Mechanisms of microparticle release from human platelets

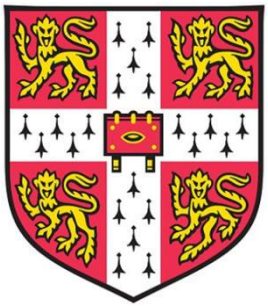

Hao Wei

Queens' College

September 2019

This thesis is submitted for the degree of

Doctor of Philosophy

Supervisor: Dr Matthew T. Harper

Department of Pharmacology

University of Cambridge

Declaration

This thesis is the result of my own work and includes nothing which is the outcome of work done in collaboration except as declared in the Preface and specified in the text. It is not substantially the same as any that I have submitted, or, is being concurrently submitted for a degree or diploma or other qualification at the University of Cambridge or any other University or similar institution except as declared in the Preface and specified in the text. I further state that no substantial part of my thesis has already been submitted, or, is being concurrently submitted for any such degree, diploma or other qualification at the University of Cambridge or any other University or similar institution except as declared in the Preface and specified in the text. It does not exceed the prescribed word limit for the relevant Degree Committee.

Abstract

Hao Wei, Mechanisms of microparticle release from human platelets

Platelets release a variety of extracellular vesicles, including platelet-derived microparticles that expose phosphatidylserine on their surface. This thesis aims to resolve the mechanisms by which pro-thrombotic microparticles are released from platelets, which have not been well-characterised. Experimental methods used include flow cytometry, Western blotting, fluorescence-based microplate assays, confocal microscopy and electron microscopy.

Intact cholesterol-rich lipid rafts were found to be required for the calpain-dependent release of microparticles from activated platelets. Microparticle release was prevented when cholesterol was depleted or sequestered from the platelet membrane. Membrane blebbing and scission in this process were independent of influx of hydrophilic ions or the endosomal sorting complex required for transport.

It was found that microparticles were also released from platelets undergoing apoptosis, which would progress to secondary necrosis *in vitro* as they were not cleared. Microparticle release in apoptotic platelets was dependent on Ca^{2+} entry, intracellular Ca^{2+} mobilisation and caspase activity, but it was largely independent of calpain. During apoptosis, caspases downregulated microparticle release from platelets in response to pro-coagulant stimuli. This may limit the pro-thrombotic consequences by providing a period of reduced capacity for platelet activation.

2-Aminoethoxydiphenyl borate (2-APB), a non-specific modulator of ion channels, was found to inhibit microparticle release from both activated and apoptotic platelets. In activated platelets, the effect of 2-APB was not related to inhibition of plasma membrane ion channels or calpain activity. In apoptotic platelets, the effect of 2-APB might be associated with inhibition of Ca^{2+} entry, although the specific target remained unclear. Future studies in identifying the target of 2-APB might provide new insights into how microparticles are released from platelets. Moreover, 2-APB may provide a scaffold for developing a pharmacological inhibitor of microparticle release.

Table of Contents

List of Figures

Chapter 6

Acknowledgements

First and foremost, I would like to thank my supervisor Dr Matthew T. Harper for his guidance, patience, knowledge and expertise. It has been great honour learning from him throughout the past three years.

I would like to thank Department of Pharmacology, Queens' College and University of Cambridge for providing the opportunity, administrative support and a world-class venue for studying and carrying out research.

I would like to thank the post-doctoral research associates Dr Nima Abbasian, Dr Bonita H. R. Apta and Dr Jessica E. Davies for offering professional advice.

I would like to thank fellow students Miss Jessica E. Berry, Mr Ivelin I. Ivanov, Miss Dora Lopresto, Mrs Sarah L. Millington and Miss Rebecca B. Riddle for creating a cordial work environment. It has been a pleasure working with all members of the Harper lab.

I would like to thank Ms Karin H. Muller at the Cambridge Advanced Imaging Centre for her guidance and supervision with electron microscopy experiments.

Last but not least, I would like to thank all the kind-hearted volunteers in the Department of Pharmacology for donating blood. Experiments could not be carried out every day without their most generous support.

Publications

Hao Wei, Jean-Daniel M. Malcor & Matthew T. Harper

Lipid rafts are essential for release of phosphatidylserine-exposing extracellular vesicles from platelets.

Scientific Reports 8, Article number: 9987 (2018)

Hao Wei & Matthew T. Harper

ABT-737 triggers caspase-dependent inhibition of platelet pro-coagulant extracellular vesicle release during apoptosis and secondary necrosis in vitro.

Thrombosis & Haemostasis 2019 Oct; 19 (10): 1665-1674

List of abbreviations

AC	adenylyl cyclase
ACD	acid citrate dextrose
ADP	adenosine diphosphate
ALG2	apoptosis-linked gene 2
ALIX	ALG2-interacting protein X
AM	acetoxymethyl ester
AMP	adenosine monophosphate
ANOVA	analysis of variance
AnxV	Annexin V
Apaf1	apoptotic protease-activating factor 1
2-APB	2-aminoethoxydiphenyl borate
APC	allophycocyanin
ATP	adenosine triphosphate
AUC	area under curve
BAK	Bcl-2 homologous antagonist killer
BAX	Bcl-2-associated X protein
BCECF	2', 7'-bis-(2-Carboxyethyl)-5-(and-6)-carboxyfluorescein
Bcl-2	B-cell lymphoma 2
Bcl-xL	B-cell lymphoma-extra large
BH3	Bcl-2 homology 3
BID	BH3-interacting domain death agonist
BSA	bovine serum albumin
cAMP	cyclic AMP
caspase	cysteine-aspartyl protease
CD	cluster of differentiation
CHAMPION-PHOENIX	Effect of Platelet Inhibition with Cangrelor during PCI on Ischemic Events
CHMP4B	charged multivesicular body protein 4B
COX	cyclooxygenase

COX IV	cytochrome c oxidase or complex IV
CRP	collagen-related peptide
CRP-XL	collagen-related peptide cross-linked
CTxB	cholera toxin B
Cx	connexin
DAPT	dual anti-platelet therapy
dH_2O	distilled water
DIC	differential interference contrast
DMSO	dimethyl sulphoxide
DRM	detergent-resistant membrane
DRP1	dynamin-related protein 1
DSM	detergent-soluble membrane
EDTA	ethylenediaminetetraacetic acid
ER	endoplasmic reticulum
ERK 1/2	extracellular signal-regulated kinase 1 and 2
ESCRT	endosomal sorting complex required for transport
EV	extracellular vesicle
FITC	fluorescein isothiocyanate
FSC	forward scatter
FVD	fixable viability dye
GAP	GTPase-activating protein
GAPDH	glyceraldehyde 3-phosphate dehydrogenase
GDP	guanosine diphosphate
GLA	γ-carboxyglutamic acid
GM1	monosialo-tetrahexosyl ganglioside
GP	glycoprotein
GPCR	G protein-coupled receptor
GPI	glycosyl phosphatidylinositol
GTP	guanosine triphosphate

H4	histone H4
HBS	HEPES-buffered saline
HEPES	hydroxyl-ethyl-piperazine-ethane-sulfonic acid
HUVEC	human umbilical vein endothelial cell
IMM	inner mitochondrial membrane
$K_{Ca}3.1$	calcium-activated potassium channel 3.1
L_d	liquid-disordered
L_o	liquid-ordered
MβCD	methyl-beta-cyclodextrin
MFI	median fluorescence intensity
MOMP	mitochondrial outer membrane permeabilisation
NCCE	non-capacitative calcium entry
NCX	sodium-calcium exchanger
NMDG	N-methyl D-glucamine
Orai	ORAI calcium release-activated calcium modulator
Panx	pannexin
PAR	protease-activated receptor
PBS	phosphate-buffered saline
PCI	percutaneous coronary intervention
PCI-CURE	Effects of pre-treatment with clopidogrel and aspirin followed by long-term therapy in patients undergoing percutaneous coronary intervention
PE	phycoerythrin
PE-Cy7	phycoerythrin-cyanine 7
PFA	paraformaldehyde
PGE_1	prostaglandin E_1
PGH_2	prostaglandin H_2
PI	phosphoinositide
PI3K	phosphoinositide 3-kinase
PIC	protease inhibitor cocktail

PIP_2	phosphatidylinositol 4, 5-biphosphate
PKA	protein kinase A
PKC	protein kinase C
PLA_2	phospholipase A_2
PLATO	Ticagrelor versus Clopidogrel in Patients with Acute Coronary Syndromes
PLT	platelet
PMP	platelet-derived microparticle
PRP	platelet-rich plasma
PS	phosphatidylserine
$PSGL_1$	P-selectin glycoprotein ligand-1
PTP1C	protein-tyrosine phosphatase 1C
RI	refractive index
RIPA	radioimmune-precipitation assay
ROCK	Rho-associated protein kinase
SDS	sodium dodecyl sulphate
SEM	standard error of mean
SERCA	sarcoplasmic / endoplasmic reticulum calcium-ATPase
SL-O	streptolysin O
SOCE	store-operated calcium entry
SSC	side scatter
STIM	stromal-interacting molecule
TEA	tetra-ethyl ammonium
TEM	transmission electron microscopy
TF	tissue factor
TMA	tetra-methyl ammonium
TMEM16F	transmembrane protein 16F
TMRM	tetra-methyl-rhodamine methyl-ester
TP	thromboxane receptor
TRAP	thrombin receptor-activating peptide

TRITON-TIMI 38	Prasugrel versus Clopidogrel in Patients with Acute Coronary Syndromes
TRPC	transient receptor potential cation channel, canonical
TRPV	transient receptor potential cation channel, vanilloid
TXA_2	thromboxane A_2
VPS	vacuolar protein sorting
vWF	von Willebrand factor
XKR8	XK-related protein 8

Chapter 1 Introduction

1.1. Platelets

Platelets are small anucleate cells in the mammalian blood circulation. In a healthy adult human, there are between 150 to 400 million platelets per millilitre of blood, generated from megakaryocytes in the bone marrow. The exact mechanism of how platelets are produced from megakaryocytes is still unclear. An early *in vitro* study showed that platelets were initially assembled and formed at one end of the megakaryocytes, before the whole cell was disintegrated to generate numerous proplatelets (Italiano et al., 1999). However, more recent studies showed that megakaryocytes extend long protrusions, mediated by dynein, into sinusoidal blood vessels in the bone marrow. Pro-platelets are then released from these protrusions under shear stress (Junt et al., 2007; Bender et al., 2015). Whatever the mechanism might be *in vivo*, a mature inactivated platelet in the blood has a biconvex discoid structure, with a diameter between 1 to 3µm (Paulus, 1975). Usually a platelet has a lifespan of around 10 days. Aged platelets are cleared by phagocytosis by macrophages in the spleen or Kupffer cells in the liver (Quach et al., 2018).

1.1.1. Platelets in haemostasis

Platelets are key players in haemostasis. By stopping bleeding at injury sites on the endothelium, platelets help to prevent outflow of blood and influx of bacteria into the blood at the same time. During the haemostatic event, platelets undergo three major processes: adhesion to a blood vessel, secretion of pro-coagulatory factors and aggregation to block the injury site.

1.1.1.1. Adhesion of platelets to blood vessels

Damage to blood vessels exposes the sub-endothelial matrix, which is made up mostly of collagen, to blood components. Derived from endothelial cells, megakaryocytes or platelets, von Willebrand factors (vWFs) in the blood circulation can anchor onto the collagen matrix. Platelets can be tethered to immobilised vWFs via the vWF receptor glycoprotein Ib (GPIb) on the platelet membrane. In this way, platelets from flowing blood are effectively linked to

the exposed collagen (Yun et al., 2016). This does not require platelet activation. However, upon binding to vWF, GPIb triggers a weak signalling pathway that leads to activation of integrins and secretion of platelet granules. In addition, the vWF-GPIb interaction slows the platelet, allowing other receptors to interact with collagen. A key receptor is membrane glycoprotein VI (GPVI), which binds collagen directly without vWF (Sarratt et al., 2005). Upon binding to collagen, GPVI triggers a strong signalling pathway that activates integrins $\alpha_{IIb}\beta_3$ (major) and $\alpha_2\beta_1$ (minor), which bind to vWF and collagen respectively. Platelets lacking GPVI cannot activate integrins during adhesion to collagen and consequently fail to stably adhere to soluble collagen (Nieswandt et al., 2001). Outside-in signalling from activated integrins further promotes platelet adhesion, leading to stable arrest of the platelet on the exposed collagen matrix.

The importance of platelet adhesion in haemostasis is shown by defects in platelet adhesion that lead to bleeding disorders. For example, deficiency or dysfunction of the GPIb complex causes the rare Bernard-Soulier syndrome (Berndt and Andrews, 2011). Defective or missing vWFs cause von Willebrand disease (Lillicrap, 2013).

1.1.1.2. Platelet activation and secretion of pro-coagulatory factors

When platelets are bound to the sub-endothelial matrix, primary interactions between surface receptors and their ligands lead to platelet activation. The platelets rapidly shoot out long processes called filopodia. The activation signals, along with shear stress, lead to release of α-granules and dense granules from platelets via the soluble N-ethylmaleimide sensitive factor attachment protein receptor (SNARE)-mediated exocytosis machinery (Berndt et al., 2014; Golebiewska et al., 2015). The α-granules contain over 300 proteins and peptides, many of which are essential to platelet function. These include vWF, multimerin, integrin $\alpha_{IIb}\beta_3$ and P-selectin (Whiteheart, 2011). P-selectin helps to recruit neutrophils by binding to its receptor P-selectin glycoprotein ligand 1 ($PSGL_1$) on the surface of neutrophils (Diacovo et al., 1996). Dense granules contain many physiological activators of platelets including ADP, ATP and Ca^{2+} (Rao, 2013). Dense granules also contain serotonin (5-HT) that leads to

constriction of vessels, which helps to slow down the flow of blood towards the injury site (Watts et al., 2012). In addition to these pre-packaged factors, activated platelets produce thromboxane A_2 (TXA_2) from arachidonic acid through the actions of cyclooxygenase 1 (COX1) and thromboxane synthase (Warner et al., 2011).

Secreted platelet activators bind to GPCRs on platelet membranes. ADP binds purinergic $P2Y_{12}$ (G_i) and $P2Y_1$ (G_q), while TXA_2 binds to TPα (G_q). In addition, thrombin, the final common protease of the coagulation cascade, activates protease-activator receptors PAR1 (G_q) and PAR4 (G_q) by proteolytic cleavage of their N-terminal domains. The G_q-linked pathway leads to activation of phospholipase C (PLC), which converts PIP_2 to diacylglycerol (DAG) and inositol triphosphate (IP_3). IP_3 acts as a second messenger that triggers Ca^{2+} release from the endoplasmic reticulum, which in turn activates CalDAG-GEF1 that promotes GDP-GTP exchange from Rap1b-GDP to Rap1b-GTP (Cifuni et al., 2008). The G_i-linked pathway downstream of $P2Y_{12}$ inhibits RASA3, which is a GTPase-activating protein that converts Rap1b-GTP to Rap1b-GDP (Stefanini et al., 2015). Therefore, G_q- and G_i-linked pathways downstream of surface GPCRs converge at Rap1b-GTP, which in turn leads to activation of talin. Talin, via its headgroup, binds to and activates integrin $\alpha_{IIb}\beta_3$ by triggering a conformational change (Petrich, 2009). This is sometimes called “inside-out signalling”.

1.1.1.3. Platelet aggregation and blood coagulation

Activated integrin $\alpha_{IIb}\beta_3$ binds fibrinogen with high affinity. Since each fibrinogen molecule can bind to two activated integrin $\alpha_{IIb}\beta_3$ molecules, it can cross-link two activated platelets. Integrin $\alpha_{IIb}\beta_3$ activation therefore underlies platelet aggregation. In general, these secretion events amplify the activation process and the inside-out signalling events associated with integrin $\alpha_{IIb}\beta_3$, recruiting more platelets for aggregation (Bennett, 2005). In this way, a non-stable primary haemostatic plug is formed that blocks the injury site. Integrin $\alpha_{IIb}\beta_3$ can also deliver outside-in signals that enhance platelet activation, granule secretion and cytoskeletal rearrangement, which further facilitate the primary haemostatic plug and thrombus formation (Durrant et al., 2017).

In addition to their central roles in forming the primary plug, platelets also contribute to the coagulation pathway. Coagulation is initially triggered by the exposure of tissue factor (TF), normally in the vessel wall but revealed to plasma coagulation factors by vessel injury. TF activates factor VII that, together with activated factor V, forms the extrinsic tenase complex. This requires a negatively-charged phospholipid surface both to accelerate the formation of activated factor X, and also to protect activated factor X from tissue factor pathway inhibitor (TFPI). The negatively-charged phospholipid surface is provided by a subpopulation of activated platelets that expose phosphatidylserine (PS) on their outer surface. By providing a negatively-charged surface to which γ-carboxyglutamic acid (GLA) domain-containing coagulation factors bind, PS markedly potentiates production of thrombin at the site of vascular injury (Hoffman and Monroe, 2001). Thrombin is a serine protease that cleaves plasma fibrinogen to form fibrin, which is cross-linked into a mesh (Swieringa et al., 2018). In this way, platelets facilitate generation of the cross-linked fibrin clot, which seals the injury site until tissues are repaired. In summary, platelets have essential functions in all three major steps of haemostasis: vasoconstriction, primary haemostasis (temporary blockage by the platelet plug) and blood coagulation (formation of the fibrin clot).

1.1.2. Platelets in thrombosis and vessel occlusion

Haemostasis maintains vascular integrity and blood flow, but pathological factors can disrupt its regulation, which can lead to uncontrolled clot formation, thrombosis and vessel occlusion in either arteries or veins. Arterial thrombosis in coronary arteries is the major trigger of acute coronary syndrome, which includes myocardial infarction and unstable angina pectoris, while venous thrombosis might lead to thromboembolism or pulmonary embolism. Activated platelets have essential roles in these thrombotic events (McFadyen et al., 2018)

The vascular endothelium continuously prevents platelet activation by releasing inhibitory factors. These include endonucleotidases that degrade ADP, thrombomodulin that inactivates thrombin, and prostacyclin that suppresses most known platelet activation

processes (Versteeg et al., 2013). This endothelium-mediated suppression is impaired not only at sites of vascular injury, but also at eroded or ruptured atherosclerotic plaques (Jackson, 2011). Many atherosclerotic plaques are rich in TF, so plaque rupture triggers the coagulation cascade. In addition, collagen is present in atherosclerotic plaques (Shekhonin et al., 1985), so platelets can be activated and aggregate at the plaques in the same way as they do at vascular injury sites. Activated platelets release secondary mediators (e.g. ADP, 5-HT, TXA_2) that recruit circulating platelets to the growing thrombus, which in turn leads to activation of more platelets and ultimately formation of a three-dimensional fibrin clot that occludes the arteries (van der Meijden and Heemskerk, 2018).

Compared to arterial thrombosis that occurs under high shear stress around ruptured plaques, venous thrombosis occurs under low shear flow and mostly around intact endothelial walls. The exact trigger for venous thrombosis is still under debate, but it usually initiates with inflammation and activation of the endothelium. Activated endothelium expresses adhesion molecules on the surface (e.g. selectin) to capture platelets and leukocytes. Attached leukocytes and platelets become activated and in turn initiate the coagulation process, which leads to fibrin deposition and clot formation (Mackman, 2012). Unlike the arterial “white clot” that is composed mainly of fibrin and platelets, the venous “red clot” encapsulates tightly packed erythrocytes at its core that are resistant to fibrinolysis under low shear flow, with activated platelets attached to fibrin at the periphery (Cines et al., 2014). Since platelet adhesion is not mediated by collagen, venous thrombi are not tightly anchored to the endothelium. They can easily dislodge to cause embolism and hence distant vessel occlusive diseases (Koupenova et al., 2017).

1.1.3. Pharmacology of anti-platelet drugs

Anti-platelet drugs are the cornerstone therapy for patients with acute coronary syndromes or stable coronary arterial diseases, and for those undergoing revascularisation procedures such as percutaneous coronary intervention (PCI) (Yousuf and Bhatt, 2011). This is because platelets are essential to forming a thrombus under the high shear conditions of a ruptured

atherosclerotic plaque and localising coagulation to this injury site. Currently four main classes of anti-platelet drugs are used either alone or in combination for clinical purposes. These include COX1 inhibitors (aspirin), $P2Y_{12}$ inhibitors (cangrelor, clopidogrel, prasugrel and ticagrelor), PAR1 antagonists (vorapaxar) and integrin $\alpha_{IIb}\beta_3$ inhibitors (abciximab, eptifibatide and tirofiban) (Figure 1.1). These drugs have proven successful in reducing morbidity and mortality associated with arterial thrombosis. However, inhibition of platelet function is inherently linked to bleeding risks, which lead to adverse cardiovascular outcomes and sometimes mortality.

1.1.3.1. Aspirin

Aspirin, the oldest anti-platelet drug, irreversibly inactivates the COX1 enzyme. COX1 mediates production of prostaglandin H_2 (PGH_2) from arachidonic acid, which is released from membrane phospholipids by phospholipase A_2 (PLA_2) upon activation of platelets. PGH_2 is transformed by TXA_2 synthase into TXA_2, which is an agonist for the TPα receptor. Patients with a rare loss-of-function mutation in the TBXA2R gene, which encodes the TPα receptor, experience mild bleeding symptoms (Mundell and Mumford, 2018). By blocking TXA_2 production, aspirin inhibits TPα-mediated platelet activation and aggregation. Aspirin's bleeding risk is correlated with both its anti-platelet effect and its inhibition of prostaglandin production that has protective effects on the gastrointestinal tract (Warner et al., 2011).

1.1.3.2. $P2Y_{12}$ antagonists

The purinergic $P2Y_{12}$ receptor mediates sustained activation of integrin $\alpha_{IIb}\beta_3$ in response to ADP stimulation. While ADP is a natural agonist for $P2Y_{12}$, ATP and many triphosphate analogues are natural antagonists of this receptor (Storey, 2001). Given the central roles of $P2Y_{12}$ in ADP-dependent secretion, platelet aggregation and procoagulant activities, inhibition of $P2Y_{12}$ carries major bleeding risks. Prolonged tail bleeding time was recorded in both $P2Y_{12}$-knockout mice and wild-type mice treated with high doses of $P2Y_{12}$ inhibitors (Andre et al., 2003; Liu et al., 2012). $P2Y_{12}$ gene mutations have been linked to bleeding in human subjects (Scavone et al., 2017). For example, a patient with rare congenital $P2Y_{12}$

deficiency caused by a point mutation in the translation initiation codon showed impaired platelet aggregation in response to ADP, and he had experienced mild bleeding tendency since childhood (Shiraga et al., 2005).

Thienopyridine pro-drugs irreversibly inhibit $P2Y_{12}$. Clopidogrel's active metabolite partitions $P2Y_{12}$ oligomers out of lipid rafts (Savi et al., 2006), which may contribute to its actions. Its efficacy for secondary prevention was confirmed in the PCI-CURE trial. Results from PCI-CURE showed that post-PCI patients using aspirin should be given clopidogrel at the same time (Mehta et al., 2001), which laid the foundation for today's dual anti-platelet therapy (DAPT) – aspirin plus clopidogrel (Mauri et al., 2014). Metabolism of clopidogrel is highly variable, with common polymorphisms in CYP2C19 reducing the formation of its active metabolite (Holmes et al., 2011). Unlike clopidogrel, the first step of prasugrel metabolism is by esterases, so it has a faster onset of action and is not affected by polymorphisms in CYP2C19 (Ancrenaz et al., 2010). In the TRITON-TIMI 38 trial, prasugrel showed significant superiority over clopidogrel for post-PCI patients in reducing cardiovascular events but increased bleeding (Wiviott et al., 2007). However, this may reflect consistency of effect of prasugrel over clopidogrel rather than greater efficacy.

$P2Y_{12}$ can also be reversibly inhibited by nucleotide derivatives. Ticagrelor is an ADP derivative and cangrelor is an ATP analogue. In the PLATO trial, ticagrelor was better than clopidogrel at preventing infarction and cardiovascular death without increasing bleeding risks (Wallentin et al., 2009). In the CHAMPION-PHOENIX trial, cangrelor used with subsequent DAPT showed clear benefits for preventing death in post-PCI patients (Bhatt et al., 2013). In addition, cangrelor, delivered by intravenous infusion, does not require metabolism and it has a very rapid onset of action about 5 to 10 minutes (Ferreiro et al., 2009). Therefore, cangrelor is more suitable for acute clinical situations and $P2Y_{12}$ inhibition in *in vitro* experimental settings.

1.1.3.3. Vorapaxar and PAR inhibition

There are two thrombin receptors on the platelet surface, the high affinity PAR1 and the low affinity PAR4 (Covic et al., 2000). Vorapaxar is an oral PAR1-selective antagonist. Based on results from TRACER and TRA-2P TIMI-50 trials, vorapaxar showed clear benefits in reducing ischaemic events when used together with DAPT, but the bleeding risk was so high that TRACER was prematurely terminated (Morrow et al., 2012; Tricoci et al., 2012). Vorapaxar has now been approved for treating cardiovascular events in patients with a history of myocardial infarction, but it is contra-indicated in patients with major bleeding histories. Vorapaxar's high bleeding risk might derive from disrupting protein C-mediated activation of PAR1, which is biased towards β-arrestin pathways that prevent endothelial apoptosis (Mosnier et al., 2012).

Novel PAR inhibitors are being developed as potential therapies. A new PAR1 antagonist class, the parmodulins, are antagonists biased towards G_q-mediated pathways and they do not inhibit β-arrestin pathways. Theoretically, they inhibit platelet aggregation without inducing endothelial damage (Aisiku et al., 2015). On the other hand, a new PAR4 antagonist BMS-986120 has demonstrated substantial anti-thrombotic activities and its bleeding risks were lower than vorapaxar in animal models (Wong et al., 2017). Clinical efficacy of parmodulins or BMS-986120 still awaits thorough investigations.

1.1.3.4. Integrin $\alpha_{IIb}\beta_3$ inhibitors and others

Currently three integrin $\alpha_{IIb}\beta_3$ inhibitors are in clinical use: a monoclonal antibody abciximab, a cyclic heptapeptide eptifibatide, and a non-peptide small molecule tirofiban. They are all ligand mimetic molecules that prevent fibrinogen from binding to activated platelets. Due to their high propensity to cause bleeding, integrin inhibitors are limited to patients with high thrombotic risks and low bleeding risks (Bosch et al., 2013). Potential novel anti-platelet therapies include GPIb or vWF inhibitors (ARC1779, caplacizumab) that disrupt the GPIb-vWF axis and a GPVI inhibitor (Revacept) that blocks collagen-mediated activation (Gachet, 2015).

Although they are effective in preventing platelet activation, anti-platelet drugs are limited by bleeding risks and highly variable efficacy in reducing cardiovascular events. Therefore, there is scope for developing new classes of drugs based on further understanding other aspects of platelets in thrombosis, e.g. the release of pro-coagulant microparticles from activated platelets.

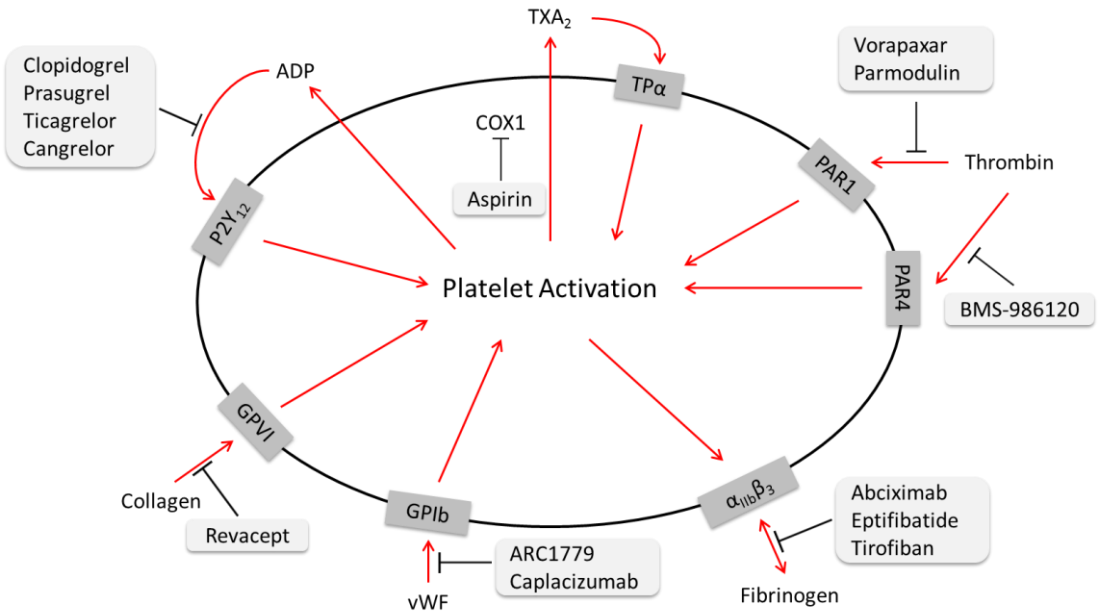

Figure 1.1: Anti-platelet drugs and their mechanisms of action

Light grey boxes for the anti- platelet drugs, dark grey boxes for receptors targeted by these drugs, red arrows for binding and/or activation, and black arrows for inhibition.

1.2. Microparticles

Extracellular vesicle (EV) is a generic term for cell-derived particles that are delimited by a lipid bilayer without a functional nucleus. All cells have the ability to produce EVs in response to activation, oxidative stress or tissue hypoxia. According to the International Society for Extracellular Vesicles, no consensus has been reached for the nomenclature of EVs that are of different sizes, origin or composition (Théry et al., 2018). This thesis adopts the standard of classifying EVs into three categories: exosomes, microparticles and apoptotic bodies (Turturici et al., 2014). Exosomes are the smallest EVs (30 to 100nm in diameter), while microparticles (also known as ectosomes) are bigger in size (100nm to 1µm in diameter). Apoptotic bodies are large membrane blebs up to 5µm in diameter that are produced exclusively during apoptotic cell disassembly (Poon et al., 2014; Hauser et al., 2017).

1.2.1. Definition of microparticles

Microparticles are a heterogeneous population of small vesicles ranging from 0.1 to 1µm in size that are derived from plasma membrane of cells (Morel et al., 2008). The presence of microparticles has been reported in a variety of body fluids, which include peripheral blood, urine, saliva, semen, synovial fluid, cerebrospinal fluid and bile (Freyssinet and Toti, 2010). Sources of microparticles in the blood circulation include platelets, leukocytes, erythrocytes, monocytes, endothelial cells and smooth muscle cells (Flaumenhaft et al., 2009). Initially identified as “platelet dust” that are released by activated platelets in human blood (Wolf, 1967), platelet-derived microparticles (PMPs) represent approximately 70 to 90% of all microparticles in the blood. They play essential roles in platelet function and various disease conditions (Żmigrodzka et al., 2016).

Microparticles are formed by direct membrane deformation and blebbing during cell activation (Morel et al., 2011). They are generally identified by phosphatidylserine (PS) on the surface, although it has been suggested that some microparticles are PS-negative (Latham et al., 2015). Similar to microparticles, apoptotic bodies are generated by membrane blebbing. They can be distinguished based on their larger sizes and components that are distinctive of apoptosis such as nuclear fragments (Akers et al., 2013).

Exosomes are a specific subtype of relatively homogenous secreted vesicles that are composed of spherical fragments of lipid bilayers from inner cell compartments (Vlassov et al., 2012). Exosome biogenesis starts with endocytosis. Early endosomes mature into multivesicular bodies (MVBs) in the cytoplasm, during which the endosomal membrane invaginates to form intraluminal vesicles (Bobrie et al., 2011). MVBs can be directed to lysosomes for degradation or transported to the vicinity of plasma membrane for exosome release (Urbanelli et al., 2013). Upon fusion of MVBs with the cell surface, exosomes are secreted into extracellular fluids in bursts. Several protein-protein interactions have been suggested to reduce the energy barriers in this process, among which the SNARE proteins facilitate membrane fusion (Hessvik and Llorente, 2018). Tetraspanins have important roles in exosome biogenesis, cargo selection, targeting and function. Two subtypes of the tetraspanin family, CD63 and CD81, are used as classical markers of exosomes (Andreu and Yáñez-Mó, 2014), although CD63 and CD81 have also been detected on the surface of microparticles secreted from certain cell lines (Crescitelli et al., 2013). In addition, exosomes are generally considered to expose little if any PS (Heijnen et al., 1999), but a recent study showed that exosomes might also expose PS (De Paoli et al., 2018).

1.2.2. Composition of microparticles

Microparticles are composed of spherical phospholipid bilayer structures that enclose cytosolic components such as enzymes, cytoskeletal proteins and RNAs from their parent cells, yet they lack a nucleus and thus synthetic capacity. Membrane markers are commonly used to identify the cell of origin, including CD41 for platelets, CD235 for erythrocytes, CD31 for endothelial cells, CD45 for leukocytes and CD14 for monocytes (Burnier et al., 2009). In particular, PMPs contain more than 40 glycoproteins (GPs) characteristic of platelets, including integrin $\alpha_{IIb}\beta_3$ (CD41), integrin β_1 (CD29) and P-selectin (CD62P). Mostly, these proteins act as adhesion molecules that initiate stimulation of recipient cells or EV internalisation by these cells (Żmigrodzka et al., 2016).

Microparticles may contain RNAs in their luminal space. Microparticles derived from endothelial progenitor cells carry coding mRNAs associated with the PI3K/AKT signalling pathway, which triggers angiogenesis in endothelial cells (Deregibus et al., 2007). Non-coding miRNAs and siRNAs have been reported in microparticles derived from embryonic stem cells, at least *in vitro* (Yuan et al., 2009). By comparison, there is no indication that DNA is present in microparticles, while exosomes and apoptotic bodies may contain traces of DNA (Kawamura et al., 2017).

Membrane lipids are the least studied components of microparticles. Some studies suggested that microparticles show a similar lipid composition as the plasma membrane, while others found specific enrichment or depletion of cholesterol, ceramide or sphingomyelin, leading to conclusions that microparticles are shed from specific regions of the plasma membrane (Pollet et al., 2018). Despite their differences in the cell of origin or the pathophysiological context, almost all microparticles expose PS at the outer membrane leaflet, which makes PS the standard marker for microparticle identification (Morel et al., 2011). However, one electron microscopy study showed that a large proportion of blood-borne EVs between 30nm to 1µm in diameter did not expose PS (Arraud et al., 2014). Whether the majority of these PS-negative EVs are exosomes or microparticles, or should be described as a separate category, remains to be resolved.

1.2.3. Functions of microparticles

Microparticles promote coagulation by providing a catalytic surface for the assembly of proteins in the coagulation cascade, which can be attributed to the presence of PS on their surface. Clotting proteins bind to PS thanks to the electrostatic interactions between the phosphate groups in the phospholipids and the tightly-bound calcium ions in the GLA domains in these proteins (Tavoosi et al., 2011). Proteins that contain a GLA domain include factors VII, IX and X, and pro-thrombin. For example, surfaces of PMPs exhibit 50-100 times higher pro-coagulant activities compared to activated platelets (Sinauridze et al., 2007).

Microparticles, especially those derived from monocytes, may harbour active TF. TF has a high affinity for coagulation factors VII and VIIa, and the TF-factor VIIa complex activates factors IX and X to initiate the extrinsic pathway of blood coagulation (Mackman et al., 2007). It was suggested that rapid accumulation of TF-exposing microparticles had important roles in thrombus formation (Lechner and Weltermann, 2008). Microparticles positive for both PS and TFs that are derived from tumour cells can potentially serve as biomarkers for identifying risks of venous thrombosis in cancer patients (Owens and Mackman, 2011).

Apart from providing pro-coagulant surfaces, microparticles can act as mediators for trans-cellular signal delivery. Microparticles carrying membrane receptors, cytosolic proteins and RNAs from their parent cells stimulate target cells, which then transform and communicate with the micro-environment in a way programmed by these contents of microparticles (Ratajczak et al., 2006). By delivering CD154, PMPs can stimulate B-cells to produce antigen-specific IgG (Sprague et al., 2008). Due to the expression of CD62P on their surface, PMPs can recruit and allow aggregation of leukocytes that express $PSGL_1$ under flow conditions (Forlow et al., 2000). When PMPs were engulfed by lung cancer cell lines, they stimulated cell proliferation, induced mRNA expression for the pro-invasive protein matrix metalloproteinase-9 and upregulated adhesion to endothelial cells (Janowska-Wieczorek et al., 2005).

Given the multi-faceted roles of microparticles, it is not surprising that elevated microparticle levels in the blood circulation have been reported in patients with hypertension (Preston et al., 2003), atherosclerosis (Wang et al., 2016), acute coronary syndromes (Mavroudis et al., 2017), myocardial infarction (Jung et al., 2012), heart failure (Berezin et al., 2015), type II diabetes (Li et al., 2016), obesity (Murakami et al., 2007), tumour progression and metastasis (Goubran et al., 2015). These associations make blood-borne microparticles attractive clinical targets and potential biomarkers of disease progression (Zhou et al., 2015).

1.2.4. How are platelet-derived microparticles released?

The mechanisms that lead to microparticle release from platelets are poorly understood. This is remarkable given their apparent contribution to many cardiovascular diseases and the details in which other platelet processes, such as granule secretion and aggregation, are understood. Microparticle release from platelets is dependent on an increase in cytosolic Ca^{2+}. Activation of platelets by a Ca^{2+} ionophore resulted in PMP release, and it was abolished when Ca^{2+} influx was inhibited (Heemskerk et al., 2002). Physiological routes for Ca^{2+} entry into platelets include purinergic $P2X_1$ receptors, the sodium-calcium exchanger (NCX), store-operated channels and transient receptor potential channels (Mahaut-Smith, 2012). It is not clear which of these channels or transporters mediate Ca^{2+} influx that ultimately leads to PMP release and whether this depends on the specific stimulus used.

An elevated level of intracellular Ca^{2+} activates calpain, a Ca^{2+}-dependent thiol protease. Activated calpain is responsible for the proteolytic cleavage of prominent cytoskeleton-associated proteins including filamin-1, gelsolin, myosin and talin (Fox et al., 1990), which in turn allows the plasma membrane to detach from the cortical actin cytoskeleton and bleb outwards. Inhibition of calpain reduced the degree of PMP release from platelets activated with thrombin, collagen or Ca^{2+} ionophore (Yano et al., 1993). Incubation of platelets with cytochalasin D, an agent that caps actin filaments and prevents their polymerisation, resulted in slow PMP release in the absence of calpain activation (Cauwenberghs et al., 2006). PMP release might also involve caspases and Rho-kinases, as described in nucleate cells (Sapet et al., 2006; Böing et al., 2013). Although caspase 3 is activated in apoptotic platelets that expose PS, it is not clear whether it has any role in platelet activation or PMP release (Kile, 2014). Activated Rho-kinases could alter the cytoskeleton and result in cellular contraction as well as membrane blebbing in platelets undergoing either apoptotic or pro-coagulant changes (Coleman et al., 2001; Paul et al., 2003).

Downstream of Ca^{2+} signalling, formation of microparticles also requires the loss of lipid asymmetry between the inner and outer leaflets of plasma membrane (Zwaal et al., 2005).

At resting state, the inner leaflet is enriched in PS, PIP_2 and phosphatidylethanolamine (PE), whereas phosphatidylcholine (PC) and sphingomyelin are predominantly distributed at the outer leaflet (Vance and Tasseva, 2013). This asymmetry is maintained by ATP-dependent transporters for inward (flip) and outward (flop) lipid translocation. In many human cells, P4-ATPase ATP11A and ATP11C act as the PS flippase (Andersen et al., 2016). When cells are activated, a rise in the intracellular Ca^{2+} concentration leads to inhibition of flippase activity. It is not enough to rapidly abolish lipid asymmetry, since uncatalysed lipid translocation is generally slow. In the meantime, scramblases whose activities are dependent on Ca^{2+} and independent of ATP might be activated to transport negatively-charged lipids including PS to the outer membrane leaflet (Bevers and Williamson, 2010). In addition, proximity of anionic phospholipids including PS might induce membrane curvature (Xu et al., 2013; Hirama et al., 2017). In this way, PS exposure is a necessary part of PMP release as well as a major contributor to its pathological effects.

In platelets, the Ca^{2+}-dependent scramblase has been identified as transmembrane protein 16F (TMEM16F). A point mutation at a splicer-acceptor site of the TMEM16F gene was identified in one patient with Scott syndrome, a rare bleeding disorder (Suzuki et al., 2010). TMEM16F-deficient platelets from Scott syndrome patients showed defects in PS exposure and PMP release *in vitro*, amongst other pro-coagulant activities, in response to physiological agonists (Mattheij et al., 2016) or a Ca^{2+} ionophore (Zwaal et al., 2004). Stimulated platelets from TMEM16F-null mice exhibited significantly lower levels of PS exposure, PMP release and *in vivo* thrombus formation compared to wild type (Fujii et al., 2015).

1.2.5. Hypothesis for the mechanism of microparticle release from platelets

Little is known beyond the calpain-dependent pathway or loss of lipid asymmetry regarding how microparticles are released from human platelets. Our working hypothesis is that it can be broken down into several stages.

Firstly, calpain-dependent breakdown dislodges cytoskeletal proteins from the membrane, which induces blebbing and sometimes membrane expansion (Miyoshi et al., 1996; Dewitt et al., 2013). Yet blebbing might also be facilitated by local increases in hydrostatic pressure through influx of hydrophilic ions followed by water. It causes the cytoplasm to flow towards those unsupported regions of the membrane where the cytoskeleton has been dislodged (Gauthier et al., 2012).

Secondly, blebbing often occurs in local regions of the plasma membrane, so there might be a specific mechanism (e.g. lipid rafts) to compartmentalise the relevant signalling complexes. For example, localisation of Ca^{2+} channels in lipid rafts might localise Ca^{2+} entry and subsequent calpain activity to these regions.

Lastly, the outward bleb needs to be pinched off. This process can be spontaneously driven by relaxation of elastic energy at a strongly curved point on the membrane (Kozlov et al., 2010), or it could be facilitated by a specialised scission mechanism (Figure 1.2).

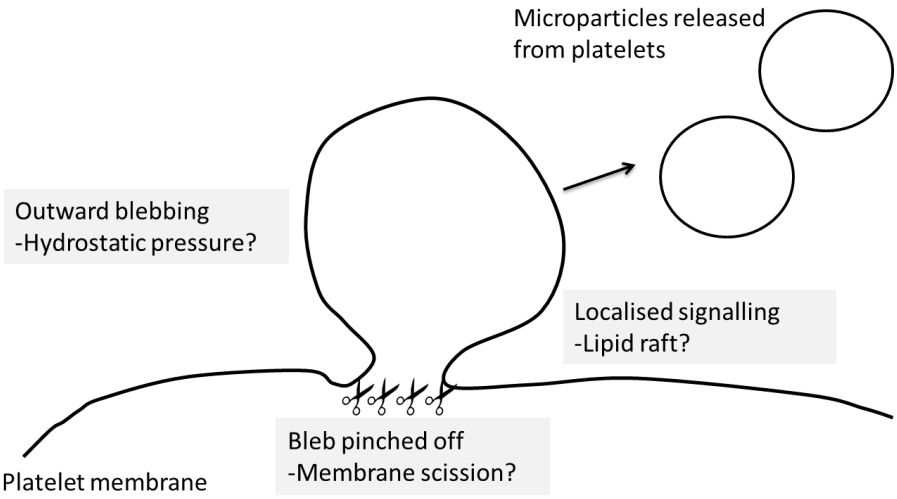

Figure 1.2: Hypothesis for the mechanism of microparticle release from platelets

(1) Increased hydrostatic pressure to induce outward membrane blebbing; (2) Lipid rafts to localise signalling events; (3) Membrane scission to pinch off membrane blebs.

1.3. Influx of ions at the platelet membrane

When microparticles are formed at the platelet membrane, outward blebbing might require local increases in pressure, possibly in the form of increased hydrostatic pressure. It could be provided by influx of Na^+ and Cl^- followed by water.

Ion influx is important for many platelet functions. Na^+ entry was shown upon activation of platelets by ADP (Feinberg et al., 1977), thrombin (Greenberg-Sepersky and Simons, 1984) and collagen (Roberts et al., 2004). It appears to have essential roles in triggering or amplifying Ca^{2+} signals. Store-operated calcium entry (SOCE) in platelets was inhibited when extracellular Na^+ was absent or when Na^+ entry was blocked by specific inhibitors (Harper et al., 2010). Na^+ entry via TRPC3 and TRPC6, followed by activation of NCX, contributes to the increase in cytosolic Ca^{2+} that ultimately triggers PS exposure when stimulated by thrombin plus collagen (Harper et al., 2013). In the presence of Cl^- channel blockers, PS exposure was reduced in response to physiological agonists but not to Ca^{2+} ionophores, so Cl^- influx may be required for membrane hyperpolarisation in stimulated platelets, which in turn is required for sustained downstream Ca^{2+} signalling events (Harper and Poole, 2013). The identity of the Cl^- channel is still under debate, but some suggested that the scramblase TMEM16F could function as a Ca^{2+}-activated Cl^- channel (Yang et al., 2012; Liu et al., 2015).

Apart from Ca^{2+} signalling and PS exposure, ion influx mediates “ballooning” in platelets. Observable under light microscopy, balloons are large PS-exposing membrane sacks (1 to 6µm in diameter) filled with small debris and devoid of organelles or the open canalicular system (Podoplelova et al., 2016). Balloon formation was significantly attenuated when platelets were incubated in medium lacking Na^+ or Cl^-, or when extracellular osmolality was increased by sucrose (Agbani et al., 2015). Water molecules might enter platelets through the aquaporin-1 channel, which was reported to be expressed in both murine and human platelets (Agbani et al., 2018). Swelling morphological changes was absent in platelets from TMEM16F-deficient mice or a patient of the rare Scott syndrome (Mattheij et al., 2016), so TMEM16F might mediate PS exposure or Cl^- entry, or both, during balloon formation.

It is not clear whether coordinated ion and water entry is needed for blebbing in PMP release, which is similar yet distinct from ballooning. The first phase of ballooning is associated with blebbing and bleb retraction before the swelling becomes irreversible (Agbani et al., 2015). However, membrane blebbing analogous to this process in cancerous cells appears reversible and independent of fluid entry (Fackler and Grosse, 2008). When ballooning was impaired by inhibiting Na^+ or Cl^- entry or blocking aquaporin-1, there was a reduction in the number of PMPs released from platelets (Agbani et al., 2017, 2018). This reduction in PMP count was based on measuring Annexin V fluorescence in microscopy images. Since microparticles are difficult to detect under light microscopy due to their small sizes, the results would be more convincing if they can be reproduced using an additional and more objective method, e.g. flow cytometry or nanoparticle tracking analysis (Théry et al., 2018).

1.4. Lipid rafts

Lipid rafts are heterogeneous, dynamic (in terms of lateral mobility) and microscopic (>300nm) domains on the plasma membrane that are enriched in saturated phospholipids, sphingolipids, glycolipids and cholesterol (Pike, 2006). These domains are formed transiently on the membrane by the collective behaviours of raft-associated lipids and proteins that interact preferentially with one another (Simons and Vaz, 2004). Enrichment of hydrophobic lipids and proteins endows lipid raft domains with increased lipid packing (or order) and decreased fluidity. Lipid rafts are present in both the inner and outer leaflets of an asymmetrical cell membrane, and they are potentially coupled across leaflets (Raghupathy et al., 2015). Functionally, lipid rafts act as platforms for the regulation of various cellular processes via selective accumulation of lipidated proteins and glycosyl phosphatidylinositol (GPI)-anchored proteins, thereby facilitating interactions between these proteins (Lingwood and Simons, 2010). This makes lipid rafts potential hubs for localised signalling cascades.

1.4.1. Studying lipid rafts

Early studies focused on isolation of lipid raft domains from the cell membrane. When detergents are applied, cellular membranes separate into two distinct fractions: detergent-soluble membranes (DSMs) and detergent-resistant membranes (DRMs) (Yu et al., 1973). Since DRMs are enriched in cholesterol, sphingolipids and GPI-anchored proteins, they became the paradigm in probing lipid raft compositions (Brown and Rose, 1992). However, DRMs cannot reflect the native lipid raft composition and organisation in living cells due to the non-physiological nature of how DRMs are extracted (Lichtenberg et al., 2005).

In parallel with differential solubilisation, artificial model membranes were developed to study principles behind raft formation. Membranes composed of miscellaneous lipids can be separated into two distinct phases: a relatively packed liquid-ordered (L_o) phase enriched in saturated lipids and cholesterol, and a relatively fluid liquid-disordered (L_d) phase enriched in unsaturated lipids (Kaiser et al., 2009). Nonetheless, it is technically difficult to integrate proteins into systems of model membranes, which limits the scope of L_o phase in modelling lipid rafts (Sezgin et al., 2012).

Microscopy has been used regularly for studying localisation, structure and composition of lipid rafts, although this is limited by the spatial resolution of the technique used. Morphologically, lipids rafts can be identified by caveolae that contain caveolin-1 protein (Parton et al., 2006). Detected by confocal microscopy, co-localisation of putative lipid raft markers (e.g. cholera toxin B) with certain molecules has been used as evidence that these molecules are associated with lipid rafts (Gupta and DeFranco, 2003). The resolution of confocal microscopy limits its use in direct assays of lipid raft structure and composition, especially in small cells such as platelets. Recently, PALM, STED and NSOM super-resolution microscopy techniques help to visualise lipid-mediated protein clustering; whereas SPT, iSCAT and FRET are powerful tools for measuring the real-time dynamics of lipid diffusion at nanometre scale (Sezgin et al., 2017). Most of these methods are dependent on fluorescent markers. As lipid behaviours are determined by molecular packing yet fluorophores are similar in size as the lipid molecules, fluorescent labels inevitably alter the native behaviour of lipids and perturb lipid raft functions (Sezgin and Schwille, 2011), which might compromise conclusions derived from fluorescence-based microscopy studies.

To study lipid raft functions, cells are treated with drugs or enzymes that interfere with cholesterol levels to disrupt lipid raft structure and function. Given its specificity and rapid onset of action, a cholesterol-depleting agent methyl-β-cyclodextrin (MβCD) is widely used. However, MβCD has off-target effects beyond cholesterol depletion, including inhibition of cholesterol-independent lateral diffusion of membrane proteins, increase in membrane permeability to ions and acute cytotoxicity (Mahammad and Parmryd, 2015). In addition, statins are used in combination with cholesterol-free medium over long incubation time (up to 24 hours) to inhibit cholesterol synthesis via the mevalonate pathway (Goodwin et al., 2005). It is not suitable for platelet studies *in vitro* because HMG-CoA reductase, the intracellular target of statins (Istvan and Deisenhofer, 2001), is not expressed in human platelets.

Ceramide confers a spontaneous curvature to the plasma membrane because of its cone-shaped structure, which might mediate membrane blebbing or invagination (Verderio et al., 2018). Drugs that interfere with sphingolipid synthesis (myriocin) or stability (tricyclic anti-depressants) have been used to disrupt lipid rafts (Miller et al., 2015; Zhao et al., 2015), but not in platelets so far. These drugs are limited by their off-target effects, because inhibiting sphingolipid metabolism or ceramide generation inevitably alters membrane properties.

1.4.2. Functions of lipid rafts

The primary function of lipid rafts is to facilitate and regulate specific protein-protein interactions as a catalytic platform, via selective accumulation and segregation of lipidated or GPI-anchored proteins at the plasma membrane. In addition, close proximity with raft lipids such as cholesterol and sphingolipids may induce conformational changes in lipid raft-associated proteins and thus affect their activities (Laganowsky et al., 2014).

The first cellular pathway discovered to be associated with lipid rafts is IgE-mediated signalling in mucosal mast cells. Under resting conditions, high affinity IgE receptors FcεRI, T-cell receptors and B-cell receptors were all found in DSMs. These key immune receptors all translocate to DRMs upon activation (Field et al., 1995). This notion was further supported when proteins of the signal transduction machineries downstream of these receptors were found to be enriched in DRMs (Filipp et al., 2004). Many immune-associated proteins at the cell surface such as DAF, CD14, CD59 and Thy-1 are GPI-anchored (Saha et al., 2016). Since then, lipid rafts have been implicated in the coordination of numerous signalling pathways in immunity, cancer, cell growth, neural development, diabetes and cardiovascular diseases (Sezgin et al., 2017).

Lipid rafts have been suggested to mediate budding of HIV viruses, which is similar in topology to microparticle release. A comparative lipidomics study found that cholesterol, sphingolipids and saturated lipids were more prevalent than unsaturated lipids in the HIV-1

viral envelope (Lorizate et al., 2013). Viral receptors and viral fusion proteins in general are preferentially partitioned into lipid raft domains on the cell surface (Teissier and Pécheur, 2007). Moreover, binding of the HIV Gag protein, a step necessary for virus assembly and budding, favours cholesterol-rich membrane domains with close packing of lipids, although it is not clear how Gag protein senses membrane domains that are of different lipid compositions (Dick et al., 2012).

1.4.3. Lipid rafts, platelets and microparticle release

Lipid raft domains are present on the platelet membrane. The first evidence came from discovery of cholesterol-rich DRMs from resting platelets (Dorahy et al., 1996). Reversible phase separation and lipid domain formation was observed under microscopy when platelets were activated by thrombin plus collagen, and it was abrogated when cholesterol was depleted by MβCD (Gousset et al., 2002).

Functions of many platelet receptors are linked to lipid rafts. Lipid rafts are required in G_i-linked signalling events downstream of the $P2Y_{12}$ receptor in response to stimulation by ADP (Quinton et al., 2005). GPVI, the major collagen receptor, is recruited to lipid rafts upon stimulation (Locke et al., 2002; Bodin et al., 2003), and lipid rafts regulate activation of platelets by GPVI agonists (Quinter et al., 2007).

The role of lipid rafts in microparticle release has been shown in several cell types. Cholesterol depletion from THP-1 monocyte membranes impaired the release of TF-bearing microparticles (Del Conde et al., 2005), while loading THP-1 monocytes with cholesterol induced PS exposure on the surface and increased microparticle release (Liu et al., 2007). Lipid rafts also control the composition of the monocyte-derived microparticles by allowing incorporation of TF, $PSGL_1$ and β_1 integrins (Rothmeier et al., 2015). Disruption of lipid rafts by MβCD or nystatin blocked microparticle release from endothelial cells in response to stimulation with angiotensin II (Burger et al., 2011). Microparticles released from erythrocytes either under storage or treated with a Ca^{2+} ionophore are enriched in the lipid

raft marker stomatin (Salzer et al., 2002, 2008). Total cholesterol content on the erythrocyte membrane decreased following the release of cholesterol-enriched vesicles (Santos et al., 2005). These studies show that lipid rafts are a conserved feature of microparticle release from cardiovascular cells. However, roles of lipid rafts in signalling including those relevant to Ca^{2+} channels are well-established (Pani and Singh, 2009). It is not always clear whether lipid rafts are involved in microparticle release itself, or in the generation of the Ca^{2+} signal that triggers microparticle release.

No previous study has directly linked lipid rafts to PMP release, yet lipid rafts have been connected to platelet membrane deformation. Upon interaction with fibrinogen or stimulation of thrombin receptors, cholesterol is redistributed to the tips of filopodia and the leading edges of spreading platelets (Heijnen et al., 2003), while cholesterol depletion impedes formation of these plasma membrane extensions (Larive et al., 2010). In addition, lipid rafts in platelets are sites of high PI metabolism (Bodin et al., 2001). Activated calpain has been shown to cleave raft-associated PIP kinases. This would lead to decreased PIP_2 levels in lipid rafts and may locally disrupt adhesion of cytoskeleton to the membrane, which favours membrane blebbing and vesicle release (Chichili and Rodgers, 2009). Finally, phospholipid content of PMPs vary slightly depending on the stimuli, but the cholesterol content in PMPs tends to be higher than that on platelet surfaces, secreted granules and intracellular membranes (Biró et al., 2005).

1.5. Membrane scission

After budding from the plasma membrane, blebs for PMPs need to be pinched off, and it requires a membrane scission mechanism. Generally the scission process starts with formation of a neck on a budding vesicle, followed by constriction of the membrane neck until it reaches a critical diameter estimated to be within 1 to 5nm. Scission occurs spontaneously when the force put on the membrane is great enough to cause constriction beyond this critical threshold (Campelo and Malhotra, 2012). Three major mechanisms have been reported under different circumstances to facilitate membrane scission in cells, namely dynamin-mediated constriction, Arf1-mediated lipid insertion and ESCRT-mediated scaffolding (Figure 1.3). They all manipulate lipid-lipid interactions within biological membranes to alter curvature of the phospholipid membrane bilayer.

1.5.1. Dynamin-mediated constriction

Dynamins are large GTPases involved in many processes including budding of transport vesicles, division of organelles, cytokinesis and pathogen resistance (Praefcke and McMahon, 2004). They can assemble into a helical coat, a ring-like structure, at necks of budding vesicles (Takei et al., 1995). Assembly of dynamin triggers its inherent GTPase activity and subsequent conformational changes constrict the necks below the critical diameter (Faelber et al., 2012). Spontaneous scission occurs at the interface between the dynamin ring and uncoated membrane, because increases in local membrane elastic energy due to curvature is the greatest at this location and the energy barrier for scission is minimised (Morlot et al., 2012). This protein machinery has been widely reported to mediate membrane scission and fusion during clathrin-mediated endocytosis (De Camilli et al., 1995; Mettlen et al., 2009). There is no evidence yet that dynamin mediates outward scission or ectocytosis, so it is unlikely to be involved in microparticle release from platelets.

1.5.2. ARF1-mediated lipid insertion

ADP-ribosylation factor 1 (Arf1) proteins are small GTPases that regulate membrane functions. Binding of GTP to Arf1 releases an N-terminal amphipathic α-helix from the protein core so that its hydrophobic residues can interact with membrane phospholipids

(Antonny et al., 1997). Insertion of this amphipathic helix into lipids causes a stacking effect leading to expansion of the outer membrane leaflet. In this way, membrane curvature is induced locally at sites of Arf1-GTP binding until constriction goes beyond the critical threshold (Beck et al., 2008). Although Arf1 has been reported in the platelet proteome (Thon et al., 2008; Haudek et al., 2009), it has not been implicated in any platelet function or EV release from any type of cells.

1.5.3. ESCRT-mediated scaffolding

The endosomal sorting complex required for transport (ESCRT) comprises a system for membrane budding and severing membrane necks from their inner surface (Hurley, 2015). The conserved membrane neck-directed activities of ESCRT are involved in a huge variety of biological processes. These include budding of HIV-1 viruses from infected cells (Gan and Gould, 2011), cytokinetic abscission checkpoint control (Carlton et al., 2012), surveillance of nuclear pore complex assembly (Webster et al., 2014), secretion of vesicles that carry Hedgehog signals during *Drosophila* wing development (Matusek et al., 2014), budding and shedding of small wounds during repair of injured cell membrane (Jimenez and Perez, 2017), and sealing of newly formed nuclear envelopes (Vietri et al., 2015).

1.5.3.1. Structure of ESCRT protein complexes

The ESCRTs were identified as five hetero-oligomeric sub-complexes called ESCRT-0, -I, -II, –III, and vacuolar protein sorting 4 (VPS4) (Katzmann et al., 2001; Babst et al., 2002; Saksena et al., 2007). Despite its name, ESCRT-0 is not a core component of the membrane budding and scission machinery. ESCRT-I and -II and apoptosis linked gene 2-interacting protein X (ALIX) are directly involved in membrane budding. They function as two branches that feed into ESCRT-III, or commonly referred to as charged multivesicular body proteins (CHMPs). ESCRT-III, in concert with VPS4, carries out scission of budding necks (Hurley and Hanson, 2010). Of these two branches, the ALIX-dependent pathway is more important for certain ESCRT functions such as EV biogenesis, virus budding and plasma membrane wound repair (Campsteijn et al., 2016). Also, damaged membrane segments are shed from the plasma membrane in the same manner as in budding of microparticles (Jimenez et al., 2014).

1.5.3.2. Mechanism of ESCRT-mediated scission

The ALIX pathway initiates with apoptosis-linked gene 2 (ALG2). ALG2 is activated by Ca^{2+} binding and it recruits ALIX to the plasma membrane (Maki et al., 2016), which in turn binds and recruits CHMP4 subunits of the ESCRT-III pathway (Scheffer et al., 2014). CHMP4B is the major binding partner of ALIX among the CHMP4 isoforms (McCullough et al., 2008). Downstream of ALIX, knockdown of CHMP4 and VPS4 genes blocked biogenesis of syndecan exosomes (Baietti et al., 2012). Upon binding to ALIX, CHMP4B self-assembles at the N-helical hairpin domain into 5nm circular polymers that are attached to the plasma membrane.

Once assembled and attached to a membrane, CHMP4B filaments have an intrinsic tendency to curve and they form conical spirals known as ESCRT-III rings. By imposing their intrinsic geometry onto the tightly-attached membrane structures, ESCRT-III rings are able to deform and distort the membrane, pushing membrane domains to bud (Hanson et al., 2008). Subsequently, constriction of the ESCRT-III spiral ring by Vps4 ATPase at the budding neck leads to membrane scission (Adell et al., 2014). As a result, vesicles are pinched off and released from the cell.

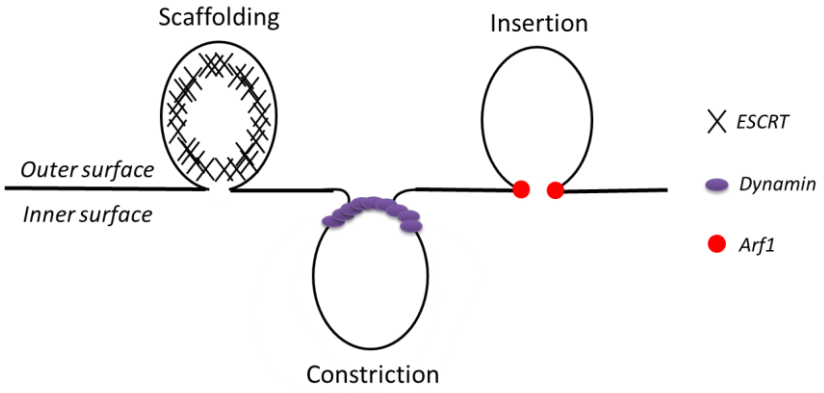

Figure 1.3: Mechanisms that facilitate membrane scission

(1) ESCRT-mediated protein scaffolding on the inside of membrane bud (e.g. membrane repair); (2) Constriction of membrane by dynamin rings on the outside of membrane bud (e.g. clathrin-mediated endocytosis); (3) Arf1-mediated lipid insertion at the neck of membrane bud (e.g. budding of vesicles of at the Golgi complex en route to the endoplasmic reticulum).

1.6. Apoptosis

Apoptosis or programmed cell death occurs during cell development, maturation and aging as a homeostatic mechanism to maintain cell populations in tissues. Unlike necrotic cells that swell until the plasma membrane ruptures, apoptotic cells shrink and the integrity of the plasma membrane is intact (Kerr et al., 1972). Apoptosis is mediated by a group of enzymes called caspases, for cysteine-aspartyl proteases (Alnemri et al., 1996). Activated caspases execute apoptosis and apoptotic cells present on their surface “eat me” signals that recruit macrophages for engulfment. In this way, dying cells can be cleared before intracellular contents are spilled out onto surrounding cells, preventing inflammation (Elmore, 2007).

1.6.1. Intrinsic and extrinsic apoptosis pathways

Apoptosis proceeds via two convergent pathways in human cells: intrinsic and extrinsic (Figure 1.4). The intrinsic apoptosis pathway is regulated by Bcl-2 family proteins, which include pro-survival Bcl-2 proteins, pro-death triggers BH3-only proteins and functionally redundant pro-death effectors BAK and BAX (Lindsten et al., 2000; Czabotar et al., 2014). In healthy cells, Bcl-2 proteins prevent apoptosis by sequestering and inhibiting BAK and BAX proteins. In response to cellular stress, cytotoxic insults or developmental cues, BH3-only members are upregulated. They bind to and inhibit Bcl-2 proteins, thereby relieving the inhibition on BAK and BAX. Activated BAK and BAX oligomerise or dimerise to form pores at the outer mitochondrial membrane, through which cytochrome c is released into the cytosol. Cytochrome c, along with Apaf1, forms apoptosome, which is a heptameric scaffolding complex that cleaves pro-caspase 9 into active caspase 9. Activated caspase 9 cleaves pro-caspase 3 into active caspase 3, which is the major cell death effector (Baig et al., 2016) .

The extrinsic apoptosis pathway is triggered by death factors of the tumour necrosis factor (TNF) superfamily including Fas ligands, TNFα and TRAIL. Binding of death ligands to their specific receptors causes oligomerisation of death domains on the intracellular side of plasma membrane. These death domains recruit pro-caspase 8 and other proteins to form a death-inducing signalling complex that facilitates cleavage of pro-caspase 8 into active

caspase 8. There are two pathways downstream of active caspase 8. In type I cells (e.g. lymphocytes), caspase 8 by itself is sufficient to cleave pro-caspase 3. In type II cells (e.g. hepatocytes), caspase 8 cleaves BID, a BH3-only protein. Cleaved BID (tBID) directly activates BAK and BAX, which induces cytochrome c release and eventually activation of caspase 3 in the same way as in the intrinsic pathway (Nagata, 2018).

Intrinsic and extrinsic apoptosis pathways converge at the caspase cascade. A recent enzymology study showed that different caspases have distinct substrate specificities (Julien et al., 2016). In total, caspases cleave more than 1,300 substrates at more than 1,700 sites in human cells (Crawford et al., 2013). For example, inhibitor of caspase-activated DNase is cleaved and DNase is released to cause apoptotic DNA fragmentation that further invokes p53 signalling (Larsen and Sørensen, 2017). ROCK1 is cleaved to induce apoptotic membrane blebbing (Zhang et al., 2018). Involvement of caspases in cell death has been extensively verified, as most proteolytic cleavages and downstream apoptotic features are ablated in the presence of pan-caspase inhibitors such as Q-VD-OPh or Z-VAD-FMK.

1.6.2. Apoptosis in platelets

Apoptosis in platelets is regulated by Bcl-extra-large (Bcl-xL), a member of the pro-survival Bcl-2 protein family. Gene disruption or pharmacological inhibition of Bcl-xL reduced platelet lifespan and caused thrombocytopenia in a dose-dependent manner, while simultaneous deletion of BAK and BAX genes prolonged platelet lifespan and caused thrombocytosis in murine models (Mason et al., 2007). Although megakaryocytes possess both functional BAK- or BAX-mediated intrinsic and Fas ligand-induced extrinsic pathways, apoptosis in platelets proceeds only through the intrinsic pathway (McArthur et al., 2018). Death receptors have not been reported on the surface of platelets, and roles of caspase 8 or the extrinsic apoptosis pathway remain elusive.

There is no consensus regarding how apoptosis is triggered in platelets in the circulation. First put forward was the “molecular clock” model stating that Bcl-xL was gradually degraded

over time and Bcl-xL levels declined relative to BAK and BAX (Dowling et al., 2010). However, Western blot analysis detected no changes in the amount of Bcl-xL proteins in platelets with significantly different age profiles (Kile, 2014), so it is likely that BH3-only proteins (e.g. BID, BIM, BAD) act as active mediators of apoptosis in platelets. There was a small extension in the lifespan of platelets from $BAD^{-/-}$ mice (Kelly et al., 2010). BAD has also been reported to be directly inhibited by PKA. Downregulation of PKA relieved its inhibition and allowed BAD to initiate platelet apoptosis by sequestering Bcl-xL (Zhao et al., 2017). In this way, apoptosis could be linked to G_i-coupled receptors such as $P2Y_{12}$ or chemokine receptor type 7 ($CXCR_7$) on the platelet surface, but definitive genetic evidence is lacking.

1.6.3. BH3-mimetic drugs

BH3-mimetic drugs tightly bind to the surface groove of pro-survival Bcl-2 proteins. By inhibiting Bcl-2 functions, BH3-mimetic drugs can induce apoptosis in cells independently of BH3-only proteins. ABT-737, the first BH3-mimetic drug ever developed, has low nanomolar affinity for Bcl-2, Bcl-xL and Bcl-w, but it has negligible affinity for Mcl-2 or Bcl-B (Park et al., 2006). ABT-737 has become a useful tool for investigating cellular apoptosis, and it has led to increased understanding of the signalling events that take place (Billard, 2013). For example, the use of ABT-737 for *in vitro* platelet studies offered insights into intracellular Ca^{2+} dynamics, caspase activity and morphological changes associated with the intrinsic apoptosis pathway (Vogler et al., 2011).

The orally available ABT-263 (navitoclax) was the first BH3-mimetic drug to enter clinical trials. It has an affinity profile similar to that of ABT-737 (Tse et al., 2008). Despite its efficacy in killing tumour cells with high Bcl-2 activity, ABT-263 provoked acute thrombocytopenia, because it inhibited Bcl-xL and induced platelet apoptosis in the blood circulation (Roberts et al., 2012).

The selective Bcl-2 inhibitor ABT-199 (venetoclax) spares platelets. It engages with the p4 hydrophobic pocket that differs in Bcl-2 (Arg103) and Bcl-xL (Glu96) (Cang et al., 2015).

ABT-199 has now been approved to treat relapsed or refractory chronic lymphocytic leukaemia with 17p deletion. Since the Bcl-2-associated intrinsic pathway acts downstream of p53, it was not surprising that the efficacy of ABT-199 was independent of p53 status (Anderson et al., 2016). In preclinical studies, ABT-199 has been shown to sensitise tumour cells to other therapies, so it has potential to enter clinical trials in combination with many other known anti-cancer agents (Adams and Cory, 2018).

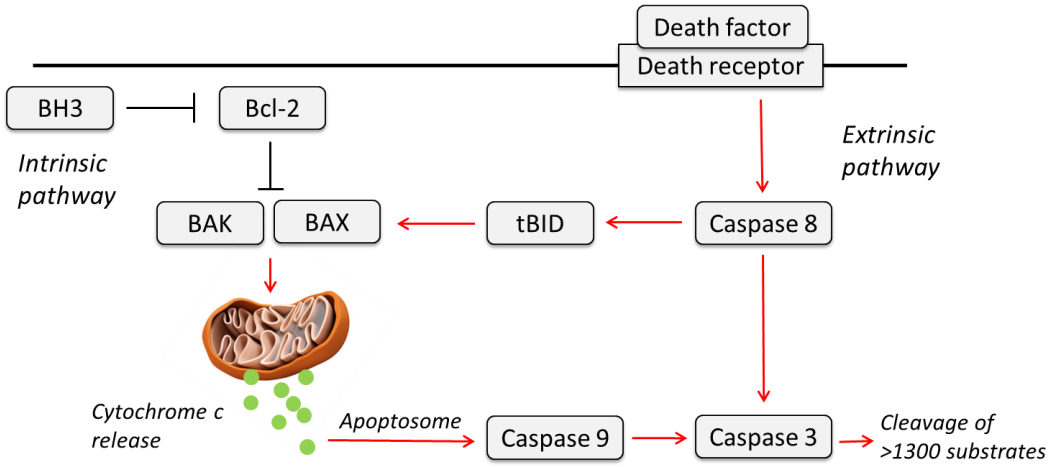

Figure 1.4: Signal transductions in apoptosis pathways

Red arrows are for activation and black arrows are for inhibition. BH3-mimetic drugs, e.g. ABT-737 and ABT-263 (navitoclax), induce apoptosis in platelets by inhibiting Bcl-xL, a member of the pro-survival Bcl-2 family.

1.6.4. Hallmark of apoptosis: PS exposure

Apoptotic cells expose PS on their surface in a caspase-dependent manner (Martin et al., 1995). Fluorescently labelled Annexin V, which specifically binds to PS (and PE) in an extracellular Ca^{2+}-dependent manner, has been the standard practice for detecting cellular apoptosis *in vitro* (Vermes et al., 1995). There are two recognition sites for caspase 3 in the cytoplasmic region of the PS flippase ATP11A (Segawa et al., 2014). Apart from flippase inhibition, a scramblase needs to be activated so that PS can be transported to the outer membrane leaflet (Bevers and Williamson, 2010). Although intracellular Ca^{2+} concentration increases during apoptosis, the Ca^{2+}-dependent scramblase TMEM16F is not indispensable for apoptotic PS exposure. TMEM16F-null platelets from a Scott syndrome patient still

exposed PS when apoptosis was induced by BH3-mimetics *in vitro* (van Kruchten et al., 2013). It agrees with an earlier hypothesis that activation-induced and apoptosis-induced PS exposure are regulated by two distinct pathways in platelets (Schoenwaelder et al., 2009).

XK-related protein 8 (XKR8) has been suggested as the Ca^{2+}-independent PS scramblase. When cells undergo apoptosis, caspase 3 cleaves XKR8 at its C-terminal tail. The truncated XKR8 undergoes dimerisation with its chaperones basigin or neuroplastin. The dimerised complex works as a non-specific scramblase that bi-directionally translocates phospholipids across membrane leaflets, so that PS can be exposed on the surface (Suzuki et al., 2016). However, there has been no evidence reporting the presence of XKR8 in human platelets. In addition, it remains to be established if there is cross-talk between the two PS mobilisation pathways in platelets. It is technically difficult to confirm whether highly activated platelets undergo apoptosis to enhance pro-coagulant activities such as PS exposure. More specifically, it is unclear whether physiological agonists can induce BAK- or BAX-mediated platelet death, partly because a potent and specific inhibitor for BAK or BAX is still lacking.

PS exposure is a necessary and sufficient "eat me" signal for cell clearance. Masking PS by pre-incubating apoptotic cells with Annexin V blocked clearance (Krahling et al., 1999). When flippase activity was inhibited, constitutive PS expression caused phagocytosis of living cells (Segawa et al., 2014). After apoptotic cells are engulfed by macrophages, they are transported along the cytoskeleton to the lysosome for degradation (Nishi et al., 2014).

1.6.5. Secondary necrosis

If apoptotic cells are not cleared rapidly by macrophage phagocytosis, they undergo secondary necrosis. Secondary necrotic cells feature plasma membrane swelling and cell lysis. Intracellular contents are released, so there might be pro-inflammatory or immunogenic consequences (Sachet et al., 2017). Recently, gasdermin E (also called deafness, autosomal dominant 5; DFNA5) was identified as a central regulator of apoptotic cell disassembly and progression to secondary necrosis. Downstream of mitochondrial damage, cytochrome c

release and the Apaf1 apoptosome pathway, DFNA5 is cleaved by caspase 3 at Asp270. The cleaved N-terminal fragments of DFNA5 self-assemble into oligomer rings that penetrate the plasma membrane from the inside. In this way, membrane permeability is increased, which causes swelling and induces secondary necrosis (Rogers et al., 2017).

It is difficult to distinguish necrotic from apoptotic platelets in experiments. Fluorescently labelled Annexin V can be used to detect PS exposed on the surface of apoptotic platelets, but Annexin V can also stain necrotic platelets because it can access the inner membrane leaflet through the ruptured plasma membrane. Necrotic cells are commonly identified by co-staining with propidium iodide, a fluorescent DNA-intercalating agent, that cannot cross the membrane of apoptotic cells (Crowley et al., 2016), but it is not applicable for anucleate platelets. In addition, some suggested that Annexin A1 was externalised only on necrotic cells (Blume et al., 2009), yet others reported that Annexin A1 began to be exposed at the early stages of apoptosis similar to the timing of PS exposure (Weyd et al., 2013).

The greatest extent of PS exposure is seen after 1 to 3 hours of treating platelets with BH3-mimetic drugs, so signalling studies often investigate these later time points (Schoenwaelder et al., 2011; Vogler et al., 2011; Rukoyatkina et al., 2013). It seems likely that an apoptotic platelet would be cleared within this time under normal circumstances, but the scavengers of apoptotic cells are not present *in vitro* and hence the apoptotic platelets will not be rapidly cleared. It is possible that secondary necrosis is initiated at these later time points. If necrosis does ensue, it then becomes necessary to review whether the classic apoptotic features reported in platelets so far should instead be associated with secondary necrosis.

1.7. 2-Aminoethoxydiphenyl borate

The drug 2-aminoethoxydiphenyl borate (2-APB) was initially developed as a cheap and fast-onset membrane-penetrable antagonist for intracellular phosphoinositide (PI) signalling. The first report of 2-APB showed that it inhibited IP_3-induced Ca^{2+} release in platelets in a concentration-dependent manner (Maruyama et al., 1997). Later, 2-APB was found to suppress Ca^{2+} signals in a variety of cells including neurons, neutrophils, cardiac myocytes and endothelial cells. Many of these studies used 2-APB to demonstrate involvement of IP_3 receptors without considering its additional effects (Bootman et al., 2002). Since then, 2-APB has been established as non-specific inhibitor of multiple Ca^{2+} channels not limited to IP_3 receptors. Rather than Ca^{2+} release, the principal antagonistic effect of 2-APB is on Ca^{2+} entry.

1.7.1. 2-APB inhibits store-operated calcium entry

2-APB inhibits store-operated calcium entry (SOCE), a process by which depletion of Ca^{2+} from the ER activates Ca^{2+} influx across the plasma membrane. SOCE helps to maintain a relatively constant Ca^{2+} concentration in the ER, which underlies protein synthesis, folding and IP_3-induced Ca^{2+} signalling (Putney et al., 2017). In platelets, SOCE can be induced by physiological agonists such as thrombin (Harper and Poole, 2011), or by pharmacological agents such as thapsigargin that inhibits SERCA pumps and depletes ER luminal Ca^{2+} (Sage et al., 2011). The inhibitory effect of 2-APB on SOCE does not involve IP_3R, but is likely to be a direct effect on SOCE in platelets (Diver et al., 2001). This is also seen in other cells. For example, in primary hepatocytes, 2-APB caused a concentration-dependent inhibition of Ca^{2+} influx without blocking IP_3-induced Ca^{2+} release (Gregory et al., 2001). In addition, Ca^{2+} entry triggered by thapsigargin was still inhibited by 2-APB in IP_3R knockout cells (Iwasaki et al., 2001), further supporting the conclusion that 2-APB directly blocks SOCE.

SOCE is mediated by two protein families: stromal interacting molecules (STIM) as the Ca^{2+} sensors in the ER and Orai as the pore-forming subunits in the plasma membrane. When Ca^{2+} is depleted from ER, Ca^{2+} dissociates from STIM, which triggers self-association and migration of STIM to the closely apposed ER-plasma membrane junctions. At these junctions, STIM oligomers interact with and activate Orai-formed channels to allow Ca^{2+} influx (Hogan and

Rao, 2015). When used at relatively high concentrations (e.g. 50μM), the inhibitory effect of 2-APB on SOCE is multi-faceted. It rapidly blocks the Orai1 pore within 90 seconds, before its direct inhibition on STIM1 develops within several minutes. 2-APB locks STIM1 in its auto-inhibitory resting state, thereby inhibiting formation of STIM1 oligomers. 2-APB also weakens interactions between STIM1 and the N-terminal region of Orai1, so it indirectly affects functional coupling between STIM1 and Orai1 (Wei et al., 2016).

Although generally denoted as an inhibitor of SOCE, 2-APB has bimodal actions. Whilst it inhibits Ca^{2+} influx at high concentrations of 25 to 100μM, 2-APB enhances SOCE at a lower range of 1 to 20μM (Putney, 2010). In a recent study, 2-APB (5μM) was found to increase the pore size of STIM1-activated Orai1 channels, which then conduct Ca^{2+} and Na^{+} (Xu et al., 2016). On the other hand, Orai2 is relatively insensitive and Orai3 is strongly activated by 2-APB even at high concentrations. 2-APB (75μM) increased the pore size of Orai3 channels by more than 40% independently of STIM1 (Schindl et al., 2008). Orai1 is the predominant member of Orai family in human platelets. Expression levels of Orai2 and Orai3 are significantly lower (Braun et al., 2009), so the stimulatory effect of 2-APB on Orai3 is likely to be negligible for platelet studies.

1.7.2. Other targets of 2-APB

2-APB inhibits canonical-type TRP channels (TRPCs). Subtypes of TRPC reportedly inhibited by 2-APB include TRPC1 (Delmas et al., 2002), TRPC3 (Trebak et al., 2002), TRPC5 (Xu et al., 2005), TRPC6 and TRPC7 (Lievremont et al., 2005). Among these subtypes, TRPC1, 3 and 6 are expressed in human platelets. The role of TRPC1 remains to be clarified. Although early reports implicated TRPC1 as a channel for SOCE (Rosado et al., 2002; Brownlow et al., 2004), platelets from TRPC1-knockout mice showed fully intact SOCE compared to wild type (Varga-Szabo et al., 2008). By contrast, TRPC3 and TRPC6 have well-established roles in store-independent calcium entry, also known as non-capacitative calcium entry (NCCE), which can be triggered in platelets by the diacylglycerol analogue, 1-Oleoyl-2-Acetyl-sn-Glycerol (OAG) (Berna-Erro et al., 2016).

Functions of TRPCs are sometimes coupled to sodium-calcium exchanger (NCX). For example, Na^+ entry via TRPC3 and TRPC6, followed by reverse activation of NCX, mediates an increase in cytosolic Ca^{2+} that ultimately triggers platelet PS exposure in response to thrombin plus collagen (Harper et al., 2013).

2-APB affects functions of vanilloid-type TRP channels (TRPVs). Whilst it inhibits TRPV6 (Voets et al., 2001; Singh et al., 2018), 2-APB is a common activator of TRPV1, 2 and 3 channels (Colton and Zhu, 2007). TRPV1 is the only TRPV subtype expressed in human platelets, and Ca^{2+} influx through TRPV1 can be triggered specifically by capsaicin (Sage et al., 2014). Functionally, TRPV1 is involved in agonist-induced 5-HT secretion from platelets, which is further associated with dense granule secretion and Ca^{2+} release during platelet activation (Harper et al., 2009).

2-APB inhibits connexin hemichannels. Opposing hemichannels dock onto each other and form gap junctions that allow direct exchange of small molecules between cytoplasm of adjacent cells (Laird and Lampe, 2018). Usually gated by Ca^{2+} (Lopez et al., 2016), connexins act as non-specific anion channels (Fiori et al., 2012). 2-APB was shown to inhibit inter-cellular transfer of molecules at both high (100μM) and low (10μM) concentrations (Griffith et al., 2005; Neijssen et al., 2005). Instead of altering single channel conductance, 2-APB inhibits gap junctions by rapidly reducing the number of channels remaining in the open state. Potency of 2-APB inhibition varies depending on specific connexin subunits (Bai et al., 2006). Roles of subunits Cx37 and Cx40 have been studied extensively in platelets using specific gap junction inhibitors and genetic knockout mice. They have important roles in fibrinogen binding, granule secretion, platelet aggregation, thrombus formation and stability, and clot retraction (Vaiyapuri et al., 2012, 2013).

2-APB may also inhibit pannexins (Willebrords et al., 2017). Pannexins are topologically analogous to connexins, although there is no sequence homology (Sosinsky et al., 2011). Pannexin subunits form plasma membrane hexameric ion channels, through which cytosolic

contents, e.g. ATP, are released to the extracellular space (Boassa et al., 2007). They can also act as Ca^{2+}-permeable gap junctions that propagate Ca^{2+} waves between cells (Vanden Abeele et al., 2006; Ishikawa et al., 2011). Pannexin subunit 1 (Panx1), but not Panx2 or Panx3, is expressed in human platelets. Inhibition of platelet Panx1 reduced Ca^{2+} influx and ATP release in response to various agonists (Taylor et al., 2014). It is thus hypothesised that ATP release through Panx1 leads to autocrine or paracrine activation of the ligand-gated $P2X_1$, which then mediates Ca^{2+} influx and ultimately platelet aggregation and thrombus formation (Molica et al., 2015, 2017).

1.7.3. Structure of 2-APB

Divergent and non-specific effects of 2-APB may derive from its structural complications. A 2-APB molecule consists of three parts: an aminoethyl chain, a boron-oxygen core and two phenyl rings. The boron atom can interact with N or O atoms in amino acids (Mc Cormack et al., 1997). The amine chain can conduct intra- and inter-molecular nucleophilic attack on boron, so 2-APB can also exist as ring-form monomers or dimers (van Rossum et al., 2000).

Several studies focused on the structure of 2-APB. When 2-APB was replaced by two analogues without an aminoethyl chain or B-O core, inhibition of platelet SOCE or activation of keratinocyte TPRV3 was not affected (Dobrydneva and Blackmore, 2001; Chung et al., 2005), so the biphenyl moiety could be the pharmacophore for these functions. Later, it was found that the phenyl rings were not essential in inhibiting SOCE, yet there was a clear correlation between the number of phenyl rings in the molecule and its ability to inhibit SOCE (Zhou et al., 2007; Dellis et al., 2011). More recently, custom-synthesised analogues enabled refined structure-function analysis of how 2-APB potentiates and inhibits SOCE in Jurkat T cells (Djillani et al., 2014, 2015).

Most 2-APB structural studies relied on analogues. Chemical structures of commercially available analogues are listed below. Compared to 2-APB, PBA is a small molecule that only retains the B-O core attached to one phenyl group. In DP3A, the B-O core is replaced by a

phosphate group. DPHD lacks the boron atom and has two methyl groups attached to the secondary amine. Diphenylborinic acid is not stable (Finch and Gardner, 1966), while DMBA provides a more stable structure where two phenyl rings are replaced by mesitylene rings. In DPBA, the terminal amine chain is replaced by another diphenylborinic group. DPTHF lacks the boron atom, yet it has a five-membered ring containing an oxygen atom, which is similar to the ring form of 2-APB monomer (Figure 1.5)

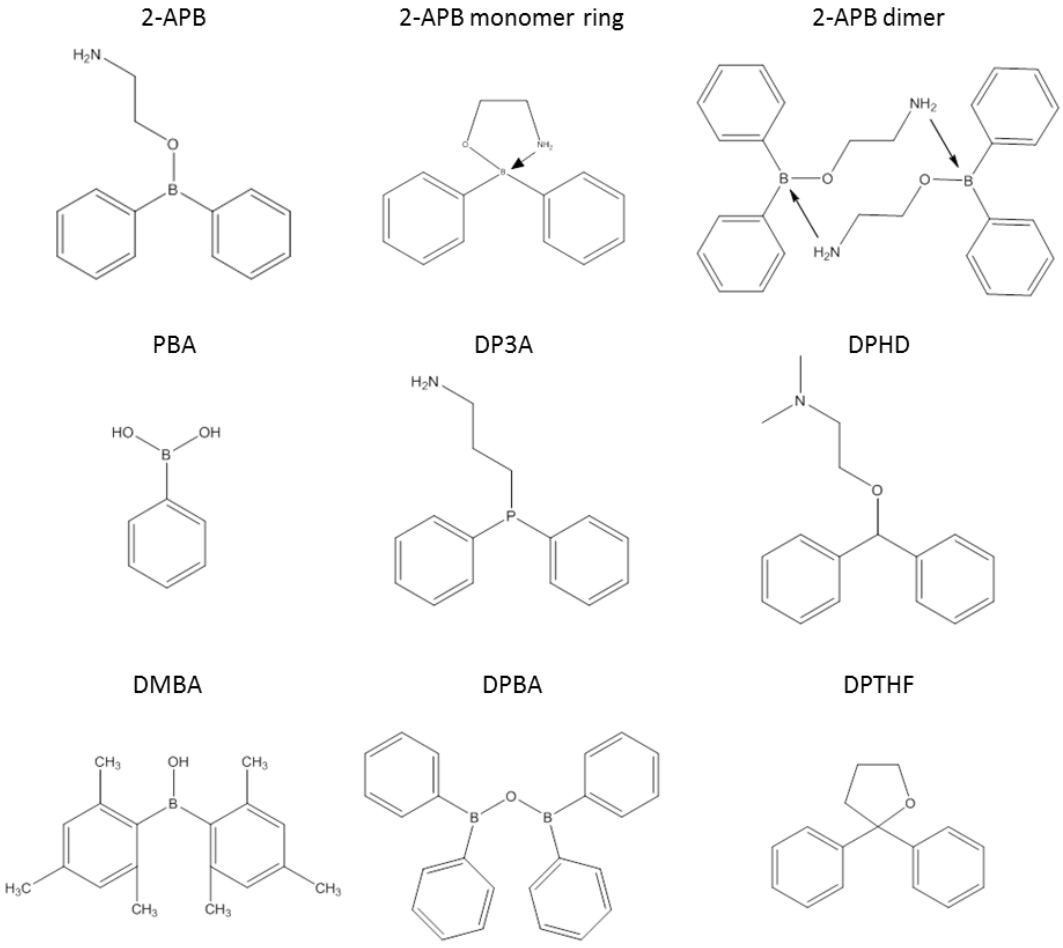

Figure 1.5: Structures of 2-APB and its analogues

2-APB: 2-aminoethoxydiphenyl borate; PBA: phenylborinic acid;

DP3A: 3-(diphenylphosphino)-1-propylamine; DPHD: diphenhydramine;

DMBA: dimesitylborinic acid; DPBA: diphenylborinic anhydride;

DPTHF: 2, 2-diphenyl tetrahydrofuran.

These structures were drawn in ChemDraw.

1.8. Aim of study

This thesis aims to understand how microparticles are released from human platelets. In the literature, there is no consensus on the method of detecting microparticles or other types of extracellular vesicles. To start with, an assay needed to be developed for the detection of platelet-derived microparticles.

Secondly, it was investigated how microparticles are released from activated human platelets. Little is known beyond the calpain-dependent pathway or loss of lipid asymmetry. A few hypotheses for this process were studied. These include influx of hydrophilic ions as a mechanism for membrane blebbing, lipid rafts as a platform for localised signalling and endosomal sorting complex required for transport as a system for membrane scission.

Thirdly, it was investigated whether and how microparticles are released from apoptotic human platelets. In terms of platelet apoptosis, little is known beyond the intrinsic apoptotic pathway and caspase-mediated phosphatidylserine exposure. Regulatory mechanisms of platelet apoptosis, secondary necrosis, and the relevant microparticle release were studied and then compared with its counterpart in activated platelets.

Finally, 2-aminoethoxydiphenyl borate (2-APB) was found to inhibit microparticle release from platelets in response to either pro-coagulant stimulation or induction of apoptosis. These two pathways for microparticle release have not been fully resolved. Studying the mechanisms behind inhibition by 2-APB, and possibly identifying its target, could bring insights into how microparticles are released from activated and apoptotic platelets.

Chapter 2 Materials and methods

2.1. Isolation of platelets from whole blood and preparation of washed platelets

Healthy, drug-free volunteers had given written, informed consent in accordance with the Declaration of Helsinki. Use of human blood for these experiments was approved by the Human Biology Research Ethics Committee, University of Cambridge, United Kingdom. Blood was drawn by venepuncture into vacuettes (Greiner) with sodium citrate (3.8% v/v in dH_2O) used as an anti-coagulant. Whole blood was gently mixed 7:1 with pre-warmed (30°C) acid citrate dextrose (ACD; 85mM tri-sodium citrate, 71mM citric acid, 111mM D-glucose).

Centrifuged at 200g for 10 minutes without brake at room temperature, whole blood was separated into platelet-rich plasma (PRP) on top and red blood cells (RBCs) at the bottom. PRP was diluted 1:1 with pre-warmed (30°C) HEPES-buffered saline (HBS; 135mM NaCl, 10mM HEPES, 3mM KCl, 1mM $MgCl_2$, 0.34mM NaH_2PO_4, pH 7.4) containing 0.9mg/ml D-glucose. Diluted PRP was supplemented with 100nM prostaglandin E_1 (PGE_1) and 0.02U/ml apyrase (Grade VII), and centrifuged at 600g for 10 minutes with brake at room temperature. The pellet was resuspended in HBS as washed platelets, counted using a Coulter counter (Beckman Coulter), and adjusted to the appropriate concentrations for specific experiments. Platelets were rested at 30°C for 30 minutes prior to stimulation or treatment with inhibitors. Calcium chloride (2mM) was added immediately prior to stimulation (Figure 2.1).

Several reagents were used to prevent platelet activation in the process of isolation from whole blood. Both sodium citrate and ACD act as anti-coagulants by the action of citrate ion, which chelates free ionised calcium and thus makes Ca^{2+} unavailable to the coagulation system. Apyrase is a highly active enzyme that catalyses hydrolysis of ATP and ADP into AMP. By breaking down ADP, it prevents activation of platelets via the purinergic receptors $P2Y_1$, $P2Y_{12}$ and $P2X_1$ (Mans et al., 1998). This also prevents desensitisation of these receptors during platelet activation. PGE_1 stimulates adenylyl cyclase (AC) activity and increases cyclic AMP (cAMP) concentrations, which inhibits the Ca^{2+} mobilisation and platelet aggregation induced by $P2Y_1$ receptor activation (Kreutz et al., 2013).

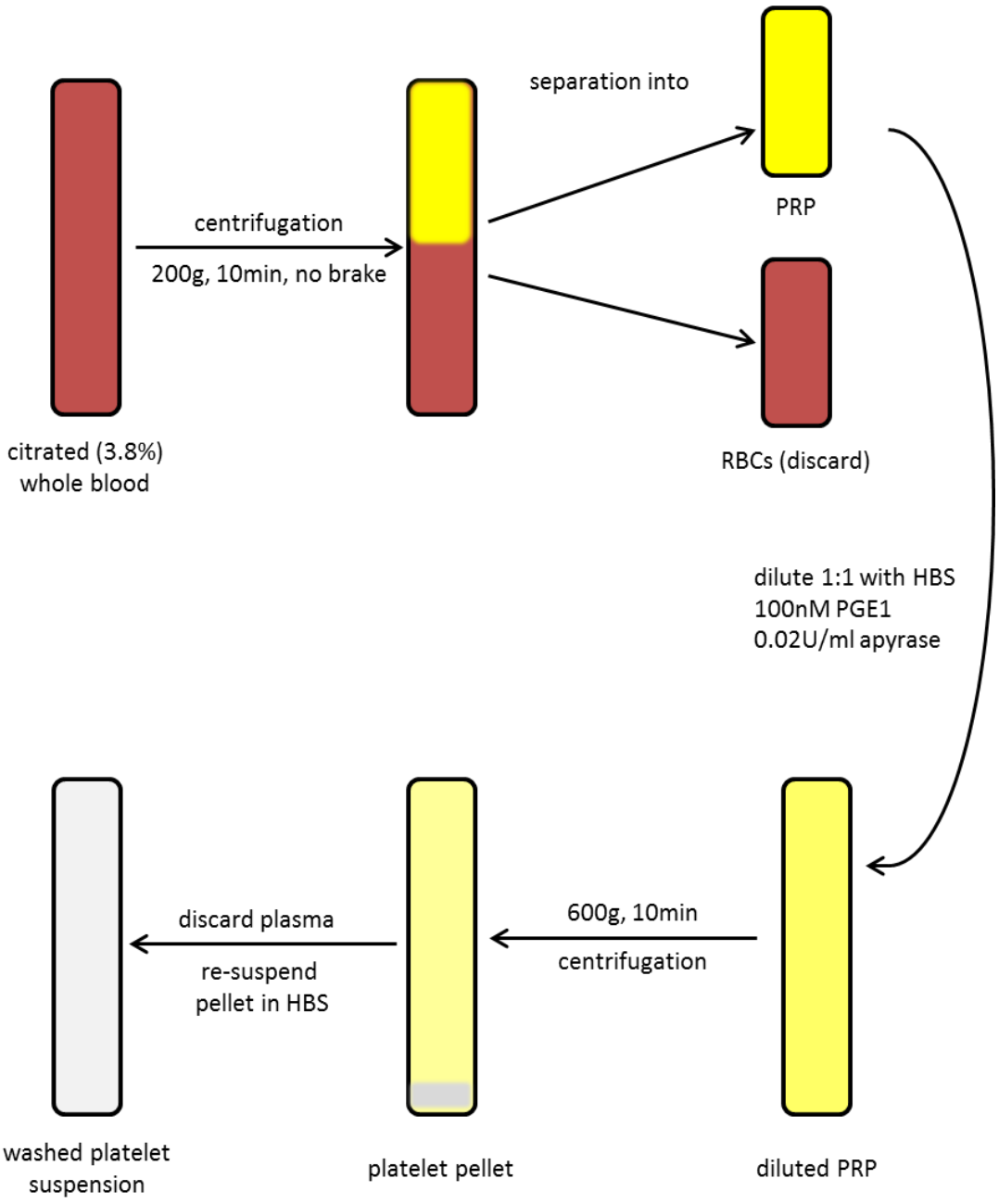

Figure 2.1: Preparation of washed platelets

2.2. Flow cytometry

Platelets (5×10^7 per ml) were rested at 30°C for 30 minutes, followed by treatment with agonists or inhibitors, as described in Chapters 3 to 6. Samples (10µl) were then stained with the appropriate dyes or conjugated antibodies (40µl in total) for 3 minutes (Table 2.1), fixed by paraformaldehyde (PFA; 1%; 250µl) and diluted by half in HBS. In most experiments, platelets were stained with Annexin V FITC to detect exposed phosphatidylserine (PS) and with anti-human CD41a PE-Cy7 to distinguish platelet-derived events (Figure 2.2A). $CaCl_2$ (2mM) was present during staining even if not present during stimulation.

Samples were acquired using a BD Accuri C6 flow cytometer at medium speed: flow rate 35µl per minute and core size 16µm. Forward scatter (FSC) and side scatter (SSC) of light were set in logarithmic scales, and the fluorescence channels were set in logarithmic gain. The 1µm gate was set in FSC using 1µm silicon dioxide beads (1 in 100,000). Event acquisition was triggered by the PE-Cy7 fluorescence of anti-human CD41a on channel FL3. The PS-binding protein, Annexin V (AnxV), was conjugated to FITC, so its fluorescence was reflected on channel FL1. Platelets were defined as events larger than 1µm positive for CD41a, whereas platelet-derived microparticles (PMPs) were defined as events smaller than 1µm positive for both CD41a and Annexin V (Figure 2.2A). Microparticle count was expressed as microparticle per platelet (PMP/PLT). This approach allowed comparison between individual experiments, as more platelets would inherently produce more PMPs.

Conjugated Antibody or Fluorescent Dye	Supplier	Code	Channel	Dilution
Annexin V APC	eBioscience	BMS306APC	FL4	1 in 100
Annexin V FITC	eBioscience	BMS306FI	FL1	1 in 100
Anti-human CD41a PE-Cy7	eBioscience	25-0419-42	FL3	1 in 100
Anti-human CD62P PE	BD Biosciences	555524	FL2	1 in 20
Calcein AM	Thermo Fisher	C1420	FL1	1 µM
Cholera toxin B FITC	Sigma	C1655	FL1	10 µg/ml
Fixable Viability Dye eFluor 660	eBioscience	65-0864	FL4	1 in 1000
Fluo4 AM	Thermo Fisher	F14201	FL1	1 µM
TMRM	Thermo Fisher	I34361	FL2	500 nM

Table 2.1: Conjugated antibodies or fluorescent dyes used for flow cytometry.

A more refined analysis of PMP release and platelet activation was enabled by fluorescently labelled markers. In CD41a +ve events smaller than 1µm, stimulation of platelets with A23187 was accompanied by an increase in the count of AnxV-positive events, i.e. PMPs (Figure 2.2B). Platelets expose PS on the surface when they are activated, so Annexin V can be used as an index for platelet activation. Resting platelets were AnxV-negative. When stimulated by A23187, platelets became activated and AnxV-positive (Figure 2.2C). PS exposure was expressed as percentage of events positive for AnxV binding in the platelet population.

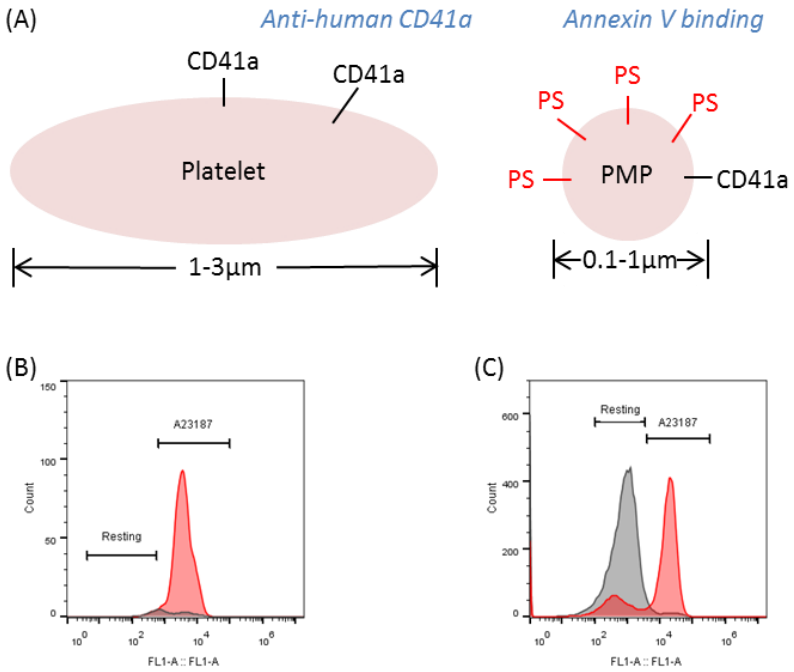

Figure 2.2: Detecting platelets and PMPs with flow cytometry

(A) Platelets are 1 to 3µm in diameter and they express CD41a molecules on their surface. CD41a can be detected by binding of a fluorescently-conjugated anti-human CD41a antibody. PMPs are 0.1 to 1µm in diameter, and they express CD41a and PS on their surface. PS can be detected by binding of fluorescently conjugated Annexin V molecules. The number of events counted by flow cytometry was an underestimate of the total number of microparticles, as only the largest EVs were predominantly acquired. (B) A23187-induced microparticle release (red) compared to resting state (black) reflected on FL1. All events in this plot are <1µm and positive for CD41a. (C) A23187-induced activation of platelets and PS exposure on surface of platelets (red) compared to resting state (black) reflected on FL1. All events in this plot are >1µm and positive for CD41a.

2.3. Confocal microscopy of filipin-stained platelets

Fresh stocks of 50mM methyl-β-cyclodextrin (MβCD) in HBS and 50mM alpha-cyclodextrin (αCD) in HBS were prepared before each experiment. Platelets were diluted 4:1 or 1:1 with 50mM cyclodextrin to achieve a final concentration of 10mM or 25mM, or HBS was added alone as vehicle, followed by incubation at 30^{o}C for 30 minutes.

Platelets (5×10^7 per ml) treated with αCD, MβCD or vehicle were fixed with 1% PFA, washed by centrifugation (600g, 10 minutes) and resuspended in 250µl phosphate buffered saline (PBS). Fixed platelets were then adhered to coverslips coated with 10µg/ml poly-L-Lysine overnight at 4^{o}C. After one gentle wash with PBS, platelets attached to coverslips were stained with 50µg/ml filipin in PBS containing 33% (v/v) fetal calf serum (FCS) for 2 hours at room temperature in the dark. Coverslips were washed gently again with PBS, before being mounted onto glass plates using Fluoromount-G (Figure 2.3).

Images were taken using a Leica SP5 confocal microscope, objective 63x oil, 405nm excitation and 411nm - 505nm emission. For quantitative analysis of platelets stained with filipin, images were obtained under identical conditions: smart gain 1142.0V, smart offset 0.6%, pinhole 90.00µm and 405nm laser 15%. Average intensity of fluorescence per platelet was measured and calculated using Fiji (Schindelin et al., 2012).

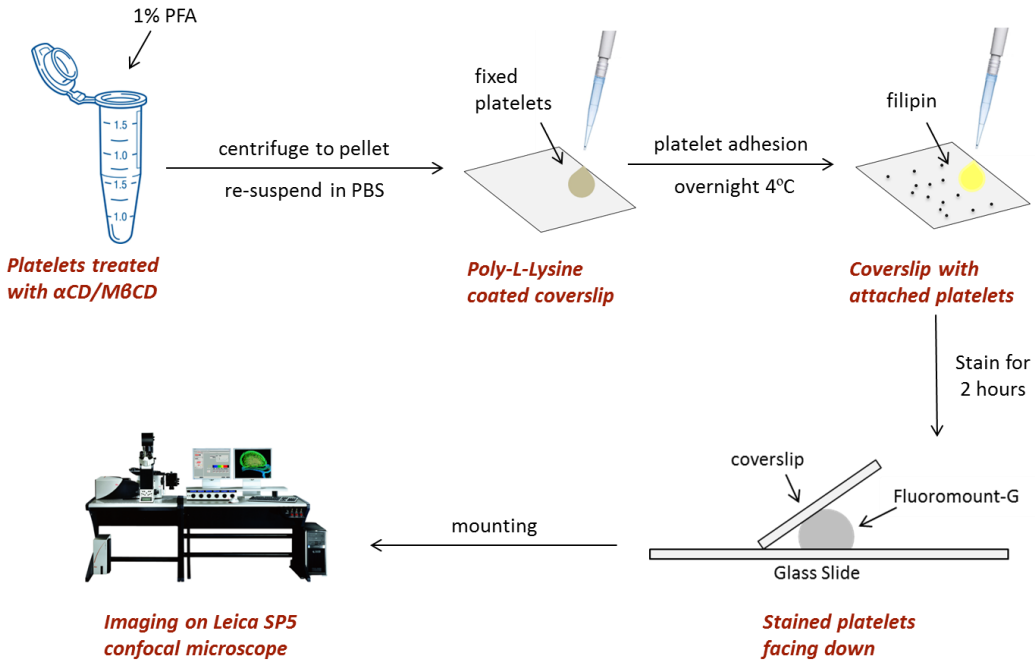

Figure 2.3: Fluorescence imaging of filipin-stained platelets by confocal microscopy

2.4. Western blotting

2.4.1. Cell culture for positive controls

HeLa cells were maintained as monolayer cultures grown at 37^{o}C in a moist atmosphere containing 5% CO_2 in 75cm cell culture flasks. The growth medium was Dulbecco's Modified Eagle Medium (DMEM) with 4.5g/L D-glucose, supplemented with FCS (10% v/v) and penicillin-streptomycin (1% v/v). HeLa cells were passaged every three days with a split ratio of 1:4. After reaching 90% confluency, HeLa cells were harvested by treating with 0.5mM EDTA and trypsin. Washed once with PBS, HeLa cell suspension was centrifuged (600g, 5 minutes, room temperature) to obtain pellets, which were then lysed for Western blot.

2.4.2. Collection of cell lysates

Western blot was performed on washed platelets (5×10^8 per ml), HeLa cells harvested from cell culture and human umbilical vein endothelial cells (HUVECs) gifted by Dr Bonita Apta. Cell pellets were lysed with radioimmune-precipitation assay (RIPA) lysis buffer (100mM Tris, 2% Triton X-100, 0.2% sodium dodecyl sulphate, 1% sodium deoxycholate, 300mM NaCl, pH 8.0) containing a protease inhibitor cocktail (PIC; 1% v/v) and 100mM dithiothreitol (DTT). Lysed pellets were incubated at 4^{o}C for 30 minutes with agitation by vortex, followed by centrifugation at 17,000g for 10 minutes to pellet membrane proteins. The supernatant was collected as cell lysate.

2.4.3. Protein assay

Bovine serum albumin (BSA) standards were prepared from 1.4 to 0mg/ml as serial dilution in dH_2O. Bradford reagent (250µl) was added to BSA standards (5µl) at each concentration and diluted samples of cell lysates (5µl), prior to incubation with gentle agitation for 10 minutes at room temperature. Protein absorbance was measured at 595nm by a Clariostar Microplate Reader (BMG Labtech). Standard curve of absorbance versus protein concentration was plotted by linear regression. Concentrations of proteins were calculated from the standard curve.

2.4.4. Gel electrophoresis and protein transfer

Cell lysates containing 20µg protein were electrophoresed on 6 to 16% polyacrylamide gels (Table 2.2) at 200V in the running buffer (19mM glycine, 25mM Tris, 0.1% SDS). Proteins were transferred from gels onto 0.45µm polyvinylidene difluoride (PVDF) membranes at 4°C for 1 hour at 100V in the transfer buffer (19mM glycine, 25mM Tris, 20% v/v methanol).

Separating Gel (10ml)

Percentage	6%	8%	10%	12%	14%	16%
Water	5.3 ml	4.6 ml	4.0 ml	3.3 ml	2.6 ml	2.0 ml
1.5M Tris pH 8.8	2.5 ml	2.5 ml	2.5 ml	2.5 ml	2.5 ml	2.5 ml
10% SDS	100 µl	100 µl	100 µl	100 µl	100 µl	100 µl
30% Acrylamide	2.0 ml	2.7 ml	3.3 ml	4.0 ml	4.7 ml	5.3 ml
10% APS	90 µl	90 µl	90 µl	90 µl	90 µl	90 µl
TEMED	10 µl	10 µl	10 µl	10 µl	10 µl	10 µl

Stacking Gel (5ml)

Percentage	4%
Water	2.94 ml
0.5M Tris pH 6.8	1.25 ml
10% SDS	50 µl
30% Acrylamide	700 µl
10% APS	50 µl
TEMED	10 µl

Table 2.2: Formula for poly-acrylamide gels. The percentage of separating gels was selected according to the size of the protein of interest. Stacking gel was layered on top of separating gel. Into the wells of stacking gels, PageRuler protein ladder (5µl) was loaded to the first lane. The remaining lanes (20µl per well) were loaded with cell lysates (20µg protein per well) mixed 3:1 with NuPAGE LDS loading buffer.

2.4.5. Treatment with antibody and membrane development

Membranes were blocked with non-fat powdered milk or BSA (5% w/v) in Tris-buffered saline-Tween (TBS-T; 137mM NaCl, 20mM Tris, 0.1% Tween-20, pH 7.6) for 1 hour at room temperature, incubated overnight at 4°C with the appropriate primary antibody (Table 2.3), and washed three times with TBS-T. To detect the primary antibody, membranes were incubated for 1 hour at room temperature with horseradish peroxidase (HRP)-conjugated anti-rabbit IgG (7074, Cell Signaling Technology; CST) or anti-mouse IgG (7076, CST), again washed three times with TBS-T. To visualise the blot, membranes were incubated for 5 minutes with SuperSignal Chemiluminescent Substrate and developed using OptiMax X-ray film processor (Protec Medizintechnik) or GeneGnome XRQ (Syngene Bio Imaging). Quantification of blots, when required, was performed using Fiji (Schindelin et al., 2012).

Antibody	Supplier	Code	Block	Dilution	Secondary
ALG2	Abcam	ab109181	5% BSA	1 in 1000	1 in 1000
ALIX	CST	2171	5% milk	1 in 1000	1 in 2000
ATP8A1	Proteintech	21565-1-AP	5% milk	1 in 1000	1 in 1000
Caspase 3	CST	9662	5% BSA	1 in 500	1 in 1000
CD41	Abcam	ab134131	5% BSA	1 in 2000	1 in 5000
CHMP4B	Santa Cruz	sc-134946	5% BSA	1 in 500	1 in 1000
COX IV	CST	4850	5% BSA	1 in 1000	1 in 10000
Cytochrome c	Santa Cruz	sc-13156	5% milk	1 in 250	1 in 2000
ERK 1/2	CST	4695	5% BSA	1 in 1000	1 in 5000
GAPDH	CST	2118	5% milk	1 in 2000	1 in 10000
Gelsolin	CST	8090	5% BSA	1 in 1000	1 in 1000
PTP1C	BD Biosciences	610125	5% milk	1 in 1000	1 in 1000
Talin	CST	T3287	5% milk	1 in 10000	1 in 10000

Table 2.3: Antibodies used for Western blotting and their optimal dilutions. Membranes were incubated with primary antibodies at 4^{o}C overnight and secondary antibodies at room temperature for 1 hour.

2.5. Fluorescence measurements by microplate reader

For measuring cytosolic Ca^{2+} concentration, PRP was loaded with 500nM Cal520 by incubation with Cal520 AM for 10 minutes. Washed platelets (5 x 10^7 per ml) were added into black 96-well plates for 150µl per well. Cal520 was excited at 492nm and fluorescence emission was detected at 520nm on FLUOstar Omega (BMG Labtech). Fluorescence was normalised to the initial fluorescence intensity of unstimulated vehicle control (F/F_0). Area under curve (AUC) for the Ca^{2+} trace above basal was calculated.

For measuring cytosolic pH, PRP was loaded with 1µg/ml 2', 7'-Bis-(2-Carboxyethyl)-5-(and-6)-Carboxyfluorescein (BCECF) by incubation with BCECF AM for 30 minutes. Washed platelets (5 x 10^7 per ml) were added into black 96-well plates for 150µl per well. BCECF was excited at 485nm and fluorescence emission was detected at 520nm on FLUOstar Omega (BMG Labtech). Fluorescence was normalised to the initial fluorescence intensity of untreated control (F/F_0).

2.6. Transmission electron microscopy

Suspensions of platelets and microparticles were centrifuged to pellet platelets at 600g for 10 minutes at room temperature. Microparticle-rich supernatant was absorbed onto glow-discharged carbon film-coated 400 mesh copper grids for 3 minutes, washed twice with distilled water, allowed to dry at room temperature, and negatively-stained with uranyl acetate (3% w/v in dH_2O) for 30 seconds. Imaging was performed using a Tecnai G2 transmission electron microscope at the Cambridge Advanced Imaging Centre (Figure 2.4).

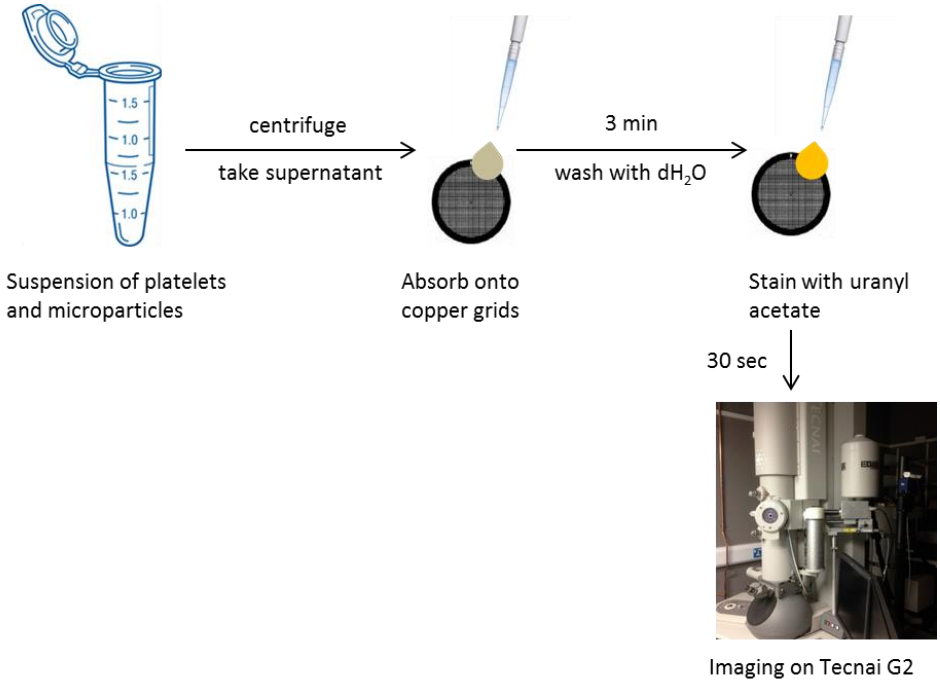

Figure 2.4: Sample preparations for transmission electron microscopy

2.7. Data Analysis

Data were reported as mean +/- standard error of mean (SEM) from at least 5 independent experiments, unless otherwise specified for preliminary experiments. Data were compared by t-test, Mann-Whitney U test, one-way or two-way ANOVA, followed by Tukey's or Dunnett's multiple comparisons test, as appropriate. Concentration-response curves were fitted using a four-parameter logistical equation and compared by extra-sum-of-squares F test, where appropriate, in GraphPad Prism v6.

2.8. Sources of reagents

Chemical, Drug or Solution	Supplier	Code
2-APB	Cayman Chemicals	64970
A23187	Sigma Aldrich	C7522
ABT-199	Selleck Chemicals	S8048
ABT-263	Selleck Chemicals	S1001
ABT-737	Selleck Chemicals	S1002
Acrylamide	Severn Biotech	20-2100-05
ADP	Sigma Aldrich	A2714
Alpha cyclodextrin	Sigma Aldrich	C4642
Amitriptyline	Sigma Aldrich	A8404
Ammonium chloride	Sigma Aldrich	A4514
Amphotericin B	Sigma Aldrich	A9528
APS	Honeywell Fluka	248614
Apyrase, grade VII	Sigma Aldrich	A6535
Aspirin	Sigma Aldrich	A5376
AT101	Selleck Chemicals	S2812
BAM7	Selleck Chemicals	S7105
BAPTA AM	Invitrogen	B1205
BCECF AM	Invitrogen	B3051
Bradford reagent	Sigma Aldrich	B6916
BSA	Sigma Aldrich	A7906
Cal520 AM	AAT Bioquest	21130
Calcium chloride	Sigma Aldrich	21115
Calpeptin	Sigma Aldrich	C8999
Cangrelor	Selleck Chemicals	S3737
Carbenoxolone	Sigma Aldrich	C4790
Choline chloride	Sigma Aldrich	C1879
CID-1067700	Cayman Chemicals	15194
Citric acid	Sigma Aldrich	C1909
CMAC, t-BOC-Leu-Met	Thermo Fisher	A6520
Complement C5b, 6	CompTech	A122
Cyclosporin A	LKT Labs	C9611
D-glucose	Fisher Scientific	G/0500/53
Digitonin	Calbiochem	300410
Diphenhydramine	Sigma Aldrich	D3630
DMBA	Sigma Aldrich	473782
DMEM	Sigma Aldrich	D6406
DMSO	Sigma Aldrich	D2650
DP3A	Sigma Aldrich	43163
DPBA	Sigma Aldrich	358835

Chemical, Drug or Solution	Supplier	Code
DPTHF	Sigma Aldrich	S408271
DTT	Sigma Aldrich	D9779
E64	Sigma Aldrich	E3132
EDTA	Sigma Aldrich	E8008
FCS	Sigma Aldrich	F2442
Filipin	Sigma Aldrich	F9765
Gap27	Tocris	1476
Glycine	Sigma Aldrich	G7126
GSK429286	Tocris	3726
GW4869	Cayman Chemicals	13127
HA14-1	Selleck Chemicals	S1071
HCl	Fisher Scientific	H/1200/PB08
HEPES	Sigma Aldrich	H3375
High Range Protein Ladder	Thermo Fisher	26625
Histone H4	New England Biolabs	M2504S
KCl	Sigma Aldrich	P3911
KH2PO4	Fisher Scientific	P/4800/53
Mdivi-1	Sigma Aldrich	M0199
Methyl beta cyclodextrin	Sigma Aldrich	M7439
$MgCl_2$	Sigma Aldrich	M2670
NaCl	Sigma Aldrich	S7653
NaH_2PO_4	Acros	207802500
NaOH	Alfa Aesar	J63736
NMDG	Acros	126845000
NuPAGE LDS sample buffer (4X)	Thermo Fisher	NP0008
Nystatin	Sigma Aldrich	N6261
OAG	Sigma Aldrich	O6754
^{10}Panx	Tocris	3348
PBA	Sigma Aldrich	78181
PBS tablet	Sigma Aldrich	P4417
Penicillin-Streptomycin	Sigma Aldrich	P4333
Pepstatin A	Sigma Aldrich	P5318
PFA, 4% in PBS	Alfa Aesar	J61899
PGE_1	Santa Cruz	sc-201223
Poly-L-lysine	Sigma Aldrich	P6282
Pre-stained Protein Ladder	Thermo Fisher	26619
Probenecid, water soluble	Thermo Fisher	P36400
Protease Inhibitor Cocktail	Sigma Aldrich	P2714
Quinine hydrochloride	Sigma Aldrich	Q1125

Chemical, Drug or Solution	Supplier	Code
Q-VD-OPh	Sigma Aldrich	SML0063
R5421	EndoTherm	ENG071
Sabutoclax	Selleck Chemicals	S8061
SAR7334	Tocris	5831
SDS	Fisher Scientific	S/5200/53
SFLLRN (TRAP6 amide)	Bachem	H-2936
SN-6	Tocris	2184
Sodium deoxycholate	Sigma Aldrich	D6750
Sodium propionate	Alfa Aesar	A17440
Streptolysin O	Sigma Aldrich	S5265
Western Blot Stripping buffer	Thermo Fisher	46430
SuperSignal Chemiluminescent Substrate	Thermo Fisher	34077
Synta66	Sigma Aldrich	SML1949
TEMED	Sigma Aldrich	T9281
TEA chloride	Sigma Aldrich	T2265
Thrombin	Sigma Aldrich	T7513
TMA chloride	Sigma Aldrich	T19526
Tris base	Sigma Aldrich	T1503
Tris HCl	Sigma Aldrich	T3253
Tri-sodium citrate	Sigma Aldrich	71405
Triton X-100	Sigma Aldrich	T9284
Trypsin	Gibco	25200-056
TW-37	Selleck Chemicals	S1121
Tween-20	Santa Cruz	sc-29113
Y27632	Sigma Aldrich	Y0503
Zymosan A	Sigma Aldrich	Z4250

Table 2.4: Sources of all chemicals, drugs and solutions.

Chapter 3 Detection of platelet-derived microparticles

3.1. Aim of study

About 75% of laboratories apply flow cytometry to detect small vesicles in experimental and clinical samples, but the method varies greatly depending on specific subjects (Lacroix et al., 2010). In this chapter, an assay was developed and optimised for detecting platelet-derived microparticles by flow cytometry.

3.2. Calibration beads

The 1µm standard is set by calibration beads, which requires optimisation due to the nature of flow cytometry. When a laser beam is directed at a particle or an aggregate of particles, it changes direction and scatters. Forward scattered light provides estimation about the size, while side scattered light provides information about the internal structure, i.e. granularity (Kim and Ligler, 2010). Refractive indices (RI) determine the scatter profiles of different cells and particles. Although calibrated at 1µm, polystyrene beads (RI = 1.598) show larger FSC values than silicon dioxide beads (RI = 1.459) in a flow cytometer (Figure 3.1A-B). Silicon dioxide beads are a better option for PMP studies, because the RI is closer to that of blood-borne EVs (RI = 1.398), though it may still be an overestimate (Gardiner et al., 2014). It contradicts the conventional microparticle counting method where the 1µm gate is set by polystyrene beads (Chandler et al., 2011; Nielsen et al., 2014; Kong et al., 2015).

The use of silicon dioxide beads was further justified by real-time acquisition of PMP release. Platelets are larger than 1µm at resting state. Upon addition of the stimulus A23187, platelets appear to shrink and produce smaller vesicles. This “shrinking” may be a reduction in size or a change in refractive index. Some “shrunken” platelets were grouped as <1µm when polystyrene beads were used, and they would be mistaken as PMPs (Figure 3.1C). On the contrary, shrunken platelets were still grouped as >1µm when silicon dioxide beads were used (Figure 3.1D). Consequently, using 1µm polystyrene beads would lead to a false increase in the PMP count, which was expressed as PMP per platelet.

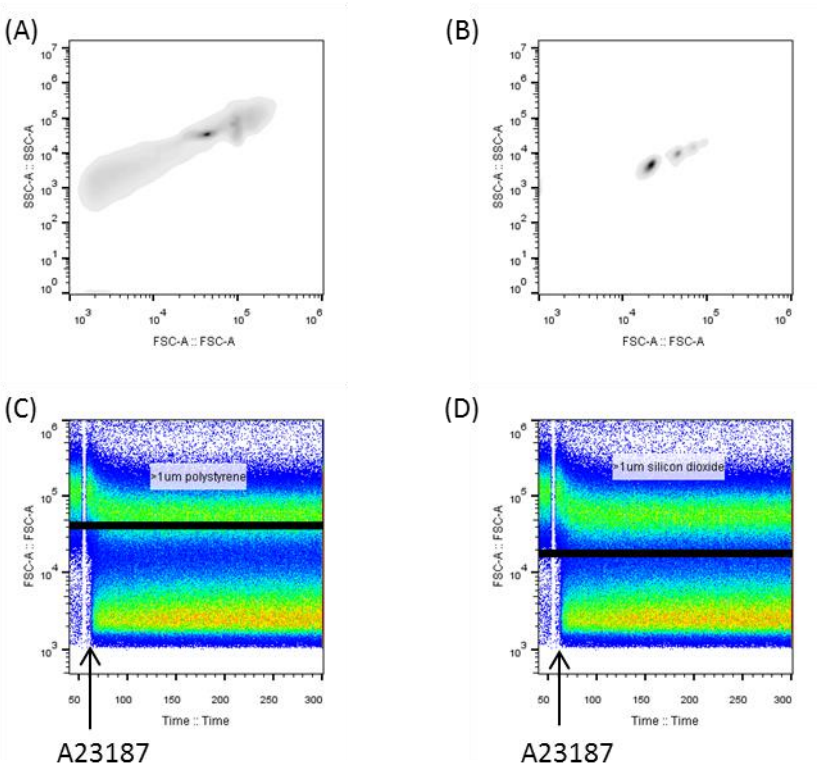

Figure 3.1: Optimisation of calibration beads

(A-B) Flow cytometry density plots of calibration beads with size reflected on forward scatter (FSC). (A) 1µm polystyrene beads (original density 10%; diluted in HBS 100,000 times). (B) 1µm silicon dioxide beads (original density 5%; diluted in HBS 100,000 times). Three spots of high density were seen. The lowest (with FSC-A between 1 x 10^4 and 2 x 10^4) represents single beads, whereas those with higher FSC-A represent more than one bead together. (C-D) Washed platelets (5 x 10^6 per ml) were stimulated with 10µM A23187 as indicated by the black arrows. Events were recorded in real time with size set by 1µm polystyrene beads in (C), and 1µm silicon dioxide beads in (D). These plots are scaled on time vs. FSC-A. These plots are representative of data from 5 different donors.

3.3. Fluorescence triggering

It is common practice in flow cytometry to use a trigger to identify and differentiate events of interest from debris and machine noise. Also known as the discriminator, the trigger is traditionally based on a FSC threshold (Boeck, 2001). However, light scattering is not the only option when a trigger is needed. There are situations where fluorescence might be a more reliable trigger, such as sorting minor sub-populations of cells (McCoy et al., 1991), detecting rare events (Rehse et al., 1995) and studying cell-derived EVs in the plasma (Arraud et al., 2016). Both platelets and PMPs stain positive for anti-human CD41a PE-Cy7, so PE-Cy7 fluorescence on channel FL3 can be used as the trigger to distinguish platelets and PMPs from background.

Size- and fluorescence-based triggers were compared. Platelets samples (unstimulated and A23187-stimulated) were triggered on size (FSC-H > 5,000) or PE-Cy7 fluorescence (FL3-H > 2,000), so events lower than a certain FSC or FL3 value were not detected. When an unstimulated sample was triggered on FL3 threshold, a high proportion of events were in the >1µm area (i.e. platelets) and few were in the <1µm area (i.e. PMPs). In contrast, a large number of events negative for CD41a fluorescence were detected in the <1µm area (i.e. debris or machine noise) when the same unstimulated sample was triggered on FSC threshold. It was similar for A23187-stimulated platelets, as more PMPs could be detected with less debris in the background when the same sample was triggered on FL3 rather than FSC threshold (Figure 3.2). Therefore, triggering on anti-human CD41a PE-Cy7 fluorescence on channel FL3 was a more suitable option for detecting platelets and PMPs.

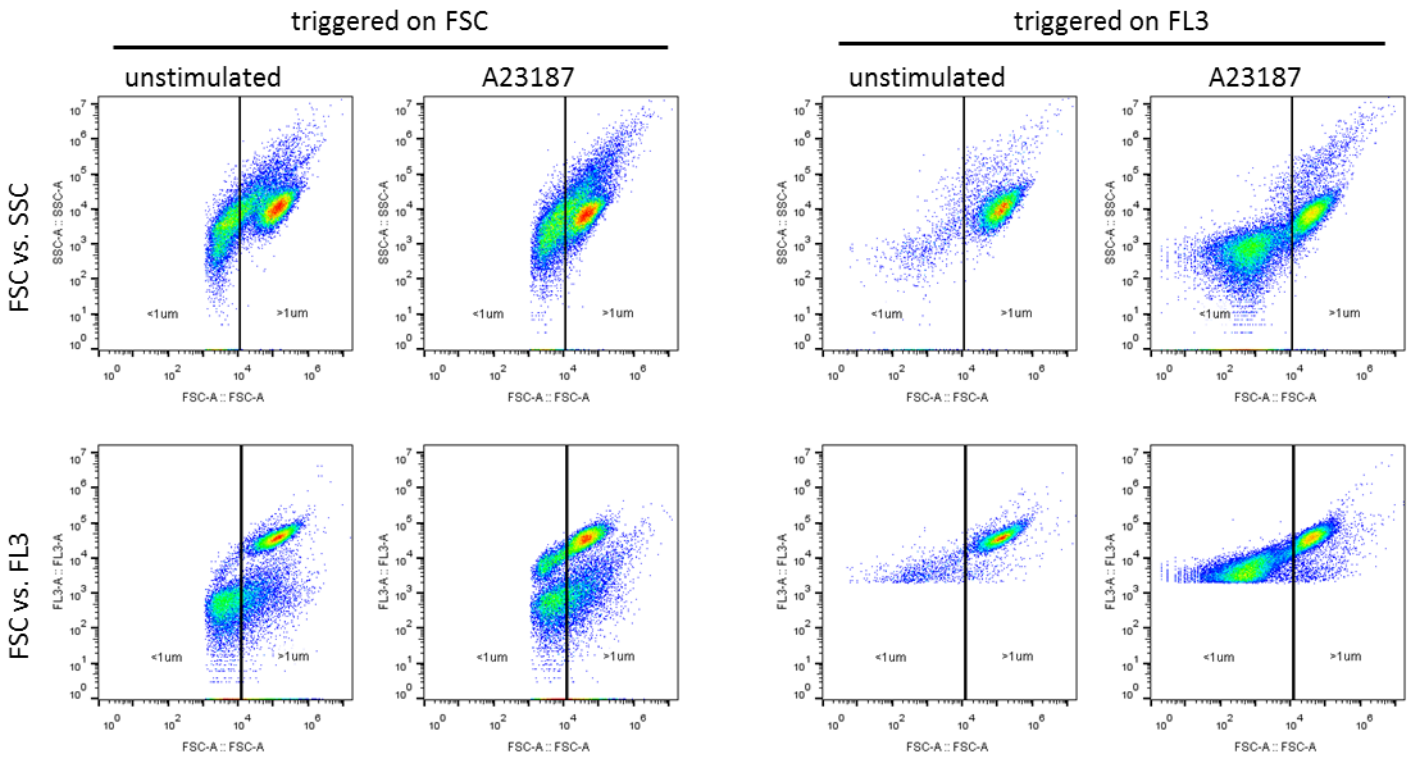

Figure 3.2: Optimisation of fluorescence triggering

Washed platelets (5 x 10^7 per ml) were stimulated with vehicle (DMSO, unstimulated) or 10µM A23187 for 10 minutes, stained with anti-human CD41a PE-Cy7 and fixed with 1% PFA. Event acquisition on flow cytometry was triggered on FSC by size (FSC-H > 5,000) or on FL3 by PE-Cy7 fluorescence (FL3-H > 2,000), as indicated. Results are scaled on FSC-A vs. SSC-A in the upper row and FSC-A vs. FL3-A in the lower row. Density plots are representative of data from 5 different donors.

3.4. Swarm detection

When poly-disperse samples are presented to a flow cytometer, a count can be generated by one large particle or a collection of small particles (i.e. swarm). Swarm detection occurs if the power of light scattered by small particles that are simultaneously present in the laser beam exceeds the detection limit (van der Pol et al., 2012). If every detected event represents one particle, the count determined by flow cytometry would be equal to the real count. A linear relationship can be obtained between the acquired count and the dilution factor on a logarithmic scale. In other words, a 1/2 dilution of the sample would result in a 50% reduction in particle count. However, neither the microparticle count nor the platelet count was halved when a representative sample of activated platelets and PMPs was diluted by half. The count determined by flow cytometer was an underestimation, and it produced a non-linear relationship on logarithmic scale. This slope turned linear and parallel to the theoretical line when the sample was diluted from 1/2 to 1/4 or 1/8 (Figure 3.3). Therefore, under our conditions, platelet samples needed to be diluted at least in half before acquisition on the flow cytometer to prevent swarm detection. In this way, a more accurate count for both platelets and PMPs could be obtained.

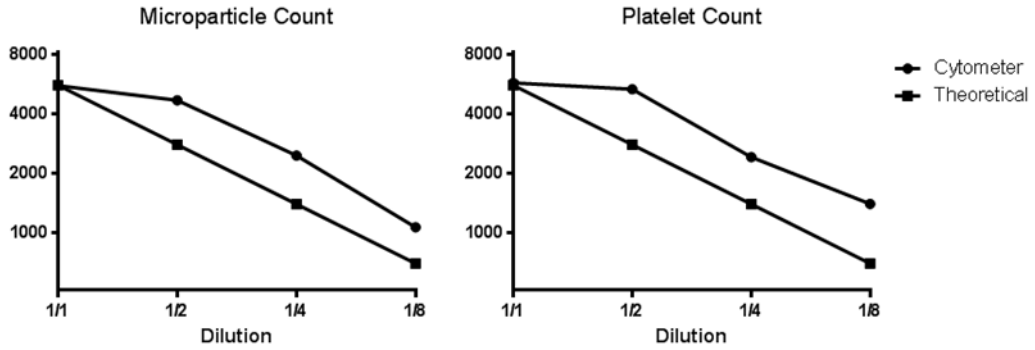

Figure 3.3: Swarm detection

A sample of A23187-stimulated platelets and PMPs was fixed by 1% PFA, diluted from 1/1 to 1/8, and acquired by flow cytometry. Changes in the microparticle count and the platelet count were plotted against the dilution factor, highlighting differences between the theoretical trend and the real trend captured by flow cytometry. Both axes are set on logarithmic scales. Results are representative of data from 5 different donors.

3.5. Optimised method for detecting platelet-derived microparticles

Microparticle release was triggered by stimulating washed platelets with the Ca^{2+} ionophore A23187. Following stimulation and staining, samples of platelets and PMPs were fixed by 1% PFA and diluted by half. Acquisition was triggered on anti-human CD41a PE-Cy7 fluorescence and the 1µm size was defined by FSC values of 1µm silicon dioxide beads. Platelets exposed PS and released PS-positive PMPs in response to increasing concentrations of A23187 (Figure 3.4).

In an unstimulated sample, the majority of events were larger than 1µm and negative for PS exposure. The positive range for Annexin V FITC fluorescence was determined separately for each experiment, so that around 2% of the resting platelets were positive on FL1-A. When platelets were stimulated with a low concentration of A23187 (0.625µM), there was a moderate yet statistically significant increase in the number of events smaller than 1µm and the percentage of platelets positive for Annexin V binding. When scaled on FSC-A vs. FL1-A, unstimulated platelets (>1µm, PS negative) are in the lower right quadrant (LR), activated platelets (>1µm, PS positive) in the upper right quadrant (UR), and PMPs (<1µm, PS positive) in the upper left quadrant (UL). Almost all platelets became activated and exposed PS on the surface when they were stimulated with a high concentration of A23187 (10µM), which was accompanied by a large increase in the number of PMPs released (Figure 3.4).

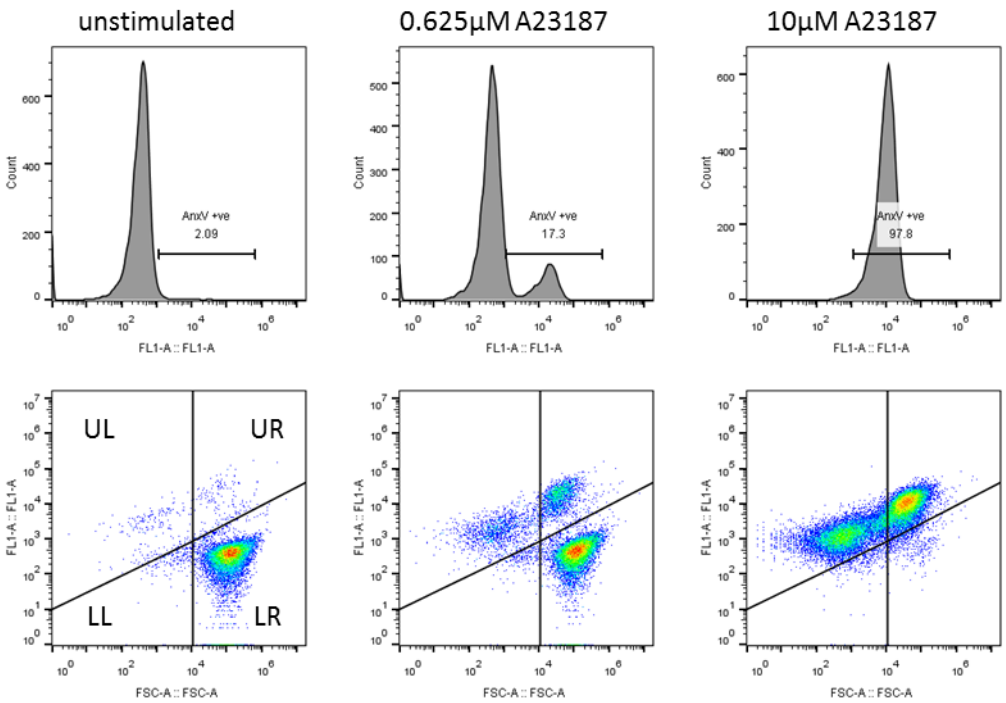

Figure 3.4: Optimised method for detecting platelet-derived microparticles

Washed platelets (5 x 10^7 per ml) were added with 2mM $CaCl_2$ and stimulated with the indicated concentration of A23187 for 10 minutes, after which samples were stained with anti-human CD41a PE-Cy7 and Annexin V FITC to detect PS exposure on channel FL1. PE-Cy7 fluorescence on FL3 was used to trigger acquisition of CD41a positive events. (Upper row) Histograms show the percentage of platelets (CD41a +ve, >1µm) positive for Annexin V binding on FL1-A, where resting platelets were arbitrarily determined as 2% positive for each individual experiment. (Lower row) Density plots show events scaled on FSC-A and FL1-A. The vertical line separating left and right was defined by FSC-A values of 1µm silicon dioxide beads. The line separating top and bottom was defined by Annexin V FITC fluorescence. Unstimulated platelets have high FSC values and low Annexin V binding (lower right quadrant, LR). Stimulation with A23187 triggered PS exposure in platelets (upper right quadrant, UR) and release of Annexin V-positive PMPs (upper left quadrant, UL). These plots are representative of data from 5 different donors.

3.6. Microparticle release can be triggered from platelets by multiple stimuli

Microparticle release can be triggered from human platelets in response to Ca^{2+} ionophore A23187 (Figure 3.4) or thrombin plus collagen-related peptide (CRP). These agonists mimic the pro-coagulant stimulation of platelets *in vivo*, which is associated with a large increase in the intracellular Ca^{2+} concentration and its downstream activation of calpain (Yano et al., 1993). In this experimental system, A23187 triggered PMP release and PS exposure on the surface of platelets in a concentration-dependent manner (Figure 3.5A-B). For PMP release, the maximum response was 0.28 ± 0.04 PMP/PLT (Mean ± SEM; n = 5) and EC_{50} was 1.20μM. For PS exposure, the maximum response was almost 100% and EC_{50} was 1.54μM.

Apart from pro-coagulant stimuli, the bacterial toxin streptolysin O (SL-O) triggers PMP release. SL-O is a subtype of streptolysin, which is a haemolytic exotoxin derived from *Streptococcus*. In its active reduced form, SL-O permeabilises platelets, allows influx of Ca^{2+} into the cytosol, and activates Ca^{2+}- and calpain-dependent responses such as the release of α-granules (Flaumenhaft et al., 1999; Rozenvayn and Flaumenhaft, 2001). Similar to A23187, SL-O triggered PMP release and PS exposure in a concentration-dependent manner in the presence of extracellular Ca^{2+} (Figure 3.5A-B). For PMP release, the maximum response was 0.16 ± 0.01 PMP/PLT (Mean ± SEM; n = 5), which was slightly lower than the maximum capacity of A23187. The EC_{50} was 89.4U/ml. For PS exposure, the maximum response was almost 100%, with its EC_{50} at 89.4U/ml.

In addition to thrombin, collagen and bacterial toxins, platelets might encounter histones in the blood circulation. Normally bound to DNA molecules in the nucleus, histones are released from necrotic cells and activated immune cells during infection such as neutrophils (Beaulieu and Freedman, 2011). Histone H4 has been found to directly activate platelets leading to thrombosis (Fuchs et al., 2011), or indirectly increase pro-coagulant activities by interacting with platelet-derived polyphosphates (Semeraro et al., 2011). When platelets were treated with histone H4, there was a concentration-dependent increase in PS exposure on the surface, which confirmed the direct activating effect histone H4 had on platelets. The

maximum response was almost 100% and the EC_{50} was 15.9µg/ml (Figure 3.5B). On the other hand, histone H4 triggered the release of a huge number of EVs that were positive for CD41a, without reducing the platelet count (Figure 3.5C). On average, each platelet released 5.27 ± 0.39 EVs in response to 40µg/ml Histone H4, and only 1.20 ± 0.26 of these EVs were positive for Annexin V (Figure 3.5A; Mean ± SEM; n = 5). It suggested that a majority of the EVs released from PS-positive platelets did not expose PS, so they were not classified as PMPs. The identity of these Annexin V-negative EVs remains unclear.

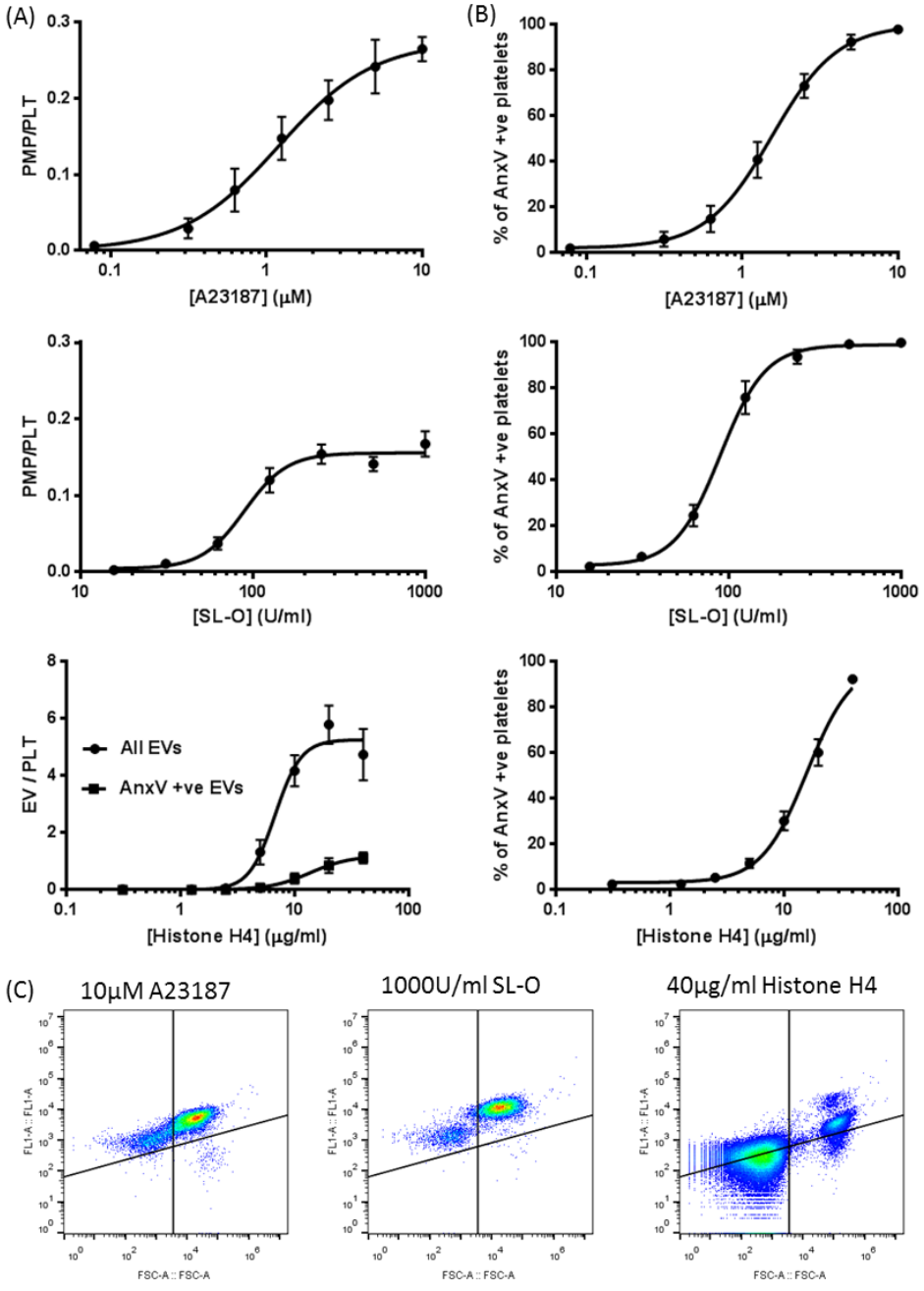

Figure 3.5: Microparticle release can be triggered from platelets by multiple stimuli

Washed platelets (5 x 10^7 per ml) were added with 2mM $CaCl_2$ and stimulated with A23187 (up to 10µM), SL-O (up to 1000U/ml), or histone H4 (up to 40µg/ml) for 10 minutes, after which samples were stained with anti-human CD41a PE-Cy7 and Annexin V FITC. Prior to stimulation, concentrated SL-O stock at 10kU/ml was reduced by 5mM DTT. (A) Microparticle release in response to A23187, SL-O or histone H4 was measured as described in Figure 3.4 (Mean ± SEM; n = 5). (B) PS exposure in response to A23187, SL-O or histone H4 was measured as described in Figure 3.4 (Mean ± SEM; n = 5). (C) Density plots of platelets stimulated with 10µM A23187, 1000U/ml SL-O and 40µg/ml histone H4. Quadrants are defined as in Figure 3.4, with Annexin V FITC fluorescence on FL1-A. These plots are representative of data from 5 different donors.

3.7. Various stimuli triggering microparticle release from platelets have differential effects on plasma membrane integrity

Ca^{2+} ionophore A23187, bacterial toxin SL-O and histone H4 were tested for their effects on platelet viability. Calcein was used to detect cell viability by measuring integrity of the plasma membrane. In its acetoxymethyl (AM) ester form, non-fluorescent calcein AM readily penetrates the plasma membrane due to its hydrophobic nature. After hydrolysis of AM by intracellular esterases, calcein cannot penetrate the plasma membrane, so it is retained in the cytoplasm in its green fluorescent form, which can be detected on channel FL1 of flow cytometry. Loss of calcein fluorescence from the platelet population indicates leakage of calcein via the plasma membrane into the surroundings, and thus loss of plasma membrane integrity.

After loading calcein into PRP for 10 minutes, excess calcein in the plasma was removed by discarding the supernatant after the second centrifugation spin during platelet isolation (Figure 2.1). Washed platelets loaded with calcein were stimulated with A23187, SL-O or histone H4 in the presence of Ca^{2+} at their respective concentrations that triggered maximal PMP release and PS exposure. Compared to unstimulated control (0.62 ± 0.06%; Mean ± SEM; n = 5), neither 10µM A23187 (1.29 ± 0.43%; Mean ± SEM; n = 5) nor 40µg/ml histone H4 (1.96 ± 0.35%; Mean ± SEM; n = 5) significantly increased the percentage of platelets negative for calcein fluorescence (Figure 3.6A-B), so A23187 and histone H4 did not affect platelet viability. By contrast, SL-O at 1000U/ml almost completely permeabilised the entire platelet population (94.2 ± 1.01%; Mean ± SEM; n = 5; Figure 3.6A-B). EC_{50} of this concentration-dependent effect was 268U/ml (Figure 3.6C).

Based on the results, A23187 was the most suitable stimulus for PMP release for two reasons. Firstly, most of the EVs released in response to A23187 exposed PS, as they were positive for Annexin V binding. Secondly, treatment with A23187 did not affect platelet viability, since membrane integrity was not compromised.

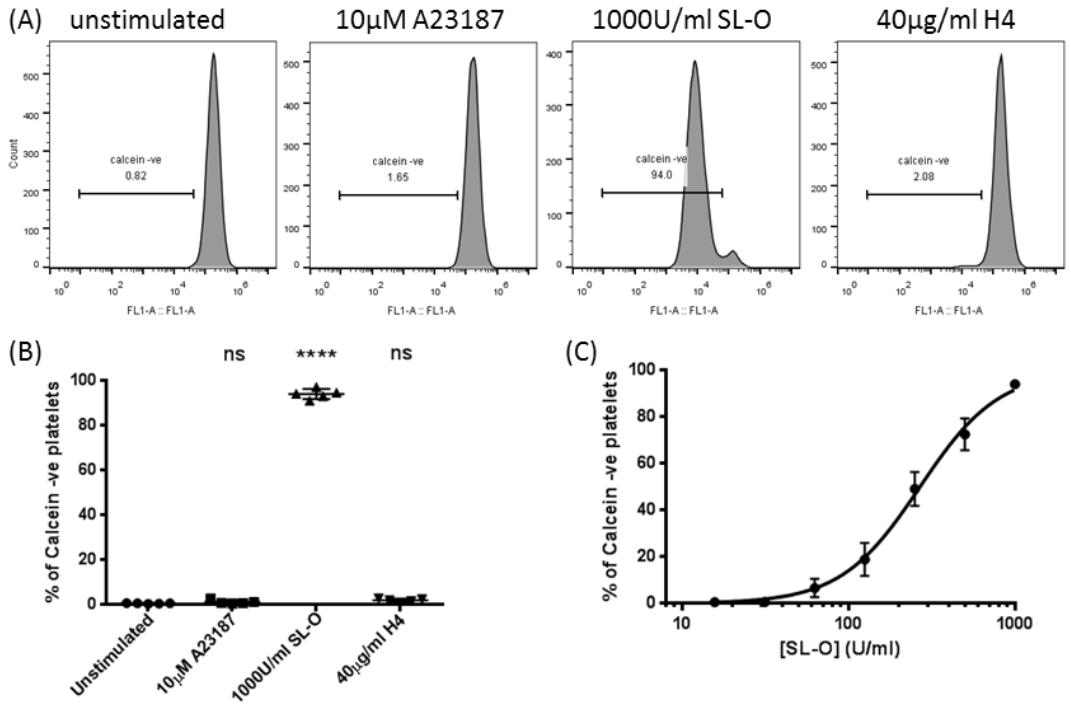

Figure 3.6: Various stimuli triggering microparticle release from platelets have differential effects on plasma membrane integrity

PRP was loaded with 1µM calcein for 10 minutes. Calcein-loaded washed platelets (5 x 10^7 per ml) were treated as indicated and stained with anti-human CD41a PE-Cy7, fluorescence of which was used to trigger acquisition of CD41a positive events. All samples were acquired live on flow cytometry. (A) Histograms show the percentage of platelets (CD41a +ve, >1µm) negative for calcein on FL1-A. (B) Percentage of platelets negative for calcein following stimulation with 10µM A23187, 1000U/ml SL-O, or 40µg/ml histone H4 for 10 minutes (Mean ± SEM; n = 5; **** $p < 0.0001$, ns: not significant, compared to unstimulated control). (C) Percentage of platelets negative for calcein following stimulation with SL-O (up to 1000U/ml) for 10 minutes (Mean ± SEM; n = 5).

3.8. Influx of sodium ions is not required for A23187-triggered microparticle release

The optimised PMP detection and counting method was used to test whether influx of Na^+ was involved in PMP release. When microparticles are released from platelets, outward blebbing of the plasma membrane requires calpain-dependent cleavage of the cytoskeleton (Yano et al., 1993). It was hypothesised that Na^+ entry into platelets, possibly coupled to Cl^- influx and then water entry, might provide the hydrostatic pressure, which could be mediated by an elevation in intracellular Ca^{2+} level. A23187 was used to cause this elevation without compromising membrane integrity.

To study if Na^+ influx is involved in PMP release, Na^+ was replaced with alternative monovalent cations. The substitute ion needed to be significantly larger than Na^+, so that it could not permeate most of the known Na^+ channels on the plasma membrane. Several types of organic cations have been used to replace Na^+ or K^+ in platelet studies. These include N-methyl D-glucamine (NMDG) (Kimura et al., 1993; Harper et al., 2010), choline (Lingjaerde, 1969) and tetra-methyl ammonium (TMA) (Kashiwagi et al., 1997).

The normal reference range of plasma Na^+ concentration in human blood is between 135mM and 145mM (Hoorn and Zietse, 2017). In this experimental system, 135mM extracellular Na^+ was present in HEPES-buffered saline (HBS) in the form of NaCl. To replace NaCl, the alternative saline contained 135mM choline chloride, TMA chloride or NMDG chloride. As NMDG chloride was not commercially available, NMDG-based HBS was titrated with 135mM HCl to compensate for Cl^-. In addition, phosphorous is present in the blood at a low concentration in the form of inorganic phosphates (Bansal, 1990). Phosphate was present in HBS as NaH_2PO_4. It was replaced by equimolar KH_2PO_4 in NMDG-, choline-, or TMA-based HBS (Table 3.1).

Different forms of HBS were used throughout the experiment to ensure depletion of extracellular Na^+. Reagents were reconstituted or diluted in specific forms of HBS for each monovalent cation, including $CaCl_2$, A23187, the Annexin V FITC plus anti-human CD41a PE-Cy7 staining buffer, and PFA. The only exceptions were the anti-coagulant reagents

sodium citrate and ACD (Figure 2.1). Na^+ present in whole blood was later removed by two centrifugation steps during isolation and preparation of washed platelets. Dilution of PRP and re-suspension of the platelet pellet were both conducted in Na^+-free HBS.

Platelets prepared and incubated in Na^+-free HBS were stimulated with A23187 for 10 minutes. PMP release, along with PS exposure, was almost completely abolished when Na^+ was replaced by equimolar NMDG. However, there was no significant inhibition or enhancement for PMP release or PS exposure in platelets incubated in choline- or TMA-based HBS compared to the conventional Na^+-based HBS (Figure 3.7A). Since substitution of Na^+ by choline or TMA did not affect PMP release, it is most likely that membrane blebbing for PMP release does not require locally increased hydrostatic pressure driven by influx of Na^+ and Cl^-.

NMDG-dependent inhibition of PMP release could be attributed to lower levels of PS exposure in the released EVs, rather than direct inhibition of EV release. When platelets in NMDG- or choline-based HBS were stimulated with the same concentration of A23187 (10μM), the number of EVs released, regardless of Annexin V staining, was similar. However, Annexin V binding was much lower for both A23187-stimulated platelets and platelet-derived EVs when platelets were incubated in NMDG-based HBS compared to those incubated in choline-based HBS (Figure 3.7A).

It was not clear why Annexin V binding was low in NMDG-based HBS. $CaCl_2$ was added to platelets prior to activation, which was confirmed by the release of EVs upon A23187 stimulation (Figure 3.7B). Na^+ was not indispensable to Annexin V binding, as it was not affected in choline- or TMA-based HBS (Figure 3.7A). In addition, Annexin V binding to heat-killed platelets was not affected in NMDG-based HBS. After platelets were killed by two cycles of 5 minutes' heating at 95^{o}C, membrane fluidity was increased, so Annexin V molecules could bind to PS distributed at the inner membrane leaflet of heat-killed platelets incubated in NMDG-based HBS (Figure 3.7C). However, Annexin V did not bind to surfaces of stimulated platelets or platelet-derived EVs that supposedly exposed PS.

(A)

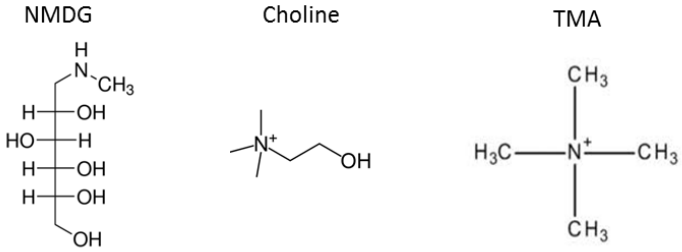

(B)

Buffer	HEPES	KCl	$MgCl_2$	NaH_2PO_4	KH_2PO_4	NaCl	NMDG	Choline Cl	TMA Cl
Sodium HBS	10mM	3mM	1mM	0.34mM	0	135mM	0	0	0
NMDG HBS	10mM	3mM	1mM	0	0.34mM	0	135mM	0	0
Choline HBS	10mM	3mM	1mM	0	0.34mM	0	0	135mM	0
TMA HBS	10mM	3mM	1mM	0	0.34mM	0	0	0	135mM

Table 3.1: Na^+ replacement. (A) Chemical Structures of NMDG, choline and TMA. (B) Recipe for different types of HBS. For every litre of NMDG-based HBS, 11.12 ml of HCl (37.5%) was added to compensate for Cl^-. To reach final pH of 7.40, NaOH was used to titrate for Na^+-based HBS, while KOH was used for Na^+-free HBS.

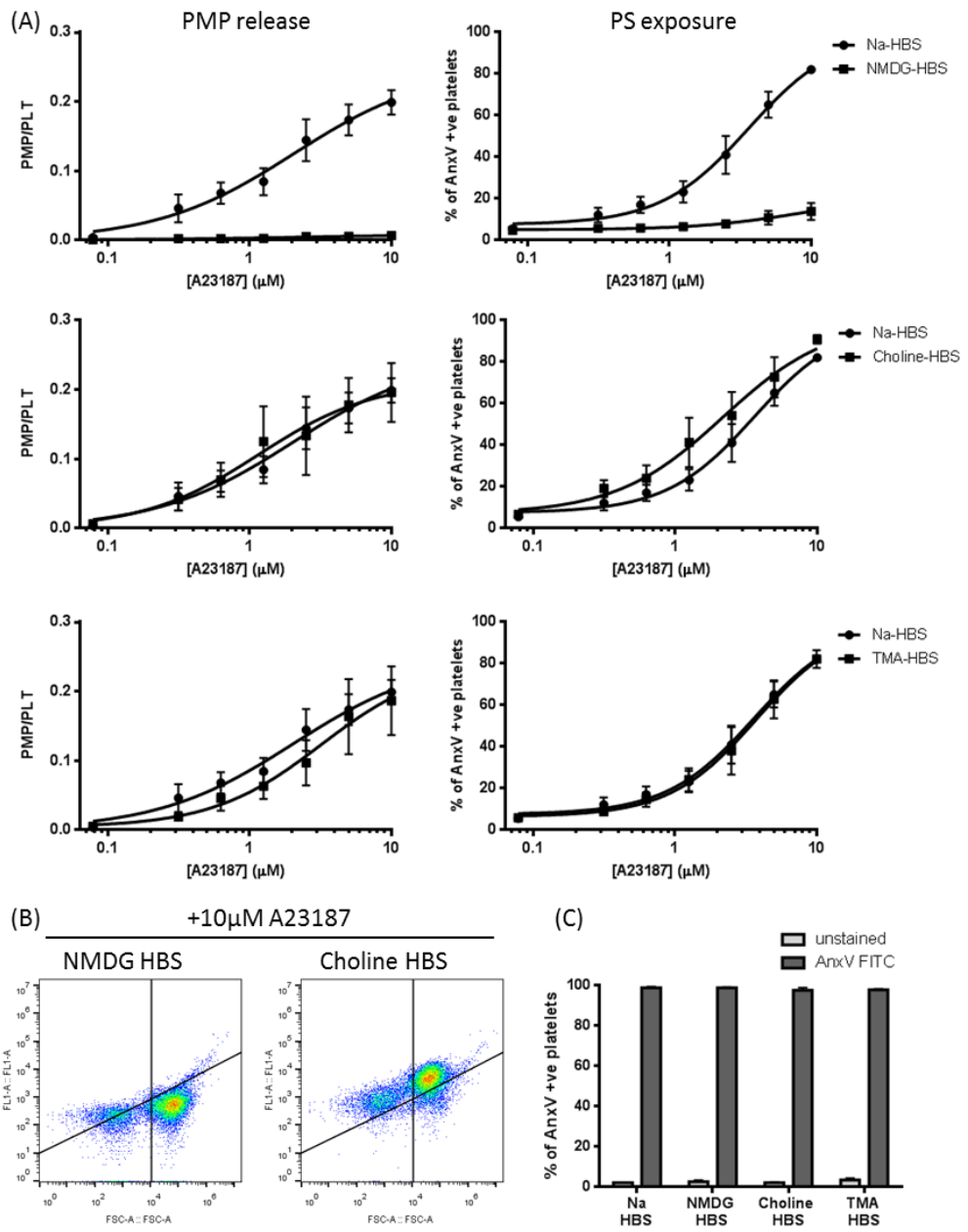

Figure 3.7: Influx of sodium ions is not required for A23187-triggered microparticle release

Washed platelets (5 x 10^7 per ml) were incubated in different types of HBS as indicated. (A) A23187-triggered PMP release and PS exposure were measured as described in Figure 3.4 (Mean ± SEM; n = 5). (B) Platelets incubated in NMDG- or choline-HBS were stimulated with 10μM A23187. Density plots are defined as in Figure 3.4, with Annexin V FITC fluorescence on FL1-A. These plots are representative of data from 5 different donors. (C) Platelets incubated in different types of HBS were heat-killed and stained with Annexin V FITC. Percentage of platelets positive for Annexin V binding was measured (Mean ± SEM; n = 3).

3.9. Discussion

In this chapter, an optimised assay for detecting PMPs was established. Samples were stained with fluorescently-conjugated Annexin V to detect PS exposure and anti-human CD41a PE-Cy7 to detect platelet-derived events. The 1µm gate was set by silicon dioxide calibration beads. To differentiate events of interest from debris and machine noise, events were triggered on PE-Cy7 fluorescence of anti-human CD41a. Samples were diluted by half in HBS before analysis using a flow cytometer, so that swarm detection could be prevented. PMPs were defined as events that were smaller than 1µm and Annexin V-positive.

It needs to be acknowledged that the number of events seen by this approach is likely to be an underestimate of the total number of PMPs. Microparticles are a heterogeneous population of EVs with their diameters ranging from 100nm to 1µm (Raposo and Stoorvogel, 2013). Flow cytometry can struggle to resolve the smaller EVs as it cannot detect particles with diameters lower than 488nm, which is the wavelength of the blue laser used to define FSC (Robert et al., 2009; van der Pol and Harrison, 2017). The model of flow cytometer used for experiments in this thesis was BD Accuri C6, which has been shown by other groups to have a limited resolution capacity (Cointe et al., 2017). Only the largest EVs were predominantly acquired. On the other hand, flow cytometry cannot detect exosomes formed by endocytosis into secretory granules and released by subsequent exocytosis, which are believed to be smaller than 100nm (van der Pol et al., 2016). All following experiments in Chapters 4 to 6 focused only on microparticle release from platelets and it does not involve any mechanistic details about exosome release.

PMP release can be triggered *in vitro* by a few different types of stimuli. Compared to SL-O or histone H4, A23187 was a more suitable choice in this experimental system. The population of EVs released from platelets in response to histone H4 was not homogeneous in terms of Annexin V binding (and thus PS exposure), so it was not definitive whether these EVs could be classified as PMPs. On the other hand, EVs released in response to SL-O were Annexin V-positive, with flow cytometry profiles identical to PMPs released in response to A23187. However, SL-O was not relevant to physiological pro-coagulant stimulation as it compromised

cell viability and caused leakage of calcein. This result is consistent with a previous report where SL-O was used to introduce antibodies into the platelet cytosol (Flaumenhaft, 2004).

As an example, the optimised PMP detection method was used to test whether ion influx mediates membrane blebbing for PMP release. Extracellular Na^+ was replaced by equimolar NMDG, choline or TMA. A23187 was used to rapidly trigger an elevation in intracellular Ca^{2+} concentration and its downstream calpain activity without compromising plasma membrane integrity. The physiological agonist, thrombin plus CRP, would not be suitable for this experiment because the catalytic activity of thrombin is dependent on Na^+ (Huntington, 2008). Substitution of Na^+ by organic monovalent cations did not significantly affect PMP release or PS exposure in response to A23187. These results ruled out the involvement of Na^+ influx-mediated membrane blebbing in the process of PMP release.

Chapter 4 Lipid rafts

4.1. Aim of study

Cholesterol-rich lipid rafts provide a platform for coordinating signalling events in platelets and other cells (Sezgin et al., 2017). Lipid rafts are involved in the release of PS-exposing extracellular vesicles from other cardiovascular cells including monocytes (Del Conde et al., 2005), endothelial cells (Burger et al., 2011) and erythrocytes (Salzer et al., 2002, 2008). In this chapter, it was investigated whether lipid rafts are required in PMP release.

4.2. Methyl-β-cyclodextrin depletes cholesterol from the platelet surface

To test whether lipid rafts are required for microparticle release, lipid rafts were disrupted by treating platelets with methyl-β-cyclodextrin (MβCD) which depletes cholesterol from the plasma membrane. Following treatment with MβCD, platelets were stained with a fluorescent dye filipin that binds to cholesterol with high affinity (Schnitzer et al., 1994; Maekawa and Fairn, 2014), before images were taken by confocal microscopy.

The intensity of filipin fluorescence has been used to measure the cholesterol content on cell surfaces (Kenworthy et al., 2004; Goodwin et al., 2005). Results generated by this semi-quantitative approach were comparable to those obtained by gas chromatography (Qin et al., 2006; Borisova et al., 2011). Filipin was only added after cells were fixed by PFA to prevent any potential damage to lipid rafts (Herbert et al., 2015; Son et al., 2015), as filipin itself might modify the cholesterol content of cell membranes (Ferraro et al., 2004). The concentration of filipin was optimised and set at 50µg/ml, which has been used on other cell lines (Halliday et al., 2005; Liu et al., 2014).

In previous studies, MβCD has been added to either washed platelet suspensions (Maurice et al., 2006; Manne et al., 2015) or platelet-rich plasma (PRP) to deplete cholesterol prior to isolation of washed platelets (Quinton et al., 2005; Quinter et al., 2007). Effects of these two strategies have not been directly compared, so a preliminary study was conducted where MβCD (10mM and 25mM) was added separately to PRP or washed platelets. Images were obtained under identical conditions, and platelets treated with MβCD showed lower levels of fluorescence intensity compared to control. When MβCD was added into PRP, filipin fluorescence of platelets was reduced to 41.0 ± 6.7% of matched controls by 10mM MβCD and 20.0 ± 2.7% of matched controls by 25mM MβCD (Figure 4.1; Mean ± SEM; n = 3). When MβCD was added into washed platelets, fluorescence of filipin was reduced to 45.8 ± 7.1% of matched controls by 10mM MβCD and 21.2 ± 3.3% of matched controls by 25mM MβCD (Figure 4.1; Mean ± SEM; n = 3). Therefore, there was no additional benefit of adding MβCD into PRP rather than washed platelets in terms of cholesterol depletion.

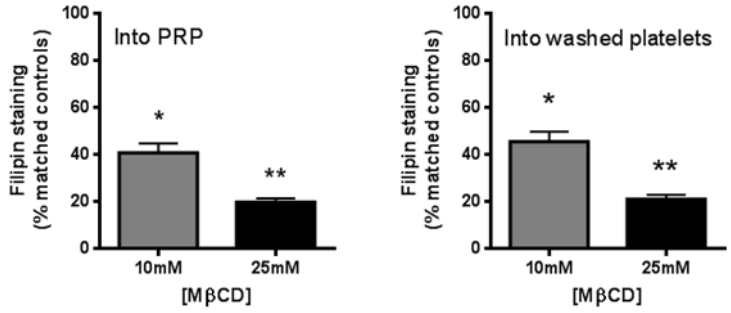

Figure 4.1: Preliminary study for treating platelets with MβCD

MβCD was added into PRP or washed platelets as indicated. Platelets (5 x 10^7 per ml) were treated with MβCD (10mM or 25mM) or vehicle (HBS) as control for 30 minutes, fixed with PFA (1%), and stained with filipin (50µg/ml). Filipin fluorescence was determined by confocal microscopy, objective 63x oil, excitation at 405nm, and emission from 411 to 505nm. Adding MβCD into PRP or washed platelets achieved similar effects in terms of reducing filipin fluorescence of platelets (Mean ± SEM; n = 3; * $p < 0.05$; ** $p < 0.01$, compared to matched vehicle controls).

A further experiment was performed by adding MβCD to washed platelets and α-cyclodextrin (αCD) was included as an additional control. While MβCD binds to and sequesters cholesterol in its hydrophobic core (Christian et al., 1997), the cavity of αCD is too small to accommodate a cholesterol molecule yet it retains many other properties of MβCD (Ohtani et al., 1989). Filipin fluorescence of platelets decreased following MβCD treatment in a concentration-dependent manner, to 51.4 ± 8.0% of matched controls by 10mM MβCD and to 30.2 ± 4.5% of matched controls by 25mM MβCD (Figure 4.2A; Mean ± SEM; n = 5). In contrast, αCD did not remove cholesterol from the platelet surface, as filipin fluorescence was at 96.5 ± 5.1% of matched controls (Figure 4.2A; Mean ± SEM; n = 5). This suggested that MβCD was both effective and specific in depleting cholesterol from the platelet membrane. By comparing fluorescence images to their differential interference contrast (DIC) counterparts, it was confirmed that filipin specifically adhered to the surface of platelets (Figure 4.2B).

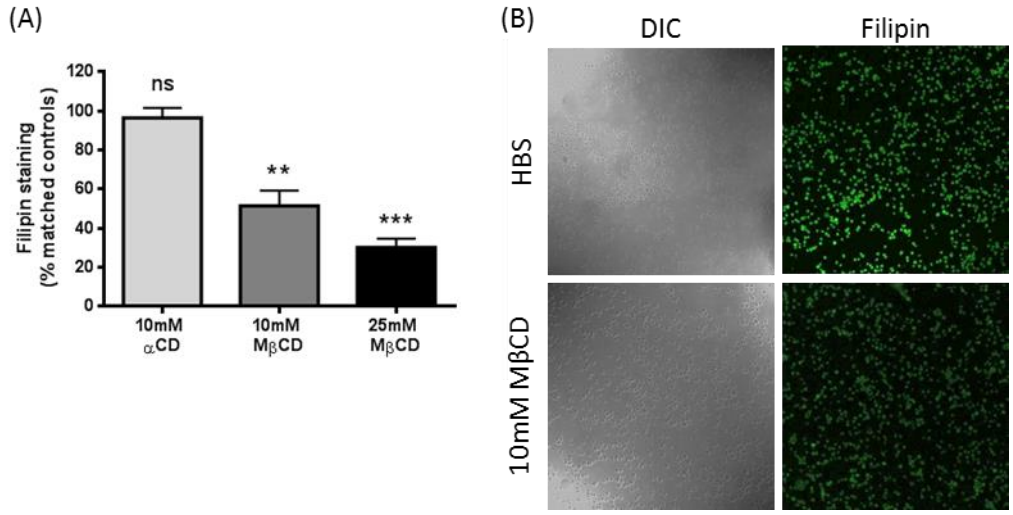

Figure 4.2: MβCD depletes cholesterol from the platelet surface

(A) MβCD (10mM or 25mM), αCD (10mM) or vehicle (HBS) was added into washed platelets suspension (5 x 10^7 per ml) for 30 minutes. MβCD-treated platelets were fixed with PFA (1%) and stained with filipin (50μg/ml). Fluorescence was determined by confocal microscopy as described in Figure 4.1 (Mean ± SEM; n = 5; ** $p < 0.01$; *** $p < 0.001$; ns, not significant, compared to matched vehicle controls). (B) Representative DIC and fluorescence images of filipin-stained platelets were taken under identical conditions.

4.3. Cholesterol depletion prevents microparticle release from platelets

Platelets were stimulated with various concentrations of A23187 and dose-response curves were plotted for PMP release and PS exposure. When platelets treated with MβCD (10mM or 25mM) were stimulated with A23187, few PS-exposing PMPs were detected (Figure 4.3A). On the contrary, PS exposure in these platelets (>1µm, CD41a +ve) was not inhibited (Figure 4.3B), which suggested that platelet activation and exposure of negatively-charged phospholipids were not affected. Consistent with this, there was no increase in Annexin V-negative vesicles (<1µm, CD41a +ve) in MβCD-treated platelet samples following A23187 stimulation (Figure 4.3D). It indicated that the lack of PS-exposing PMPs in these samples resulted directly from inhibition of vesicle release, rather than inhibition of PS exposure (hence not detected as Annexin V-positive events). Meanwhile, αCD (10mM) had no effect on PMP release or PS exposure (Figure 4.3A-B). Since αCD can be used as control for any effect of MβCD independent of cholesterol (Zidovetzki and Levitan, 2007), inhibition of PMP release caused by MβCD could be attributed to cholesterol depletion from the platelet membrane. The inhibitory effect of MβCD for PMP release was concentration-dependent (Figure 4.3C).

Flow cytometry can only detect the largest microparticles (between 488nm and 1µm), so a more sensitive method for detecting particles was required to confirm the flow cytometry data. In transmission electron microscopy (TEM), an image is formed when a beam of electrons is transmitted through a thin specimen and then focused to create an image on a screen or a film (Momen-Heravi et al., 2012). It offers a spatial resolution three orders of magnitude shorter than the wavelength of visible light, at around 0.5nm (Pisitkun et al., 2004). Moreover, TEM has been widely used to characterise EVs (Baran et al., 2010; Miranda et al., 2010), including microparticles released from human platelets stimulated by thrombin, CRP or A23187 (Aatonen et al., 2014).

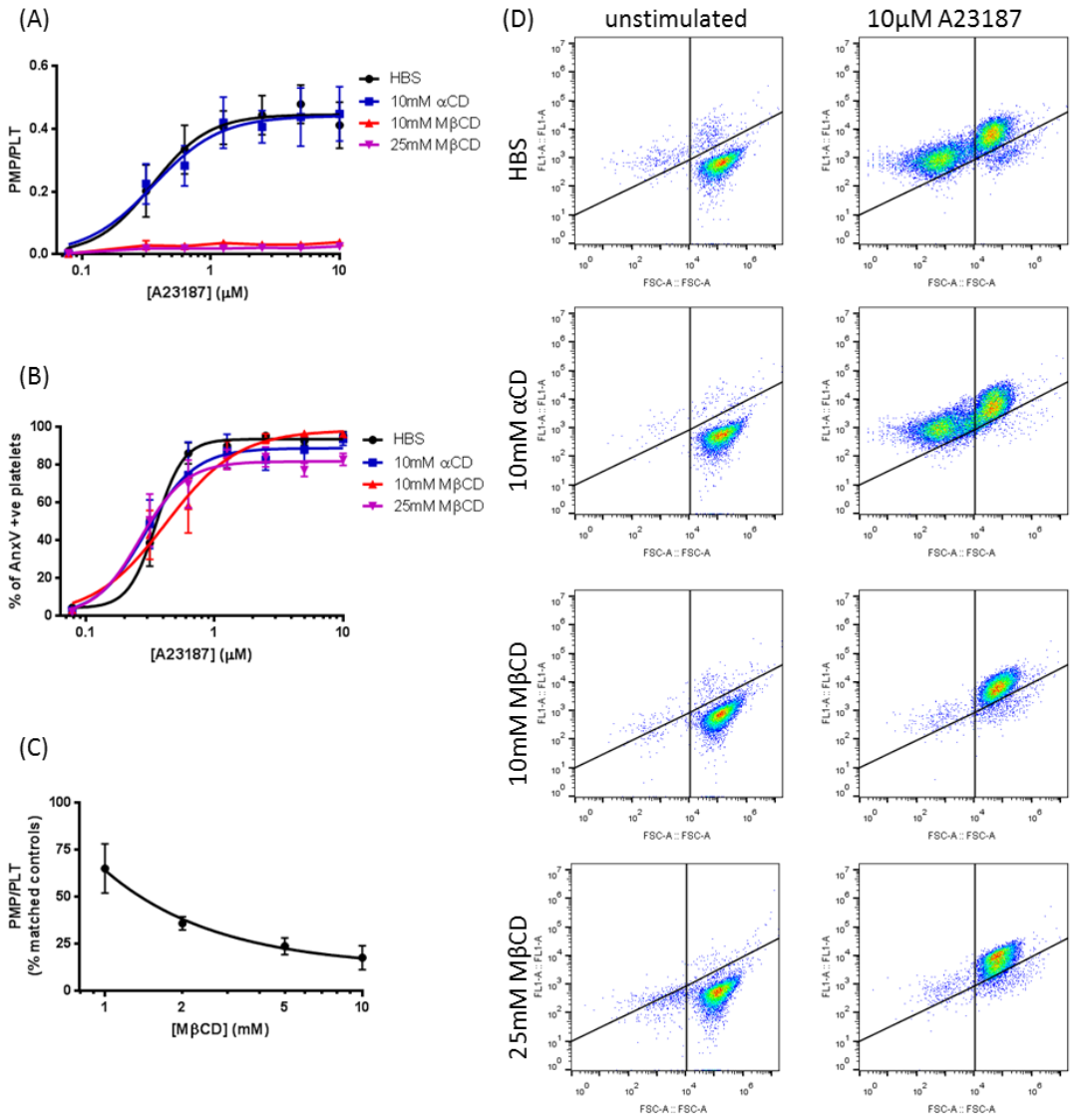

Figure 4.3: Cholesterol depletion prevents microparticle release from platelets

Washed platelets (5 x 10^7 per ml) were treated with MβCD (10mM or 25mM), αCD (10mM) or vehicle (HBS) as control for 30 minutes, prior to stimulation with A23187 for 10 minutes. (A) PMP release was measured as described in Figure 3.4 (Mean ± SEM; n = 5). (B) PS exposure was measured as described in Figure 3.4 (Mean ± SEM; n = 5). (C) Washed platelets (5 x 10^7 per ml) were treated with indicated concentrations of MβCD (1 to 10mM) or vehicle (HBS) for 30 minutes, prior to stimulation with 10μM A23187 for 10 minutes. PMP release was measured and normalised to matched vehicle controls (Mean ± SEM; n = 5). (D) Density plots of platelets treated as indicated. Quadrants are defined as in Figure 3.4, with Annexin V FITC fluorescence on FL1-A. These plots are representative of data from 5 different donors.

PMPs were isolated by centrifugation, absorbed onto glow-discharged copper grids, negatively-stained with uranyl acetate, and visualised by TEM. Small vesicles could be detected in large numbers in the supernatant of platelets stimulated with 10µM A23187 (Figure 4.4). Consistent with flow cytometry data, few particles were observed in the supernatant of unstimulated platelets or 10mM MβCD-treated platelets stimulated with A23187 (Figure 4.4). Although of different sizes, the majority of these vesicles were smaller than 500nm in diameter, which is below the detection limit of light-based experimental approaches. It further suggested that the number of events counted by flow cytometry was an underestimate of the total number of microparticles.

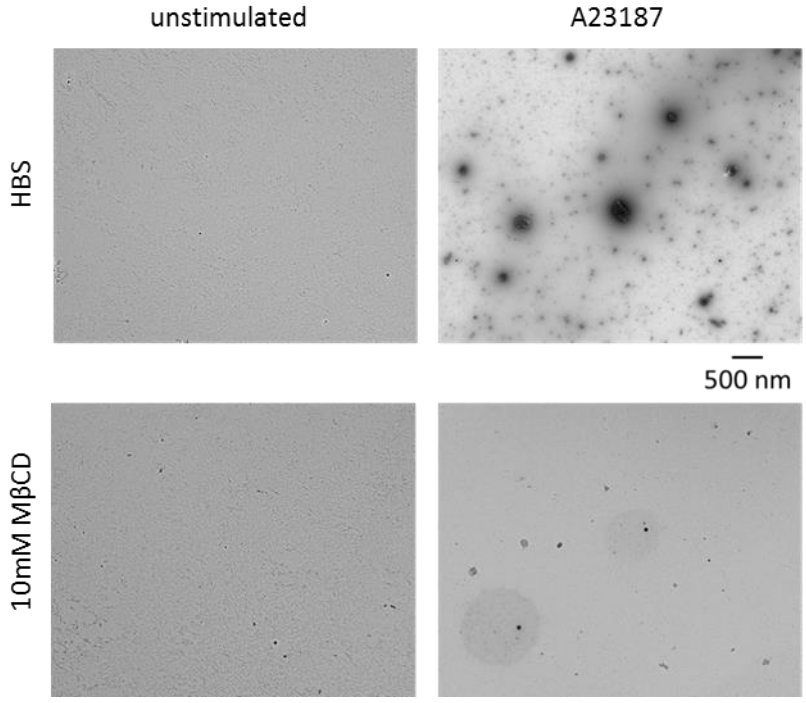

Figure 4.4: Transmission electron microscopy images

TEM images confirm that cholesterol depletion prevents microparticle release from platelets. Washed platelets (5 x 10^7 per ml) were treated with 10mM MβCD or vehicle (HBS) for 30 minutes, stimulated with 10µM A23187 for 10 minutes, and centrifuged at 600g for 10 minutes to pellet platelets. The supernatant was collected and processed for microscopy. These images are representative of results from 4 different donors.

It was not clear whether platelet viability was maintained after cholesterol depletion. If platelets were killed, MβCD could have been configured as an unspecific inhibitor that led to production of fewer PMPs. The effect of MβCD treatment on plasma membrane integrity was assessed using a fluorescent fixable viability dye (FVD) eFluor 660. With a molecular weight of 1.6kDa, FVD cannot permeate intact plasma membranes. Only cells with compromised membrane integrity would be labelled positive for FVD fluorescence. FVD was chosen over calcein in this experiment, because FVD is retained by cells even after fixation with PFA, making the experimental design more convenient.

Heat-killed platelets were used as positive control, while platelets in the resting state were used as negative control. After platelets had been killed by two cycles of 5 minutes of heating, membrane fluidity was increased. As they were permeable to FVD, heat-killed platelets showed strong FVD fluorescence. Heat-killed platelets were also positive for Annexin V FITC binding because Annexin V molecules could reach the cytoplasm and access PS distributed at the inner membrane leaflet. By contrast, resting platelets were negative for both FVD and Annexin V binding (Figure 4.5).

Neither MβCD treatment, nor A23187 stimulation for 10 minutes, led to an increase in FVD fluorescence in platelets. The efficacy of A23187 in this experiment was validated as all stimulated platelets exposed PS (Figure 4.5). This suggested that cholesterol depletion by MβCD did not cause platelet death or reduced stimulation. Therefore, lipid raft disruption does not prevent PMP release by reducing platelet viability.

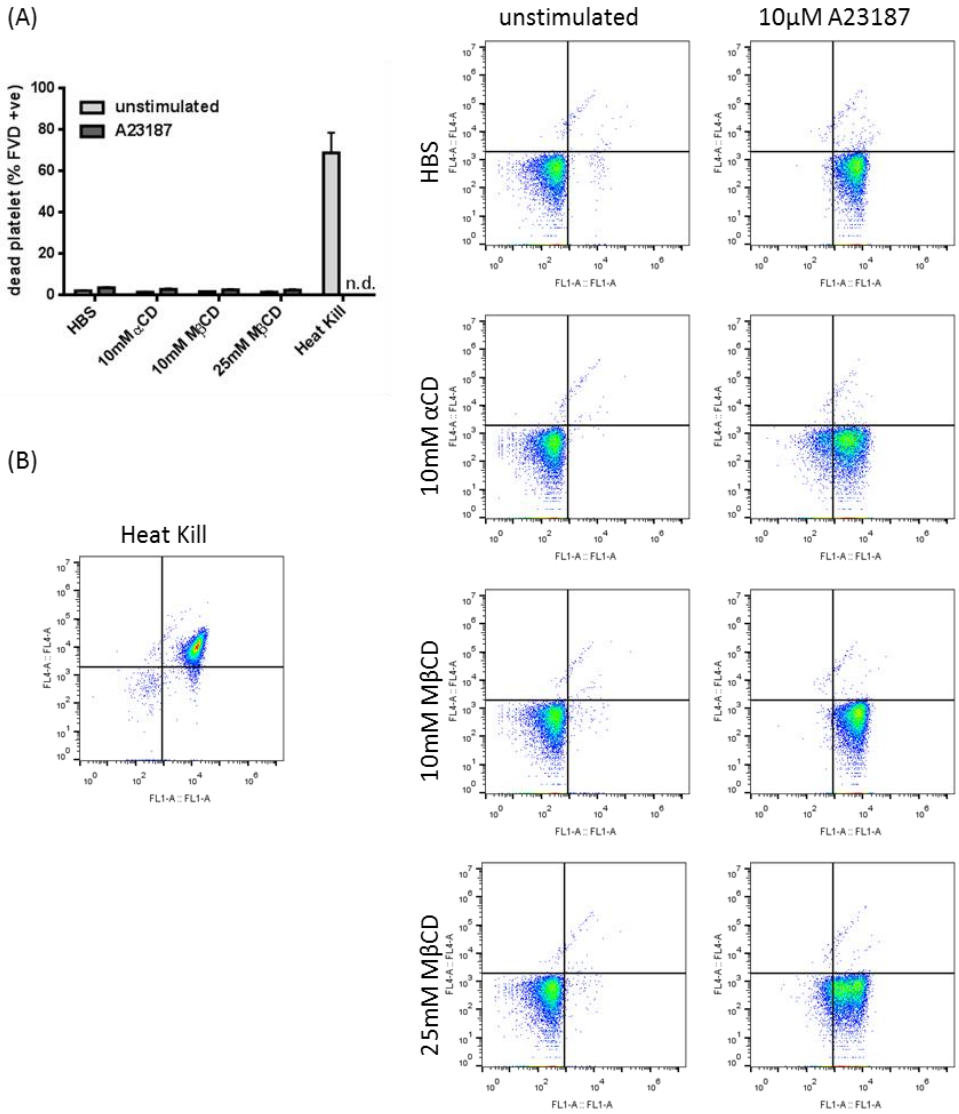

Figure 4.5: Cholesterol depletion does not affect platelet viability

Platelets (5 x 10^7 per ml) were treated with MβCD (10mM and 25mM), αCD (10mM) or vehicle (HBS) for 30 minutes, prior to stimulation with 10μM A23187 for 10 minutes. After this, platelets were stained with anti-human CD41a PE-Cy7, Annexin V FITC, and FVD eFluor 660. (A) Percentage of dead platelets (FVD +ve) in the entire platelet population (>1μm, CD41a +ve) (Mean ± SEM; n = 5; n.d.: not determined). (B) Density plots of platelets (>1μm, CD41a +ve) with Annexin V FITC on FL1-A and FVD fluorescence on FL4-A. Platelets were treated as indicated. These plots are representative of data from 5 different donors.

4.4. Cholesterol depletion inhibits microparticle release from platelets in response to physiological stimulation

Although A23187 effectively stimulated PMP release, it is possible that the mechanism of PMP release in response to A23187 does not mimic the mechanism by which PMPs are released in response to physiological activators. Major physiological agonists for platelets include ADP, thrombin receptor-activating peptide (TRAP), thrombin and collagen-related peptide (CRP). ADP activates the purinergic $P2Y_1$ and $P2Y_{12}$ receptors. $P2Y_1$ is a G_q-coupled GPCR that regulates shape change, aggregation and TXA_2 generation (Yuan et al., 2016). $P2Y_{12}$ is a G_i-coupled GPCR that potentiates platelet aggregation, procoagulant activities and dense granule secretion (Cattaneo, 2015). Thrombin activates platelets via PAR1 and PAR4 (Brass, 2003), while the short peptide sequence SFLLRN (TRAP6 amide) specifically targets PAR1. PAR activation initiates platelets for aggregation, coagulation and haemostasis (De Candia, 2012). CRP mimics collagen that activates GPVI. CRP is a highly potent GPVI agonist only in its cross-linked form (CRP-XL), in which a specific quaternary protein structure is introduced (Achison et al., 1996).

Platelets were stimulated with high concentrations of ADP, SFLLRN, thrombin, CRP-XL, and CRP-XL plus thrombin. Of all agonists, none could stimulate PMP release by itself and only thrombin was moderately effective for PS exposure. Dual stimulation with thrombin plus CRP-XL significantly promoted both PMP release and PS exposure (Figure 4.6A-B).

Effects of cholesterol depletion were then measured in platelets activated with CRP-XL plus thrombin. Treatment with MβCD (10mM, 30 minutes) inhibited PMP release (Figure 4.6C), so lipid rafts might also be important in this process in platelets stimulated with physiological activators. However, MβCD treatment also significantly inhibited PS exposure (Figure 4.6D), which suggested that platelet receptors or Ca^{2+} channels might be affected by cholesterol depletion. For this reason, further lipid raft-associated studies were continued with A23187 rather than physiological activators.

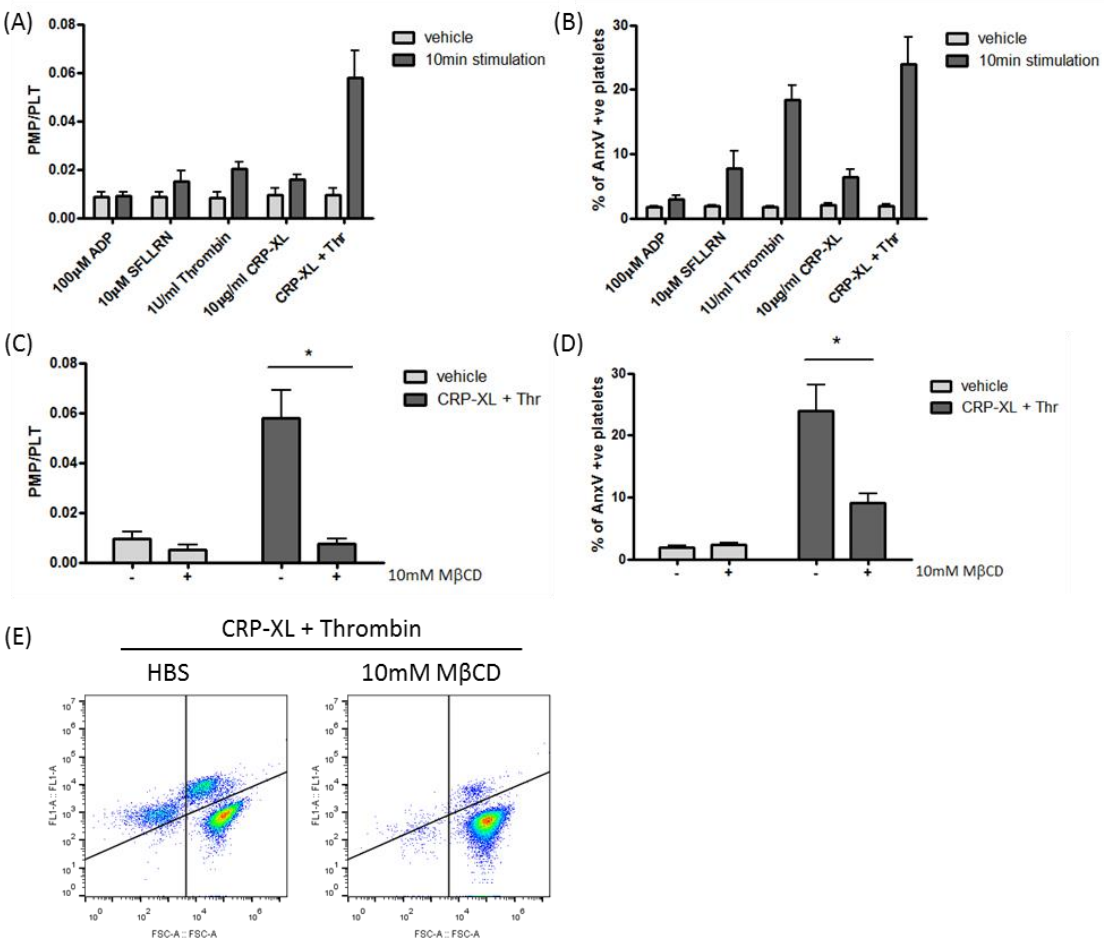

Figure 4.6: Cholesterol depletion inhibits microparticle release from platelets in response to physiological stimulation

(A-B) Washed platelets (5 x 10^7 per ml) were stimulated for 10 minutes with 100µM ADP, 10µM SFLLRN, 1U/ml thrombin, 10µg/ml CRP-XL (synthesised by Dr. J.D.M Malcor), and 10µg/ml CRP-XL plus 1U/ml thrombin or vehicle (HBS) as control. PMP release and PS exposure were measured as described in Figure 3.4 (Mean ± SEM; n = 5). (C-D) Washed platelets (5 x 10^7 per ml) were treated with 10mM MβCD (+) or vehicle (HBS) as control (-) for 30 minutes, prior to stimulation with CRP-XL (10µg/ml) plus thrombin (1U/ml) or vehicle (HBS) for 10 minutes. PMP release and PS exposure were measured as described in Figure 3.4 (Mean ± SEM; n = 5; * $p < 0.05$, compared to vehicle). (E) Density plots of MβCD- or vehicle (HBS)-treated platelets stimulated with CRP-XL (10µg/ml) plus thrombin (1U/ml). Quadrants are defined as described in Figure 3.4, with Annexin V FITC fluorescence on FL1-A. These plots are representative of data from 5 different donors.

4.5. Cholesterol depletion by an antifungal drug also prevents microparticle release from platelets

Apart from cyclodextrin, some antifungal drugs can interact with membrane lipids including cholesterol. Filipin forms complexes with membrane cholesterol when applied to unfixed cells and disrupts lipid rafts (Bolard, 1986; Bang et al., 2005). Platelets treated with filipin released significantly fewer PMPs with no effect on PS exposure in response to A23187. The inhibitory effect of filipin on PMP release was concentration-dependent (Figure 4.7).

Amphotericin B, a structurally-related polyene macrolide antibiotic, is used intravenously to treat deep fungal infections by disintegrating fungal membranes (Gallis et al., 1990). Found only in fungal cells, ergosterol changes the dynamic properties of and stabilises the lipid bilayer structure. Amphotericin B has a higher selectivity for ergosterol over its mammalian counterpart cholesterol (Kamiński, 2014). When used over the same range of concentrations as filipin, Amphotericin B had no significant effect on PMP release or PS exposure in response to A23187 (Figure 4.7). These data indicate that cholesterol depletion prevents the release of microparticles from human platelets.

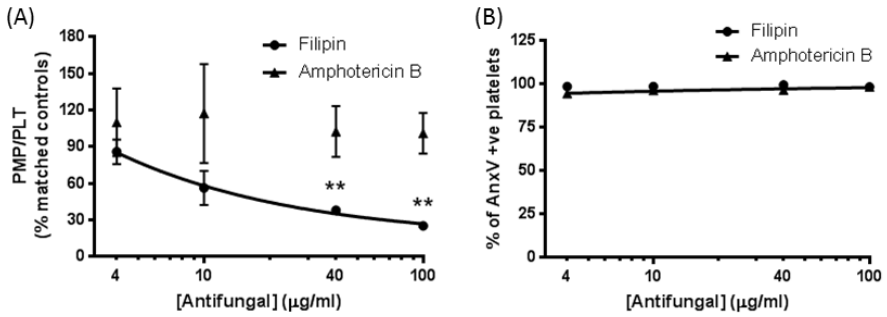

Figure 4.7: Cholesterol depletion by an antifungal drug also prevents microparticle release from platelets

Washed platelets (5 x 10^7 per ml) were treated with the indicated concentrations of filipin or amphotericin B (4, 10, 40, 100µg/ml), or vehicle (DMSO) as control for 30 minutes, prior to stimulation with 10µM A23187 for 10 minutes. (A) PMP release was measured as in Figure 3.4 and normalised to matched vehicle controls (Mean ± SEM; n = 5; ** $p < 0.01$, compared to control). (B) PS exposure was measured as described in Figure 3.4 (Mean ± SEM; n = 5).

4.6. Cholera toxin B, a lipid raft marker, binds to platelets and platelet-derived microparticles

Experiments above studied the importance of lipid rafts in PMP release based on results from cholesterol depletion. An alternative method independent of cholesterol was used to probe lipid rafts in platelets. Cholera toxin subunit B (CTxB) from *Vibrio cholerae*, the membrane binding unit of cholera toxin, has been widely identified as a marker of lipid rafts. CTxB binds with high avidity to monosialo-tetrahexosyl ganglioside (GM1) on the host cell membrane and GM1 is itself confined to lipid rafts (Heyningen S Van, 1974). The B subunit alone is not toxic, so CTxB-treated cells do not become necrotic. Unlike the A subunit, CTxB itself possesses no intrinsic adenylyl cyclase (AC) activity, so it can be exogenously added to cells for lipid raft-associated studies (Day and Kenworthy, 2015).

A FITC conjugate of CTxB has been used to stain GM1 in human cells and measured by flow cytometry (Zhang et al., 2014; Bhat et al., 2015). Unlike other conjugated antibodies, CTxB FITC was added to platelet samples after they had been fixed with PFA, because CTxB can cross-link membrane domains on live cells, forming large stabilised lipid rafts. In a purified model system, lipids reorganised into distinct, resolvable CTxB-enriched liquid-ordered (L_o) and CTxB-depleted liquid-disordered (L_d) domains following the addition of CTxB (Hammond et al., 2005). Similarly, in cytoskeleton-free membrane vesicles that were still attached to cells, addition of CTxB induced the emergence of a slower diffusing phase enriched in cholesterol, i.e. L_o or lipid raft, which then selectively reorganised the lateral distribution of membrane proteins (Lingwood et al., 2008).

In addition, fixing cells before staining with CTxB prevents internalisation of CTxB FITC and thus intracellular staining. In a previous study on T cells, FITC fluorescence of CTxB increased upon cell activation when these cells were fixed before staining, yet significant uptake of CTxB FITC into cells occurred when non-fixed cells were stained (Blank et al., 2007). Similarly, platelets were negative for fluorescence on FL1 when they were stained with CTxB FITC prior to fixation. When platelets were stained with CTxB FITC after fixation with PFA, they were positive for the binding of CTxB (Figure 4.8A).

CTxB FITC bound to unstimulated platelets, as MFI on FL1-A increased significantly for CTxB FITC-stained platelets compared to unstained samples (Figure 4.8A), which confirmed the presence of lipid raft domains on the platelet membrane. PMPs also stained positive for CTxB FITC (Figure 4.8B). In this experiment, CTxB FITC fluorescence was recorded on channel FL1, so Annexin V FITC was omitted (however, as shown in Figure 3.4, the majority of platelet-derived EVs that could be detected were positive for Annexin V). Of all EVs detected, 74.7 ± 0.8% (Mean ± SEM; n = 5) were positive for CTxB FITC binding (indicated by the gate in Figure 4.8C).

Following stimulation with A23187, MFI of CTxB FITC bound to intact platelets decreased, as its specific staining reduced to 78.4 ± 6.0% (Mean ± SEM; n=5) of matched controls (Figure 4.8A). This suggests that GM1 is lost from platelets into PMPs and supports the hypothesis that PMPs are released from sites of lipid rafts.

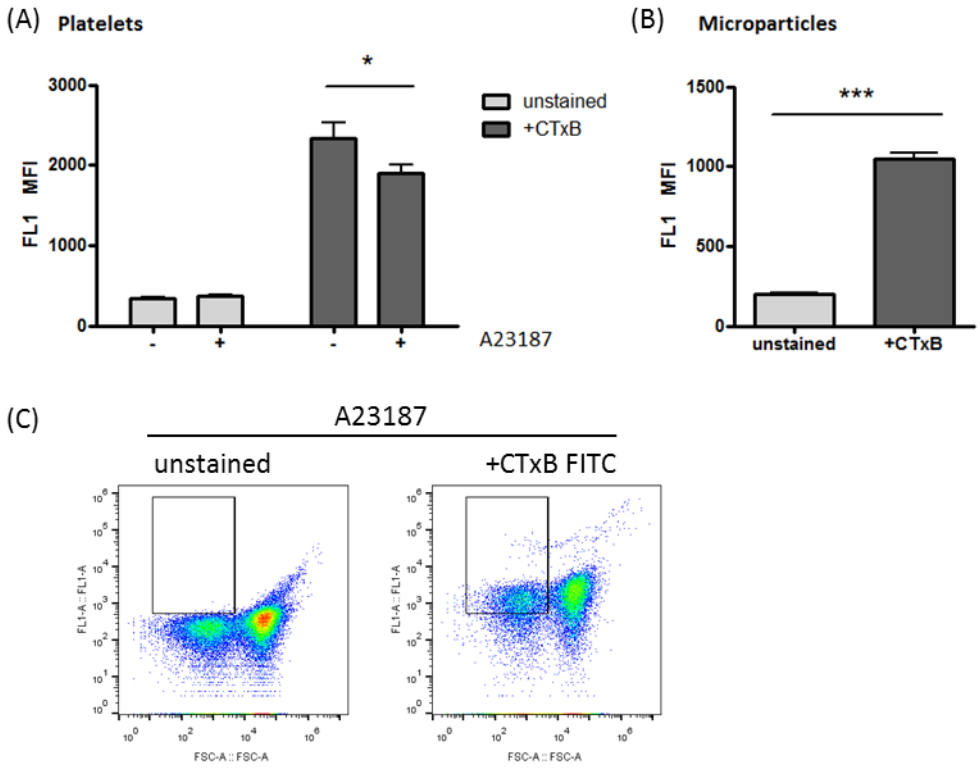

Figure 4.8: Cholera toxin B, a marker of lipid rafts, binds to platelets and platelet-derived microparticles

(A) Washed platelets (5 x 10^7 per ml), unstimulated (-) or stimulated with 10µM A23187 for 10 minutes (+), were stained with anti-human CD41a PE-Cy7, fixed with 1% PFA, then stained with 10µg/ml cholera toxin subunit B FITC conjugate and measured by flow cytometry. Event acquisition was triggered by PE-Cy7 fluorescence on FL3. MFI on FL1-A for FTIC fluorescence is shown for stained and unstained platelets. Stimulation with A23187 led to a significant reduction in CTxB binding to platelets (Mean ± SEM; n = 5, * $p < 0.05$). (B) MFI on FL1-A for stained and unstained microparticles from platelets stimulated with A23187 in the same experiment. PMPs were positive for CTxB binding (Mean ± SEM; n = 5, *** $p < 0.001$). (C) Density plots of platelets stimulated with A23187, with CTxB FITC fluorescence on FL1-A. Left: an unstained sample; Right: the same sample stained with CTxB FITC. The black rectangular box gates for PMPs positive for CTxB binding. These plots are representative of data from 5 different donors.

4.7. Cholesterol depletion does not affect calpain activity

Calpain, an intracellular Ca^{2+}-dependent protease, is important for microparticle release from human platelets (Fox et al., 1991; Yano et al., 1993). Inhibition of calpain reduces the degree of PMP release in response to thrombin and CRP (Shcherbina and Remold-O'Donnell, 1999). A rise in intracellular Ca^{2+} concentration leads to activation of calpain, which cleaves prominent cytoskeletal proteins such as filamin-1, talin and myosin (Morel et al., 2011). This may uncouple the plasma membrane from the cytoskeleton and result in cellular contraction and membrane blebbing.

The role of calpain in PMP release was confirmed in this experimental system. Platelets were treated with calpeptin, a cell-penetrative inhibitor specific for calpain (Tsujinaka et al., 1988). Calpeptin (140μM) significantly inhibited PMP release in response to A23187 (Figure 4.9A). It also increased the proportion of platelets that bound Annexin V at lower concentrations of A23187 (Figure 4.9B; $p = 0.0008$). These results are consistent with a previous report where complete inhibition of calpain by calpeptin (100μM) enhanced PS exposure, measured by Annexin V binding, on platelet surface (Bachelot-Loza et al., 2006).

Calpain activity in platelets can be measured by cleavage of talin, which is a cytosolic substrate of calpain highly expressed in platelets (Mattheij et al., 2013). In Western blot, a monoclonal anti-talin antibody recognised an epitope at 225kDa and a fragment at 190kDa obtained by protease cleavage (Soslau et al., 2014). In platelets in the resting state, both bands could be detected (Figure 4.9C). It might reflect baseline calpain activity, which has also been reported in platelets under storage (Cauwenberghs et al., 2006). Stimulation with A23187 led to complete cleavage of talin and the upper band at 225kDa disappeared (Figure 4.9C), suggesting that calpain was activated upon influx of Ca^{2+}. Cleavage of talin, including the baseline activity, was inhibited by prior treatment with calpeptin, either with or without A23187 stimulation, since no band could be detected at 190kDa (Figure 4.9C). These results confirmed that cleavage of talin could be used as a reliable indicator of calpain activity.

Cleavage of talin was then used to measure calpain activity in platelets where lipid rafts were disrupted. Incubation of platelets with MβCD (10mM and 25mM) or αCD (10mM) did not affect the baseline calpain activity in the resting state. Following stimulation with A23187, cleavage of talin was not affected by pre-treatment with MβCD or αCD either (Figure 4.9D). It suggests that cholesterol depletion does not affect influx of Ca^{2+} through the plasma membrane, Ca^{2+}-dependent activation of calpain in the cytosol, or subsequent protease activities of calpain. This confirms that cytosolic activities of calpain in platelets are not localised to lipid raft domains on the membrane (Huang and Wang, 2001). The effects of lipid raft disruption on PMP release are more likely to be focused at the platelet membrane, downstream of the Ca^{2+}-dependent signalling events.

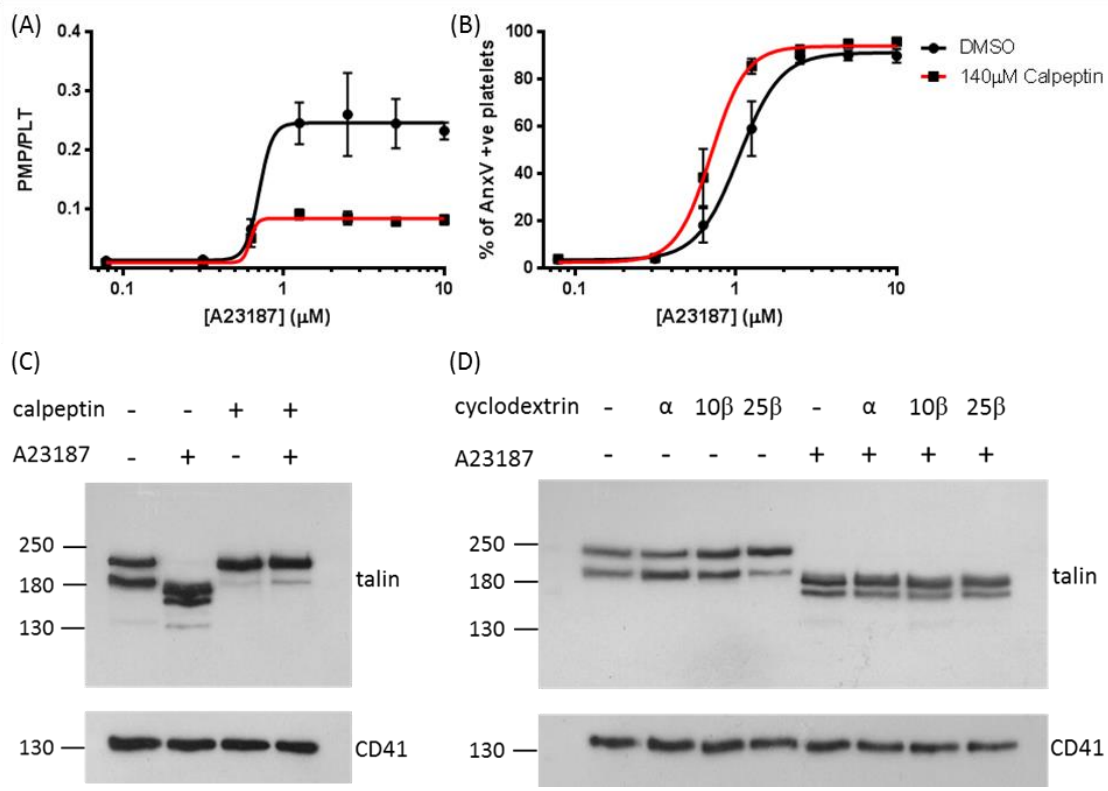

Figure 4.9: Cholesterol depletion does not affect calpain activity

(A-B) Washed platelets (5 x 10^7 per ml) were treated with calpeptin (140μM) or vehicle (DMSO) as control for 30 minutes, prior to stimulation with A23187 for 10 minutes. (A) PMP release was measured as described in Figure 3.4 (Mean ± SEM; n = 5). (B) PS exposure was measured as described in Figure 3.4 (Mean ± SEM; n = 5). (C) Washed platelets (5 x 10^8 per ml) were treated as indicated with 140μM calpeptin (+) or vehicle (-) for 30 minutes, prior to stimulation with 10μM A23187 for 10 minutes where indicated, and then lysed by RIPA buffer. Proteins (20μg) were separated by SDS-PAGE on a 6% poly-acrylamide gel. Talin was detected with anti-talin antibody (1 in 10000). Membranes were stripped and re-probed for CD41 with anti-CD41 antibody (1 in 2000) as a loading control. Calpain-mediated cleavage of talin was triggered by A23187 and inhibited by calpeptin. The blots are representative of 5 independent experiments. (D) Washed platelets (5 x 10^8 per ml) were treated as indicated with 10mM αCD (α), 10mM MβCD (10β), 25mM MβCD (25β) or vehicle (-) as control for 30 minutes, prior to stimulation with 10μM A23187 for 10 minutes where indicated. A23187-triggered talin cleavage was not affected by MβCD. These blots are representative of data from 5 different donors.

4.8. $P2Y_{12}$ and thromboxane signalling are not required for A23187-triggered microparticle release in platelets

The ADP receptor $P2Y_{12}$ and the thromboxane receptor TPα have been reported to reside in lipid rafts on platelet surface (Quinton et al., 2005; Moscardó et al., 2014). To determine if disruption of these two pathways could account for the effect of cholesterol depletion, platelets were treated with the $P2Y_{12}$ antagonist, cangrelor (AR-C 69931MX; 10μM), or the COX inhibitor, aspirin (100μM). Cangrelor was chosen over the pro-drug clopidogrel, because it has a rapid onset of action independent of metabolic conversion (Ferreiro et al., 2009). TXA_2 is the primary end product of COX1-dependent metabolism of arachidonic acid via the intermediate product prostaglandin H_2. By inhibiting COX enzymes, aspirin blocks TXA_2 biosynthesis, thereby removing the major TPα agonist (Davì et al., 2012). Neither drug had any significant effect on PMP release or PS exposure in response to A23187 (Figure 4.10).

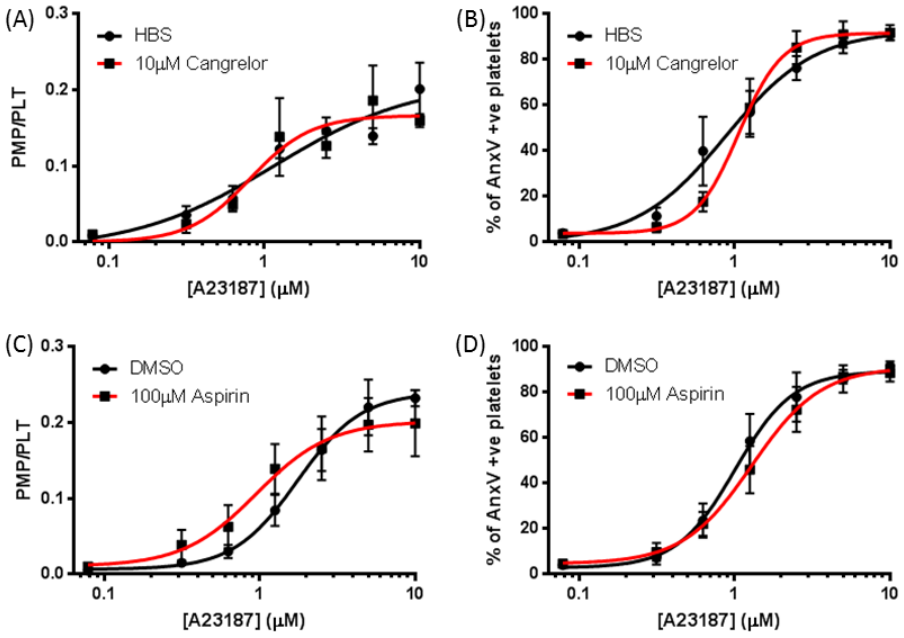

Figure 4.10: $P2Y_{12}$ and thromboxane signalling are not required for A23187-triggered microparticle release in platelets

Washed platelets (5 x 10^7 per ml) were treated for 30 minutes with the $P2Y_{12}$ inhibitor cangrelor (10μM) or vehicle (HBS) as control in (A-B), or the COX inhibitor aspirin (100μM) or vehicle (DMSO) as control in (C-D), prior to stimulation with A23187 for 10 minutes. (A, C) PMP release was measured as described in Figure 3.4 (Mean ± SEM; n = 5). (B, D) PS exposure was measured as described in Figure 3.4 (Mean ± SEM; n = 5).

4.9. ESCRT-associated proteins are not expressed in human platelets

The ESCRT complex comprises a system for membrane budding and severing membrane necks from their inner surface (Hurley, 2015). In a previous study, ESCRT-0 was found to bind to lipid rafts. Local membrane curvature in these domains further recruits other ESCRT-associated proteins, which helps to stabilise the membrane neck (Babst, 2011). Also, a raft-associated protein, flotillin-1, was found to be involved in recognition and sorting of cargoes by ESCRTs (Meister et al., 2017). On the other hand, microparticle release is topologically similar to viral budding and shedding of small wounds, both of which are mediated by ESCRT proteins (Jimenez and Perez, 2017). More importantly, ESCRT proteins have been reported to mediate EV release from erythrocytes (Prudent et al., 2015). Here, ESCRT-mediated scaffolding was studied as a potential lipid raft-associated mechanism that facilitates membrane scission.

Since pharmacological modulators are not available for the ESCRT pathway, RNA interference has been the tool of choice in most ESCRT-associated studies (Hurley, 2015). For example, the sequence for ESCRT recruitment in wound repair was illustrated using siRNA for ALG2 and shRNA for ALIX in HeLa cells (Scheffer et al., 2014). However, RNA interference-based methods are not applicable for platelets as platelets do not possess a genome (Garraud and Cognasse, 2015). The few options left include probing for ESCRT expression levels by Western blot and visualising ESCRT localisation in the cytoplasm by fluorescent microscopy.

Three ESCRT-associated proteins apoptosis-linked gene 2 (ALG2; 21kDa), ALG2-interacting protein X (ALIX; 95kDa) and charged multiple vesicular protein 4B (CHMP4B; 25kDa) were selected to be probed by Western blot, because these proteins are crucial to the biogenesis of EVs in general (Akers et al., 2013). None of the three proteins were found to be expressed in human platelets, or their expression levels were too low to be detected. As control, all three ESCRT-associated proteins were detected in lysates from human umbilical vein endothelial cells (HUVECs) and HeLa cells (Figure 4.11).

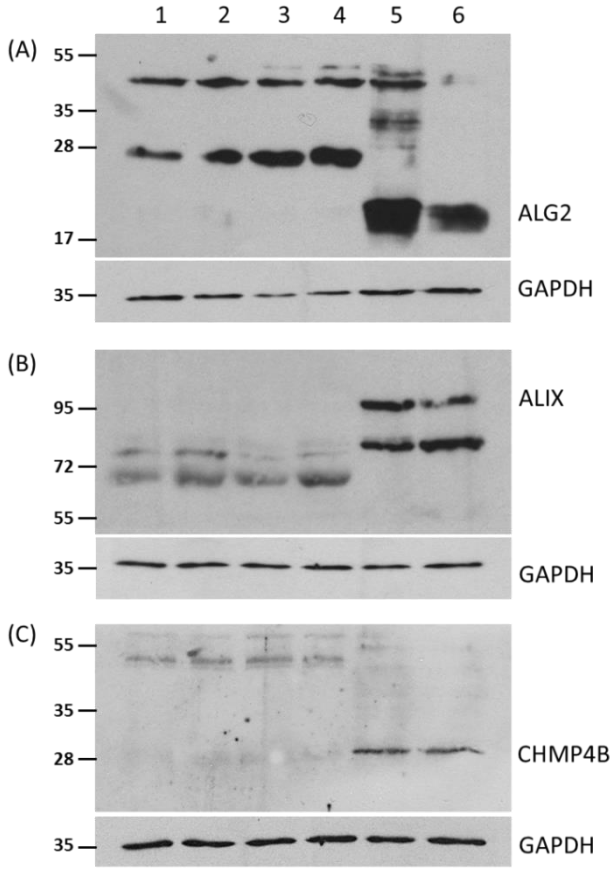

Figure 4.11: ESCRT-associated proteins are not expressed in human platelets

Washed platelets (5 x 10^8 per ml) were lysed in RIPA buffer. Proteins (20µg) were separated by SDS-PAGE and detected with (A) anti-ALG-2 antibody (1 in 1000; 14% poly-acrylamide gel), (B) anti-ALIX antibody (1 in 1000; 8% poly-acrylamide gel), and (C) anti-CHMP4B antibody (1 in 500; 14% poly-acrylamide gel). Membranes were stripped and re-probed for GAPDH with anti-GAPDH antibody (1 in 2000) as a loading control. Lanes on the blots are: 1-4 for platelets from four individual blood donors, 5 for HUVECs and 6 for HeLa cells. HUVECs and HeLa cells acted as positive controls for the ESCRT-associated proteins.

4.10. Discussion

In this chapter, it was shown that intact cholesterol-rich lipid rafts are required for PMP release. MβCD, a widely used lipid raft disruptor, depleted cholesterol from platelets and prevented PMP release. Filipin, which binds and sequesters membrane cholesterol, also prevented PMP release. In contrast, amphotericin B, a structurally-related polyene antibiotic, had no effect on PMP release. Cholera toxin B (CTxB) binds to the lipid raft marker, GM1 ganglioside. CTxB readily bound to PMPs, whereas CTxB binding to platelets was reduced by stimulation with A23187, suggesting that GM1 ganglioside was lost from platelets during PMP release. Together, these data indicate that lipid rafts have an essential role in PMP release. This is consistent with a previous report that PMPs are enriched in cholesterol relative to the membrane fractions of unstimulated platelets (Biró et al., 2005).

How lipid rafts contribute to PMP release is still unclear. Little is known beyond calpain activity and PS exposure. Lipid raft disruption did not disrupt PS exposure, since MβCD or filipin had no effect on Annexin V binding to stimulated platelets. Inhibition of PMP release was not due to a selective deficit of PS exposure in the released EVs either, since there was no increase in Annexin V-negative vesicles following stimulation of MβCD-treated platelets. In addition, lipid raft disruption did not affect intracellular calpain activity, since calpain-dependent cleavage of talin was not affected.

Although it is not a physiological stimulus for platelets, A23187 was chosen over more physiological agonists such as thrombin and collagen for two reasons. Firstly, PS-positive microparticles are released from platelets that expose PS on their surface (Briedé et al., 1999). Not all physiological activators, even in combination, are able to cause PS exposure in platelets (Harper and Poole, 2013; Harper et al., 2013), but PS exposure can be achieved in the entire platelet population by A23187 when used at high concentrations. Secondly, signalling pathways relevant to PMP release might be affected when lipid rafts are disrupted. Using a Ca^{2+} ionophore allows platelet stimulation to bypass receptor activation and its subsequent Ca^{2+} signalling mechanisms, such as SOCE (Brownlow et al., 2004).

Inhibition of PMP release by MβCD pre-treatment in response to thrombin plus CRP-XL might reflect inhibition of PS exposure, which is required for formation of PMPs on platelet surface. The PS scramblase TMEM16F itself does not appear to be affected by cholesterol depletion, as MβCD pre-treatment did not affect PS exposure in platelets activated by A23187. Rather, cholesterol depletion is more likely to affect the receptors, ion channels or signalling molecules required for triggering PS exposure upstream of TMEM16F in response to physiological agonists, including type I protein kinase A (Raslan et al., 2015) and TRPC6 (Harper et al., 2013). Intact lipid rafts are also necessary for SOCE, which is another major route for Ca^{2+} entry leading to PS exposure (Harper and Poole, 2013).

Although $P2Y_{12}$ and TPα receptors have been found in platelet lipid rafts, neither inhibition of $P2Y_{12}$ with cangrelor, nor inhibition of TXA_2 synthesis with aspirin, significantly affected A23187-stimulated PMP release or PS exposure. In contrast, PMP release induced by SFLLRN or thrombin plus convulxin was inhibited by pre-treatment with cangrelor (Behan et al., 2005; Kahner et al., 2008). Similarly, arachidonic acid was found to induce PMP release, which was inhibited by aspirin (Giacomazzi et al., 2016). This indicates that activation of $P2Y_{12}$ and TPα enhances signalling downstream of receptor stimulation, potentially by promoting Ca^{2+} mobilisation and signalling. They are not directly involved in the PMP release mechanism, since inhibition of these receptor activities could be circumvented by the use of A23187.

Membrane scission in PMP release is not mediated by the ESCRT machinery, which has been implicated in lipid rafts. Absence of ESCRT-associated proteins in platelets does not contradict early studies. ALG2 was only reported in platelets when mass spectroscopy-derived peptide fragments were compared with a computational data base (Lewandrowski et al., 2009). ALIX and CHMP4B were reported in platelets when a combinatorial ligand library was used to specifically concentrate and capture low-abundance proteins (Guerrier et al., 2007). The expression levels of ALIX, ALG2 and CHMP4B in platelets, if any, would be too low to underlie PMP release, which is a rapidly-triggered process with high turnover rates.

Chapter 5 Apoptosis

5.1. Aim of study

In terms of apoptosis in human platelets, little is known beyond the intrinsic pathway regulated by Bcl-xL and PS exposure mediated by caspases. Activated PS-exposing platelets tend to release PS-positive PMPs (Morel et al., 2011). Release of EVs, including exosomes and microparticles, has been reported as a hallmark of cellular apoptosis in general (Caruso and Poon, 2018). In this chapter, it was investigated whether PMPs are released when platelets undergo apoptosis. If this is the case, other questions include how this process is regulated in platelets, and how apoptotic PMP release links to stimulatory PMP release from platelets.

5.2. ABT-737 triggers Ca^{2+}-dependent apoptosis and microparticle release in platelets

To investigate platelet apoptosis *in vitro*, washed human platelets were treated with the BH3-mimetic drug ABT-737 (10μM) for up to 3 hours. PS exposure was detected by Annexin V FITC binding. ABT-737-treated platelets showed two levels of stimulated Annexin V binding, medium and high (Figure 5.1A). Two levels of positive Annexin V binding were consistent with a previous report (van Kruchten et al., 2013).

Coincident with development of platelets with high Annexin V binding, Annexin V-positive PMPs were released (Figure 5.1C). PMPs were detected via flow cytometry as described in Figure 3.4, so PMPs detected here are likely an underestimate of the total number of EVs present. This result shows that PMPs are released from apoptotic platelets.

ABT-737 also triggered a slow increase in intracellular Ca^{2+} concentration ($[Ca^{2+}]_i$), which was detected by loading platelets with Fluo-4 or Cal520 (Figure 5.1D). Fluo-4 fluorescence was measured live using flow cytometry in platelets (>1μm, CD41a +ve) discretely at the indicated time points. Since the earliest time analysed in this experiment was 10 minutes, the previously-reported transient (<1min) increase in $[Ca^{2+}]_i$ was not detected in this assay (Harper and Poole, 2012). By comparison, Cal520 fluorescence was measured using a microplate reader continuously every minute throughout 3 hours of incubation. A rapid,

though not transient, increase in $[Ca^{2+}]_i$ was detected, as the initial fluorescence intensity of ABT-737-treated platelets was 1.26 ± 0.07 times higher than that of vehicle control (Mean ± SEM; n = 5). Results from Fluo-4- and Cal520-based assays followed the same trend. Further experiments for $[Ca^{2+}]_i$ measurement were conducted using Cal520 on a microplate reader because of its continuity and high throughput.

The increase in $[Ca^{2+}]_i$ was largely dependent on the presence of extracellular Ca^{2+} (Figure 5.1D), which indicated that it was largely due to Ca^{2+} entry. Ca^{2+} entry was required for ABT-737-triggered PS exposure and PMP release, as both were significantly inhibited in the absence of extracellular Ca^{2+} (Figure 5.1B-C). Notably, $CaCl_2$ was present in the Annexin V staining buffer, as is required for Annexin V binding to PS. In control experiments, Annexin V readily bound to heat-killed platelets when $CaCl_2$ was absent during the treatment and only present in the staining buffer (see Figure 5.2A below, for an example).

In contrast, chelation of intracellular Ca^{2+} by treating platelets with BAPTA AM (20μM) had less effect on PS exposure. The total percentage of Annexin V-positive platelets was not affected. Instead, the percentage of high Annexin V platelets was reduced (at 180 minutes, 5.9 ± 0.8% showed high Annexin V binding in BAPTA-loaded platelets, compared to 42.7 ± 6.3%; n = 5; $p < 0.001$) and the percentage of medium Annexin V platelets correspondingly increased (at 180 minutes, 50.3 ± 2.2% showed medium Annexin V binding in BAPTA-loaded platelets, compared to 38.8 ± 4.3%; n = 5; $p < 0.01$), so that the total percentage of Annexin V-positive platelets was only slightly reduced (at 180 minutes, 56.2 ± 2.3% were positive for Annexin V binding in BAPTA-loaded platelets, compared to 81.5 ± 2.4%; n = 5; $p < 0.05$). PMP release was abolished when ABT-737-treated platelets were co-incubated with BAPTA (Figure 5.1C). Chelation of intracellular Ca^{2+} by BAPTA was confirmed by $[Ca^{2+}]_i$ assay (Figure 5.1D). This suggested that PMP release was linked to the development of platelets with high Annexin V binding during apoptosis, rather than platelets with medium Annexin V binding.

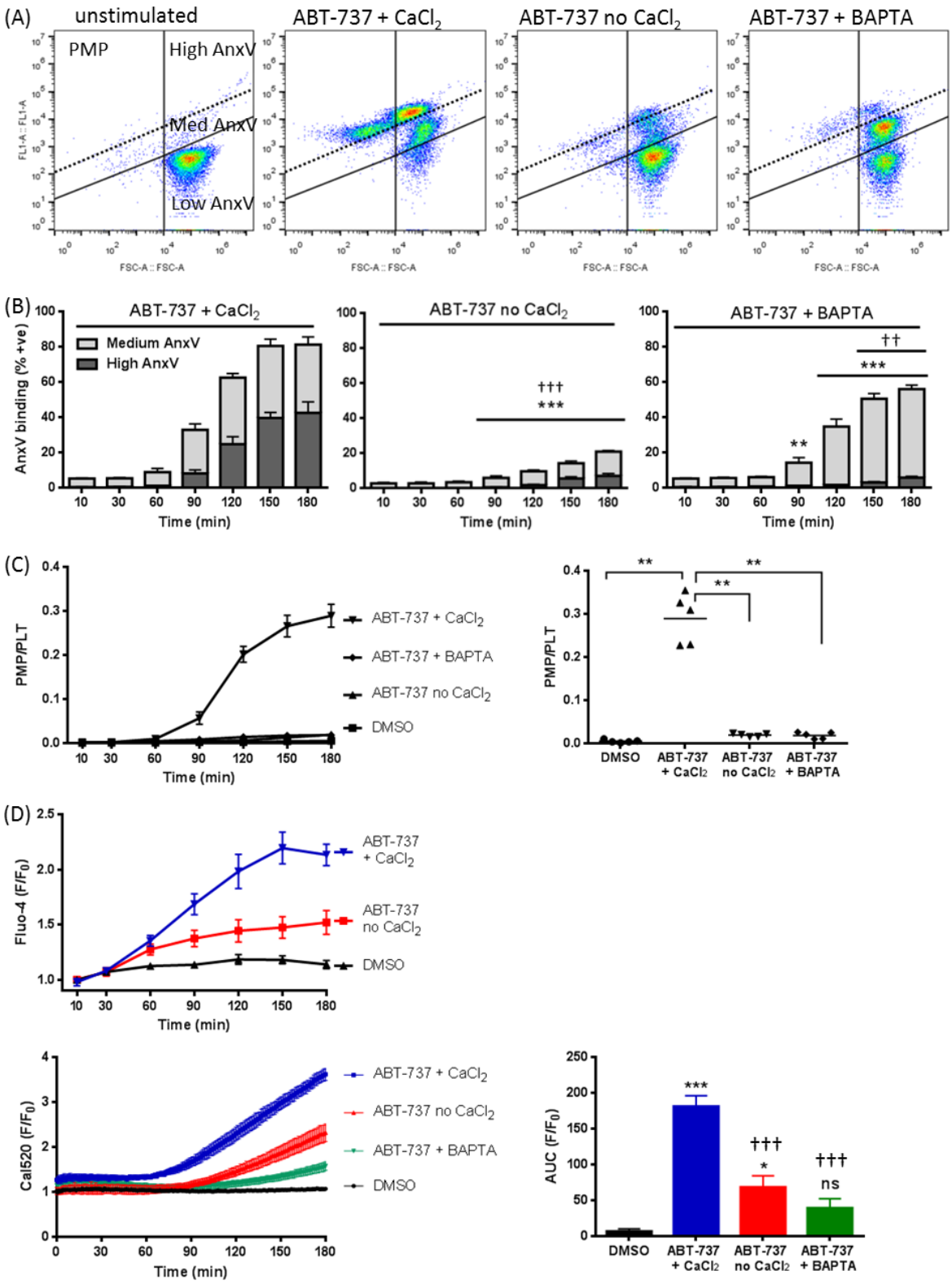
(A)
unstimulated
ABT-737 + CaCl2
ABT-737 no CaCl2
ABT-737 + BAPTA
PMP
High AnxV
Med AnxV
Low AnxV
FL1-A :: FL1-A
FSC-A :: FSC-A
(B)
ABT-737 + CaCl2
ABT-737 no CaCl2
ABT-737 + BAPTA
Medium AnxV
High AnxV
AnxV binding (% +ve)
Time (min)
†††
***
**
††
(C)
PMP/PLT
Time (min)
ABT-737 + CaCl2
ABT-737 + BAPTA
ABT-737 no CaCl2
DMSO
(D)
Fluo-4 (F/F0)
Cal520 (F/F0)
AUC (F/F0)
ns
*

Figure 5.1: ABT-737 triggers Ca^{2+}-dependent apoptosis and microparticle release in platelets.

Washed platelets (5 x 10^7 per ml) were stimulated with 10µM ABT-737 or vehicle (DMSO) for 3 hours with or without 2mM extracellular $CaCl_2$, or with 20µM BAPTA AM in the presence of 2mM $CaCl_2$, after which samples were stained with anti-human CD41a PE-Cy7 and Annexin V FITC to detect PS exposure. PE-Cy7 fluorescence on FL3 was used to trigger acquisition of CD41a positive events. (A) The panels show density plots of events from low density (blue) to high density (red) on FSC-A and FITC fluorescence on FL1-A. The vertical line separating left and right was defined by FSC-A values of 1µm silicon dioxide beads. Unstimulated platelets have high FSC-A and low Annexin V binding. Stimulation with ABT-737 triggers PS exposure at two levels, detected as medium and high Annexin V binding. These plots are representative of data from 5 different donors. (B) PS exposure in platelets treated with 10µM ABT-737 at the indicated times was measured as described in Figure 3.4. Percentage of platelets positive for medium or high Annexin V binding was shown separately (Mean ± SEM; n = 5; ** $p < 0.01$, *** $p < 0.001$ for high Annexin V binding compared to platelets treated with 10µM ABT-737 plus 2mM $CaCl_2$; †† $p < 0.01$, ††† $p < 0.001$ for medium Annexin V binding compared to platelets treated with 10µM ABT-737 plus 2mM $CaCl_2$). (C) Number of Annexin V-positive PMPs released in platelets treated with 10µM ABT-737 at the indicated times (left) and only at the endpoint of 180 minutes (right), measured as described in Figure 3.4 (Mean ± SEM; n = 5, ** $p < 0.01$). (D) Intracellular Ca^{2+} assay of platelets treated with 10µM ABT-737, where PRP was loaded with 1µM Fluo-4 (upper) or 500nM Cal520 (lower) for 10 minutes (Mean ± SEM; n = 5). Fluorescence was normalised to the initial fluorescence intensity of vehicle control prior to stimulation (F/F_0). Area under curve (AUC) above basal was calculated for the Cal520-based Ca^{2+} trace (Mean ± SEM; n = 5; * $p < 0.05$, *** $p < 0.001$, ns: not significant, compared to unstimulated control; ††† $p < 0.001$ compared to platelets treated with 10µM ABT-737 plus 2mM $CaCl_2$).

5.3. ABT-737 triggers secondary necrosis in platelets

During the course of ABT-737 treatment, some platelets gradually lost plasma membrane integrity, as detected by loss of calcein fluorescence from the cytosol (Figure 5.2A). It was proposed that these platelets had progressed to secondary necrosis at later stages. Following 3 hours of treatment with ABT-737 in the presence of 2mM $CaCl_2$, 31.1 ± 1.3% (Figure 5.2B; Mean ± SEM; n = 5) of platelets had lost plasma membrane integrity. For positive control, almost all heat-killed platelets (97.8 ± 1.3%; Mean ± SEM; n = 5) lost plasma membrane integrity. Heat-killed platelets were positive for Annexin V fluorescence since Annexin V molecules had access to PS distributed at the inner leaflet of plasma membrane (Figure 5.2A). In contrast, following 3 hours of treatment with vehicle (DMSO), only 1.4 ± 0.1% of platelets lost plasma membrane integrity (Mean ± SEM; n = 5).

ABT-737 triggers secondary necrosis in a Ca^{2+}-dependent manner. Absence of extracellular Ca^{2+} prevented secondary necrosis, with only 1.6 ± 0.2% (Figure 5.2B; Mean ± SEM; n = 5) of platelets losing plasma membrane integrity. BAPTA also prevented ABT-737-triggered secondary necrosis, with only 6.0 ± 0.4% (Figure 5.2B; Mean ± SEM; n = 5) of platelets losing plasma membrane integrity. This suggested that higher levels of PS exposure triggered by ABT-737, detected as high Annexin V binding, could at least be partially attributed to secondary necrosis.

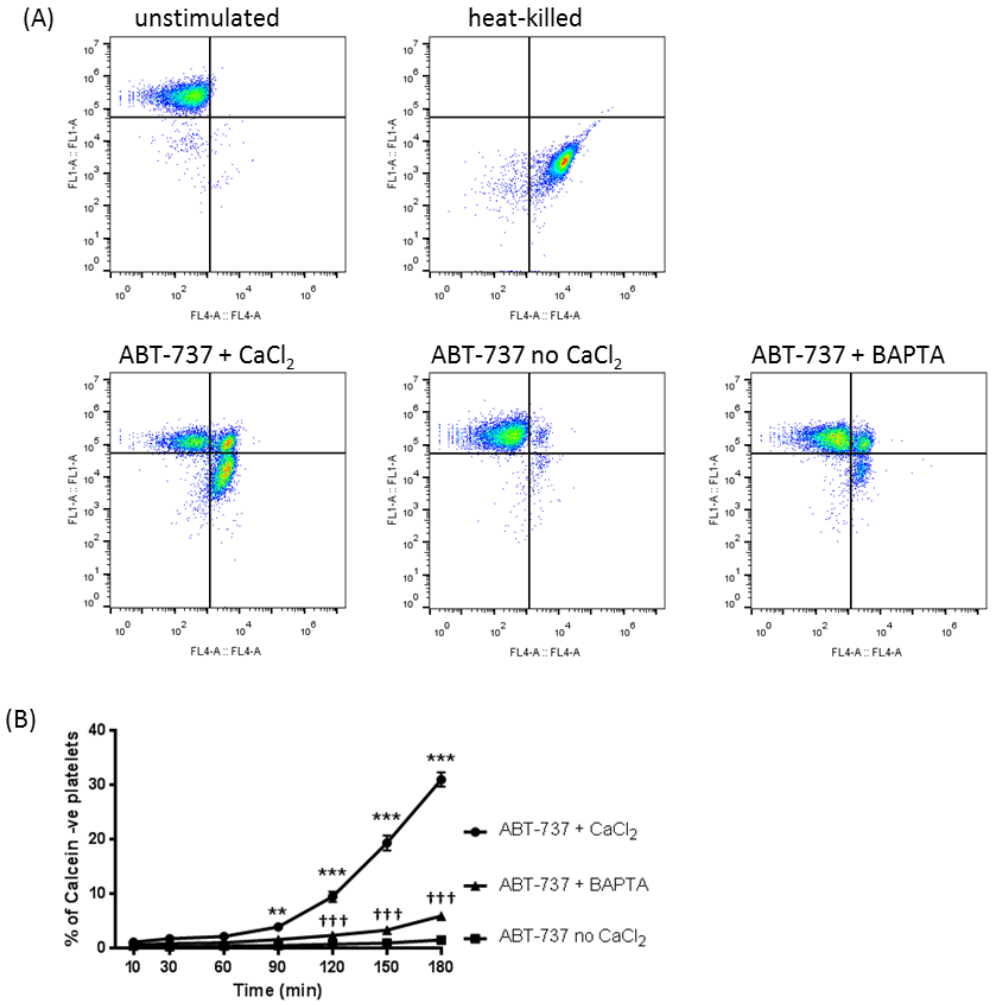

Figure 5.2: ABT-737 triggers secondary necrosis in platelets

PRP was loaded with 1µM calcein for 10 minutes. Calcein-loaded washed platelets (5 x 10^7 per ml) were treated as indicated and stained with anti-human CD41a PE-Cy7 and Annexin V APC. Samples were acquired live with flow cytometry and triggered on PE-Cy7 fluorescence on FL3. (A) Density plots are gated on platelets (CD41a +ve, >1µm) after 180 minutes of ABT-737 incubation and scaled on FL1-A for calcein and FL4-A for Annexin V APC. These plots are representative of data from 5 different donors. Unstimulated platelets are a negative control and heat-killed platelets are a positive control for loss of calcein. (B) The percentage of platelets negative for calcein at the indicated time points (Mean ± SEM; n = 5; *** $p < 0.001$ for ABT-737 + $CaCl_2$ vs. ABT-737 no $CaCl_2$; ††† $p < 0.001$ for ABT-737 + $CaCl_2$ vs. ABT-737 + BAPTA).

5.4. ABT-737-triggered apoptosis and microparticle release are dependent on caspase and only partially dependent on calpain

Cell death mechanisms often require intracellular proteases (Vanden Berghe et al., 2014). Two proteases, caspase and calpain, were examined for their roles in platelet apoptosis and its associated PMP release. Caspases have well-established roles in cell death through initiating and executing a cascade of protein cleavage and degradation (Elmore, 2007). On the other hand, calpain has been reported as a major effector of necrotic death. Its substrates include cytoskeletal proteins, ion channels and transporters, adhesion molecules, kinases, phosphatases and phospholipases (Liu et al., 2004; Zong and Thompson, 2006).

Firstly, platelets were treated with a cell-permeable pan-caspase inhibitor Q-VD-OPh (50µM) prior to stimulation with ABT-737. When caspases were inhibited, PS exposure on the surface of platelets was almost completely abolished (Figure 5.3A). At 180 minutes, only 3.0 ± 0.5% of Q-VD-OPh-treated platelets were positive for Annexin V binding compared to 81.5 ± 2.4% of controls (Figure 5.3B; Mean ± SEM; n = 5; $p < 0.001$). Caspase inhibition also suppressed PMP release (Figure 5.3C) and Ca^{2+} entry throughout 180 minutes (Figure 5.3D). This suggests that caspase activities are upstream of Ca^{2+} mobilisation and phospholipid scramblase activation during platelet apoptosis, which includes both the Ca^{2+}-dependent TMEM16F responsible for higher PS exposure and the unidentified caspase-dependent scramblase responsible for lower PS exposure.

Compared to caspase, calpain has a relatively limited role in apoptosis and PMP release. Platelets were treated with calpeptin (140µM) prior to stimulation with ABT-737. Calpeptin partially inhibited high Annexin V binding, with a slight yet statistically insignificant increase in medium Annexin V binding (Figure 5.3B). At 180 minutes, 20.1 ± 4.3% showed high Annexin V binding in calpeptin-treated platelets, compared to 42.7 ± 6.3% in vehicle control (Figure 5.3B; Mean ± SEM; n = 5; $p < 0.01$), while 44.8 ± 4.5% showed medium Annexin V binding in calpeptin-treated platelets, compared to 38.8 ± 4.3% in vehicle control (Figure 5.3B; Mean ± SEM; n = 5; not significant).

Although calpain was required for A23187-triggered PMP release (Figure 4.9), calpeptin had a statistically significant whilst small inhibitory effect on PMP release in response to ABT-737 (Figure 5.3C). In addition, calpeptin-treated platelets showed significant, but not complete, suppression of the slow increase in intracellular Ca^{2+} concentration (Figure 5.3D).

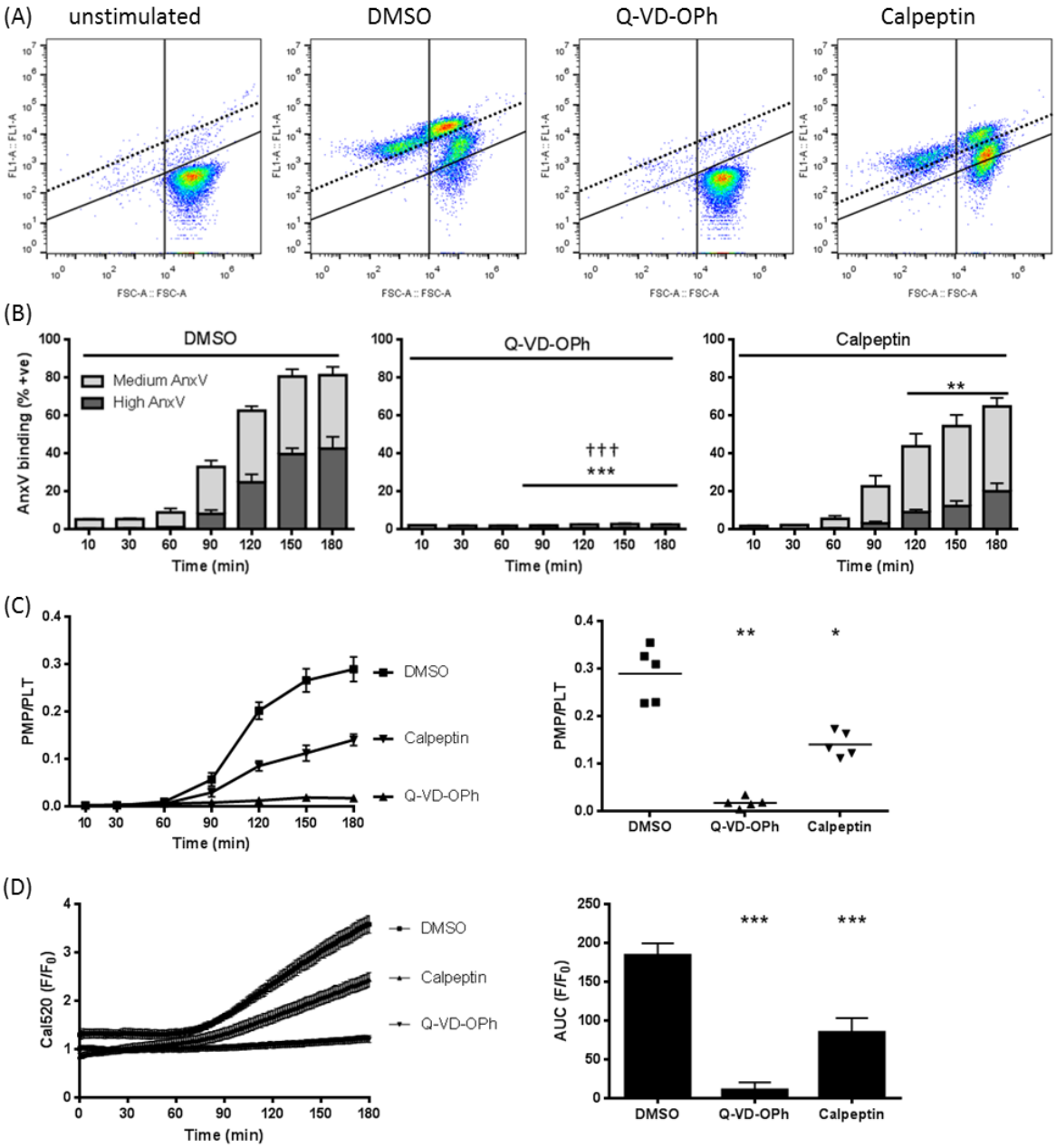

Figure 5.3: ABT-737-triggered apoptosis and microparticle release are dependent on caspase and only partially dependent on calpain

Washed platelets (5 x 10^7 per ml) were treated with the caspase inhibitor, Q-VD-OPh (50μM), or the calpain inhibitor, calpeptin (140μM), or vehicle control (DMSO) for 30 minutes, prior to stimulation with 10μM ABT-737 in the presence of 2mM extracellular $CaCl_2$ for 3 hours. (A) Density plots of platelets treated as indicated after 180 minutes of ABT-737 incubation. Unstimulated control is included. Quadrants are defined as in Figure 5.1, with Annexin V FITC fluorescence on FL1-A. These plots are representative of data from 5 different donors. (B) PS exposure was measured as described in Figure 5.1. The panel shows percentage of platelets positive for medium and high Annexin V binding at the indicated time points (Mean ± SEM; n = 5; ** $p < 0.01$, *** $p < 0.001$ for high Annexin V binding compared to vehicle; ††† $p < 0.001$ for medium Annexin V binding compared to vehicle). (C) PMP release was measured as described in Figure 5.1. The left panel shows the number of PMPs released in platelets treated as indicated at the indicated time points. The right panel shows the number of PMPs released in platelets treated as indicated after 180 minutes of ABT-737 incubation (n = 5, * $p < 0.05$, ** $p < 0.01$ compared to vehicle). (D) Intracellular Ca^{2+} assay of platelets treated with the indicated drugs, where PRP was loaded with 500nM Cal520 for 10 minutes. Fluorescence was normalised to initial fluorescence intensity of untreated platelets prior to stimulation (F/F_0). AUC above basal was calculated (Mean ± SEM; n = 5; *** $p < 0.001$ compared to vehicle).

5.5. ABT-737-triggered secondary necrosis requires caspase and calpain

Caspase and calpain were then examined for their roles in ABT-737-triggered secondary necrosis. Calcein-loaded platelets were pre-treated with Q-VD-OPh or calpeptin prior to stimulation with ABT-737. Caspase activities were required for secondary necrosis. Inhibition of caspases abolished this process, because only 1.7 ± 0.1% of Q-VD-OPh-treated platelets were negative for calcein fluorescence compared to 31.1 ± 1.3% of vehicle-treated controls at 180 minutes (Figure 5.4B; Mean ± SEM; n = 5; $p < 0.001$).

Inhibition of calpain by calpeptin also significantly inhibited loss of calcein fluorescence in platelets treated with ABT-737 (at 180 minutes, 8.3 ± 1.9% of calpeptin-treated platelets were negative for calcein fluorescence compared to 31.1 ± 1.3% of vehicle-treated controls; Figure 5.4B; Mean ± SEM; n = 5; $p < 0.001$), so low levels of calpain activity in apoptotic platelets led to loss of plasma membrane integrity. This may account for the small apparent role of calpain in PMP release, high levels of PS exposure (high Annexin V binding) and Ca^{2+} entry.

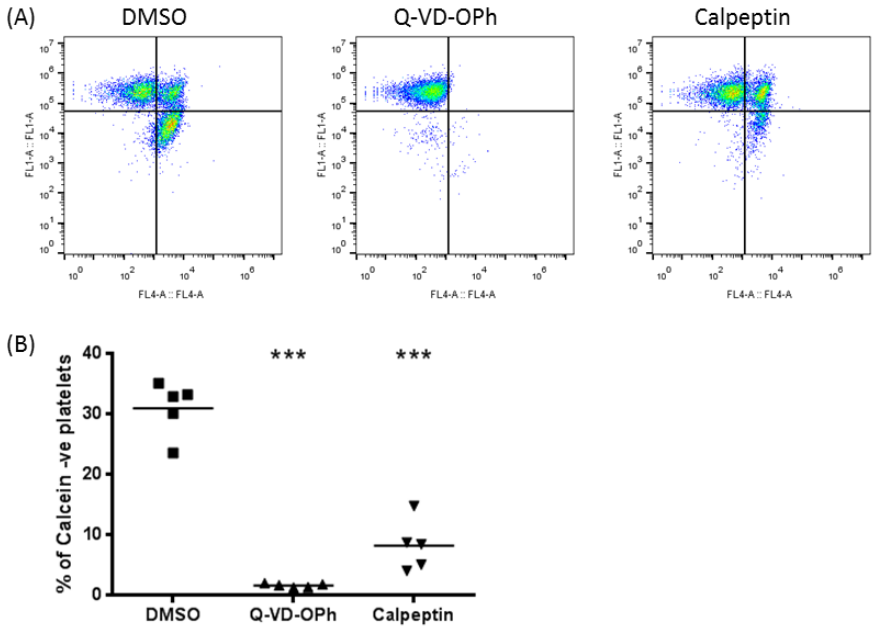

Figure 5.4: ABT-737-triggered secondary necrosis requires caspase and calpain

PRP was loaded with 1µM calcein for 10 minutes. Calcein-loaded washed platelets (5 x 10^7 per ml) were treated with Q-VD-OPh (50µM), or calpeptin (140µM), or vehicle control (DMSO) for 30 minutes, prior to stimulation with 10µM ABT-737 in the presence of 2mM extracellular $CaCl_2$ for 3 hours. Platelets were then stained with anti-human CD41a PE-Cy7 and Annexin V APC. Samples were acquired live with flow cytometry and triggered on PE-Cy7 fluorescence on FL3. (A) Density plots of platelets treated as indicated. Quadrants are defined as in Figure 5.2, with calcein fluorescence on FL1-A and Annexin V APC fluorescence on FL4-A. These plots are representative of data from 5 different donors. (B) The percentage of platelets negative for calcein fluorescence at 180 minutes (n = 5; *** $p < 0.001$ compared to vehicle).

5.6. ABT-737 triggers significant caspase activities and weak calpain activity

Caspase and calpain activities were examined by Western blotting. ABT-737 induced self-cleavage of caspase 3 into its active effector fragment, which then cleaved its substrate gelsolin within 60 minutes. Caspase-dependent cleavage of gelsolin was inhibited in the presence of Q-VD-OPh (Figure 5.5A). The onset of caspase 3 cleavage activities was slightly earlier than that of Ca^{2+} entry, PS exposure, PMP release or loss of plasma membrane integrity. This confirms that these apoptotic and secondary necrotic features are dependent on and thus downstream of caspase activities.

Cleavage of talin by calpain was weak, as its pattern in ABT-737-stimulated platelets was similar to untreated control (Figure 5.5B). By contrast, cleavage of another calpain substrate ATP8A1 was more prominent in platelets treated with ABT-737 (Jing et al., 2019). It may suggest that calpain activity is biased towards different substrates during platelet activation and apoptosis.

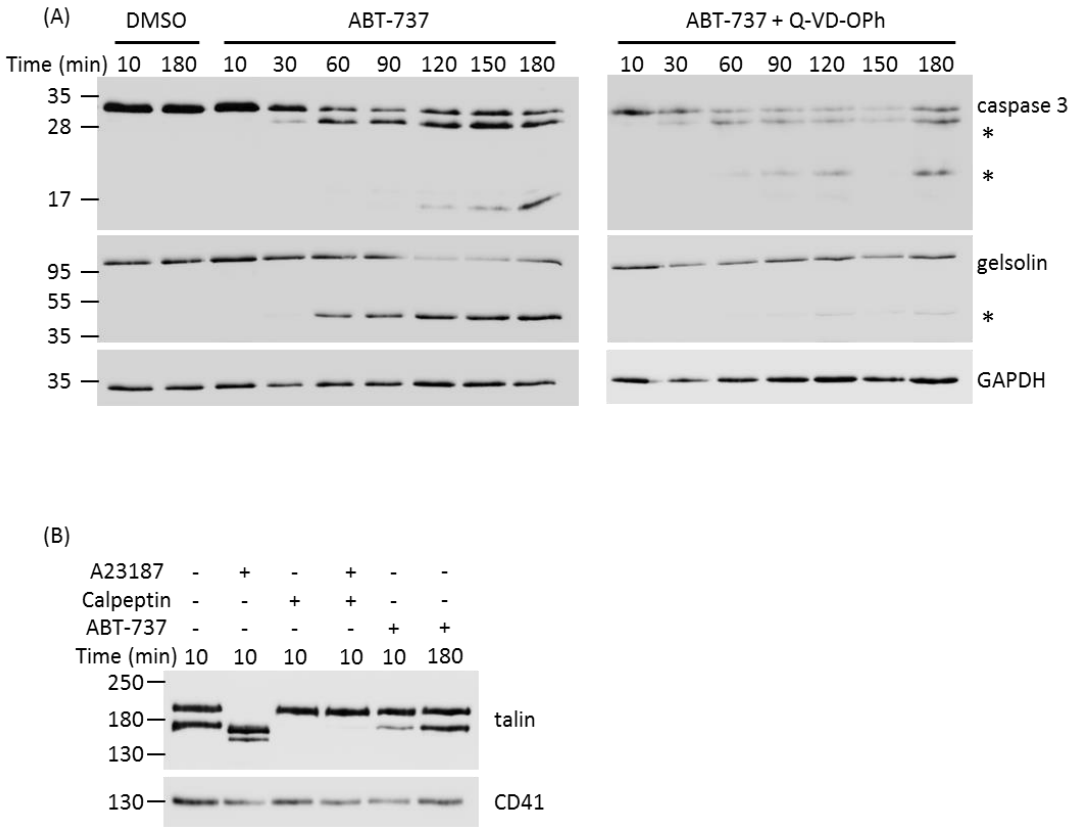

Figure 5.5: ABT-737 triggers significant caspase activities and weak calpain activity

(A) Washed platelets (5 x 10^8 per ml) were treated with ABT-737 (10µM) with or without Q-VD-OPh (50µM), or vehicle (DMSO) as control for the indicated times, before being lysed with RIPA buffer. Proteins (20µg) were separated by SDS-PAGE on a 16% poly-acrylamide gel. Caspase 3 was detected with anti-caspase 3 antibody (1 in 500), stripped and re-probed for gelsolin with anti-gelsolin antibody (1 in 1000), again stripped and re-probed for GAPDH with anti-GAPDH antibody (1 in 2000) as a loading control. Asterisks (*) indicate cleavage products. (B) Washed platelets (5 x 10^8 per ml) were treated with A23187 (10µM), calpeptin (140µM) or ABT-737 (10µM) as indicated, and lysed with RIPA buffer. Talin and the loading control CD41 were probed as described in Figure 4.9. These blots are representative of data from 5 different donors.

5.7. ABT-737 triggers cytochrome c release from mitochondria and loss of mitochondrial membrane potential in platelets

Effects of apoptosis on platelet mitochondria were studied. Mitochondrial outer membrane permeabilisation (MOMP) occurs in the early stages of apoptotic cell death. Activated pro-death BAK and BAX proteins perforate the outer mitochondrial membrane, which allows the release of cytochrome c from the mitochondrial intermembrane space into the cytosol (Nagata, 2018). To examine retention of cytochrome c, digitonin had been transiently applied to selectively permeabilise the plasma membrane without damaging the outer mitochondrial membrane. After washing digitonin-treated cells by centrifugation, the supernatant containing released cytochrome c was discarded (Campos et al., 2006).

In this experiment, digitonin treatment was optimised to 0.05% (w/v) for 2 minutes for platelets at 5 x 10^8 per ml. After washing out released cytochrome c, the digitonin-resistant pellet showed loss of the cytosol marker extracellular signal-regulated kinases 1 and 2 (ERK 1/2), but retained the mitochondrial marker cytochrome c oxidase or complex IV (COX IV). ABT-737 triggered cytochrome c release within 10 minutes, which is consistent with a previous report (Choo et al., 2017). Release of cytochrome c was not delayed or inhibited in the presence of Q-VD-OPh or BAPTA (Figure 5.6A). This confirmed that MOMP is independent of intracellular Ca^{2+} levels and it occurs upstream of caspase activation.

To monitor the loss of mitochondrial membrane potential, platelets were treated with tetra-methyl-rhodamine methyl-ester (TMRM). After penetrating the plasma membrane, TMRM is readily sequestered by active mitochondria. Loss of TMRM from cells is linked to disruption of the inner mitochondrial membrane (IMM) (Jobe et al., 2008). Slower than cytochrome c release, loss of TMRM from the mitochondria was temporally coincident with Ca^{2+} entry, PS exposure and PMP release. It was abolished by Q-VD-OPh, partially inhibited by BAPTA, but not affected by calpeptin (Figure 5.6B). This showed that IMM disruption and loss of mitochondrial membrane potential were regulated by Ca^{2+} entry and caspases, and largely independent of calpain.

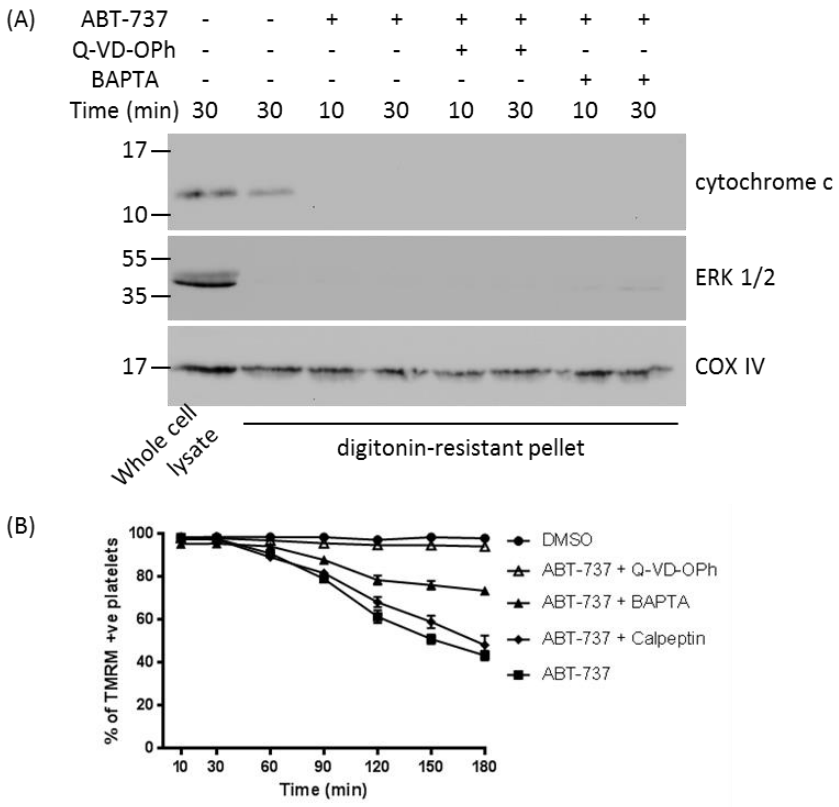

Figure 5.6: ABT-737 triggers cytochrome c release from mitochondria and loss of mitochondrial membrane potential in platelets

(A) Washed platelets (5 x 10^8 per ml) were treated with 50µM Q-VD-OPh or 20µM BAPTA AM where indicated, before treatment with 10µM ABT-737 for 10 to 30 minutes. Platelets were briefly permeabilised with 0.05% (w/v) digitonin for 2 minutes and the cytosol-rich fraction removed by centrifugation (600g, 10 minutes), after which digitonin-resistant pellets were lysed with RIPA buffer. Proteins (20µg) were separated by SDS-PAGE on a 16% poly-acrylamide gel. Cytochrome c was detected with anti-cytochrome c antibody (1 in 250), stripped and re-probed for ERK 1/2 with anti-ERK 1/2 antibody (1 in 1000), again stripped and re-probed for COX IV with anti-COX IV antibody (1 in 1000). Whole cell lysate was included as a control. These blots are representative of data from 5 different donors. (B) Washed platelets (5 x 10^7 per ml) were loaded with 500nM TMRM for 30 minutes and treated with 50µM Q-VD-OPh, 20µM BAPTA AM or 140µM calpeptin where indicated, prior to treatment with 10µM ABT-737 for the time indicated. Platelets were stained with anti-human CD41a PE-Cy7. Percentage of platelets (CD41a +ve, >1µm) positive for TMRM fluorescence on FL2 was shown (Mean ± SEM; n = 5).

5.8. Calpain-dependent release of microparticles is downregulated during apoptosis

It was surprising that calpain was only weakly involved in ABT-737-triggered PMP release, since calpain is required for PMP release in response to A23187 (Figure 4.9) or procoagulant stimuli (Yano et al., 1993). It was hypothesised that ABT-737 treatment might somehow reduce the ability of calpain to promote PMP release. To investigate this hypothesis, platelets were treated with ABT-737 for 3 hours without extracellular Ca^{2+}, as very few PMPs were released under this condition (Figure 5.1). These platelets were then stimulated with A23187 for 10 minutes in the presence of extracellular Ca^{2+} to trigger a large increase in intracellular Ca^{2+} concentration (Figure 5.7A). A23187 was used rather than physiological agonists, such as thrombin and CRP-XL, since ABT-737 disrupts responses to these agonists through shedding of GPVI and GPIb (Schoenwaelder et al., 2011; Vogler et al., 2011), yet A23187 can bypass these disruptions.

As control, A23187 rapidly triggered PMP release in the presence of 2mM $CaCl_2$ in untreated platelets. ABT-737 treatment significantly inhibited PMP release in response to subsequent stimulation with A23187 plus $CaCl_2$ (Figure 5.7B). PS exposure in response to A23187 was not affected (Figure 5.7C). Caspase activation inhibited the ability of platelets to release PMPs in response to A23187. The importance of this process was seen when apoptosis was triggered by ABT-737 yet caspases were inhibited by Q-VD-OPh. Compared to control, these platelets released more PMPs in response to A23187 (Figure 5.7B), yet PS exposure was at similar levels (Figure 5.7C). Therefore, ABT-737 makes platelets more sensitive to A23187 stimulation if caspases are not activated.

Caspase and calpain activities in this experiment were confirmed by Western blot. Although A23187 triggered calpain-dependent self-cleavage of caspase 3, it did not activate the cell death-related effector cascade, as indicated by cleavage of gelsolin (Figure 5.7E). ABT-737 still triggered caspase 3 activity in the absence of extracellular Ca^{2+}, which was inhibited by Q-VD-OPh (Figure 5.7E). A23187-triggered calpain activity was not affected by activation of caspases. A23187, in the presence of $CaCl_2$, was still able to activate calpain regardless of treatment with ABT-737 and Q-VD-OPh, as shown by cleavage talin (Figure 5.7E).

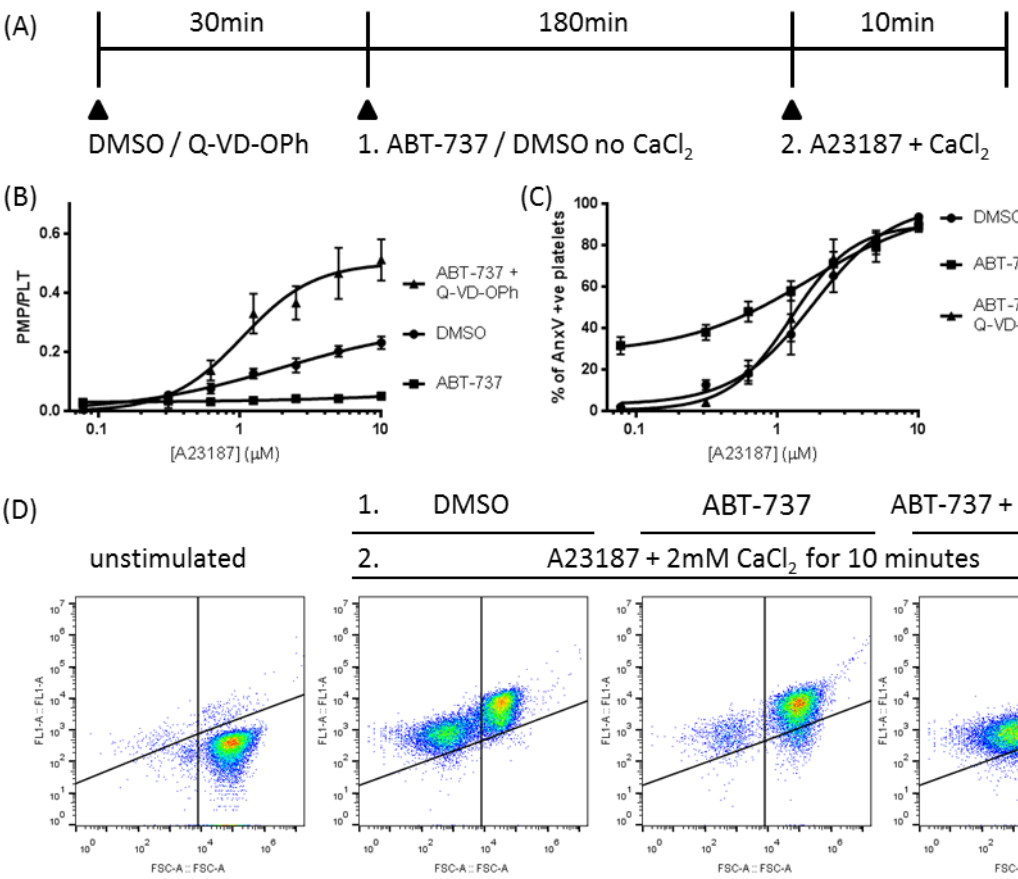
(A)
30min
180min
10min
DMSO / Q-VD-OPh
1. ABT-737 / DMSO no CaCl2
2. A23187 + CaCl2
(B)
PMP/PLT
[A23187] (μM)
ABT-737 + Q-VD-OPh
DMSO
ABT-737
(C)
% of AnxV +ve platelets
[A23187] (μM)
DMSO
ABT-737
ABT-737 + Q-VD-OPh

(D)
1. DMSO
ABT-737
ABT-737 + Q-VD-OPh
unstimulated
2. A23187 + 2mM CaCl2 for 10 minutes
FL1-A :: FL1-A
FSC-A :: FSC-A

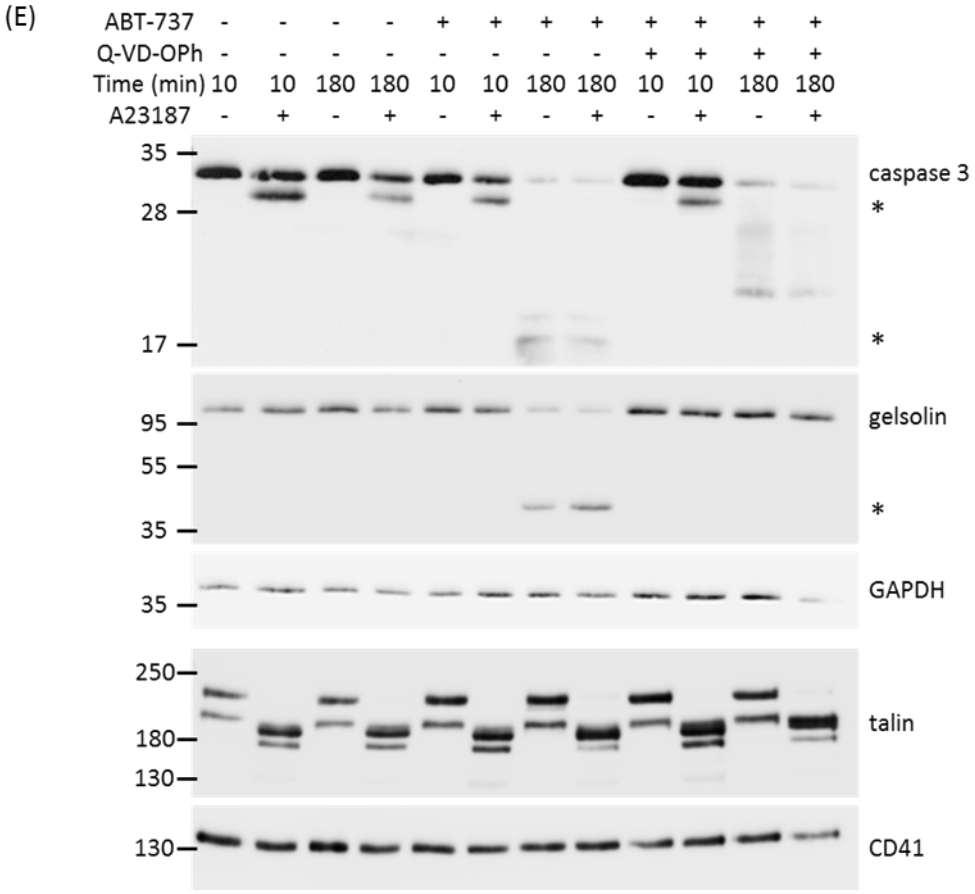
(E)
ABT-737 - - - - + + + + + + + +
Q-VD-OPh - - - - - - - - + + + +
Time (min) 10 10 180 180 10 10 180 180 10 10 180 180
A23187 - + - + - + - + - + - +
35
28
17
caspase 3
*
*
95
55
35
gelsolin
*
35
GAPDH
250
180
130
talin
130
CD41

Figure 5.7: Calpain-dependent microparticle release is downregulated during apoptosis

(A) Scheme of the experiment. Washed platelets (5 x 10^7 per ml) were treated with 50µM Q-VD-OPh or vehicle (DMSO) for 30 minutes, prior to 10µM ABT-737 or vehicle (DMSO) in the absence of extracellular $CaCl_2$. After 3 hours of ABT-737, platelets were stimulated with A23187 for 10 minutes in the presence of 2mM $CaCl_2$. (B-C) A23187-stimulated platelets were stained with anti-human CD41a PE-Cy7 and Annexin V FITC. PMP release and PS exposure were measured as described in Figure 3.4 (Mean ± SEM; n = 5). (D) Density plots of platelets treated as indicated. Quadrants are defined as described in Figure 3.4, with Annexin V FITC fluorescence on FL1-A. These plots are representative of data from 5 different donors. (E) Washed platelets (5 x 10^8 per ml) were treated with 10µM ABT-737 (or DMSO), with or without 50µM Q-VD-OPh in the absence of extracellular Ca^{2+} for 10 or 180 minutes as indicated, prior to stimulation with 10µM A23187 (or DMSO) in the presence of 2mM $CaCl_2$ for 10 minutes as indicated and lysed with RIPA buffer. (Top) Proteins (20µg) were separated with SDS-PAGE on a 16% poly-acrylamide gel. Caspase 3, gelsolin and the loading control GAPDH were probed as described in Figure 5.5. Asterisks (*) indicate cleavage products. (Bottom) Proteins (20µg) were separated with SDS-PAGE on a 6% poly-acrylamide gel. Talin and the loading control CD41 were probed as described in Figure 4.9. These blots are representative of data from 5 different donors.

5.9. ABT-737 is the most suitable drug for studying platelet apoptosis and necrosis *in vitro*

Multiple drugs can trigger apoptosis in cells. Similar to ABT-737, clinically used BH3-mimetics ABT-199 (venetoclax) and ABT-263 (navitoclax) inhibit Bcl-2 proteins (Wilson et al., 2010; Souers et al., 2013). BAM7 selectively binds and activates BAX, independently of BAK or Bcl-2 proteins (Gavathiotis et al., 2012). AT-101 inhibits Mcl-1, Bcl-2 and Bcl-xL with high affinity, and it induces caspase-dependent apoptosis in various cancer cell lines both *in vivo* and *in vitro* (Paoluzzi et al., 2008; Zerp et al., 2009). HA14-1, a non-peptide ligand of a Bcl-2 surface pocket, showed cytotoxic effects *in vitro* (Skommer et al., 2006), yet it did not directly affect growth of tumour cells *in vivo* (Manero et al., 2006). The pan-Bcl-2 inhibitor sabutoclax suppresses tumour cell growth through activation of BAK and BAX both *in vivo* and *in vitro* (Wei et al., 2010; Dash et al., 2011). TW-37 was shown to inhibit proliferation and induce apoptosis in lymphoma cells without any significant effect on normal peripheral blood lymphocytes. However, its affinity has only been determined *in vitro* for recombinant Bcl-2, Bcl-xL and Mcl-1 proteins in cell-free assays (Mohammad et al., 2007). Of these pro-death drugs, only ABT-199, ABT-263 and ABT-737 have been applied to platelets.

To investigate their effects *in vitro*, pro-death drugs were added to platelets for 3 hours. At a low concentration (100nM), none of the drugs triggered PS exposure or PMP release. At a medium concentration (1μM), ABT-737 was the only drug that triggered apoptosis (64.5 ± 2.9% of platelets were AnxV +ve and PMP/PLT = 0.09 ± 0.02; n=5). At a high concentration (10μM), ABT-263, ABT-737, AT-101, HA14-1 and sabutoclax triggered PMP release and PS exposure. By contrast, ABT-199, BAM7 and TW-7 did not lead to any significant increase in PMP release or PS exposure, which corresponds to the specificities of these drugs on Bcl-xL (Figure 5.8A-B). ABT-263 and sabutoclax were less potent than ABT-737 for triggering PMP release, while AT-101 and HA14-1 were at least equally potent (for PMP/PLT: ABT-263 = 0.05 ± 0.02, ABT-737 = 0.23 ± 0.03, AT-101 = 0.23 ± 0.05, HA14-1 = 0.29 ± 0.03, sabutoclax = 0.11 ± 0.03; n = 5). ABT-263 was weaker than ABT-737 for triggering PS exposure, while the rest were equally potent (for % of AnxV +ve: ABT-263 = 49.4 ± 4.9%, ABT-737 = 76.0 ± 3.7%, AT-101 = 60.6 ± 12.8%, HA14-1 = 80.6 ± 6.2%, sabutoclax = 71.6 ± 8.5%; n = 5).

To understand their pro-death effects, platelets were treated with ABT-263, AT-101, HA14-1 or sabutoclax (10μM) in the presence of Q-VD-OPh or calpeptin, or in the absence of extracellular $CaCl_2$. Responses to all drugs were dependent on Ca^{2+} entry, as PMP release and PS exposure were abolished in the absence of extracellular $CaCl_2$. Apoptosis triggered by ABT-263 was similar to that triggered by ABT-737, as it was dependent on caspases and largely independent of calpain. By contrast, platelet death in response to AT-101, HA14-1 or sabutoclax was mechanistically distinct. Caspase inhibition by Q-VD-OPh did not abolish PMP release or suppress PS exposure; whereas calpain inhibition by calpeptin was largely insignificant at least in terms of PS exposure (Figure 5.8C-D).

ABT-263, AT-101, HA14-1 and sabutoclax were further examined for their capacity in inducing necrosis, again measured by loss of cytosolic calcein. Apoptosis in ABT-263-treated platelets did not progress to secondary necrosis, as only 2.5 ± 0.7% of the platelets were negative for calcein (Figure 5.8F). By comparison, treatment with AT-101, HA14-1 or sabutoclax produced variable results. These drugs were more potent than ABT-737 in triggering necrosis in platelets from some blood donors, yet they did not cause necrosis in platelets from other donors (Figure 5.8F).

Based on the results above, ABT-737 is the most suitable drug for studying platelet apoptosis and necrosis *in vitro*. ABT-199, BAM7 and TW-37 did not trigger apoptosis in platelets, as suggested by little increase in PMP release or PS exposure. ABT-263 was similar to ABT-737 in terms of mechanistic details, but it was less potent and did not lead to secondary necrosis in platelets. Rather than inhibiting Bcl-xL and thus leading to activation of effector caspases, AT-101, HA14-1 and sabutoclax triggered PMP release and PS exposure in platelets potentially through off-target effects that are yet to be resolved. Whether these drugs trigger secondary necrosis might be subject to individual differences between blood donors.

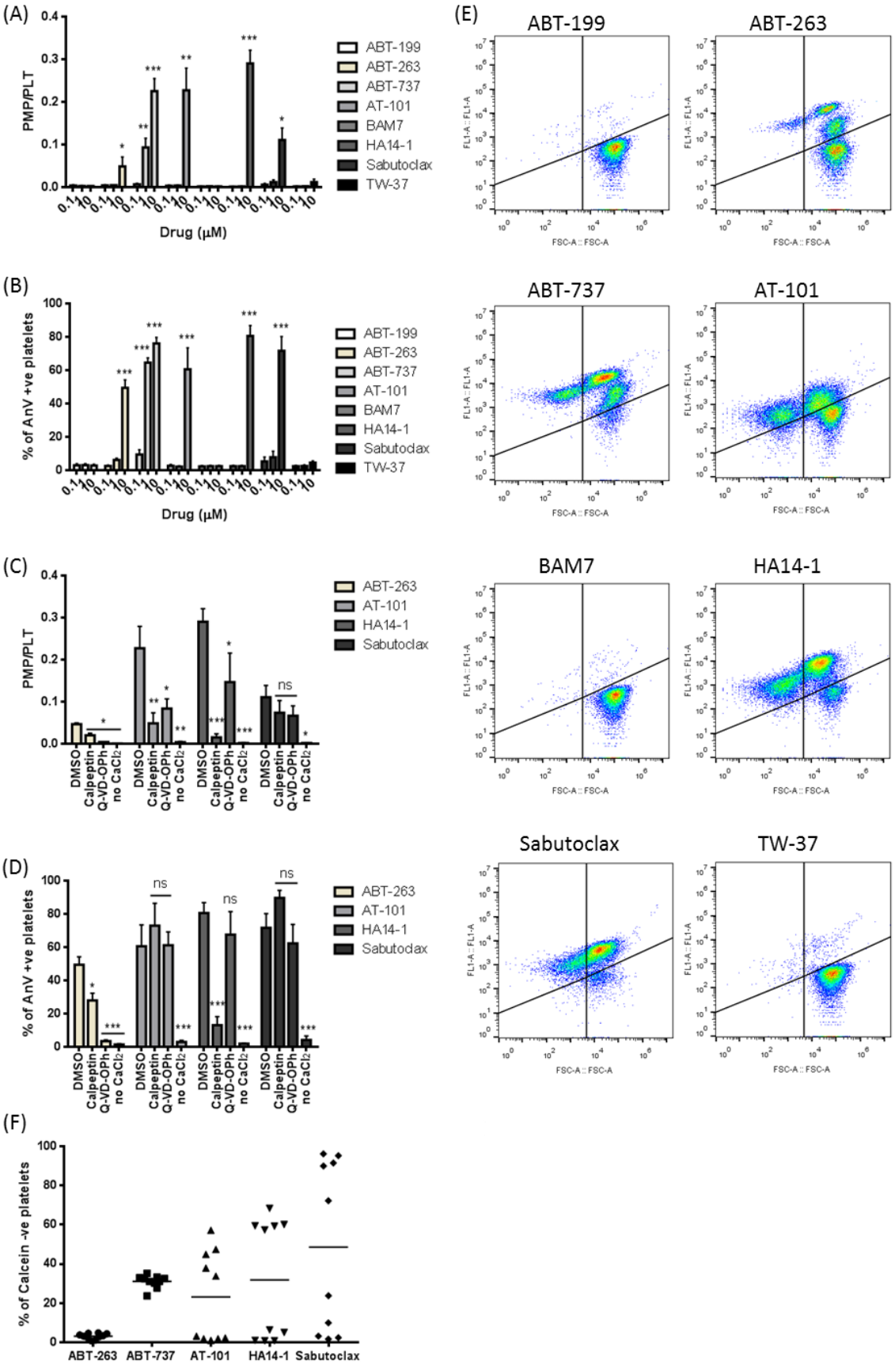
(A)
PMP/PLT
Drug (μM)
ABT-199
ABT-263
ABT-737
AT-101
BAM7
HA14-1
Sabutoclax
TW-37
(B)
% of AnV +ve platelets
Drug (μM)
(C)
PMP/PLT
DMSO
Calpeptin
Q-VD-OPh
no CaCl2
ns
(D)
% of AnV +ve platelets
(E)
ABT-199
ABT-263
ABT-737
AT-101
BAM7
HA14-1
Sabutoclax
TW-37
FL1-A :: FL1-A
FSC-A :: FSC-A
(F)
% of Calcein -ve platelets
ABT-263
ABT-737
AT-101
HA14-1
Sabutoclax

Figure 5.8: ABT-737 is the most suitable drug for studying platelet apoptosis and necrosis *in vitro*

(A-B) Washed platelets (5 x 10^7 per ml) were treated with 0.1µM, 1µM or 10µM of ABT-199, ABT-263, ABT-737, AT-101, BAM7, HA14-1, sabutoclax or TW-37 in the presence of extracellular $CaCl_2$ for 3 hours. PMP release and PS exposure were measured as described in Figure 5.1 (Mean ± SEM; n = 5; * $p < 0.05$, ** $p < 0.01$, *** $p < 0.001$, compared to vehicle). (C-D) Washed platelets (5 x 10^7 per ml) were treated with calpeptin (140µM), Q-VD-OPh (50µM) or vehicle control (DMSO) for 30 minutes, prior to stimulation with 10µM ABT-263, AT-101, HA14-1 or sabutoclax in the presence of extracellular $CaCl_2$ for 3 hours. Platelets were also stimulated in the absence of $CaCl_2$ with each drug for 3 hours. PMP release and PS exposure were measured as described in Figure 5.1 (Mean ± SEM; n = 5; * $p < 0.05$, ** $p < 0.01$, *** $p < 0.001$, ns: not significant, compared to vehicle of each drug). (E) Density plots of platelets treated for 3 hours with 10µM of the pro-apoptotic drugs, as indicated. Quadrants are defined as in Figure 5.1, with Annexin V FITC fluorescence on FL1-A. These plots are representative of data from 5 different donors. (F) PRP was loaded with 1µM calcein for 10 minutes. Calcein-loaded washed platelets (5 x 10^7 per ml) were treated with 10µM ABT-263, ABT-737, AT-101, HA14-1 or sabutoclax in the presence of 2mM extracellular $CaCl_2$ for 3 hours. Loss of calcein fluorescence was measured as described in Figure 3.6 (n = 10).

5.10. Discussion

In this chapter, it was shown that PMPs were released from platelets during apoptosis, which progressed to secondary necrosis *in vitro* as they were not cleared. This PMP release was dependent on Ca^{2+} entry and caspases, but largely independent of calpain. Intracellular signalling events involved in stages of apoptosis and secondary necrosis were differentially regulated by Ca^{2+} entry, caspases and calpain activity. During platelet apoptosis, caspases downregulate calpain-dependent PMP release in response to pro-coagulant stimuli (Figure 5.9).

Two levels of Annexin V binding were detected in platelets in response to ABT-737. This is consistent with a previous report where apoptosis was induced in platelets from healthy donors (van Kruchten et al., 2013). When platelets from a Scott Syndrome patient were treated with ABT-737, most Annexin V-positive platelets showed medium Annexin V binding (van Kruchten et al., 2013). Similarly, medium Annexin V binding was detected when platelets from TMEM16F$^{-/-}$ mice were treated with ABT-737 (Mattheij et al., 2016). This suggests that high level of PS exposure (high Annexin V binding) is mediated by the Ca^{2+}-dependent phospholipid scramblase TMEM16F, which is defective in Scott Syndrome (Suzuki et al., 2010). PMPs also appear to derive from platelets of high Annexin V binding. On the other hand, medium levels of PS exposure (medium Annexin V binding) might be mediated by the caspase-activated scramblase XKR8 (Suzuki et al., 2016), though it has not been reported in platelets so far.

Apoptosis was largely dependent on Ca^{2+} entry, as it was substantially reduced in the absence of extracellular Ca^{2+}. Interestingly, chelation of intracellular Ca^{2+} had less effect. Intracellular BAPTA significantly inhibited the large rise in $[Ca^{2+}]_i$, which was required to activate TMEM16F for high PS exposure. By contrast, BAPTA had little effect on the TMEM16F-independent medium PS exposure. It is possible that there is an additional role for extracellular Ca^{2+}. This may be to support Ca^{2+} entry, or there might be an extracellular site of action for an unidentified platelet scramblase (Hampton et al., 1996). The precise roles that Ca^{2+} plays in these two pathways for PS exposure are worth further investigations.

After prolonged treatment with ABT-737, some platelets lost plasma membrane integrity, suggesting that these platelets had entered secondary necrosis. The progression to necrosis required caspases, extracellular and intracellular Ca^{2+}, and calpain. This has important implications for interpreting results from *in vitro* studies. Many ABT-737-triggered signalling events were attributed to apoptosis (Rukoyatkina et al., 2013; Zhang et al., 2013; Chatterjee et al., 2014), but they may instead be associated with secondary necrosis.

It is unlikely that platelets normally reach secondary necrosis *in vivo*, but rapid induction of apoptosis (e.g. chemotherapy) in many platelets could temporarily overwhelm the capacity for clearance. Circulating PS-positive platelets were readily detectable following ABT-737 administration in mice, with a 90% reduction in platelet count (Schoenwaelder et al., 2011). Impaired clearance and accumulation of secondary necrotic cells have been associated with activation of the adaptive immune system and chronic inflammation (Sachet et al., 2017). Necrotic cells were found to release damage-associated molecular patterns (DAMPs) that activate innate immune cells via receptors including toll-like receptors (Chen and Nuñez, 2010; Krysko et al., 2011). Some DAMPs are associated with thrombosis (Wang et al., 2014; Vogel et al., 2015). Impaired clearance of apoptotic cells is also associated with development of auto-antibodies against intracellular antigens and subsequently chronic inflammation (Mahajan et al., 2016; Sachet et al., 2017). Although consequences of platelet secondary necrosis are yet to be determined, a large number of circulating secondary necrotic cells would have the potential to promote acute and chronic inflammation.

Responses from secondary necrotic platelets may have been modified by prior activation of caspases. It was found that caspases downregulated calpain-dependent PMP release in response to A23187 and an acute rise in $[Ca^{2+}]_i$, which may provide a period of reduced capacity to activate platelets. When apoptosis was triggered yet caspases were inhibited, platelets became more sensitive to pro-coagulant stimuli, as they released more PMPs in response to A23187. This might be linked to disruption of mitochondrial functions during apoptosis (Tait and Green, 2013). ABT-737 triggered caspase-independent MOMP within 10 minutes (cytochrome c release), which then gradually led to IMM disruption (loss of TMRM).

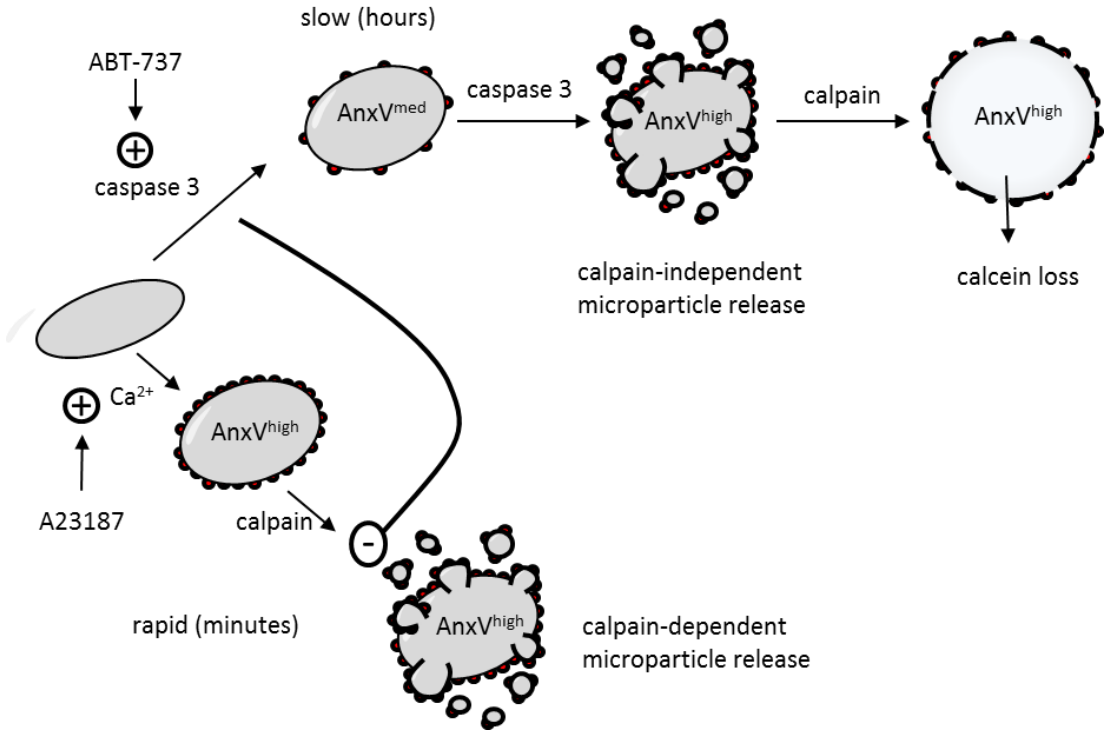

Figure 5.9: Apoptosis and microparticle release in human platelets

ABT-737-triggered responses in platelets *in vitro* are not a single apoptotic event, but a temporal sequence of stages that can be distinguished by their sensitivity to different inhibitors. Medium levels of PS exposure (medium Annexin V binding; $AnxV^{med}$) is triggered in a caspase-dependent manner. There is a slow progression to high levels of PS exposure (high Annexin V binding; $AnxV^{high}$), which is blocked by chelation of intracellular Ca^{2+}. PMPs are released in a calpain-independent manner from platelets with high levels of PS exposure, but absent from platelets with medium levels of PS exposure. Platelets slowly become secondary necrotic and feature loss of plasma membrane integrity (measured by loss of calcein), which is partially dependent on calpain. Caspase activation is required for all apoptotic responses, including PS exposure, PMP release, Ca^{2+} entry and loss of membrane integrity. Caspase activation also downregulates the rapid release of PMPs in response to A23187 and the acute increase in intracellular Ca^{2+} that follows.

Chapter 6 2-Aminoethoxydiphenyl borate as an inhibitor for microparticle release from platelets

6.1. Aim of study

Initially developed as a cheap and fast-acting antagonist for intracellular phosphoinositide signalling, 2-aminoethoxydiphenyl borate (2-APB) has now been established as a non-specific blocker of numerous ion channels, particularly Ca^{2+} channels. In preliminary experiments, 2-APB was found to significantly inhibit microparticle release from platelets in response to either pro-coagulant stimulation (A23187) or apoptosis (ABT-737). Neither of these two microparticle release pathways has been fully understood. In this chapter, the effects of 2-APB were characterised in an effort to better understand their inhibition.

6.2. 2-APB inhibits A23187-triggered microparticle release from platelets

When platelets were treated with 2-APB (100μM), PMP release was significantly inhibited compared to platelets treated with vehicle (DMSO) at all concentrations of A23187 tested (Figure 6.1A). PS exposure was only weakly affected (Figure 6.1B). When 10μM A23187 was used, the inhibitory effect of 2-APB on PMP release was concentration-dependent (pIC_{50} = 4.45 ± 0.09; IC_{50} approximately 35μM; Mean ± SEM; n = 5; Figure 6.1C), again with little effect on PS exposure (Figure 6.1D).

To assess the reversibility of 2-APB-mediated inhibition on PMP release, platelets were treated with 2-APB (100μM) or vehicle (DMSO) and then washed by centrifugation. This procedure of washing platelets resulted in slightly greater sensitivity to A23187 (for PMP release, pEC_{50} = 5.77 ± 0.20 prior to washing, pEC_{50} = 6.16 ± 0.12 after washing; Mean ± SEM; n = 5). After washing, platelets treated with 2-APB still released significantly fewer PMPs in response to A23187 (Figure 6.1F). Notably, there was no difference in PS exposure between 2-APB-treated platelets and vehicle control at any concentration of A23187 used (Figure 6.1G). Therefore, 2-APB inhibits A23187-triggered PMP release and this inhibition is not related to the weak inhibition of PS exposure.

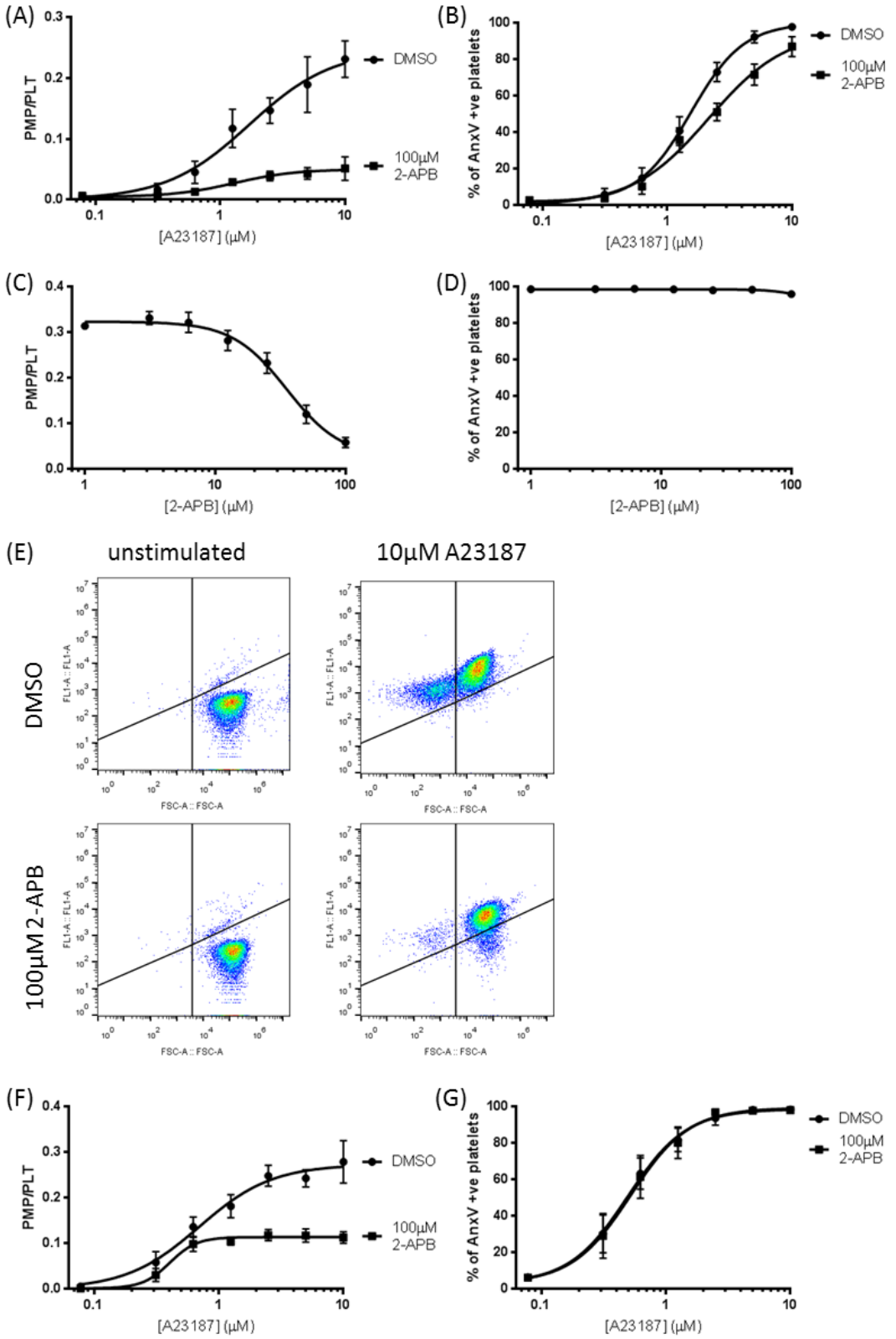
(A)
PMP/PLT
[A23187] (μM)
DMSO
100μM 2-APB
(B)
% of AnxV +ve platelets
[A23187] (μM)
DMSO
100μM 2-APB
(C)
PMP/PLT
[2-APB] (μM)
(D)
% of AnxV +ve platelets
[2-APB] (μM)
(E)
unstimulated
10μM A23187
DMSO
100μM 2-APB
FL1-A :: FL1-A
FSC-A :: FSC-A
(F)
PMP/PLT
[A23187] (μM)
DMSO
100μM 2-APB
(G)
% of AnxV +ve platelets
[A23187] (μM)
DMSO
100μM 2-APB

Figure 6.1: 2-APB inhibits A23187-triggered microparticle release from platelets

(A-B) Washed platelets (5 x 10^7 per ml) were treated with 100µM 2-APB or vehicle control (DMSO) for 30 minutes, prior to stimulation with A23187 for 10 minutes. PMP release and PS exposure were measured as described in Figure 3.4 (Mean ± SEM; n = 5). (C-D) Washed platelets (5 x 10^7 per ml) were treated with indicated concentrations of 2-APB (1 to 100µM), prior to stimulation with 10µM A23187 for 10 minutes. PMP release and PS exposure were measured as described in Figure 3.4 (Mean ± SEM; n = 5). (E) Density plots of platelets treated as indicated. Quadrants are defined as in Figure 3.4, with Annexin V FITC fluorescence on FL1-A. These plots are representative of data from 5 different donors. (F-G) Washed platelets (5 x 10^7 per ml) were treated with 100µM 2-APB or vehicle control (DMSO) for 30 minutes, followed by a second washing step by centrifugation (600g, 10 minutes) in the presence of apyrase (0.02U/ml) and PGE_1 (100nM). Resuspended platelets (5 x 10^7 per ml) were stimulated with A23187 for 10 minutes. PMP release and PS exposure were measured as described in Figure 3.4 (Mean ± SEM; n = 5).

6.3. DPBA and DP3A, two 2-APB analogues, inhibit A23187-triggered microparticle release

A small panel of compounds structurally related to 2-APB were used to investigate inhibition of A23187-triggered PMP release. Compounds used in this study include phenylborinic acid (PBA), dimesitylborinic acid (DMBA), diphenhydramine (DPHD), 2, 2-diphenyl tetrahydrofuran (DPTHF), diphenylborinic anhydride (DPBA) and 3-(diphenylphosphino)-1-propylamine (DP3A). For chemical structures of these compounds, please refer to Figure 1.5. Each of these compounds was applied to platelets in the same way as 2-APB (100μM, 30 minutes). PBA, DMBA, DPHD and DPTHF did not affect PMP release or PS exposure in response to A23187 (Figure 6.2A-B).

DPBA significantly inhibited PMP release in response to A23187 (Figure 6.2A). PS exposure was also inhibited, but the level of inhibition was not to the same extent as PMP release (Figure 6.2B). When 10μM A23187 was used, the inhibitory effect of DPBA on PMP release was concentration-dependent (pIC_{50} = 4.55 ± 0.32; IC_{50} approximately 28μM; Mean ± SEM; n = 5; Figure 6.2C). The small inhibitory effect of DPBA on A23187-triggered PS exposure was ambiguous (Figure 6.2D), as its predicted IC_{50} value (565.5μM) exceeded the range of concentrations used (1 to 100μM). It was therefore considered ineffective.

DP3A also significantly inhibited PMP release in response to A23187 (Figure 6.2A), yet PS exposure was not affected (Figure 6.2B). When 10μM A23187 was used, the inhibitory effect of DP3A on PMP release was also concentration-dependent (pIC_{50} = 4.38 ± 0.14; IC_{50} approximately 42μM; Mean ± SEM; n = 5; Figure 6.2C), again without any effect on PS exposure (Figure 6.2D).

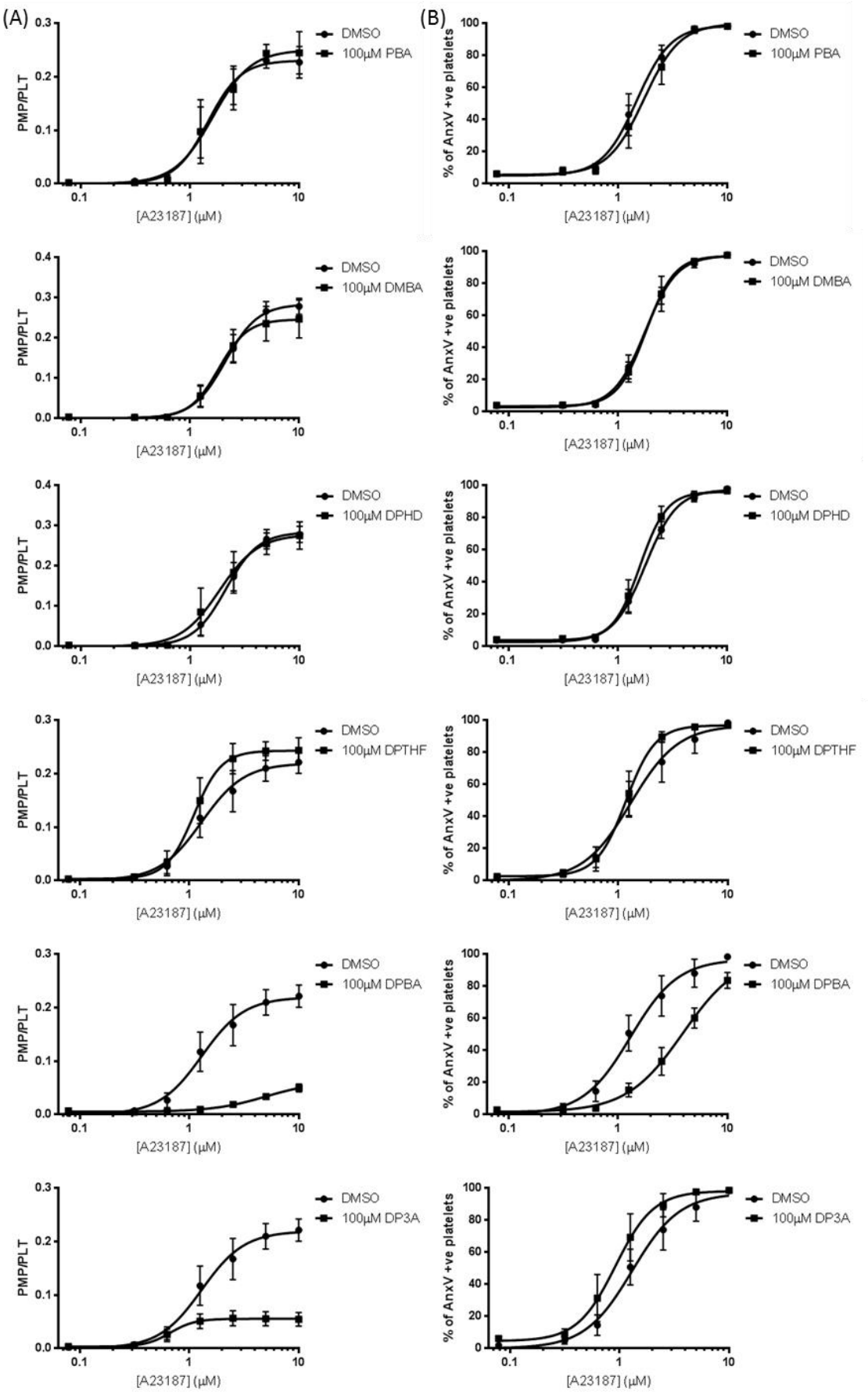
(A)
(B)
PMP/PLT
% of AnxV +ve platelets
[A23187] (μM)
DMSO
100μM PBA
100μM DMBA
100μM DPHD
100μM DPTHF
100μM DPBA
100μM DP3A

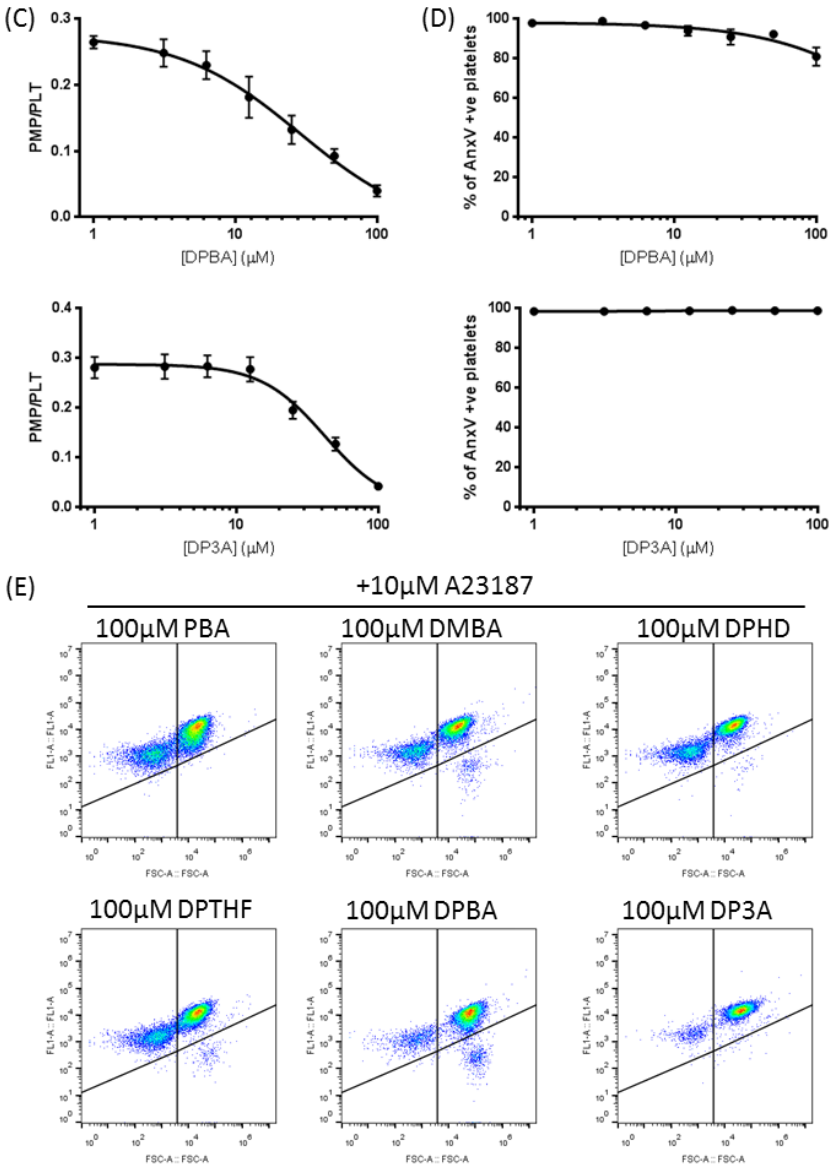

Figure 6.2: DPBA and DP3A inhibit A23187-triggered microparticle release

(A-B) Washed platelets (5 x 10^7 per ml) were treated as indicated with 100μM PBA, DMBA, DPHD, DPTHF, DPBA, DP3A or vehicle control (DMSO) for 30 minutes, prior to stimulation with A23187 for 10 minutes. PMP release and PS exposure were measured as described in Figure 3.4 (Mean ± SEM; n = 5). (C-D) Washed platelets (5 x 10^7 per ml) were treated with indicated concentrations of DPBA or DP3A (1 to 100μM), prior to stimulation with 10μM A23187 for 10 minutes. PMP release and PS exposure were measured as described in Figure 3.4 (Mean ± SEM; n = 5). (E) Density plots of platelets treated as indicated. Quadrants are defined as in Figure 3.4, with Annexin V FITC fluorescence on FL1-A. These plots are representative of data from 5 different donors.

6.4. 2-APB and DPBA, but not DP3A, inhibit A23187-triggered Ca^{2+} entry

2-APB and its analogues were tested for their effects on A23187-triggered Ca^{2+} entry by the Cal520-based intracellular $[Ca^{2+}]_i$ assay on a microplate reader as described previously. Treatment with A23187 (10μM) immediately triggered a large increase in fluorescence intensities of Cal520-loaded platelets, which indicated Ca^{2+} entry into the platelet cytosol (Figure 6.3A). Results were compared by area under curve for the Ca^{2+} trace throughout 10 minutes of A23187 stimulation (Figure 6.3B).

As control, platelets were treated with specific inhibitors of Ca^{2+} entry pathways, including SN-6 that blocks NCX (Harper and Sage, 2007), SAR7334 that blocks TRPC6 and thus NCCE (Hou et al., 2018; Zhou et al., 2018), Synta66 that blocks Orai1 and thus SOCE (van Kruchten et al., 2012; Tian et al., 2016) and a combination of SN-6, SAR7334 and Synta66. TRPC and Orai1 channels are known targets of 2-APB. Functions of TPRC channels are sometimes coupled to NCX (see introduction chapter 1.7). These inhibitors of calcium entry pathways, singly or combined, did not significantly affect Ca^{2+} entry in response to A23187 (Figure 6.3A, B; 1st row). As expected, inhibition of these pathways did not inhibit PMP release or PS exposure in response to A23187 (Figure 6.3C-D). These data confirmed that A23187 could bypass any contribution of plasma membrane Ca^{2+} entry pathways.

Treating platelets with 2-APB or DPBA, but not DP3A, inhibited A23187-triggered Ca^{2+} entry in a concentration-dependent manner (Figure 6.3A-B; 2nd, 4th and 5th rows). This suggested that there is no direct link between the inhibition of Cal520 fluorescence and inhibition of PMP release. Analogues that did not inhibit PMP release (PBA, DMBA, DPHD and DPTHF) had no effect on A23187-triggered Ca^{2+} entry into platelets (Figure 6.3A-B, 3rd row).

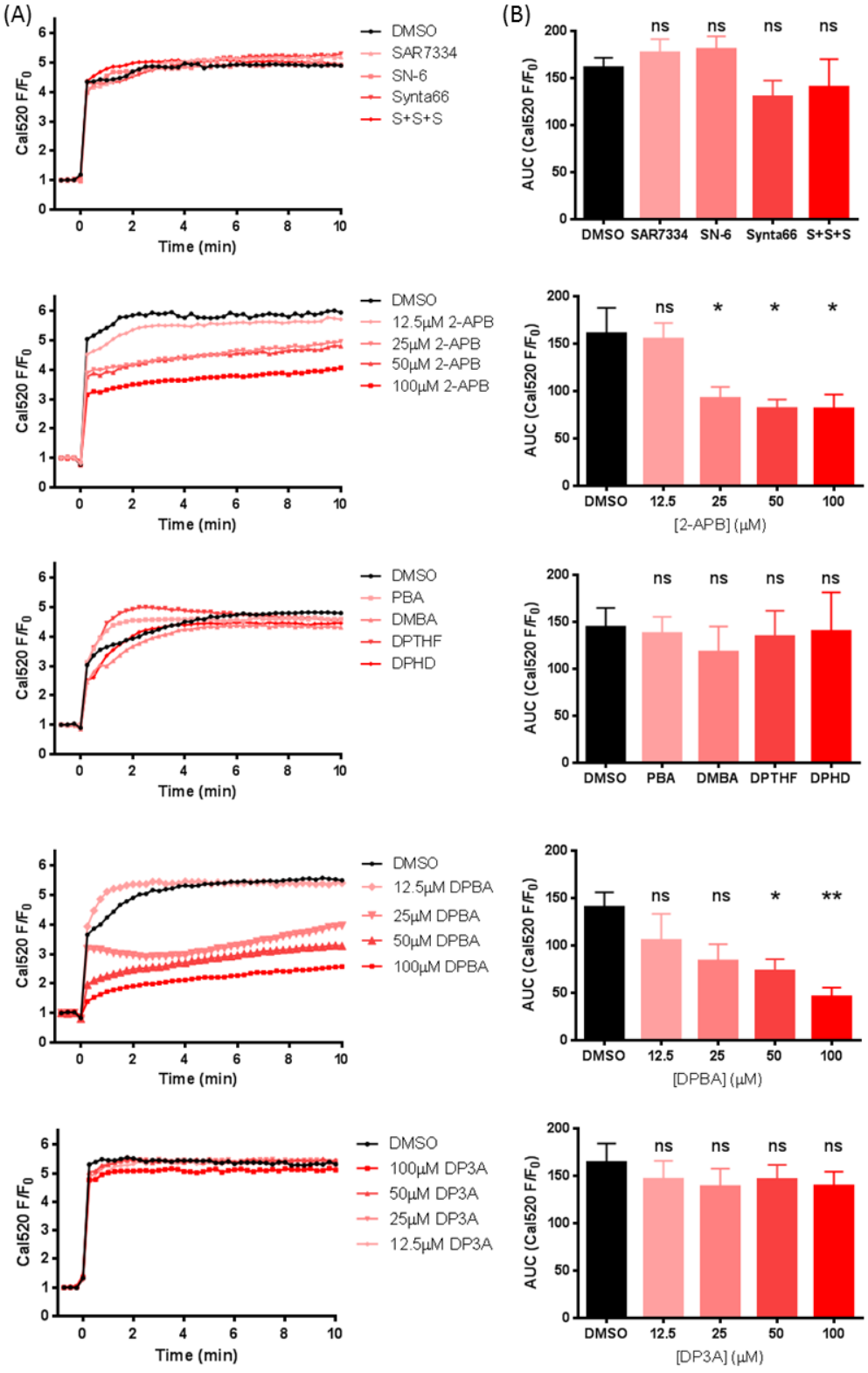
(A)
(B)
Cal520 F/F0
Time (min)
DMSO
SAR7334
SN-6
Synta66
S+S+S
AUC (Cal520 F/F0)
ns
DMSO SAR7334 SN-6 Synta66 S+S+S
12.5μM 2-APB
25μM 2-APB
50μM 2-APB
100μM 2-APB
*
DMSO 12.5 25 50 100
[2-APB] (μM)
PBA
DMBA
DPTHF
DPHD
DMSO PBA DMBA DPTHF DPHD
12.5μM DPBA
25μM DPBA
50μM DPBA
100μM DPBA
**
[DPBA] (μM)
100μM DP3A
50μM DP3A
25μM DP3A
12.5μM DP3A
[DP3A] (μM)

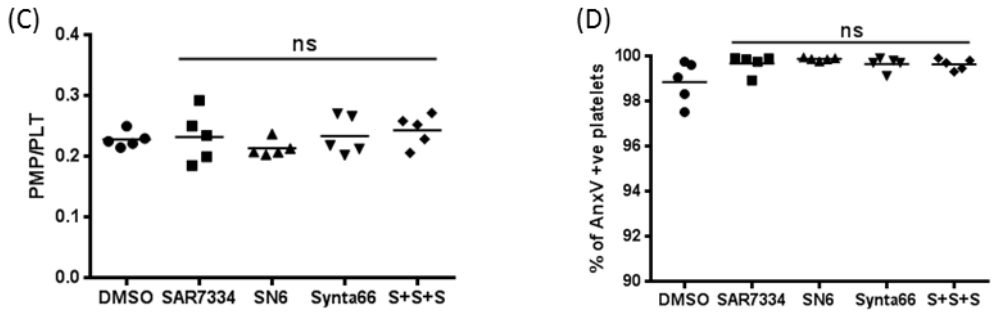

Figure 6.3: 2-APB and DPBA, but not DP3A, inhibit A23187-triggered Ca^{2+} entry

PRP was loaded with 500nM Cal520 for 10 minutes. Cal520-loaded washed platelets (5 x 10^7 per ml) were treated for 30 minutes with SN-6 (50µM), SAR7334 (1µM), Synta66 (10µM), SN-6 plus SAR7334 plus Synta66 (S+S+S), 2-APB (12.5 to 100µM), DPBA (12.5 to 100µM), DP3A (12.5 to 100µM), PBA (100µM), DMBA (100µM), DPTHF (100µM), DPHD (100µM) or vehicle control (DMSO), prior to stimulation with 10µM A23187 for 10 minutes. Cal520 fluorescence values were recorded every 15 seconds and normalised to the initial fluorescence intensity of vehicle-treated control prior to stimulation (F/F_0). (A) Representative Ca^{2+} trace. A23187 was added into platelets at minute 0. (B) AUC above basal was calculated (Mean ± SEM; n = 5; * $p < 0.05$, ** $p < 0.01$, ns: not significant, compared to vehicle). (C-D) Washed platelets (5 x 10^7 per ml) were treated with SAR7334 (1µM), SN6 (50µM), Synta66 (10µM), SAR7334 plus SN6 plus Synta66 (S+S+S), or vehicle control (DMSO) for 30 minutes, prior to stimulation with 10µM A23187 for 10 minutes. PMP release and PS exposure were measured as described in Figure 3.4 (n = 5; ns: not significant, compared to vehicle).

6.5. Mild changes in intracellular pH do not affect A23187-triggered microparticle release

It was investigated whether the effect of 2-APB on Cal520 fluorescence might be an artefact due to a change in cytosolic pH. Addition of NH_4Cl to unstimulated Cal520-loaded platelets, which was expected to result in rapid intracellular alkalinisation, gave a rapid increase in fluorescence. Similarly, addition of extracellular NaOH also increased the signals. By contrast, extracellular HCl had little effect on the Cal520 signals in unstimulated platelets (Figure 6.4A). Although A23187 rapidly increased Cal520 fluorescence to a plateau (which was expected as the dye was likely to be saturated with Ca^{2+} under these conditions), this fluorescence signal could be further increased by extracellular NH_4Cl or NaOH. It could also be decreased by extracellular HCl, suggesting that H^+ had entered stimulated platelets (Figure 6.4B). Together, these data showed that Cal520 fluorescence is highly sensitive to pH, consistent with a previous report that signals of intracellular Ca^{2+} indicators are subject to pH changes (Paredes et al., 2008).

To determine whether 2-APB affects cytosolic pH, platelets were loaded with the cell-permeable pH-sensitive carboxyfluorescein dye BCECF (Han and Burgess, 2010). As control, BCECF-loaded platelets were treated with HCl and NH_4Cl. NH_4Cl (100mM) immediately increased the BCECF signal to 1.27 ± 0.02 times that of vehicle-treated control (F/F_0; Mean ± SEM; n = 5; Figure 6.4C), indicating cytosolic alkalinisation, which slowly reversed. HCl (1mM) immediately decreased the BCECF signal to 0.90 ± 0.01 times that of vehicle (F/F_0; Mean ± SEM; n = 5; Figure 6.4C), indicating cytosolic acidification. By comparison, changes in BCECF signals induced by 2-APB or any of the analogues over 30 minutes of incubation were all within the range of 0.95 to 1.12 (F/F_0; n = 5; Figure 6.4D). This suggested that 2-APB did not significantly affect cytosolic pH. Moreover, the effect of 2-APB and DPBA on Cal520 fluorescence was not an artefact of decreased cytosolic pH.

Furthermore, it was tested if PMP release could be affected by intracellular pH. Platelets were treated with HCl (1mM) or NH_4Cl (100mM), followed by immediate stimulation with A23187 to temporally match the rapid induction of pH changes. PMP release and PS exposure in response to A23187 was not significantly affected by modulation of pH in either direction (Figure 6.4E-F). This suggested that a change in cytosolic pH does not account for the inhibitory effect of 2-APB on PMP release.

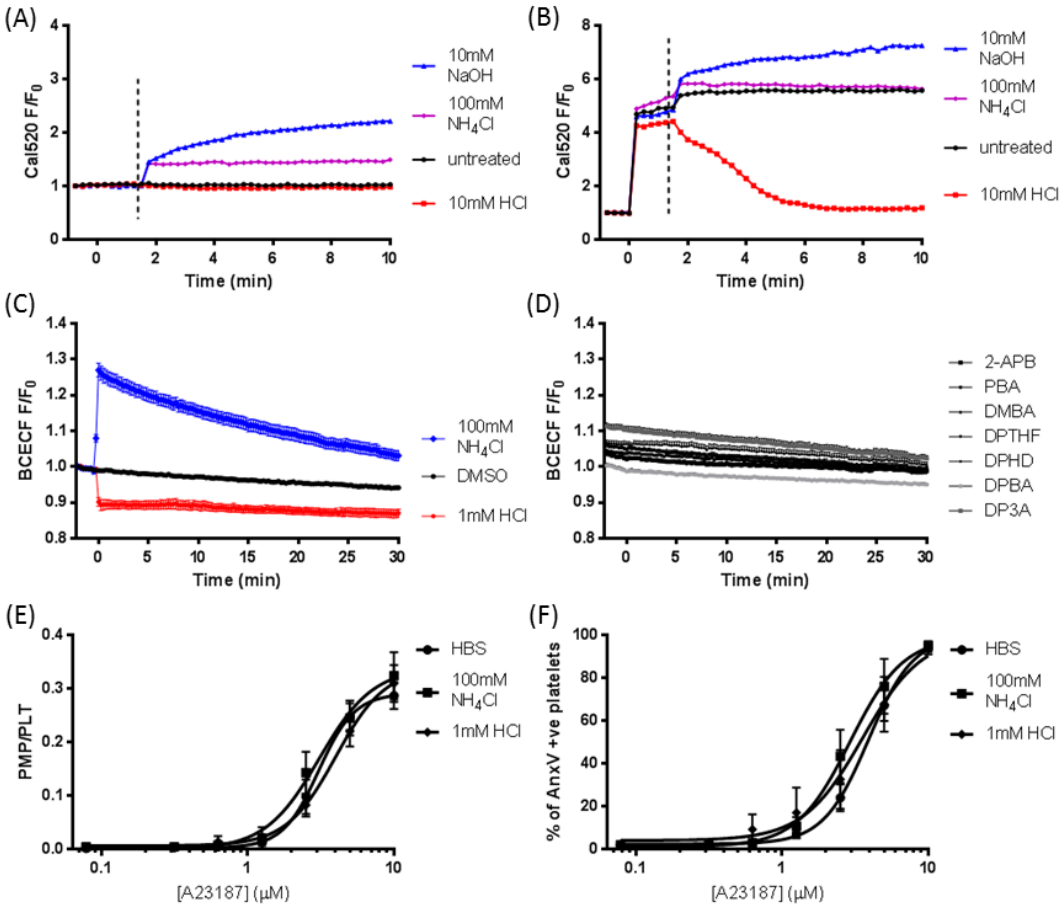

Figure 6.4: Mild changes in intracellular pH do not affect A23187-triggered microparticle release

(A-B) PRP was loaded with 500nM Cal520 for 10 minutes. (A) Cal520-loaded washed platelets (5 x 10^7 per ml) were treated with HCl (10mM), NaOH (10mM) or NH_4Cl (100mM) at the time point indicated by the dashed line. (B) Cal520-loaded washed platelets (5 x 10^7 per ml) were stimulated with 10µM A23187 at minute 0, followed by HCl (10mM), NaOH (10mM) or NH_4Cl (100mM) at the time point indicated by the dashed line. These traces are representative of data from 5 different donors. (C-D) PRP was loaded with 1µg/ml BCECF for 30 minutes. BCECF-loaded washed platelets (5 x 10^7 per ml) were treated as indicated. Fluorescence was recorded for 30 minutes and normalised to the initial fluorescence intensity of vehicle control (DMSO) prior to stimulation (F/F_0). (C) Platelets were treated with acid (1mM HCl) or base (100mM NH_4Cl) at minute 0 (Mean ± SEM; n = 5). (D) Platelets were manually added with 2-APB or its analogues (all 100µM), immediately before the recording started (Mean ± SEM; n = 5). (E-F) Washed platelets (5 x 10^7 per ml) were treated with 1mM HCl, 100mM NH_4Cl or vehicle control (HBS), immediately followed by stimulation with A23187 for 10 minutes. PMP release and PS exposure were measured as described in Figure 3.4 (Mean ± SEM; n = 5).

6.6. 2-APB does not inhibit microparticle release by blocking Ca^{2+}-activated K^+ channels

2-APB has been reported to inhibit Ca^{2+}-activated K^+ channels (K_{Ca}) following activation of SOCE in human erythroleukemia cells (Littlechild et al., 2015). These channels might be required for PS exposure and PMP release (Wolfs et al., 2006). Experiments were performed to test if PMP release was associated with K_{Ca} channels, the presence of which has been recorded in platelets (Mahaut-Smith, 2012).

Quinine and tetra-ethyl ammonium (TEA), two non-selective blockers (Fatherazi and Cook, 1991), were used to block K_{Ca} channels. They have not been applied to platelets before. The concentrations used were slightly higher than the saturated effective dose previously reported in other cell lines (Kozak et al., 1998). Neither quinine nor TEA significantly affected PMP release or PS exposure in response to A23187 (Figure 6.5).

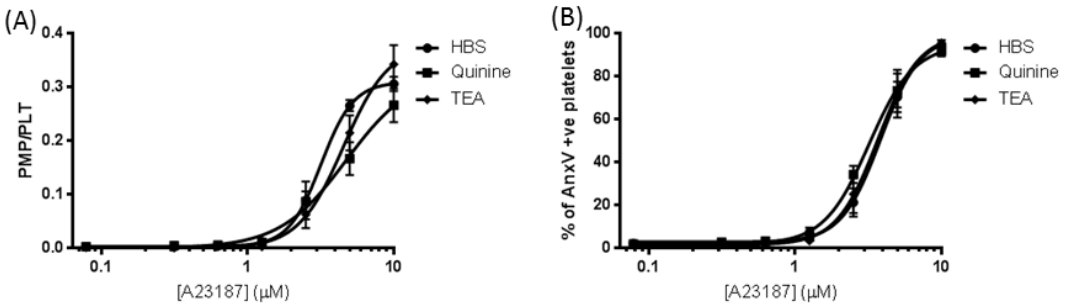

Figure 6.5: 2-APB does not inhibit microparticle release by blocking Ca^{2+}-activated K^+ channels

Washed platelets (5 x 10^7 per ml) were treated with 500μM quinine, 30mM TEA or vehicle control (HBS) for 30 minutes, prior to stimulation with A23187 for 10 minutes. PMP release and PS exposure were measured as described in Figure 3.4 (Mean ± SEM; n = 5).

6.7. 2-APB, DPBA and DP3A inhibit streptolysin O-triggered microparticle release

Similar to A23187, streptolysin O (SL-O) triggers PMP release in the presence of extracellular Ca^{2+} in a concentration-dependent manner (Figure 3.5). Perforation of platelet membrane by SL-O bypasses all channels on the plasma membrane, not limited to Ca^{2+} channels, and enables Ca^{2+} to reach its intracellular target calpain (Figure 3.6). To test if any membrane channel is involved in 2-APB-mediated inhibition of PMP release, SL-O (1000U/ml) was applied to platelets treated with 2-APB and its analogues.

Treatment with calpeptin inhibited SL-O-triggered PMP release (Figure 6.6A), which confirmed its dependence on calpain activity. 2-APB, DPBA and DP3A significantly inhibited PMP release in response to SL-O, while PBA, DMBA, DPHD and DPTHF did not (Figure 6.6A). PS exposure in response to SL-O was not prevented by any of these drugs (Figure 6.6B). 2-APB, DPBA and DP3A did not inhibit efficacy of SL-O in terms of membrane perforation, as calcein leakage from SL-O-treated platelets was not significantly prevented by these drugs (Figure 6.6D).

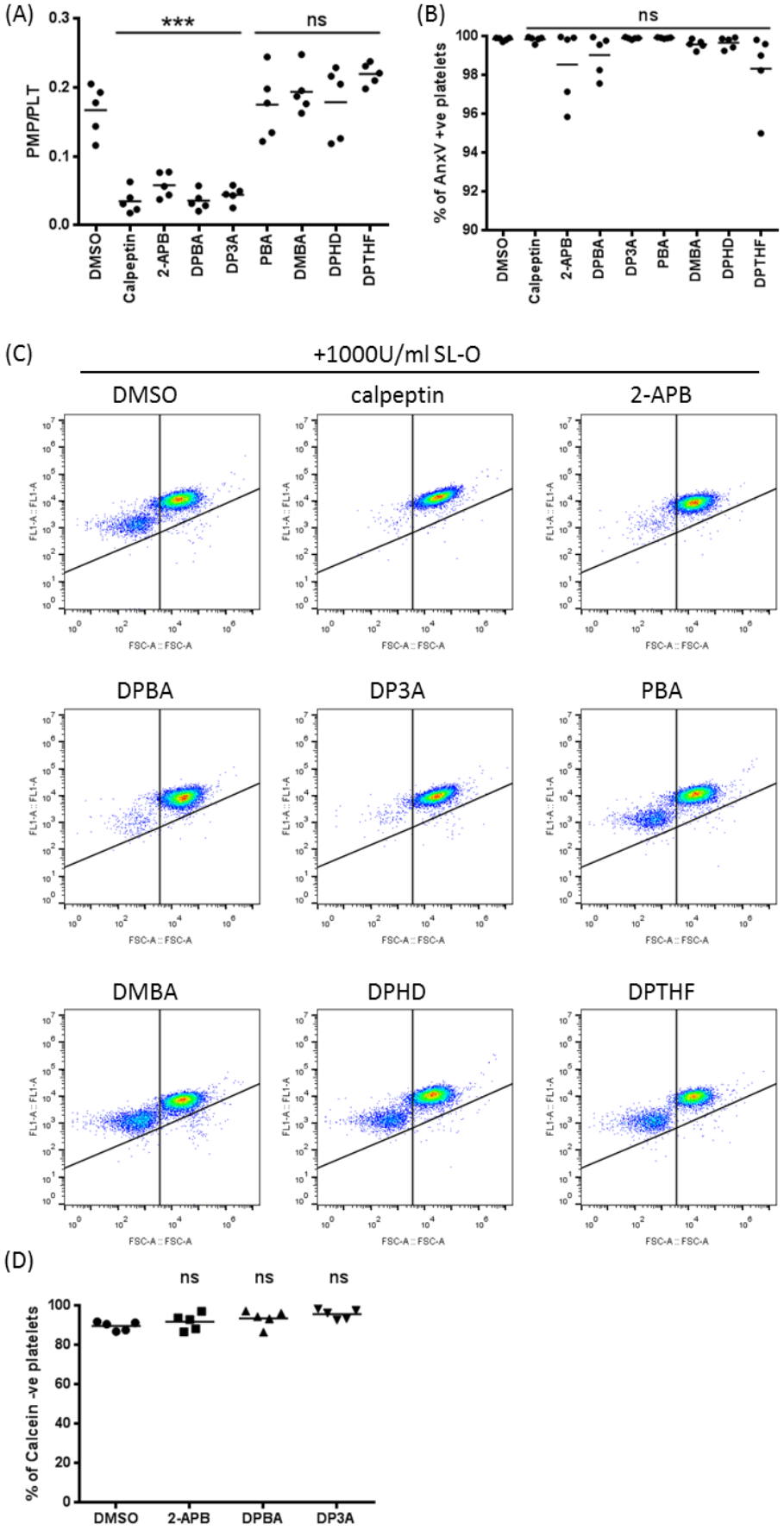
(A)
PMP/PLT
***
ns
DMSO
Calpeptin
2-APB
DPBA
DP3A
PBA
DMBA
DPHD
DPTHF
(B)
% of AnxV +ve platelets
ns
(C)
+1000U/ml SL-O
DMSO
calpeptin
2-APB
DPBA
DP3A
PBA
DMBA
DPHD
DPTHF
FL1-A :: FL1-A
FSC-A :: FSC-A
(D)
% of Calcein -ve platelets
ns
ns
ns
DMSO
2-APB
DPBA
DP3A

Figure 6.6: 2-APB, DPBA and DP3A inhibit streptolysin O-triggered microparticle release

(A-B) Washed platelets (5 x 10^7 per ml) were treated with calpeptin (140μM), 2-APB or its analogues (100μM), or vehicle control (DMSO) for 30 minutes, prior to stimulation with 1000U/ml SL-O in the presence of 2mM $CaCl_2$ for 10 minutes. PMP release and PS exposure were measured as described in Figure 3.4 (n = 5; *** $p < 0.001$, ns: not significant, compared to vehicle). (C) Density plots of platelets stimulated with 1000U/ml SL-O. Quadrants are defined as in Figure 3.4, with Annexin V FITC fluorescence on FL1-A. These plots are representative of data from 5 different donors. (D) PRP was loaded with 1μM calcein for 10 minutes. Calcein-loaded washed platelets (5 x 10^7 per ml) were treated with 100μM 2-APB, DPBA or DP3A, or vehicle control (DMSO) for 30 minutes, prior to stimulation with 1000U/ml SL-O in the presence of 2mM $CaCl_2$ for 10 minutes. Loss of calcein fluorescence was measured as described in Figure 3.6 (n = 5; ns: not significant, compared to vehicle).

6.8. 2-APB and DPBA, but not DP3A, partially inhibit A23187-triggered calpain activity

Calpain is required for the Ca^{2+}-dependent PMP release following stimulation with either A23187 or SL-O (Figures 4.9 & 6.6). Calpain inhibition by 2-APB was reported in HeLa cells (Splettstoesser et al., 2007). Therefore, it was tested whether 2-APB and its analogues affected calpain activity in platelets. Intracellular targets of calpain in platelets include talin (Figure 4.9), phospholipid flippase ATP8A1 (Jing et al., 2019), caspase 3 (Figure 5.7), and protein tyrosine phosphatase 1C (PTP1C) (Falet et al., 1998).

Calpain activity was measured by the extent of cleavage of these proteins via Western blot. As control, A23187 stimulation and its subsequent Ca^{2+} influx led to cleavage of talin, ATP8A1, caspase 3 and PTP1C, which was inhibited in the presence of calpeptin (Figure 6.7A). At a high concentration of 100µM, 2-APB and DPBA partially inhibited calpain-dependent cleavage of all four proteins (Figure 6.7A), which was not observed following treatment with DP3A, PBA, DMBA, DPHD or DPTHF (Figure 6.7A). Inhibitory effects of 2-APB and DPBA on calpain activity were concentration-dependent (Figure 6.7B). Cleavage of talin and caspase 3 by calpain was quantified (Figure 6.7C).

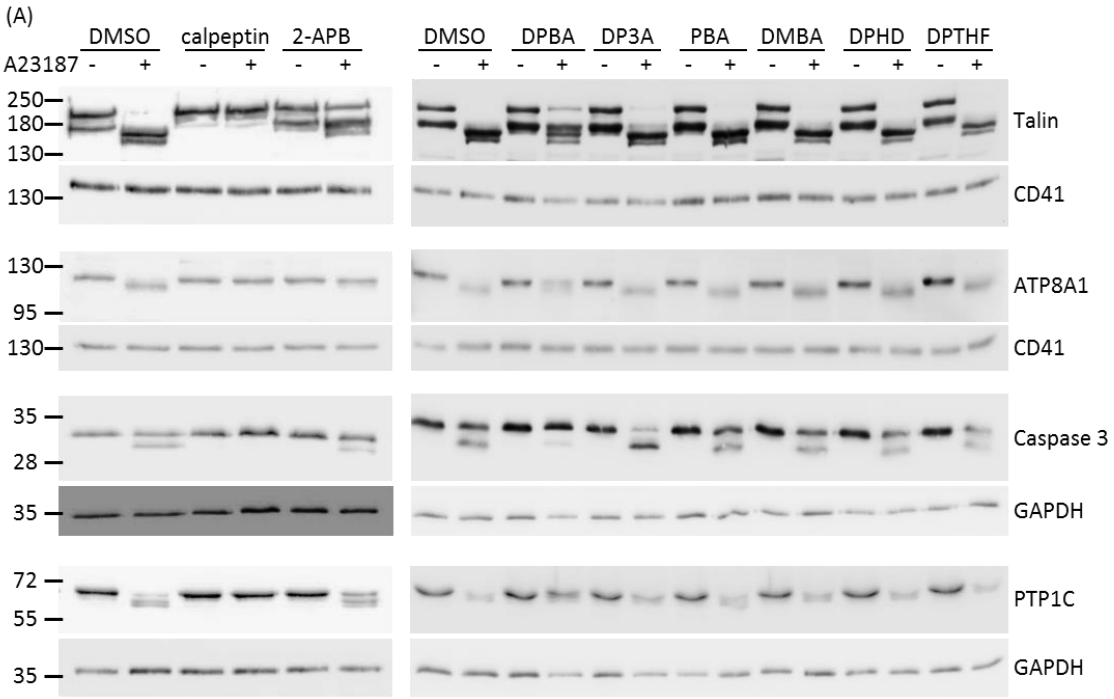

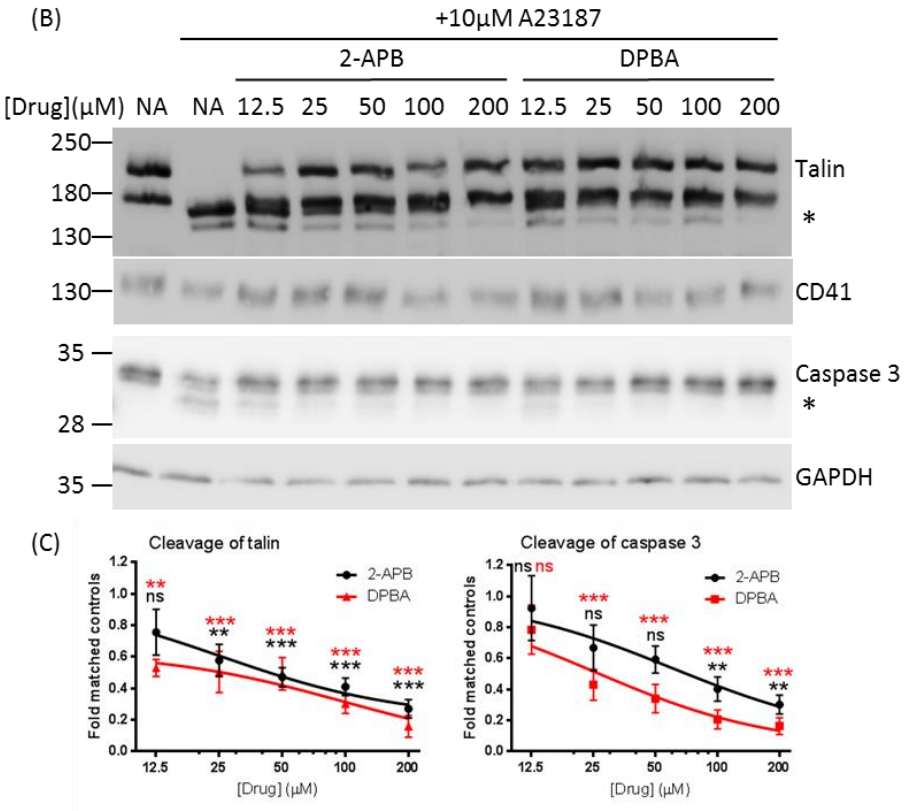

Figure 6.7: 2-APB and DPBA, but not DP3A, partially inhibit A23187-triggered calpain activity

Washed platelets (5 x 10^8 per ml) were treated with the indicated drugs for 30 minutes, prior to stimulation with A23187 (+) or vehicle (-) for 10 minutes and lysed with RIPA buffer. Proteins (20µg) were separated with SDS-PAGE on a 6% poly-acrylamide gel, probed for talin as described in Figure 4.9 and ATP8A1 with anti-ATP8A1 antibody (1 in 1000), stripped and re-probed for CD41 as a loading control. Also, proteins (20µg) were separated with SDS-PAGE on a 12% poly-acrylamide gel, probed for caspase 3 as described in Figure 5.5 and PTP1C with anti-PTP1C antibody (1 in 1000), stripped and re-probed for GAPDH as a loading control. (A) Platelets were treated with calpeptin (140µM), 2-APB ,DPBA, DP3A, PBA, DMBA, DPHD, DPTHF (100µM), or vehicle control (DMSO). (B) Platelets were treated with 2-APB (12.5µM to 200µM), DPBA (12.5µM to 200µM), or vehicle control (DMSO; NA). Asterisks (*) indicate the cleaved protein fragment to be quantified. (C) Intensity of cleaved protein fragment was divided by intensity of the loading control, which was then normalised to that of matched vehicle controls. Dose-response inhibition curves were plotted (Mean ± SEM; n = 5; ** $p < 0.01$, *** $p < 0.001$, ns: not significant, compared to matched vehicle controls).

6.9. 2-APB inhibits ABT-737-triggered microparticle release and Ca^{2+} entry

To investigate whether 2-APB also affects PMP release during apoptosis *in vitro*, platelets treated with 2-APB (100µM) were stimulated with ABT-737 in the presence of extracellular $CaCl_2$. Although PS exposure was not affected (Figure 6.8A-B), platelets treated with 2-APB showed lower levels of PMP release (Figure 6.8C). Ca^{2+} entry in response to ABT-737 was inhibited (Figure 6.8D). Secondary necrosis, measured by loss of calcein, was not affected (Figure 6.8E).

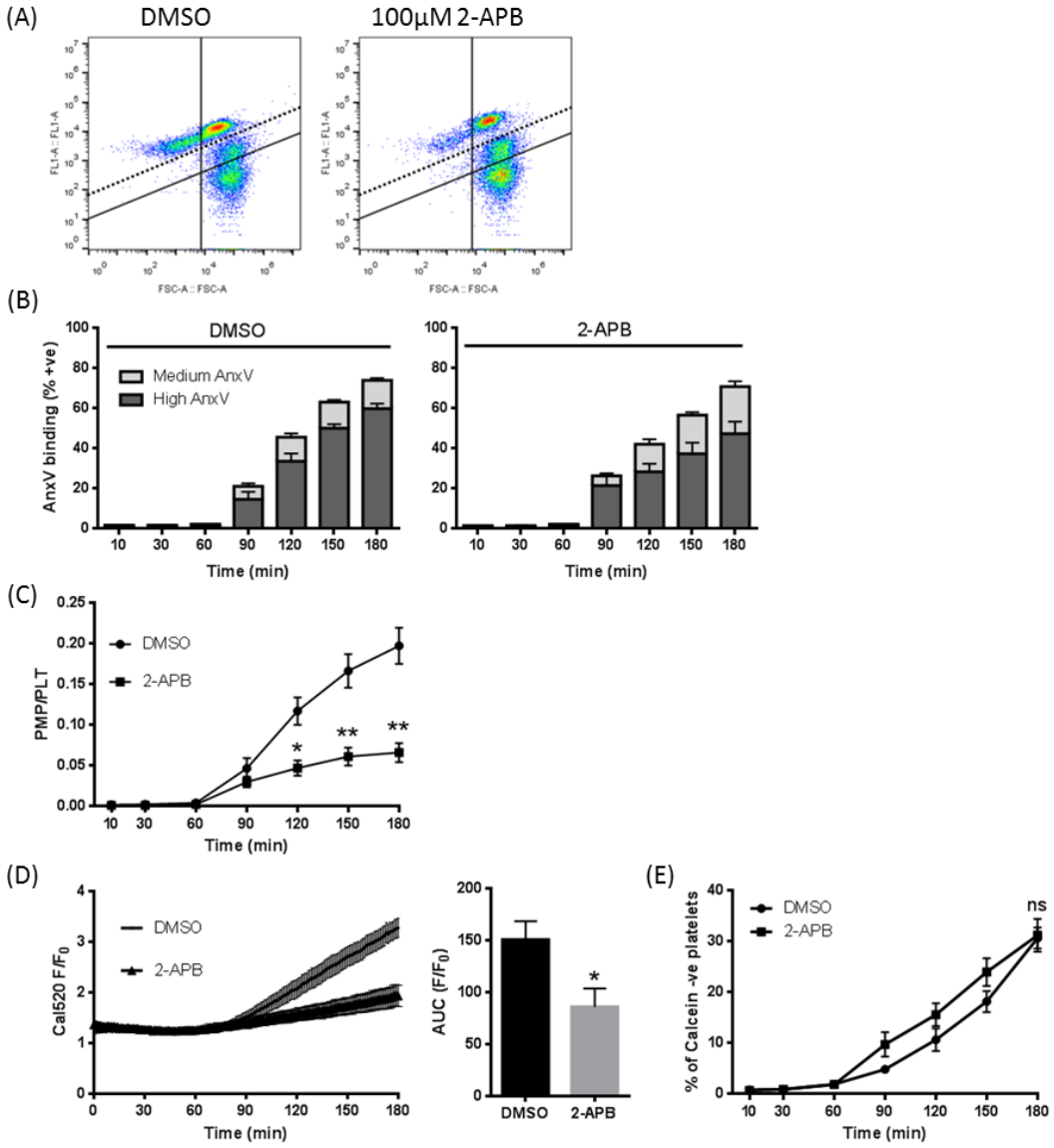

Figure 6.8: 2-APB inhibits ABT-737-triggered microparticle release and Ca^{2+} entry

Washed platelets (5 x 10^7 per ml) were treated with 2-APB (100µM) or vehicle control (DMSO) for 30 minutes, prior to stimulation with 10µM ABT-737 in the presence of 2mM $CaCl_2$ for 3 hours. (A) Density plots of platelets treated as indicated after 3 hours of ABT-737 treatment. Quadrants are defined as in Figure 5.1, with Annexin V FITC fluorescence on FL1-A. These plots are representative of data from 5 different donors. (B) PS exposure, detected as medium and high Annexin V binding, was measured as described in Figure 5.1 (Mean ± SEM; n = 5). (C) PMP release at the indicated time points was measured as described in Figure 3.4 (Mean ± SEM; n = 5; * $p < 0.05$, ** $p < 0.01$, compared to vehicle at the same time point). (D) PRP was loaded with 500nM Cal520. Cal520-loaded washed platelets (5 x 10^7 per ml) were treated as indicated. Calcium trace was recorded as described in Figure 5.1 and AUC above basal was calculated (Mean ± SEM; n = 5; * $p < 0.05$ compared to vehicle). (E) PRP was loaded with 1µM calcein. Calcein-loaded washed platelets (5 x 10^7 per ml) were treated as indicated. Loss of calcein fluorescence was measured as described in Figure 3.6 at the indicated time points (Mean ± SEM; n = 5; ns: not significant, compared to vehicle).

6.10. ABT-737-triggered microparticle release is independent of Ca^{2+} entry pathways on the plasma membrane

Inhibition of ABT-737-triggered PMP release by 2-APB was associated with reduced Ca^{2+} entry (Figure 6.8D), so inhibitors of calcium entry pathways SN6, SAR7334 and Synta66 were screened. These inhibitors, singly or combined, did not significantly affect PS exposure, PMP release or Ca^{2+} entry in response to ABT-737 (Figure 6.9). Therefore, NCX, TRPC6 and Orai1 are not involved in Ca^{2+} entry or PMP release during apoptosis. Inhibition of Ca^{2+} entry pathways by 2-APB does not explain its effect on ABT-737-triggered PMP release.

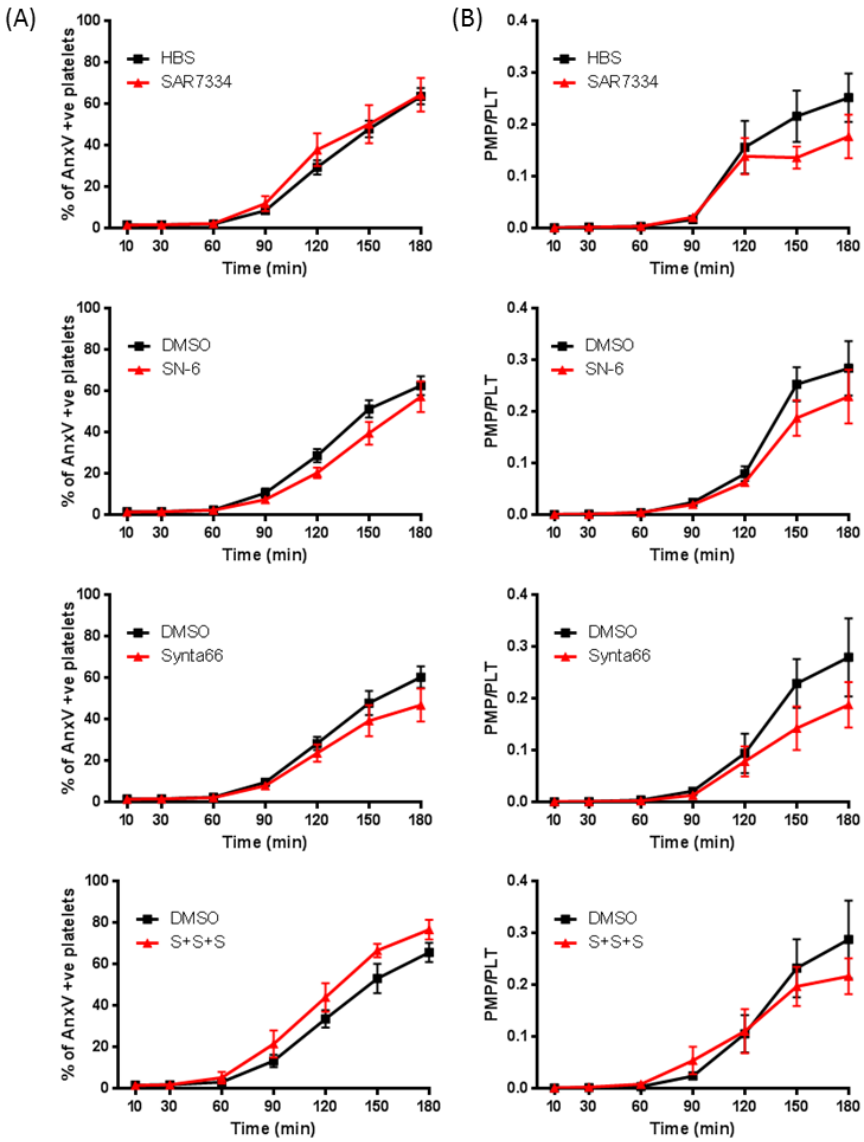

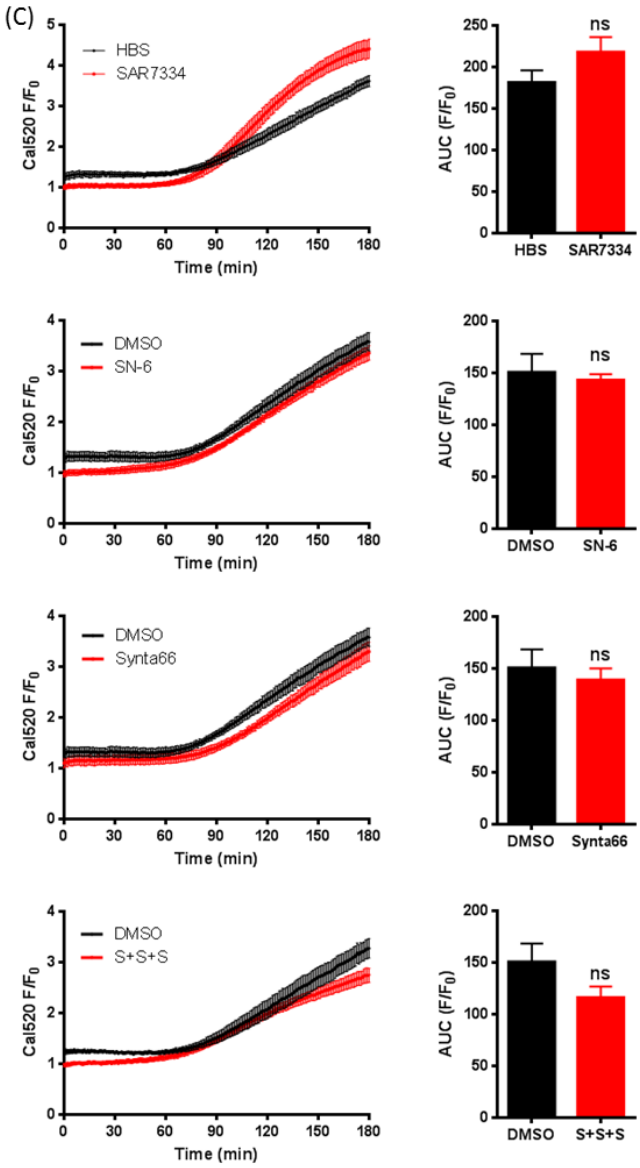

Figure 6.9: ABT-737-triggered microparticle release is independent of Ca^{2+} entry pathways on the plasma membrane

Washed platelets (5 x 10^7 per ml) were treated with SAR7334 (1µM) or vehicle (HBS), SN-6 (50µM), Synta66 (10µM), SAR7334 plus SN-6 plus Synta66 (S+S+S), or vehicle control (DMSO) for 30 minutes, prior to stimulation with 10µM ABT-737 in the presence of 2mM $CaCl_2$ for 3 hours. (A-B) PS exposure and PMP release were measured as described in Figure 5.1 (Mean ± SEM; n = 5). (C) Calcium trace in Cal520-loaded platelets was recorded for 180 minutes as described in Figure 5.1. AUC above basal was calculated (Mean ± SEM; n = 5; ns: not significant, compared to vehicle).

6.11. ABT-737-triggered microparticle release may be dependent on gap junction channels

Apart from selective Ca^{2+} channels, 2-APB also inhibits gap junctions that potentially act as routes for Ca^{2+} flow into cells (Griffith et al., 2005; Neijssen et al., 2005). Connexins and pannexins, two types of gap junction subunits, were reported in platelets (Taylor et al., 2014; Vaiyapuri et al., 2015). To investigate whether gap junctions are the effective target of 2-APB in terms of ABT-737-triggered PMP release, platelets were treated with carbenoxolone and probenecid, two non-specific gap junction inhibitors. Concentrations of these drugs used were similar to those in previous studies (Packham et al., 1996; Ye et al., 2009).

Carbenoxolone and probenecid had divergent effects on ABT-737-triggered responses in platelets. PS exposure, at medium but not high levels, was inhibited by carbenoxolone, yet PMP release and secondary necrosis were not affected. On the other hand, PS exposure, at high but not medium levels, PMP release and secondary necrosis were inhibited by probenecid (Figure 6.10A-C). This suggested that ABT-737-triggered PMP release was associated with platelets that showed high levels of PS exposure and loss of plasma membrane integrity, consistent with previous findings derived from chelating intracellular Ca^{2+} by BAPTA (Figures 5.1 & 5.2). However, Ca^{2+} entry was reduced when platelets were treated with either carbenoxolone or probenecid (Figure 6.10D), so the exact link between PMP release and Ca^{2+} entry during apoptosis *in vitro* remains unclear.

To further understand how gap junctions may contribute to PMP release and Ca^{2+} entry, platelets were treated with more selective inhibitors. Gap27, a peptide derived from Cx43, has high specificities for connexin subtypes Cx40 and Cx43 (Vaiyapuri et al., 2013). On the other hand, ^{10}Panx, a Panx1 mimetic peptide, specifically blocks the pannexin subtype Panx1 (Pelegrin and Surprenant, 2006). Concentrations of these drugs used were similar to those in previous studies (Manohar et al., 2012; Vaiyapuri et al., 2012). Neither peptide had any effect on A23187-triggered PS exposure, PMP release or Ca^{2+} entry (Figure 6.10E-G).

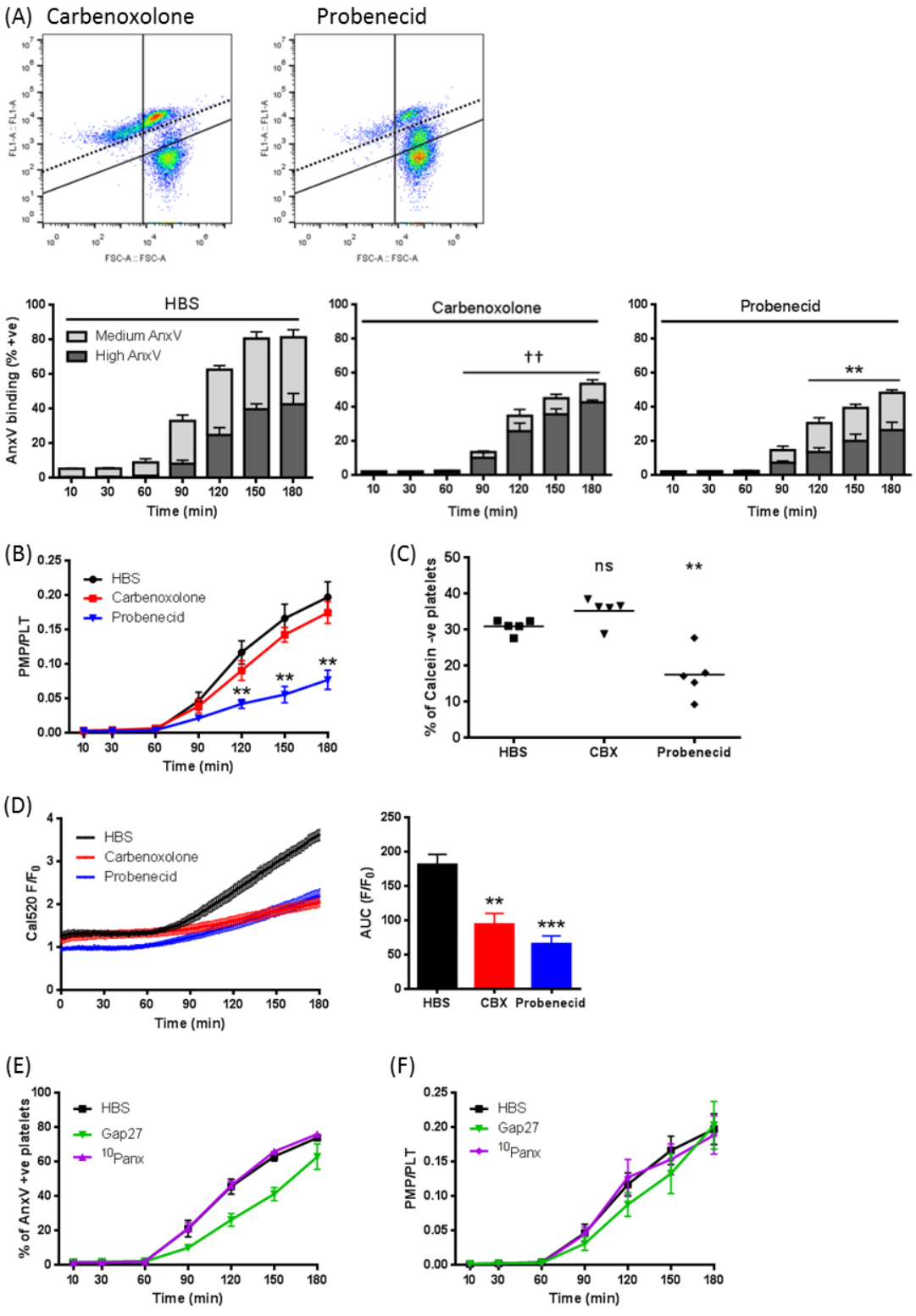
(A) Carbenoxolone
Probenecid
FL1-A :: FL1-A
FSC-A :: FSC-A
HBS
Carbenoxolone
Probenecid
Medium AnxV
High AnxV
AnxV binding (% +ve)
Time (min)
††
**
(B)
HBS
Carbenoxolone
Probenecid
PMP/PLT
Time (min)
(C)
ns
**
% of Calcein -ve platelets
HBS
CBX
Probenecid
(D)
Cal520 F/F0
AUC (F/F0)
***
(E)
Gap27
10Panx
% of AnxV +ve platelets
(F)

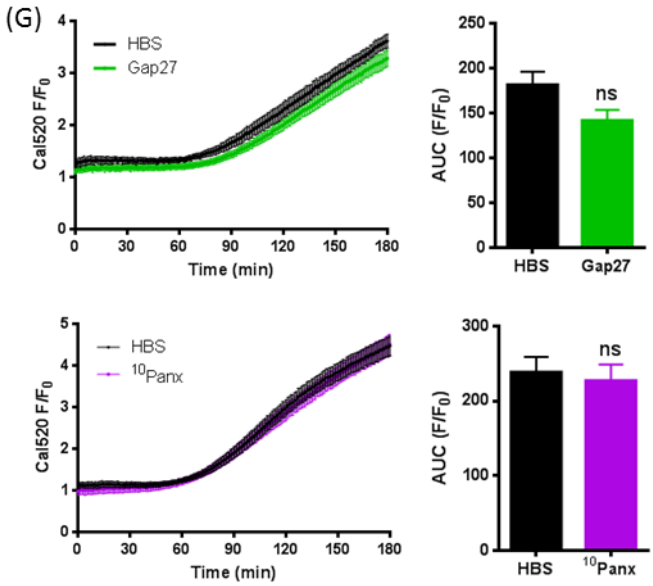

Figure 6.10: ABT-737-triggered microparticle release and Ca^{2+} entry might be dependent on gap junction channels

(A-D) Washed platelets (5 x 10^7 per ml) were treated with carbenoxolone (CBX; 30µM), probenecid (2mM), or vehicle control (HBS) prior to stimulation with 10µM ABT-737 in the presence of 2mM $CaCl_2$ for 3 hours. (A) PS exposure was measured as described in Figure 5.1 (Mean ± SEM; n = 5; ** $p < 0.01$, compared to high Annexin V binding of vehicle; †† $p < 0.01$, compared to medium Annexin V binding of vehicle). Density plots are representative of data from 5 different donors. (B) PMP release was measured as described in Figure 5.1 (Mean ± SEM; n = 5; ** $p < 0.01$, compared to vehicle). (C) Loss of calcein fluorescence in calcein-loaded platelets after 180 minutes was measured as described in Figure 3.6 (n = 5; ** $p < 0.01$, ns: not significant, compared to vehicle). (D) Calcium trace in Cal520-loaded platelets was recorded as described in Figure 5.1. AUC above basal was calculated (Mean ± SEM; n = 5; ** $p < 0.01$, *** $p < 0.001$, compared to vehicle). (E-G) Washed platelets (5 x 10^7 per ml) were treated with Gap27 (100µg/ml), ^{10}Panx (200µM) or vehicle control (HBS), prior to stimulation with 10µM ABT-737 in the presence of 2mM $CaCl_2$ for 3 hours. (E) PS exposure was measured as described in Figure 5.1 (Mean ± SEM; n = 5). (F) PMP release was measured as described in Figure 5.1 (Mean ± SEM; n = 5). (G) Calcium trace was record in Cal520-loaded platelets as described in Figure 5.1. AUC above basal was calculated (Mean ± SEM; n = 5; ns: not significant, compared to vehicle).

6.12. Discussion

In this chapter, it was found that 2-aminoethoxydiphenyl borate (2-APB), a cell-permeable modulator of numerous ion channels, inhibited PMP release in response to A23187. It was surprising since A23187 was expected to bypass any contribution of plasma membrane Ca^{2+} channels. It is not likely that 2-APB directly inhibits scramblase TMEM16F that leads to PS exposure, because platelet Annexin V binding was largely unaffected under conditions where PMP release was almost completely inhibited. Although a small inhibition of platelet Annexin V binding was observed when 2-APB was present, this was fully reversed by washing the platelets, whereas inhibition of PMP release was not readily reversed.

To understand this effect, a panel of structurally related compounds was used, which included DPBA, DP3A, DMBA, DPHD, DPTHF and PBA. Of these compounds, DPBA and DP3A inhibited PMP release with similar potency to 2-APB, so neither the amine group nor the boron-oxygen core is essential for inhibition. Interestingly, the pattern of active and inactive analogues was similar to that reported for inhibiting interleukin (Il)-1β release from murine macrophages (Baldwin et al., 2017). In that study, the effect was attributed to inhibition of NLRP3 inflammasome. Since Il-1β may be released in microparticles (MacKenzie et al., 2001), inhibition of microparticle release could potentially contribute to inhibition of Il-1β release.

PMP release in response to streptolysin O (SL-O) was also inhibited by 2-APB, DPBA and DP3A. This showed that 2-APB-mediated inhibition of Ca^{2+}-induced PMP release could not be attributed to inhibition of plasma membrane ion channels, because these channels were effectively bypassed by the use of SL-O. Consistent with this, blockers of Orai1, TRPC6, NCX or K_{Ca} channels had no effect on A23187-triggered PMP release. On the other hand, PBA, DMBA, DPHD and DPTHF did not inhibit PMP release when they could access intracellular proteins in response to stimulation with SL-O. Therefore, lack of inhibition by these 2-APB analogues was not due to insufficient penetration of membrane. It is likely that 2-APB, DPBA and DP3A have an intracellular target in PMP release separate to plasma membrane ion channels, for which the inactive analogues have low affinities.

At first sight, the observation that 2-APB inhibited A23187-induced increase in Cal520 signals leads to the opposite conclusion, as it suggested that 2-APB inhibited the rise in $[Ca^{2+}]_i$. It is unclear whether this is a real inhibition of $[Ca^{2+}]_i$, or an artefact on Cal520 signals. It was tested whether 2-APB induced cytosolic acidification, as 2-APB has been reported to acidify the cytoplasm of Jurkat T lymphocytes (Chokshi et al., 2012), although this effect might be specific to certain cell types. Cal520 signals were also shown to be pH-sensitive. However, 2-APB did not significantly affect intracellular pH, as measured by BCECF fluorescence, suggesting that cytosolic acidification does not explain the reduced Cal520 signals. In addition, extracellular addition of NH_4Cl and HCl did alter intracellular pH without affecting PMP release. Therefore, 2-APB does not inhibit PMP release by altering intracellular pH.

It is possible that 2-APB does inhibit the A23187-triggered increase in $[Ca^{2+}]_I$ rather than artefactually decrease Cal520 signals, although the mechanism is unclear. Data showed that it did not involve Orai1 or TRPC6, the major channels for Ca^{2+} entry into platelets. Inhibition of Ca^{2+} signalling could account for the weak inhibition of PS exposure and calpain activity by 2-APB and DPBA. However, it cannot fully explain inhibition of PMP release, because DP3A did not have any effect on Ca^{2+} signalling, PS exposure or calpain activity. Together, these data suggest that there is a target of 2-APB, independent of plasma membrane ion channels or Ca^{2+} signalling, that is required for PMP release (Figure 6.11). DP3A is likely to inhibit the same target without these other effects. DP3A may be a better scaffold from which to develop a more selective inhibitor of PMP release.

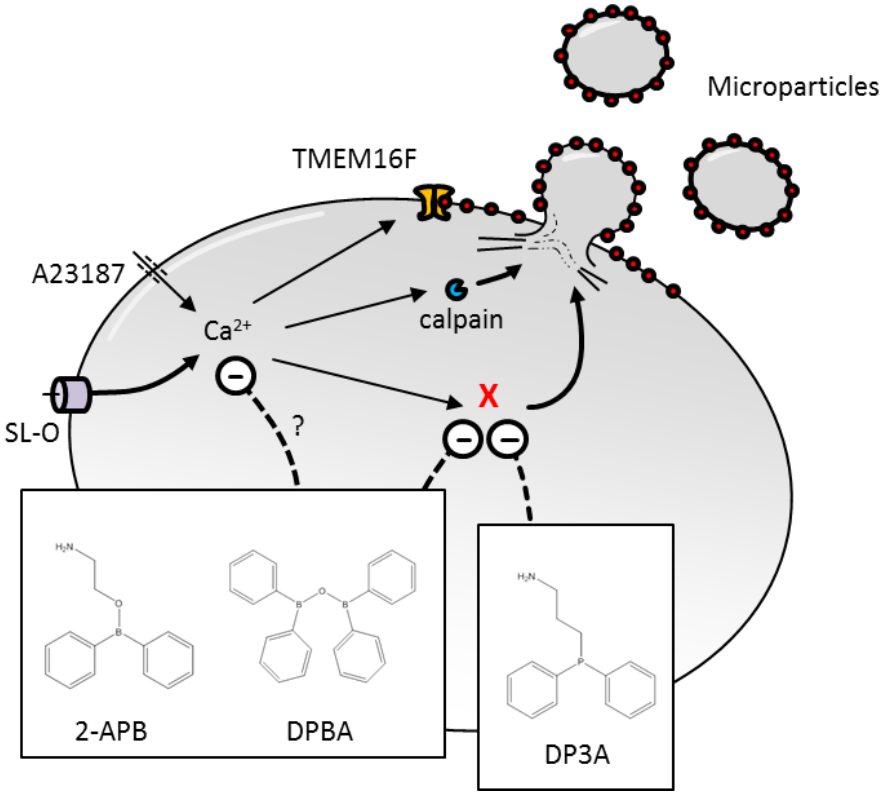

Figure 6.11: Summary of the targets of 2-APB

2-APB, along with its analogues DPBA and DP3A, inhibits PMP release in response to A23187 or SL-O. 2-APB and DPBA also inhibit A23187-triggered rise in Cal520 fluorescence signals, which may indicate inhibition of Ca^{2+} signalling or may be an artefact. Inhibition of Ca^{2+} signalling by 2-APB and DPBA may explain weak inhibition of TMEM16F and calpain. In contrast, DP3A does not inhibit Ca^{2+} signalling, TMEM16F or calpain. 2-APB, DPBA and DP3A have a common intracellular target required for PMP release that is yet to be resolved (as indicated by "X").

In addition to that triggered by A23187, PMP release triggered by ABT-737 was also found to be inhibited by 2-APB. Unlike BAPTA, calpeptin or Q-VD-OPh, 2-APB did not inhibit cell death. PS exposure and loss of calcein were not affected in platelets treated with 2-APB. Rather, this inhibitory effect might be linked to reduced Ca^{2+} entry. Ca^{2+} entry during ABT-737-triggered apoptosis was independent of NCX, SOCE and NCCE at the plasma membrane, as it was not affected by inhibitors of Ca^{2+} entry pathways including SN-6, Synta66 or SAR7334.

Inhibition of ABT-737-triggered PMP release by 2-APB might potentially result from inhibition of gap junctions, which, although they are often associated with anion movement, could act as bi-directional conduits for Ca^{2+} flow (Fiori et al., 2012). Two non-specific gap junction blockers, carbenoxolone and probenecid, were used. Whilst carbenoxolone only inhibited medium levels of PS exposure but not PMP release, probenecid was shown to attenuate most of the apoptotic features, including PS exposure (high levels), PMP release, Ca^{2+} entry and secondary necrosis. Divergence of effects between the two blockers might be explained by their off-target effects related to apoptosis in platelets.

In chapter 5, it was found that secondary necrosis was dependent on Ca^{2+}, as loss of calcein was inhibited in the absence of extracellular Ca^{2+} or in the presence of BAPTA. However, both 2-APB and carbenoxolone significantly, though not completely, inhibited Ca^{2+} entry, yet secondary necrosis was not affected by either drug. This suggested that secondary necrosis might be regulated by localised, rather than global, Ca^{2+} signalling events within the cytosol.

Amongst various subunits that constitute gap junctions, pannexin 1 (Panx1) has been found to be activated by caspase cleavage (Sandilos et al., 2012). Truncated Panx1 mediates signal release and plasma membrane permeability during apoptosis (Chekeni et al., 2010). Also, connexin 43 (Cx43) has been implicated in apoptotic transformation of HeLa cells (Kalvelyte et al., 2003; Kameritsch et al., 2013). However, subtype-specific mimetic peptides, ^{10}Panx (for Panx1) and Gap27 (for Cx40 and Cx43), did not inhibit PS exposure, PMP release or Ca^{2+} entry in response to ABT-737.

It is still unclear how 2-APB inhibits ABT-737-triggered PMP release. It might be linked to reduced Ca^{2+} entry via an unknown route, or it could be attributed to the same unidentified intracellular target underlying A23187-triggered PMP release. Future studies into 2-APB and its target might provide a scaffold for developing a pharmacological inhibitor of microparticle release from platelets in response to both activation and apoptosis.

Chapter 7 General discussion and future directions

7.1. Detection of platelet-derived microparticles

This thesis aims to understand how microparticles are released from human platelets. An assay was developed for the detection of PMPs by flow cytometry. A sample of platelets and PMPs was stained with fluorescently-conjugated Annexin V molecules to detect PS exposure and anti-human CD41a PE-Cy7 to detect events that were derived from platelets. The 1μm gate was set by silicon dioxide calibration beads. To differentiate events of interest from debris and machine noise, events were triggered on PE-Cy7 fluorescence of anti-human CD41a. Samples were diluted by half in HBS before analysis using a flow cytometer, so that swarm detection could be prevented. PMPs were defined as events smaller than 1μm and positive for Annexin V binding. It needs to be acknowledged that the number of events seen by this approach is likely an underestimate of the total number of PMPs, since flow cytometry can struggle to resolve the smaller EVs. However, this assay has proved useful for investigating the pharmacology of PMP release.

A few types of stimuli can be used to trigger PMP release. These include physiological agonists thrombin plus CRP-XL, a Ca^{2+} ionophore A23187, a bacterial toxin SL-O, and histone H4. Compared to thrombin plus CRP-XL, A23187 allowed platelet stimulation to bypass receptor activation and its subsequent Ca^{2+} signalling mechanisms. Compared to SL-O, A23187 did not cause perforation of plasma membrane. In addition, the population of EVs released from platelets in response to histone H4 was not homogeneous in terms of PS exposure, so it was not definitive whether these EVs could be classified as PMPs. Therefore, A23187 was the most suitable stimulus for further investigations into the mechanisms of PMP release.

7.2. Lipid rafts, membrane blebbing and scission

It was shown that cholesterol-rich lipid rafts are required for PMP release in response to A23187. A23187-triggered PMP release was prevented by MβCD that depletes cholesterol from membranes. It was also inhibited by filipin that sequesters membrane cholesterol, but not by amphotericin B, a structurally-related polyene antifungal that does not disrupt cholesterol. The importance of lipid rafts in PMP release was supported by data from using cholera toxin B (CTxB) that binds to GM1 ganglioside, an alternative marker of lipid rafts. CTxB bound to PMPs, whereas CTxB binding to platelets was reduced by A23187 stimulation.

How lipid rafts contribute to PMP release is still unclear. Lipid raft disruption did not affect PS exposure, since MβCD or filipin had no effect on Annexin V binding to A23187-stimulated platelets. Lipid raft disruption did not affect intracellular calpain activity, since MβCD had no effect on calpain-dependent cleavage of talin. Inhibition of either $P2Y_{12}$ or TPα, both of which have been found in lipid rafts, did not affect A23187-triggered PMP release, so these receptors are not directly involved in the PMP release mechanism. One future approach would be to compare the proteomes of platelet lipid rafts and of PMPs to identify novel regulators of PMP release.

In the lipid raft domains, membrane curvature may be generated by protein crowding. Even in a cell-free lamellar vesicle system, lateral pressure created by protein-protein interactions was shown to cause membrane bending (Stachowiak et al., 2012). Enrichment of regulatory proteins and budding microparticles in lipid rafts could alone be sufficient to drive outward blebbing, which is independent of Na^+ influx-mediated increases in hydrostatic pressure.

After blebs are formed on the platelet surface, they are pinched off to form PMPs. Membrane scission is independent of the ESCRT system, because ESCRT-associated proteins are not expressed in human platelets. It is possible that scission during PMP release occurs spontaneously when lipid raft-facilitated protein crowding creates a curvature force beyond the threshold for constriction.

7.3. Apoptosis

In addition to stimulated platelets, platelets undergoing apoptosis also release PMPs. In this thesis, apoptosis was triggered in platelets primarily by a BH3-mimetic drug ABT-737 that inhibits Bcl-xL and initiates the intrinsic apoptotic pathway. Two levels of PS exposure were detected in platelets in response to ABT-737. While high PS exposure is mediated by the Ca^{2+}-dependent TMEM16F, medium PS exposure is likely to be mediated by an unknown caspase-dependent scramblase. PMPs are released from platelets with high PS exposure, but absent from platelets with medium PS exposure. Contrary to that triggered by A23187, PMP release triggered by ABT-737 is dependent on caspases and largely independent of calpain.

Apoptotic platelets would progress to secondary necrosis if they are not cleared, including under *in vitro* conditions due to lack of scavenger cells. Mediated by caspases and partially calpain, secondary necrosis in platelets shows loss of plasma integrity and high PS exposure. This has important implications for *in vitro* studies, because some of the signalling events that were associated with apoptosis may rather reflect secondary necrosis.

Two pathways of PMP release are linked with each other, one being stimulation-related and the other cell death-related. It was found that ABT-737-triggered activation of caspases downregulated calpain-dependent PMP release in response to A23187 and an acute rise in $[Ca^{2+}]_i$. However, when apoptosis was triggered yet caspases were inhibited, platelets released more PMPs in response to A23187. Therefore, during the early apoptotic phase, caspases may protect platelets from potential immunogenic effects of pro-thrombotic stimuli by down-regulating the capacity for rapid PMP release.

7.4. 2-aminoethoxydiphenyl borate as an inhibitor of microparticle release

2-APB, a cell-permeable modulator of numerous ion channels, was found to inhibit A23187-triggered PMP release. DPBA and DP3A, two structurally-related compounds, also inhibit A23187-triggered PMP release with similar potency to 2-APB.

It is not clear how 2-APB and its analogues lead to inhibition of A23187-triggered PMP release. A few hypotheses were tested and ruled out. These include Ca^{2+} entry into cytosol, ion channels or transporters on the plasma membrane, and calpain activity. The inhibitory effects of 2-APB might be attributed to an unidentified intracellular target.

2-APB was also found to inhibit ABT-737-triggered PMP release. Rather than PS exposure and secondary necrosis, Ca^{2+} entry into platelets was inhibited by 2-APB during ABT-737-triggered apoptosis. NCX, SOCE and NCCE were ruled out as the route for Ca^{2+} entry. Results from inhibiting gap junctions, with drugs of varying specificities, were difficult to interpret.

Therefore, 2-APB's inhibitory effect on ABT-737-triggered PMP release might be linked to reduced Ca^{2+} entry via an unknown route, or to the same intracellular target underlying A23187-triggered PMP release. Future studies in identifying the target of 2-APB, followed by *in silico* docking of 2-APB and its analogues, might provide new insights into how microparticles are released from both activated and apoptotic platelets.

7.5. Future direction: other pro-death stimuli that trigger microparticle release

In section 5.9, it was found that PMP release could be triggered by a few pro-death drugs in addition to ABT-737, including ABT-263, AT-101, HA14-1 and sabutoclax. AT-101, HA14-1 and sabutoclax triggered PMP release largely independently of caspases, as PMP release and PS exposure in response to these drugs were not abolished in the presence of Q-VD-OPh (Figure 5.8C-D). Also, loss of plasma membrane integrity in response to these drugs was highly variable depending on specific donors (Figure 5.8F). These data suggest that AT-101, HA14-1 and sabutoclax might trigger PMP release via a third pathway, independent of calpain (e.g. in response to A23187 or thrombin plus CRP-XL) or caspases (e.g. in response to ABT-737 or ABT-263).

Experiments can be performed in the future to characterise this unidentified pathway leading to PMP release. A few hypotheses for the intracellular targets of AT-101, HA14-1 and sabutoclax include Ca^{2+}-dependent protease family cathepsin, mitochondria permeability transition pore (MPTP) and Rho-associated protein kinase (ROCK). Since the effects of these drugs were all dependent on extracellular Ca^{2+}, the routes for Ca^{2+} entry into platelets in response to AT-101, HA14-1 and sabutoclax are also worth further investigations.

7.6. Limitations of studies in this thesis

PMP detection in this thesis relied primarily on flow cytometry, but flow cytometry is limited by its resolution in detecting small vesicles. For example, PMPs with diameters below 488nm could not be detected. Although some results were confirmed by the use of transmission electron microscopy, a more objective and efficient method could be used to detect PMPs in parallel to flow cytometry. This include nanoparticle tracking analysis, which has been used for counting microparticles derived from platelets, endothelial cells and macrophages (Aatonen et al., 2014; Abbasian et al., 2015; Marchini et al., 2016).

Platelet functions were mostly studied by flow cytometry, Western blotting and microplate assays. These include PS exposure, PMP release, cell viability, $[Ca^{2+}]_i$ assay, pH measurement and protein expression. Some experiments in this thesis focused on the platelet membrane (e.g. lipid rafts, membrane leakage). It would be interesting to visualise these results by scanning electron microscopy, which has been used on platelets before (Schoenwaelder et al., 2011; Vasina et al., 2011). These include the topology of membranes from pro-coagulant, apoptotic and secondary necrotic platelets treated with various inhibitors such as 2-APB.

Studies in this thesis relied heavily on pharmacology. Platelets were applied with specific activators, inhibitors or disruptors. If conditions allowed, some of the studies could be performed with platelets from knockout or knockdown mice. Some existing and viable targets for gene modification that might be useful include TMEM16F (Mattheij et al., 2016), Bcl-xL (Kodama et al., 2011), Cx37 and Cx40 (Vaiyapuri et al., 2012, 2013).

Finally, the scope of this thesis is limited to platelets. Some experiments could be extended to other cardiovascular cells. For example, 2-APB and its structural analogues can be applied to endothelial cells, testing if the release of endothelial cell-derived microparticles is inhibited in response to A23187 or ABT-737. These results could help reveal commonalities and differences in pathways of microparticle release from different cells, which in turn might bring insights into the mechanisms of PMP release.

7.7. Concluding remarks

Taken together, this thesis has made some contributions in understanding the mechanisms of microparticle release from human platelets.

It was found that cholesterol-rich lipid rafts are required for the calpain-dependent release of microparticles from platelets in response to pro-coagulant stimuli. Membrane blebbing in this process is not mediated by local influx of Na^+. Membrane scission in this process is not mediated by the endosomal sorting complex required for transport. It was also found that microparticles are released from platelets in response to pro-apoptotic triggers, which is dependent on caspases but largely independent of calpain. Microparticle release from apoptotic platelets is associated with high levels of phosphatidylserine exposure and secondary necrosis. Caspase activity during platelet apoptosis downregulates the calpain-dependent microparticle release in response to pro-coagulant stimuli. 2-Aminoethoxydiphenyl borate (2-APB) was found to inhibit microparticle release from platelets under both stimulatory and apoptotic conditions. The effects of 2-APB have been characterised, although the intracellular target of 2-APB remains unknown.

There are a few avenues for future studies into the subject. These include identifying novel regulators of microparticle release from platelets, using nanoparticle tracking analysis and platelets from knockout mice in parallel with flow cytometry and pharmacology, and extending these experiments to other cells in the cardiovascular system.

References

Aatonen, M.T., Ohman, T., Nyman, T.A., Laitinen, S., Grönholm, M., and Siljander, P.R.-M. (2014). Isolation and characterization of platelet-derived extracellular vesicles. J. Extracell. Vesicles *3*:.

Abbasian, N., Burton, J.O., Herbert, K.E., Tregunna, B.-E., Brown, J.R., Ghaderi-Najafabadi, M., et al. (2015). Hyperphosphatemia, Phosphoprotein Phosphatases, and Microparticle Release in Vascular Endothelial Cells. J. Am. Soc. Nephrol. JASN *26*: 2152–2162.

Achison, M., Joel, C., Hargreaves, P.G., Sage, S.O., Barnes, M.J., and Farndale, R.W. (1996). Signals elicited from human platelets by synthetic, triple helical, collagen-like peptides. Blood Coagul. Fibrinolysis Int. J. Haemost. Thromb. *7*: 149–152.

Adams, J.M., and Cory, S. (2018). The BCL-2 arbiters of apoptosis and their growing role as cancer targets. Cell Death Differ. *25*: 27–36.

Adell, M.A.Y., Vogel, G.F., Pakdel, M., Müller, M., Lindner, H., Hess, M.W., et al. (2014). Coordinated binding of Vps4 to ESCRT-III drives membrane neck constriction during MVB vesicle formation. J. Cell Biol. *205*: 33–49.

Agbani, E.O., Bosch, M.T.J. van den, Brown, E., Williams, C.M., Mattheij, N.J.A., Cosemans, J.M.E.M., et al. (2015). Coordinated Membrane Ballooning and Procoagulant Spreading in Human Platelets. Circulation *132*: 1414–1424.

Agbani, E.O., Williams, C.M., Hers, I., and Poole, A.W. (2017). Membrane Ballooning in Aggregated Platelets is Synchronised and Mediates a Surge in Microvesiculation. Sci. Rep. *7*:.

Agbani, E.O., Williams, C.M., Li, Y., Bosch, M.T. van den, Moore, S.F., Mauroux, A., et al. (2018). Aquaporin-1 regulates platelet procoagulant membrane dynamics and in vivo thrombosis. JCI Insight *3*:.

Aisiku, O., Peters, C.G., De Ceunynck, K., Ghosh, C.C., Dilks, J.R., Fustolo-Gunnink, S.F., et al. (2015). Parmodulins inhibit thrombus formation without inducing endothelial injury caused by vorapaxar. Blood *125*: 1976–1985.

Akers, J.C., Gonda, D., Kim, R., Carter, B.S., and Chen, C.C. (2013). Biogenesis of extracellular vesicles (EV): exosomes, microvesicles, retrovirus-like vesicles, and apoptotic bodies. J. Neurooncol. *113*: 1–11.

Alnemri, E.S., Livingston, D.J., Nicholson, D.W., Salvesen, G., Thornberry, N.A., Wong, W.W., et al. (1996). Human ICE/CED-3 protease nomenclature. Cell *87*: 171.

Ancrenaz, V., Daali, Y., Fontana, P., Besson, M., Samer, C., Dayer, P., et al. (2010). Impact of genetic polymorphisms and drug-drug interactions on clopidogrel and prasugrel response variability. Curr. Drug Metab. *11*: 667–677.

Andersen, J.P., Vestergaard, A.L., Mikkelsen, S.A., Mogensen, L.S., Chalat, M., and Molday, R.S. (2016). P4-ATPases as Phospholipid Flippases—Structure, Function, and Enigmas. Front. Physiol. *7*:.

Anderson, M.A., Deng, J., Seymour, J.F., Tam, C., Kim, S.Y., Fein, J., et al. (2016). The BCL2 selective inhibitor venetoclax induces rapid onset apoptosis of CLL cells in patients via a TP53-independent mechanism. Blood *127*: 3215–3224.

Andre, P., Delaney, S.M., LaRocca, T., Vincent, D., DeGuzman, F., Jurek, M., et al. (2003). P2Y12 regulates platelet adhesion/activation, thrombus growth, and thrombus stability in injured arteries. J. Clin. Invest. *112*: 398–406.

Andreu, Z., and Yáñez-Mó, M. (2014). Tetraspanins in Extracellular Vesicle Formation and Function. Front. Immunol. *5*:.

Antonny, B., Beraud-Dufour, S., Chardin, P., and Chabre, M. (1997). N-terminal hydrophobic residues of the G-protein ADP-ribosylation factor-1 insert into membrane phospholipids upon GDP to GTP exchange. Biochemistry *36*: 4675–4684.

Arraud, N., Gounou, C., Turpin, D., and Brisson, A.R. (2016). Fluorescence triggering: A general strategy for enumerating and phenotyping extracellular vesicles by flow cytometry. Cytom. Part J. Int. Soc. Anal. Cytol. *89*: 184–195.

Arraud, N., Linares, R., Tan, S., Gounou, C., Pasquet, J.-M., Mornet, S., et al. (2014). Extracellular vesicles from blood plasma: determination of their morphology, size, phenotype and concentration. J. Thromb. Haemost. JTH *12*: 614–627.

Babst, M. (2011). MVB vesicle formation: ESCRT-dependent, ESCRT-independent and everything in between. Curr. Opin. Cell Biol. *23*: 452–457.

Babst, M., Katzmann, D.J., Snyder, W.B., Wendland, B., and Emr, S.D. (2002). Endosome-associated complex, ESCRT-II, recruits transport machinery for protein sorting at the multivesicular body. Dev. Cell *3*: 283–289.

Bachelot-Loza, C., Badol, P., Brohard-Bohn, B., Fraiz, N., Cano, E., and Rendu, F. (2006). Differential regulation of platelet aggregation and aminophospholipid exposure by calpain. Br. J. Haematol. *133*: 419–426.

Bai, D., Corsso, C. del, Srinivas, M., and Spray, D.C. (2006). Block of specific gap junction channel subtypes by 2-aminoethoxydiphenyl borate (2-APB). J. Pharmacol. Exp. Ther. *319*: 1452–1458.

Baietti, M.F., Zhang, Z., Mortier, E., Melchior, A., Degeest, G., Geeraerts, A., et al. (2012). Syndecan-syntenin-ALIX regulates the biogenesis of exosomes. Nat. Cell Biol. *14*: 677–685.

Baig, S., Seevasant, I., Mohamad, J., Mukheem, A., Huri, H.Z., and Kamarul, T. (2016). Potential of apoptotic pathway-targeted cancer therapeutic research: Where do we stand? Cell Death Dis. *7*: e2058.

Baldwin, A.G., Rivers-Auty, J., Daniels, M.J.D., White, C.S., Schwalbe, C.H., Schilling, T., et al. (2017). Boron-Based Inhibitors of the NLRP3 Inflammasome. Cell Chem. Biol. *24*: 1321-1335.e5.

Bang, B., Gniadecki, R., and Gajkowska, B. (2005). Disruption of lipid rafts causes apoptotic cell death in HaCaT keratinocytes. Exp. Dermatol. *14*: 266–272.

Bansal, V.K. (1990). Serum Inorganic Phosphorus. In Clinical Methods: The History, Physical, and Laboratory Examinations, H.K. Walker, W.D. Hall, and J.W. Hurst, eds. (Boston: Butterworths), p.

Baran, J., Baj-Krzyworzeka, M., Weglarczyk, K., Szatanek, R., Zembala, M., Barbasz, J., et al. (2010). Circulating tumour-derived microvesicles in plasma of gastric cancer patients. Cancer Immunol. Immunother. CII *59*: 841–850.

Beaulieu, L.M., and Freedman, J.E. (2011). Inflammation & the platelet histone trap. Blood *118*: 1714–1715.

Beck, R., Sun, Z., Adolf, F., Rutz, C., Bassler, J., Wild, K., et al. (2008). Membrane curvature induced by Arf1-GTP is essential for vesicle formation. Proc. Natl. Acad. Sci. U. S. A. *105*: 11731–11736.

Behan, M.W.H., Fox, S.C., Heptinstall, S., and Storey, R.F. (2005). Inhibitory effects of P2Y12 receptor antagonists on TRAP-induced platelet aggregation, procoagulant activity, microparticle formation and intracellular calcium responses in patients with acute coronary syndromes. Platelets *16*: 73–80.

Bender, M., Thon, J.N., Ehrlicher, A.J., Wu, S., Mazutis, L., Deschmann, E., et al. (2015). Microtubule sliding drives proplatelet elongation and is dependent on cytoplasmic dynein. Blood *125*: 860–868.

Bennett, J.S. (2005). Structure and function of the platelet integrin αIIbβ3. J. Clin. Invest. *115*: 3363–3369.

Berezin, A.E., Kremzer, A.A., Berezina, T.A., and Martovitskaya, Y.V. (2015). Pattern of circulating microparticles in chronic heart failure patients with metabolic syndrome: Relevance to neurohumoral and inflammatory activation. BBA Clin. *4*: 69–75.

Berna-Erro, A., Jardín, I., Smani, T., and Rosado, J.A. (2016). Regulation of Platelet Function by Orai, STIM and TRP. Adv. Exp. Med. Biol. *898*: 157–181.

Berndt, M.C., and Andrews, R.K. (2011). Bernard-Soulier syndrome. Haematologica *96*: 355–359.

Berndt, M.C., Metharom, P., and Andrews, R.K. (2014). Primary haemostasis: newer insights. Haemoph. Off. J. World Fed. Hemoph. *20 Suppl 4*: 15–22.

Bevers, E.M., and Williamson, P.L. (2010). Phospholipid scramblase: an update. FEBS Lett. *584*: 2724–2730.

Bhat, N.M., Adams, C.M., Chen, Y., Bieber, M.M., and Teng, N.N.H. (2015). Identification of Cell Surface Straight Chain Poly-N-Acetyl-Lactosamine Bearing Protein Ligands for VH4-34-Encoded Natural IgM Antibodies. J. Immunol. Baltim. Md 1950 *195*: 5178–5188.

Bhatt, D.L., Stone, G.W., Mahaffey, K.W., Gibson, C.M., Steg, P.G., Hamm, C.W., et al. (2013). Effect of platelet inhibition with cangrelor during PCI on ischemic events. N. Engl. J. Med. *368*: 1303–1313.

Billard, C. (2013). BH3 mimetics: status of the field and new developments. Mol. Cancer Ther. *12*: 1691–1700.

Biró, E., Akkerman, J.W.N., Hoek, F.J., Gorter, G., Pronk, L.M., Sturk, A., et al. (2005). The phospholipid composition and cholesterol content of platelet-derived microparticles: a comparison with platelet membrane fractions. J. Thromb. Haemost. JTH *3*: 2754–2763.

Blank, N., Schiller, M., Krienke, S., Wabnitz, G., Ho, A.D., and Lorenz, H.-M. (2007). Cholera toxin binds to lipid rafts but has a limited specificity for ganglioside GM1. Immunol. Cell Biol. *85*: 378–382.

Blume, K.E., Soeroes, S., Waibel, M., Keppeler, H., Wesselborg, S., Herrmann, M., et al. (2009). Cell surface externalization of annexin A1 as a failsafe mechanism preventing inflammatory responses during secondary necrosis. J. Immunol. Baltim. Md 1950 *183*: 8138–8147.

Boassa, D., Ambrosi, C., Qiu, F., Dahl, G., Gaietta, G., and Sosinsky, G. (2007). Pannexin1 channels contain a glycosylation site that targets the hexamer to the plasma membrane. J. Biol. Chem. *282*: 31733–31743.

Bobrie, A., Colombo, M., Raposo, G., and Théry, C. (2011). Exosome secretion: molecular mechanisms and roles in immune responses. Traffic Cph. Den. *12*: 1659–1668.

Bodin, S., Giuriato, S., Ragab, J., Humbel, B.M., Viala, C., Vieu, C., et al. (2001). Production of phosphatidylinositol 3,4,5-trisphosphate and phosphatidic acid in platelet rafts: evidence for a critical role of cholesterol-enriched domains in human platelet activation. Biochemistry *40*: 15290–15299.

Bodin, S., Tronchère, H., and Payrastre, B. (2003). Lipid rafts are critical membrane domains in blood platelet activation processes. Biochim. Biophys. Acta *1610*: 247–257.

Boeck, G. (2001). Current status of flow cytometry in cell and molecular biology. Int. Rev. Cytol. *204*: 239–298.

Böing, A.N., Stap, J., Hau, C.M., Afink, G.B., Ris-Stalpers, C., Reits, E.A., et al. (2013). Active caspase-3 is removed from cells by release of caspase-3-enriched vesicles. Biochim. Biophys. Acta *1833*: 1844–1852.

Bolard, J. (1986). How do the polyene macrolide antibiotics affect the cellular membrane properties? Biochim. Biophys. Acta *864*: 257–304.

Bootman, M.D., Collins, T.J., Mackenzie, L., Roderick, H.L., Berridge, M.J., and Peppiatt, C.M. (2002). 2-aminoethoxydiphenyl borate (2-APB) is a reliable blocker of store-operated Ca2+ entry but an inconsistent inhibitor of InsP3-induced Ca2+ release. FASEB J. Off. Publ. Fed. Am. Soc. Exp. Biol. *16*: 1145–1150.

Borisova, T., Kasatkina, L., and Ostapchenko, L. (2011). The proton gradient of secretory granules and glutamate transport in blood platelets during cholesterol depletion of the plasma membrane by methyl-β-cyclodextrin. Neurochem. Int. *59*: 965–975.

Bosch, X., Marrugat, J., and Sanchis, J. (2013). Platelet glycoprotein IIb/IIIa blockers during percutaneous coronary intervention and as the initial medical treatment of non-ST segment elevation acute coronary syndromes. Cochrane Database Syst. Rev. CD002130.

Brass, L.F. (2003). Thrombin and platelet activation. Chest *124*: 18S-25S.

Braun, A., Varga-Szabo, D., Kleinschnitz, C., Pleines, I., Bender, M., Austinat, M., et al. (2009). Orai1 (CRACM1) is the platelet SOC channel and essential for pathological thrombus formation. Blood *113*: 2056–2063.

Briedé, J.J., Heemskerk, J.W., Hemker, H.C., and Lindhout, T. (1999). Heterogeneity in microparticle formation and exposure of anionic phospholipids at the plasma membrane of single adherent platelets. Biochim. Biophys. Acta *1451*: 163–172.

Brown, D.A., and Rose, J.K. (1992). Sorting of GPI-anchored proteins to glycolipid-enriched membrane subdomains during transport to the apical cell surface. Cell *68*: 533–544.

Brownlow, S.L., Harper, A.G.S., Harper, M.T., and Sage, S.O. (2004). A role for hTRPC1 and lipid raft domains in store-mediated calcium entry in human platelets. Cell Calcium *35*: 107–113.

Burger, D., Montezano, A.C., Nishigaki, N., He, Y., Carter, A., and Touyz, R.M. (2011). Endothelial microparticle formation by angiotensin II is mediated via Ang II receptor type I/NADPH oxidase/ Rho kinase pathways targeted to lipid rafts. Arterioscler. Thromb. Vasc. Biol. *31*: 1898–1907.

Burnier, L., Fontana, P., Kwak, B.R., and Angelillo-Scherrer, A. (2009). Cell-derived microparticles in haemostasis and vascular medicine. Thromb. Haemost. *101*: 439–451.

Campelo, F., and Malhotra, V. (2012). Membrane fission: the biogenesis of transport carriers. Annu. Rev. Biochem. *81*: 407–427.

Campos, C.B.L., Paim, B.A., Cosso, R.G., Castilho, R.F., Rottenberg, H., and Vercesi, A.E. (2006). Method for monitoring of mitochondrial cytochrome c release during cell death: Immunodetection of cytochrome c by flow cytometry after selective permeabilization of the plasma membrane. Cytom. Part J. Int. Soc. Anal. Cytol. *69*: 515–523.

Campsteijn, C., Vietri, M., and Stenmark, H. (2016). Novel ESCRT functions in cell biology: spiraling out of control? Curr. Opin. Cell Biol. *41*: 1–8.

Cang, S., Iragavarapu, C., Savooji, J., Song, Y., and Liu, D. (2015). ABT-199 (venetoclax) and BCL-2 inhibitors in clinical development. J. Hematol. Oncol.J Hematol Oncol *8*: 129.

Carlton, J.G., Caballe, A., Agromayor, M., Kloc, M., and Martin-Serrano, J. (2012). ESCRT-III governs the Aurora B-mediated abscission checkpoint through CHMP4C. Science *336*: 220–225.

Caruso, S., and Poon, I.K.H. (2018). Apoptotic Cell-Derived Extracellular Vesicles: More Than Just Debris. Front. Immunol. *9*: 1486.

Cattaneo, M. (2015). P2Y12 receptors: structure and function. J. Thromb. Haemost. JTH *13 Suppl 1*: S10-16.

Cauwenberghs, S., Feijge, M.A.H., Harper, A.G.S., Sage, S.O., Curvers, J., and Heemskerk, J.W.M. (2006). Shedding of procoagulant microparticles from unstimulated platelets by integrin-mediated destabilization of actin cytoskeleton. FEBS Lett. *580*: 5313–5320.

Chandler, W.L., Yeung, W., and Tait, J.F. (2011). A new microparticle size calibration standard for use in measuring smaller microparticles using a new flow cytometer. J. Thromb. Haemost. JTH *9*: 1216–1224.

Chatterjee, M., Borst, O., Walker, B., Fotinos, A., Vogel, S., Seizer, P., et al. (2014). Macrophage migration inhibitory factor limits activation-induced apoptosis of platelets via CXCR7-dependent Akt signaling. Circ. Res. *115*: 939–949.

Chekeni, F.B., Elliott, M.R., Sandilos, J.K., Walk, S.F., Kinchen, J.M., Lazarowski, E.R., et al. (2010). Pannexin 1 channels mediate 'find-me' signal release and membrane permeability during apoptosis. Nature *467*: 863–867.

Chen, G.Y., and Nuñez, G. (2010). Sterile inflammation: sensing and reacting to damage. Nat. Rev. Immunol. *10*: 826–837.

Chichili, G.R., and Rodgers, W. (2009). Cytoskeleton-membrane interactions in membrane raft structure. Cell. Mol. Life Sci. CMLS *66*: 2319–2328.

Chokshi, R., Fruasaha, P., and Kozak, J.A. (2012). 2-aminoethyl diphenyl borinate (2-APB) inhibits TRPM7 channels through an intracellular acidification mechanism. Channels Austin Tex *6*: 362–369.

Choo, H.-J., Kholmukhamedov, A., Zhou, C., and Jobe, S. (2017). Inner Mitochondrial Membrane Disruption Links Apoptotic and Agonist-Initiated Phosphatidylserine Externalization in Platelets. Arterioscler. Thromb. Vasc. Biol. *37*: 1503–1512.

Christian, A.E., Haynes, M.P., Phillips, M.C., and Rothblat, G.H. (1997). Use of cyclodextrins for manipulating cellular cholesterol content. J. Lipid Res. *38*: 2264–2272.

Chung, M.-K., Güler, A.D., and Caterina, M.J. (2005). Biphasic currents evoked by chemical or thermal activation of the heat-gated ion channel, TRPV3. J. Biol. Chem. *280*: 15928–15941.

Cifuni, S.M., Wagner, D.D., and Bergmeier, W. (2008). CalDAG-GEFI and protein kinase C represent alternative pathways leading to activation of integrin αIIbβ3 in platelets. Blood *112*: 1696–1703.

Cines, D.B., Lebedeva, T., Nagaswami, C., Hayes, V., Massefski, W., Litvinov, R.I., et al. (2014). Clot contraction: compression of erythrocytes into tightly packed polyhedra and redistribution of platelets and fibrin. Blood *123*: 1596–1603.

Cointe, S., Judicone, C., Robert, S., Mooberry, M.J., Poncelet, P., Wauben, M., et al. (2017). Standardization of microparticle enumeration across different flow cytometry platforms: results of a multicenter collaborative workshop. J. Thromb. Haemost. JTH *15*: 187–193.

Coleman, M.L., Sahai, E.A., Yeo, M., Bosch, M., Dewar, A., and Olson, M.F. (2001). Membrane blebbing during apoptosis results from caspase-mediated activation of ROCK I. Nat. Cell Biol. *3*: 339–345.

Colton, C.K., and Zhu, M.X. (2007). 2-Aminoethoxydiphenyl borate as a common activator of TRPV1, TRPV2, and TRPV3 channels. Handb. Exp. Pharmacol. 173–187.

Covic, L., Gresser, A.L., and Kuliopulos, A. (2000). Biphasic kinetics of activation and signaling for PAR1 and PAR4 thrombin receptors in platelets. Biochemistry *39*: 5458–5467.

Crawford, E.D., Seaman, J.E., Agard, N., Hsu, G.W., Julien, O., Mahrus, S., et al. (2013). The DegraBase: a database of proteolysis in healthy and apoptotic human cells. Mol. Cell. Proteomics MCP *12*: 813–824.

Crescitelli, R., Lässer, C., Szabó, T.G., Kittel, A., Eldh, M., Dianzani, I., et al. (2013). Distinct RNA profiles in subpopulations of extracellular vesicles: apoptotic bodies, microvesicles and exosomes. J. Extracell. Vesicles *2*:.

Crowley, L.C., Marfell, B.J., Scott, A.P., and Waterhouse, N.J. (2016). Quantitation of Apoptosis and Necrosis by Annexin V Binding, Propidium Iodide Uptake, and Flow Cytometry. Cold Spring Harb. Protoc. *2016*:.

Czabotar, P.E., Lessene, G., Strasser, A., and Adams, J.M. (2014). Control of apoptosis by the BCL-2 protein family: implications for physiology and therapy. Nat. Rev. Mol. Cell Biol. *15*: 49–63.

Dash, R., Azab, B., Quinn, B.A., Shen, X., Wang, X.-Y., Das, S.K., et al. (2011). Apogossypol derivative BI-97C1 (Sabutoclax) targeting Mcl-1 sensitizes prostate cancer cells to mda-7/IL-24-mediated toxicity. Proc. Natl. Acad. Sci. U. S. A. *108*: 8785–8790.

Davì, G., Santilli, F., and Vazzana, N. (2012). Thromboxane receptors antagonists and/or synthase inhibitors. Handb. Exp. Pharmacol. 261–286.

Day, C.A., and Kenworthy, A.K. (2015). Functions of cholera toxin B-subunit as a raft cross-linker. Essays Biochem. *57*: 135–145.

De Camilli, P., Takei, K., and McPherson, P.S. (1995). The function of dynamin in endocytosis. Curr. Opin. Neurobiol. *5*: 559–565.

De Candia, E. (2012). Mechanisms of platelet activation by thrombin: a short history. Thromb. Res. *129*: 250–256.

De Paoli, S.H., Tegegn, T.Z., Elhelu, O.K., Strader, M.B., Patel, M., Diduch, L.L., et al. (2018). Dissecting the biochemical architecture and morphological release pathways of the human platelet extracellular vesiculome. Cell. Mol. Life Sci. CMLS.

Del Conde, I., Shrimpton, C.N., Thiagarajan, P., and López, J.A. (2005). Tissue-factor-bearing microvesicles arise from lipid rafts and fuse with activated platelets to initiate coagulation. Blood *106*: 1604–1611.

Dellis, O., Mercier, P., and Chomienne, C. (2011). The boron-oxygen core of borinate esters is responsible for the store-operated calcium entry potentiation ability. BMC Pharmacol. *11*: 1.

Delmas, P., Wanaverbecq, N., Abogadie, F.C., Mistry, M., and Brown, D.A. (2002). Signaling microdomains define the specificity of receptor-mediated InsP(3) pathways in neurons. Neuron *34*: 209–220.

Deregibus, M.C., Cantaluppi, V., Calogero, R., Lo Iacono, M., Tetta, C., Biancone, L., et al. (2007). Endothelial progenitor cell derived microvesicles activate an angiogenic program in endothelial cells by a horizontal transfer of mRNA. Blood *110*: 2440–2448.

Dewitt, S., Francis, R.J., and Hallett, M.B. (2013). Ca2+ and calpain control membrane expansion during the rapid cell spreading of neutrophils. J. Cell Sci. *126*: 4627–4635.

Diacovo, T.G., Roth, S.J., Buccola, J.M., Bainton, D.F., and Springer, T.A. (1996). Neutrophil rolling, arrest, and transmigration across activated, surface-adherent platelets via sequential action of P-selectin and the beta 2-integrin CD11b/CD18. Blood *88*: 146–157.

Dick, R.A., Goh, S.L., Feigenson, G.W., and Vogt, V.M. (2012). HIV-1 Gag protein can sense the cholesterol and acyl chain environment in model membranes. Proc. Natl. Acad. Sci. U. S. A. *109*: 18761–18766.

Diver, J.M., Sage, S.O., and Rosado, J.A. (2001). The inositol trisphosphate receptor antagonist 2-aminoethoxydiphenylborate (2-APB) blocks Ca2+ entry channels in human platelets: cautions for its use in studying Ca2+ influx. Cell Calcium *30*: 323–329.

Djillani, A., Doignon, I., Luyten, T., Lamkhioued, B., Gangloff, S.C., Parys, J.B., et al. (2015). Potentiation of the store-operated calcium entry (SOCE) induces phytohemagglutinin-activated Jurkat T cell apoptosis. Cell Calcium *58*: 171–185.

Djillani, A., Nüße, O., and Dellis, O. (2014). Characterization of novel store-operated calcium entry effectors. Biochim. Biophys. Acta *1843*: 2341–2347.

Dobrydneva, Y., and Blackmore, P. (2001). 2-Aminoethoxydiphenyl borate directly inhibits store-operated calcium entry channels in human platelets. Mol. Pharmacol. *60*: 541–552.

Dorahy, D.J., Lincz, L.F., Meldrum, C.J., and Burns, G.F. (1996). Biochemical isolation of a membrane microdomain from resting platelets highly enriched in the plasma membrane glycoprotein CD36. Biochem. J. *319 (Pt 1)*: 67–72.

Dowling, M.R., Josefsson, E.C., Henley, K.J., Hodgkin, P.D., and Kile, B.T. (2010). Platelet senescence is regulated by an internal timer, not damage inflicted by hits. Blood *116*: 1776–1778.

Durrant, T.N., Bosch, M.T. van den, and Hers, I. (2017). Integrin αIIbβ3 outside-in signaling. Blood *130*: 1607–1619.

Elmore, S. (2007). Apoptosis: a review of programmed cell death. Toxicol. Pathol. *35*: 495–516.

Fackler, O.T., and Grosse, R. (2008). Cell motility through plasma membrane blebbing. J. Cell Biol. *181*: 879–884.

Faelber, K., Held, M., Gao, S., Posor, Y., Haucke, V., Noé, F., et al. (2012). Structural insights into dynamin-mediated membrane fission. Struct. Lond. Engl. 1993 *20*: 1621–1628.

Falet, H., Pain, S., and Rendu, F. (1998). Tyrosine unphosphorylated platelet SHP-1 is a substrate for calpain. Biochem. Biophys. Res. Commun. *252*: 51–55.

Fatherazi, S., and Cook, D.L. (1991). Specificity of tetraethylammonium and quinine for three K channels in insulin-secreting cells. J. Membr. Biol. *120*: 105–114.

Feinberg, H., Sandler, W.C., Scorer, M., Le Breton, G.C., Grossman, B., and Born, G.V. (1977). Movement of sodium into human platelets induced by ADP. Biochim. Biophys. Acta *470*: 317–324.

Ferraro, J.T., Daneshmand, M., Bizios, R., and Rizzo, V. (2004). Depletion of plasma membrane cholesterol dampens hydrostatic pressure and shear stress-induced mechanotransduction pathways in osteoblast cultures. Am. J. Physiol. Cell Physiol. *286*: C831-839.

Ferreiro, J.L., Ueno, M., and Angiolillo, D.J. (2009). Cangrelor: a review on its mechanism of action and clinical development. Expert Rev. Cardiovasc. Ther. *7*: 1195–1201.

Field, K.A., Holowka, D., and Baird, B. (1995). Fc epsilon RI-mediated recruitment of p53/56lyn to detergent-resistant membrane domains accompanies cellular signaling. Proc. Natl. Acad. Sci. U. S. A. *92*: 9201–9205.

Filipp, D., Leung, B.L., Zhang, J., Veillette, A., and Julius, M. (2004). Enrichment of lck in lipid rafts regulates colocalized fyn activation and the initiation of proximal signals through TCR alpha beta. J. Immunol. Baltim. Md 1950 *172*: 4266–4274.

Finch, A., and Gardner, P.J. (1966). Thermochemistry of phenylboronic acid, diphenylborinic acid, and their anhydrides. Trans. Faraday Soc. *62*: 3314–3318.

Fiori, M.C., Figueroa, V., Zoghbi, M.E., Saéz, J.C., Reuss, L., and Altenberg, G.A. (2012). Permeation of calcium through purified connexin 26 hemichannels. J. Biol. Chem. *287*: 40826–40834.

Flaumenhaft, R. (2004). Platelet permeabilization. Methods Mol. Biol. Clifton NJ *273*: 365–378.

Flaumenhaft, R., Croce, K., Chen, E., Furie, B., and Furie, B.C. (1999). Proteins of the exocytotic core complex mediate platelet alpha-granule secretion. Roles of vesicle-associated membrane protein, SNAP-23, and syntaxin 4. J. Biol. Chem. *274*: 2492–2501.

Flaumenhaft, R., Dilks, J.R., Richardson, J., Alden, E., Patel-Hett, S.R., Battinelli, E., et al. (2009). Megakaryocyte-derived microparticles: direct visualization and distinction from platelet-derived microparticles. Blood *113*: 1112–1121.

Forlow, S.B., McEver, R.P., and Nollert, M.U. (2000). Leukocyte-leukocyte interactions mediated by platelet microparticles under flow. Blood *95*: 1317–1323.

Fox, J.E., Austin, C.D., Reynolds, C.C., and Steffen, P.K. (1991). Evidence that agonist-induced activation of calpain causes the shedding of procoagulant-containing microvesicles from the membrane of aggregating platelets. J. Biol. Chem. *266*: 13289–13295.

Fox, J.E., Reynolds, C.C., and Austin, C.D. (1990). The role of calpain in stimulus-response coupling: evidence that calpain mediates agonist-induced expression of procoagulant activity in platelets. Blood *76*: 2510–2519.

Freyssinet, J.-M., and Toti, F. (2010). Formation of procoagulant microparticles and properties. Thromb. Res. *125 Suppl 1*: S46-48.

Fuchs, T.A., Bhandari, A.A., and Wagner, D.D. (2011). Histones induce rapid and profound thrombocytopenia in mice. Blood *118*: 3708–3714.

Fujii, T., Sakata, A., Nishimura, S., Eto, K., and Nagata, S. (2015). TMEM16F is required for phosphatidylserine exposure and microparticle release in activated mouse platelets. Proc. Natl. Acad. Sci. U. S. A. *112*: 12800–12805.

Gachet, C. (2015). Antiplatelet drugs: which targets for which treatments? J. Thromb. Haemost. JTH *13 Suppl 1*: S313-322.

Gallis, H.A., Drew, R.H., and Pickard, W.W. (1990). Amphotericin B: 30 years of clinical experience. Rev. Infect. Dis. *12*: 308–329.

Gan, X., and Gould, S.J. (2011). Identification of an inhibitory budding signal that blocks the release of HIV particles and exosome/microvesicle proteins. Mol. Biol. Cell *22*: 817–830.

Gardiner, C., Shaw, M., Hole, P., Smith, J., Tannetta, D., Redman, C.W., et al. (2014). Measurement of refractive index by nanoparticle tracking analysis reveals heterogeneity in extracellular vesicles. J. Extracell. Vesicles *3*: 25361.

Garraud, O., and Cognasse, F. (2015). Are Platelets Cells? And if Yes, are They Immune Cells? Front. Immunol. *6*: 70.

Gauthier, N.C., Masters, T.A., and Sheetz, M.P. (2012). Mechanical feedback between membrane tension and dynamics. Trends Cell Biol. *22*: 527–535.

Gavathiotis, E., Reyna, D.E., Bellairs, J.A., Leshchiner, E.S., and Walensky, L.D. (2012). Direct and selective small-molecule activation of proapoptotic BAX. Nat. Chem. Biol. *8*: 639–645.

Giacomazzi, A., Degan, M., Calabria, S., Meneguzzi, A., and Minuz, P. (2016). Antiplatelet Agents Inhibit the Generation of Platelet-Derived Microparticles. Front. Pharmacol. *7*: 314.

Golebiewska, E.M., Harper, M.T., Williams, C.M., Savage, J.S., Goggs, R., Fischer von Mollard, G., et al. (2015). Syntaxin 8 regulates platelet dense granule secretion, aggregation, and thrombus stability. J. Biol. Chem. *290*: 1536–1545.

Goodwin, J.S., Drake, K.R., Remmert, C.L., and Kenworthy, A.K. (2005). Ras diffusion is sensitive to plasma membrane viscosity. Biophys. J. *89*: 1398–1410.

Goubran, H., Sabry, W., Kotb, R., Seghatchian, J., and Burnouf, T. (2015). Platelet microparticles and cancer: An intimate cross-talk. Transfus. Apher. Sci. Off. J. World Apher. Assoc. Off. J. Eur. Soc. Haemapheresis *53*: 168–172.

Gousset, K., Wolkers, W.F., Tsvetkova, N.M., Oliver, A.E., Field, C.L., Walker, N.J., et al. (2002). Evidence for a physiological role for membrane rafts in human platelets. J. Cell. Physiol. *190*: 117–128.

Greenberg-Sepersky, S.M., and Simons, E.R. (1984). Cation gradient dependence of the steps in thrombin stimulation of human platelets. J. Biol. Chem. *259*: 1502–1508.

Gregory, R.B., Rychkov, G., and Barritt, G.J. (2001). Evidence that 2-aminoethyl diphenylborate is a novel inhibitor of store-operated Ca2+ channels in liver cells, and acts through a mechanism which does not involve inositol trisphosphate receptors. Biochem. J. *354*: 285–290.

Griffith, T.M., Chaytor, A.T., Bakker, L.M., and Edwards, D.H. (2005). 5-Methyltetrahydrofolate and tetrahydrobiopterin can modulate electrotonically mediated endothelium-dependent vascular relaxation. Proc. Natl. Acad. Sci. U. S. A. *102*: 7008–7013.

Guerrier, L., Claverol, S., Fortis, F., Rinalducci, S., Timperio, A.M., Antonioli, P., et al. (2007). Exploring the platelet proteome via combinatorial, hexapeptide ligand libraries. J. Proteome Res. *6*: 4290–4303.

Gupta, N., and DeFranco, A.L. (2003). Visualizing lipid raft dynamics and early signaling events during antigen receptor-mediated B-lymphocyte activation. Mol. Biol. Cell *14*: 432–444.

Halliday, G.M., Ophof, A., Broe, M., Jensen, P.H., Kettle, E., Fedorow, H., et al. (2005). Alpha-synuclein redistributes to neuromelanin lipid in the substantia nigra early in Parkinson's disease. Brain J. Neurol. *128*: 2654–2664.

Hammond, A.T., Heberle, F.A., Baumgart, T., Holowka, D., Baird, B., and Feigenson, G.W. (2005). Crosslinking a lipid raft component triggers liquid ordered-liquid disordered phase separation in model plasma membranes. Proc. Natl. Acad. Sci. U. S. A. *102*: 6320–6325.

Hampton, M.B., Vanags, D.M., Pörn-Ares, M.I., and Orrenius, S. (1996). Involvement of extracellular calcium in phosphatidylserine exposure during apoptosis. FEBS Lett. *399*: 277–282.

Han, J., and Burgess, K. (2010). Fluorescent indicators for intracellular pH. Chem. Rev. *110*: 2709–2728.

Hanson, P.I., Roth, R., Lin, Y., and Heuser, J.E. (2008). Plasma membrane deformation by circular arrays of ESCRT-III protein filaments. J. Cell Biol. *180*: 389–402.

Harper, A.G.S., Brownlow, S.L., and Sage, S.O. (2009). A role for TRPV1 in agonist-evoked activation of human platelets. J. Thromb. Haemost. JTH *7*: 330–338.

Harper, A.G.S., and Sage, S.O. (2007). A key role for reverse Na+/Ca2+ exchange influenced by the actin cytoskeleton in store-operated Ca2+ entry in human platelets: evidence against the de novo conformational coupling hypothesis. Cell Calcium *42*: 606–617.

Harper, M.T., Londoño, J.E.C., Quick, K., Londoño, J.C., Flockerzi, V., Philipp, S.E., et al. (2013). Transient receptor potential channels function as a coincidence signal detector mediating phosphatidylserine exposure. Sci. Signal. *6*: ra50.

Harper, M.T., Molkentin, J.D., and Poole, A.W. (2010). Protein kinase C alpha enhances sodium-calcium exchange during store-operated calcium entry in mouse platelets. Cell Calcium *48*: 333–340.

Harper, M.T., and Poole, A.W. (2011). Store-operated calcium entry and non-capacitative calcium entry have distinct roles in thrombin-induced calcium signalling in human platelets. Cell Calcium *50*: 351–358.

Harper, M.T., and Poole, A.W. (2012). Bcl-xL-inhibitory BH3 mimetic ABT-737 depletes platelet calcium stores. Blood *119*: 4337–4338.

Harper, M.T., and Poole, A.W. (2013). Chloride channels are necessary for full platelet phosphatidylserine exposure and procoagulant activity. Cell Death Dis. *4*: e969.

Haudek, V.J., Slany, A., Gundacker, N.C., Wimmer, H., Drach, J., and Gerner, C. (2009). Proteome maps of the main human peripheral blood constituents. J. Proteome Res. *8*: 3834–3843.

Hauser, P., Wang, S., and Didenko, V.V. (2017). Apoptotic Bodies: Selective Detection in Extracellular Vesicles. Methods Mol. Biol. Clifton NJ *1554*: 193–200.

Heemskerk, J.W.M., Bevers, E.M., and Lindhout, T. (2002). Platelet activation and blood coagulation. Thromb. Haemost. *88*: 186–193.

Heijnen, H.F., Schiel, A.E., Fijnheer, R., Geuze, H.J., and Sixma, J.J. (1999). Activated platelets release two types of membrane vesicles: microvesicles by surface shedding and exosomes derived from exocytosis of multivesicular bodies and alpha-granules. Blood *94*: 3791–3799.

Heijnen, H.F.G., Van Lier, M., Waaijenborg, S., Ohno-Iwashita, Y., Waheed, A.A., Inomata, M., et al. (2003). Concentration of rafts in platelet filopodia correlates with recruitment of c-Src and CD63 to these domains. J. Thromb. Haemost. JTH *1*: 1161–1173.

Herbert, A.S., Davidson, C., Kuehne, A.I., Bakken, R., Braigen, S.Z., Gunn, K.E., et al. (2015). Niemann-pick C1 is essential for ebolavirus replication and pathogenesis in vivo. MBio *6*: e00565-00515.

Hessvik, N.P., and Llorente, A. (2018). Current knowledge on exosome biogenesis and release. Cell. Mol. Life Sci. CMLS *75*: 193–208.

Heyningen S Van, null (1974). Cholera toxin: interaction of subunits with ganglioside GM1. Science *183*: 656–657.

Hirama, T., Lu, S.M., Kay, J.G., Maekawa, M., Kozlov, M.M., Grinstein, S., et al. (2017). Membrane curvature induced by proximity of anionic phospholipids can initiate endocytosis. Nat. Commun. *8*: 1393.

Hoffman, M., and Monroe, D.M. (2001). A cell-based model of hemostasis. Thromb. Haemost. *85*: 958–965.

Hogan, P.G., and Rao, A. (2015). Store-operated calcium entry: Mechanisms and modulation. Biochem. Biophys. Res. Commun. *460*: 40–49.

Holmes, M.V., Perel, P., Shah, T., Hingorani, A.D., and Casas, J.P. (2011). CYP2C19 genotype, clopidogrel metabolism, platelet function, and cardiovascular events: a systematic review and meta-analysis. JAMA *306*: 2704–2714.

Hoorn, E.J., and Zietse, R. (2017). Diagnosis and Treatment of Hyponatremia: Compilation of the Guidelines. J. Am. Soc. Nephrol. JASN *28*: 1340–1349.

Hou, X., Xiao, H., Zhang, Y., Zeng, X., Huang, M., Chen, X., et al. (2018). Transient receptor potential channel 6 knockdown prevents apoptosis of renal tubular epithelial cells upon oxidative stress via autophagy activation. Cell Death Dis. *9*:.

Huang, Y., and Wang, K.K. (2001). The calpain family and human disease. Trends Mol. Med. *7*: 355–362.

Huntington, J.A. (2008). How Na+ Activates Thrombin – A Review of the Functional and Structural Data. Biol. Chem. *389*: 1025–1035.

Hurley, J.H. (2015). ESCRTs are everywhere. EMBO J. *34*: 2398–2407.

Hurley, J.H., and Hanson, P.I. (2010). Membrane budding and scission by the ESCRT machinery: it's all in the neck. Nat. Rev. Mol. Cell Biol. *11*: 556–566.

Ishikawa, M., Iwamoto, T., Nakamura, T., Doyle, A., Fukumoto, S., and Yamada, Y. (2011). Pannexin 3 functions as an ER Ca(2+) channel, hemichannel, and gap junction to promote osteoblast differentiation. J. Cell Biol. *193*: 1257–1274.

Istvan, E.S., and Deisenhofer, J. (2001). Structural mechanism for statin inhibition of HMG-CoA reductase. Science *292*: 1160–1164.

Italiano, J.E., Lecine, P., Shivdasani, R.A., and Hartwig, J.H. (1999). Blood platelets are assembled principally at the ends of proplatelet processes produced by differentiated megakaryocytes. J. Cell Biol. *147*: 1299–1312.

Iwasaki, H., Mori, Y., Hara, Y., Uchida, K., Zhou, H., and Mikoshiba, K. (2001). 2-Aminoethoxydiphenyl borate (2-APB) inhibits capacitative calcium entry independently of the function of inositol 1,4,5-trisphosphate receptors. Receptors Channels *7*: 429–439.

Jackson, S.P. (2011). Arterial thrombosis--insidious, unpredictable and deadly. Nat. Med. *17*: 1423–1436.

Janowska-Wieczorek, A., Wysoczynski, M., Kijowski, J., Marquez-Curtis, L., Machalinski, B., Ratajczak, J., et al. (2005). Microvesicles derived from activated platelets induce metastasis and angiogenesis in lung cancer. Int. J. Cancer *113*: 752–760.

Jimenez, A.J., Maiuri, P., Lafaurie-Janvore, J., Divoux, S., Piel, M., and Perez, F. (2014). ESCRT machinery is required for plasma membrane repair. Science *343*: 1247136.

Jimenez, A.J., and Perez, F. (2017). Plasma membrane repair: the adaptable cell life-insurance. Curr. Opin. Cell Biol. *47*: 99–107.

Jing, W., Yabas, M., Bröer, A., Coupland, L., Gardiner, E.E., Enders, A., et al. (2019). Calpain cleaves phospholipid flippase ATP8A1 during apoptosis in platelets. Blood Adv. *3*: 219–229.

Jobe, S.M., Wilson, K.M., Leo, L., Raimondi, A., Molkentin, J.D., Lentz, S.R., et al. (2008). Critical role for the mitochondrial permeability transition pore and cyclophilin D in platelet activation and thrombosis. Blood *111*: 1257–1265.

Julien, O., Zhuang, M., Wiita, A.P., O'Donoghue, A.J., Knudsen, G.M., Craik, C.S., et al. (2016). Quantitative MS-based enzymology of caspases reveals distinct protein substrate specificities, hierarchies, and cellular roles. Proc. Natl. Acad. Sci. U. S. A. *113*: E2001-2010.

Jung, C., Sörensson, P., Saleh, N., Arheden, H., Rydén, L., and Pernow, J. (2012). Circulating endothelial and platelet derived microparticles reflect the size of myocardium at risk in patients with ST-elevation myocardial infarction. Atherosclerosis *221*: 226–231.

Junt, T., Schulze, H., Chen, Z., Massberg, S., Goerge, T., Krueger, A., et al. (2007). Dynamic visualization of thrombopoiesis within bone marrow. Science *317*: 1767–1770.

Kahner, B.N., Dorsam, R.T., and Kunapuli, S.P. (2008). Role of P2Y receptor subtypes in platelet-derived microparticle generation. Front. Biosci. J. Virtual Libr. *13*: 433–439.

Kaiser, H.-J., Lingwood, D., Levental, I., Sampaio, J.L., Kalvodova, L., Rajendran, L., et al. (2009). Order of lipid phases in model and plasma membranes. Proc. Natl. Acad. Sci. U. S. A. *106*: 16645–16650.

Kalvelyte, A., Imbrasaite, A., Bukauskiene, A., Verselis, V.K., and Bukauskas, F.F. (2003). Connexins and apoptotic transformation. Biochem. Pharmacol. *66*: 1661–1672.

Kameritsch, P., Khandoga, N., Pohl, U., and Pogoda, K. (2013). Gap junctional communication promotes apoptosis in a connexin-type-dependent manner. Cell Death Dis. *4*: e584.

Kamiński, D.M. (2014). Recent progress in the study of the interactions of amphotericin B with cholesterol and ergosterol in lipid environments. Eur. Biophys. J. EBJ *43*: 453–467.

Kashiwagi, H., Schwartz, M.A., Eigenthaler, M., Davis, K.A., Ginsberg, M.H., and Shattil, S.J. (1997). Affinity modulation of platelet integrin alphaIIbbeta3 by beta3-endonexin, a selective binding partner of the beta3 integrin cytoplasmic tail. J. Cell Biol. *137*: 1433–1443.

Katzmann, D.J., Babst, M., and Emr, S.D. (2001). Ubiquitin-dependent sorting into the multivesicular body pathway requires the function of a conserved endosomal protein sorting complex, ESCRT-I. Cell *106*: 145–155.

Kawamura, Y., Yamamoto, Y., Sato, T.-A., and Ochiya, T. (2017). Extracellular vesicles as trans-genomic agents: Emerging roles in disease and evolution. Cancer Sci. *108*: 824–830.

Kelly, P.N., White, M.J., Goschnick, M.W., Fairfax, K.A., Tarlinton, D.M., Kinkel, S.A., et al. (2010). Individual and overlapping roles of BH3-only proteins Bim and Bad in apoptosis of lymphocytes and platelets and in suppression of thymic lymphoma development. Cell Death Differ. *17*: 1655–1664.

Kenworthy, A.K., Nichols, B.J., Remmert, C.L., Hendrix, G.M., Kumar, M., Zimmerberg, J., et al. (2004). Dynamics of putative raft-associated proteins at the cell surface. J. Cell Biol. *165*: 735–746.

Kerr, J.F., Wyllie, A.H., and Currie, A.R. (1972). Apoptosis: a basic biological phenomenon with wide-ranging implications in tissue kinetics. Br. J. Cancer *26*: 239–257.

Kile, B.T. (2014). The role of apoptosis in megakaryocytes and platelets. Br. J. Haematol. *165*: 217–226.

Kim, J.S., and Ligler, F.S. (2010). Utilization of microparticles in next-generation assays for microflow cytometers. Anal. Bioanal. Chem. *398*: 2373–2382.

Kimura, M., Aviv, A., and Reeves, J.P. (1993). K(+)-dependent Na+/Ca2+ exchange in human platelets. J. Biol. Chem. *268*: 6874–6877.

Kodama, T., Takehara, T., Hikita, H., Shimizu, S., Shigekawa, M., Li, W., et al. (2011). BH3-only activator proteins Bid and Bim are dispensable for Bak/Bax-dependent thrombocyte apoptosis induced by Bcl-xL deficiency: molecular requisites for the mitochondrial pathway to apoptosis in platelets. J. Biol. Chem. *286*: 13905–13913.

Kong, F., Zhang, L., Wang, H., Yuan, G., Guo, A., Li, Q., et al. (2015). Impact of collection, isolation and storage methodology of circulating microvesicles on flow cytometric analysis. Exp. Ther. Med. *10*: 2093–2101.

Koupenova, M., Kehrel, B.E., Corkrey, H.A., and Freedman, J.E. (2017). Thrombosis and platelets: an update. Eur. Heart J. *38*: 785–791.

Kozak, J.A., Misler, S., and Logothetis, D.E. (1998). Characterization of a Ca2+-activated K+ current in insulin-secreting murine betaTC-3 cells. J. Physiol. *509 (Pt 2)*: 355–370.

Kozlov, M.M., McMahon, H.T., and Chernomordik, L.V. (2010). Protein-driven membrane stresses in fusion and fission. Trends Biochem. Sci. *35*: 699–706.

Krahling, S., Callahan, M.K., Williamson, P., and Schlegel, R.A. (1999). Exposure of phosphatidylserine is a general feature in the phagocytosis of apoptotic lymphocytes by macrophages. Cell Death Differ. *6*: 183–189.

Kreutz, R.P., Nystrom, P., Kreutz, Y., Miao, J., Kovacs, R., Desta, Z., et al. (2013). Inhibition of platelet aggregation by prostaglandin E1 (PGE1) in diabetic patients during therapy with clopidogrel and aspirin. Platelets *24*: 145–150.

Kruchten, R. van, Braun, A., Feijge, M.A.H., Kuijpers, M.J.E., Rivera-Galdos, R., Kraft, P., et al. (2012). Antithrombotic potential of blockers of store-operated calcium channels in platelets. Arterioscler. Thromb. Vasc. Biol. *32*: 1717–1723.

Kruchten, R. van, Mattheij, N.J.A., Saunders, C., Feijge, M.A.H., Swieringa, F., Wolfs, J.L.N., et al. (2013). Both TMEM16F-dependent and TMEM16F-independent pathways contribute to phosphatidylserine exposure in platelet apoptosis and platelet activation. Blood *121*: 1850–1857.

Krysko, D.V., Agostinis, P., Krysko, O., Garg, A.D., Bachert, C., Lambrecht, B.N., et al. (2011). Emerging role of damage-associated molecular patterns derived from mitochondria in inflammation. Trends Immunol. *32*: 157–164.

Lacroix, R., Robert, S., Poncelet, P., Kasthuri, R.S., Key, N.S., Dignat-George, F., et al. (2010). Standardization of platelet-derived microparticle enumeration by flow cytometry with calibrated beads: results of the International Society on Thrombosis and Haemostasis SSC Collaborative workshop. J. Thromb. Haemost. JTH *8*: 2571–2574.

Laganowsky, A., Reading, E., Allison, T.M., Ulmschneider, M.B., Degiacomi, M.T., Baldwin, A.J., et al. (2014). Membrane proteins bind lipids selectively to modulate their structure and function. Nature *510*: 172–175.

Laird, D.W., and Lampe, P.D. (2018). Therapeutic strategies targeting connexins. Nat. Rev. Drug Discov.

Larive, R.M., Baisamy, L., Urbach, S., Coopman, P., and Bettache, N. (2010). Cell membrane extensions, generated by mechanical constraint, are associated with a sustained lipid raft patching and an increased cell signaling. Biochim. Biophys. Acta *1798*: 389–400.

Larsen, B.D., and Sørensen, C.S. (2017). The caspase-activated DNase: apoptosis and beyond. FEBS J. *284*: 1160–1170.

Latham, S.L., Tiberti, N., Gokoolparsadh, N., Holdaway, K., Couraud, P.O., Grau, G.E.R., et al. (2015). Immuno-analysis of microparticles: probing at the limits of detection. Sci. Rep. *5*: 16314.

Lechner, D., and Weltermann, A. (2008). Circulating tissue factor-exposing microparticles. Thromb. Res. *122 Suppl 1*: S47-54.

Lewandrowski, U., Wortelkamp, S., Lohrig, K., Zahedi, R.P., Wolters, D.A., Walter, U., et al. (2009). Platelet membrane proteomics: a novel repository for functional research. Blood *114*: e10-19.

Li, S., Wei, J., Zhang, C., Li, X., Meng, W., Mo, X., et al. (2016). Cell-Derived Microparticles in Patients with Type 2 Diabetes Mellitus: a Systematic Review and Meta-Analysis. Cell. Physiol. Biochem. Int. J. Exp. Cell. Physiol. Biochem. Pharmacol. *39*: 2439–2450.

Lichtenberg, D., Goñi, F.M., and Heerklotz, H. (2005). Detergent-resistant membranes should not be identified with membrane rafts. Trends Biochem. Sci. *30*: 430–436.

Lievremont, J.-P., Bird, G.S., and Putney, J.W. (2005). Mechanism of inhibition of TRPC cation channels by 2-aminoethoxydiphenylborane. Mol. Pharmacol. *68*: 758–762.

Lillicrap, D. (2013). von Willebrand disease: advances in pathogenetic understanding, diagnosis, and therapy. Blood *122*: 3735–3740.

Lindsten, T., Ross, A.J., King, A., Zong, W.X., Rathmell, J.C., Shiels, H.A., et al. (2000). The combined functions of proapoptotic Bcl-2 family members bak and bax are essential for normal development of multiple tissues. Mol. Cell *6*: 1389–1399.

Lingjaerde, O. (1969). Uptake of serotonin in blood platelets: Dependence on sodium and chloride, and inhibition by choline. FEBS Lett. *3*: 103–106.

Lingwood, D., Ries, J., Schwille, P., and Simons, K. (2008). Plasma membranes are poised for activation of raft phase coalescence at physiological temperature. Proc. Natl. Acad. Sci. U. S. A. *105*: 10005–10010.

Lingwood, D., and Simons, K. (2010). Lipid rafts as a membrane-organizing principle. Science *327*: 46–50.

Littlechild, R., Zaidman, N., Khodaverdi, D., and Mason, M.J. (2015). Inhibition of KCa3.1 by depolarisation and 2-aminoethoxydiphenyl borate (2-APB) during Ca^{2+} release activated Ca^{2+} (CRAC) entry in human erythroleukemia (HEL) cells: Implications for the interpretation of 2-APB inhibition of CRAC entry. Cell Calcium *57*: 76–88.

Liu, G., Liu, G., Chen, H., Borst, O., Gawaz, M., Vortkamp, A., et al. (2015). Involvement of Ca2+ Activated Cl- Channel Ano6 in Platelet Activation and Apoptosis. Cell. Physiol. Biochem. Int. J. Exp. Cell. Physiol. Biochem. Pharmacol. *37*: 1934–1944.

Liu, M.-L., Reilly, M.P., Casasanto, P., McKenzie, S.E., and Williams, K.J. (2007). Cholesterol enrichment of human monocyte/macrophages induces surface exposure of phosphatidylserine and the release of biologically-active tissue factor-positive microvesicles. Arterioscler. Thromb. Vasc. Biol. *27*: 430–435.

Liu, R., Li, J., Zhang, T., Zou, L., Chen, Y., Wang, K., et al. (2014). Itraconazole suppresses the growth of glioblastoma through induction of autophagy: involvement of abnormal cholesterol trafficking. Autophagy *10*: 1241–1255.

Liu, X., Van Vleet, T., and Schnellmann, R.G. (2004). The role of calpain in oncotic cell death. Annu. Rev. Pharmacol. Toxicol. *44*: 349–370.

Liu, Y., Jennings, N.L., Dart, A.M., and Du, X.-J. (2012). Standardizing a simpler, more sensitive and accurate tail bleeding assay in mice. World J. Exp. Med. *2*: 30–36.

Locke, D., Chen, H., Liu, Y., Liu, C., and Kahn, M.L. (2002). Lipid rafts orchestrate signaling by the platelet receptor glycoprotein VI. J. Biol. Chem. *277*: 18801–18809.

Lopez, W., Ramachandran, J., Alsamarah, A., Luo, Y., Harris, A.L., and Contreras, J.E. (2016). Mechanism of gating by calcium in connexin hemichannels. Proc. Natl. Acad. Sci. U. S. A. *113*: E7986–E7995.

Lorizate, M., Sachsenheimer, T., Glass, B., Habermann, A., Gerl, M.J., Kräusslich, H.-G., et al. (2013). Comparative lipidomics analysis of HIV-1 particles and their producer cell membrane in different cell lines. Cell. Microbiol. *15*: 292–304.

MacKenzie, A., Wilson, H.L., Kiss-Toth, E., Dower, S.K., North, R.A., and Surprenant, A. (2001). Rapid secretion of interleukin-1beta by microvesicle shedding. Immunity *15*: 825–835.

Mackman, N. (2012). New insights into the mechanisms of venous thrombosis. J. Clin. Invest. *122*: 2331–2336.

Mackman, N., Tilley, R.E., and Key, N.S. (2007). Role of the extrinsic pathway of blood coagulation in hemostasis and thrombosis. Arterioscler. Thromb. Vasc. Biol. *27*: 1687–1693.

Maekawa, M., and Fairn, G.D. (2014). Molecular probes to visualize the location, organization and dynamics of lipids. J. Cell Sci. *127*: 4801–4812.

Mahajan, A., Herrmann, M., and Muñoz, L.E. (2016). Clearance Deficiency and Cell Death Pathways: A Model for the Pathogenesis of SLE. Front. Immunol. *7*: 35.

Mahammad, S., and Parmryd, I. (2015). Cholesterol depletion using methyl-β-cyclodextrin. Methods Mol. Biol. Clifton NJ *1232*: 91–102.

Mahaut-Smith, M.P. (2012). The unique contribution of ion channels to platelet and megakaryocyte function. J. Thromb. Haemost. JTH *10*: 1722–1732.

Maki, M., Takahara, T., and Shibata, H. (2016). Multifaceted Roles of ALG-2 in Ca(2+)-Regulated Membrane Trafficking. Int. J. Mol. Sci. *17*:.

Manero, F., Gautier, F., Gallenne, T., Cauquil, N., Grée, D., Cartron, P.-F., et al. (2006). The small organic compound HA14-1 prevents Bcl-2 interaction with Bax to sensitize malignant glioma cells to induction of cell death. Cancer Res. *66*: 2757–2764.

Manne, B.K., Badolia, R., Dangelmaier, C.A., and Kunapuli, S.P. (2015). C-type lectin like receptor 2 (CLEC-2) signals independently of lipid raft microdomains in platelets. Biochem. Pharmacol. *93*: 163–170.

Manohar, M., Hirsh, M.I., Chen, Y., Woehrle, T., Karande, A.A., and Junger, W.G. (2012). ATP release and autocrine signaling through P2X4 receptors regulate γδ T cell activation. J. Leukoc. Biol. *92*: 787–794.

Mans, B.J., Gaspar, A.R., Louw, A.I., and Neitz, A.W. (1998). Apyrase activity and platelet aggregation inhibitors in the tick Ornithodoros savignyi (Acari: Argasidae). Exp. Appl. Acarol. *22*: 353–366.

Marchini, J.F., Miyakawa, A.A., Tarasoutchi, F., Krieger, J.E., Lemos, P., and Croce, K. (2016). Endothelial, platelet, and macrophage microparticle levels do not change acutely following transcatheter aortic valve replacement. J. Negat. Results Biomed. *15*:.

Martin, S.J., Reutelingsperger, C.P., McGahon, A.J., Rader, J.A., Schie, R.C. van, LaFace, D.M., et al. (1995). Early redistribution of plasma membrane phosphatidylserine is a general feature of apoptosis regardless of the initiating stimulus: inhibition by overexpression of Bcl-2 and Abl. J. Exp. Med. *182*: 1545–1556.

Maruyama, T., Kanaji, T., Nakade, S., Kanno, T., and Mikoshiba, K. (1997). 2APB, 2-aminoethoxydiphenyl borate, a membrane-penetrable modulator of Ins(1,4,5)P3-induced Ca2+ release. J. Biochem. (Tokyo) *122*: 498–505.

Mason, K.D., Carpinelli, M.R., Fletcher, J.I., Collinge, J.E., Hilton, A.A., Ellis, S., et al. (2007). Programmed anuclear cell death delimits platelet life span. Cell *128*: 1173–1186.

Mattheij, N.J.A., Braun, A., Kruchten, R. van, Castoldi, E., Pircher, J., Baaten, C.C.F.M.J., et al. (2016). Survival protein anoctamin-6 controls multiple platelet responses including phospholipid scrambling, swelling, and protein cleavage. FASEB J. Off. Publ. Fed. Am. Soc. Exp. Biol. *30*: 727–737.

Mattheij, N.J.A., Gilio, K., Kruchten, R. van, Jobe, S.M., Wieschhaus, A.J., Chishti, A.H., et al. (2013). Dual mechanism of integrin αIIbβ3 closure in procoagulant platelets. J. Biol. Chem. *288*: 13325–13336.

Matusek, T., Wendler, F., Polès, S., Pizette, S., D'Angelo, G., Fürthauer, M., et al. (2014). The ESCRT machinery regulates the secretion and long-range activity of Hedgehog. Nature *516*: 99–103.

Mauri, L., Kereiakes, D.J., Yeh, R.W., Driscoll-Shempp, P., Cutlip, D.E., Steg, P.G., et al. (2014). Twelve or 30 months of dual antiplatelet therapy after drug-eluting stents. N. Engl. J. Med. *371*: 2155–2166.

Maurice, P., Waeckel, L., Pires, V., Sonnet, P., Lemesle, M., Arbeille, B., et al. (2006). The platelet receptor for type III collagen (TIIICBP) is present in platelet membrane lipid microdomains (rafts). Histochem. Cell Biol. *125*: 407–417.

Mavroudis, C.A., Eleftheriou, D., Hong, Y., Majumder, B., Koganti, S., Sapsford, R., et al. (2017). Microparticles in acute coronary syndrome. Thromb. Res. *156*: 109–116.

Mc Cormack, T., Baumeister, W., Grenier, L., Moomaw, C., Plamondon, L., Pramanik, B., et al. (1997). Active site-directed inhibitors of Rhodococcus 20 S proteasome. Kinetics and mechanism. J. Biol. Chem. *272*: 26103–26109.

McArthur, K., Chappaz, S., and Kile, B.T. (2018). Apoptosis in megakaryocytes and platelets: the life and death of a lineage. Blood *131*: 605–610.

McCoy, J.P., Chambers, W.H., Lakomy, R., Campbell, J.A., and Stewart, C.C. (1991). Sorting minor subpopulations of cells: use of fluorescence as the triggering signal. Cytometry *12*: 268–274.

McCullough, J., Fisher, R.D., Whitby, F.G., Sundquist, W.I., and Hill, C.P. (2008). ALIX-CHMP4 interactions in the human ESCRT pathway. Proc. Natl. Acad. Sci. U. S. A. *105*: 7687–7691.

McFadyen, J.D., Schaff, M., and Peter, K. (2018). Current and future antiplatelet therapies: emphasis on preserving haemostasis. Nat. Rev. Cardiol. *15*: 181–191.

Mehta, S.R., Yusuf, S., Peters, R.J., Bertrand, M.E., Lewis, B.S., Natarajan, M.K., et al. (2001). Effects of pretreatment with clopidogrel and aspirin followed by long-term therapy in patients undergoing percutaneous coronary intervention: the PCI-CURE study. Lancet Lond. Engl. *358*: 527–533.

Meijden, P.E.J. van der, and Heemskerk, J.W.M. (2018). Platelet biology and functions: new concepts and clinical perspectives. Nat. Rev. Cardiol.

Meister, M., Bänfer, S., Gärtner, U., Koskimies, J., Amaddii, M., Jacob, R., et al. (2017). Regulation of cargo transfer between ESCRT-0 and ESCRT-I complexes by flotillin-1 during endosomal sorting of ubiquitinated cargo. Oncogenesis *6*: e344.

Mettlen, M., Pucadyil, T., Ramachandran, R., and Schmid, S.L. (2009). Dissecting dynamin's role in clathrin-mediated endocytosis. Biochem. Soc. Trans. *37*: 1022–1026.

Miller, H., Castro-Gomes, T., Corrotte, M., Tam, C., Maugel, T.K., Andrews, N.W., et al. (2015). Lipid raft–dependent plasma membrane repair interferes with the activation of B lymphocytes. J. Cell Biol. *211*: 1193–1205.

Miranda, K.C., Bond, D.T., McKee, M., Skog, J., Păunescu, T.G., Da Silva, N., et al. (2010). Nucleic acids within urinary exosomes/microvesicles are potential biomarkers for renal disease. Kidney Int. *78*: 191–199.

Miyoshi, H., Umeshita, K., Sakon, M., Imajoh-Ohmi, S., Fujitani, K., Gotoh, M., et al. (1996). Calpain activation in plasma membrane bleb formation during tert-butyl hydroperoxide-induced rat hepatocyte injury. Gastroenterology *110*: 1897–1904.

Mohammad, R.M., Goustin, A.S., Aboukameel, A., Chen, B., Banerjee, S., Wang, G., et al. (2007). Preclinical studies of TW-37, a new nonpeptidic small-molecule inhibitor of Bcl-2, in diffuse large cell lymphoma xenograft model reveal drug action on both Bcl-2 and Mcl-1. Clin. Cancer Res. Off. J. Am. Assoc. Cancer Res. *13*: 2226–2235.

Molica, F., Morel, S., Meens, M.J., Denis, J.-F., Bradfield, P.F., Penuela, S., et al. (2015). Functional role of a polymorphism in the Pannexin1 gene in collagen-induced platelet aggregation. Thromb. Haemost. *114*: 325–336.

Molica, F., Stierlin, F.B., Fontana, P., and Kwak, B.R. (2017). Pannexin- and Connexin-Mediated Intercellular Communication in Platelet Function. Int. J. Mol. Sci. *18*:.

Momen-Heravi, F., Balaj, L., Alian, S., Tigges, J., Toxavidis, V., Ericsson, M., et al. (2012). Alternative methods for characterization of extracellular vesicles. Front. Physiol. *3*: 354.

Morel, O., Jesel, L., Freyssinet, J.-M., and Toti, F. (2011). Cellular mechanisms underlying the formation of circulating microparticles. Arterioscler. Thromb. Vasc. Biol. *31*: 15–26.

Morel, O., Morel, N., Freyssinet, J.-M., and Toti, F. (2008). Platelet microparticles and vascular cells interactions: a checkpoint between the haemostatic and thrombotic responses. Platelets *19*: 9–23.

Morlot, S., Galli, V., Klein, M., Chiaruttini, N., Manzi, J., Humbert, F., et al. (2012). Membrane shape at the edge of the dynamin helix sets location and duration of the fission reaction. Cell *151*: 619–629.

Morrow, D.A., Braunwald, E., Bonaca, M.P., Ameriso, S.F., Dalby, A.J., Fish, M.P., et al. (2012). Vorapaxar in the secondary prevention of atherothrombotic events. N. Engl. J. Med. *366*: 1404–1413.

Moscardó, A., Vallés, J., Latorre, A., and Santos, M.T. (2014). The association of thromboxane A2 receptor with lipid rafts is a determinant for platelet functional responses. FEBS Lett. *588*: 3154–3159.

Mosnier, L.O., Sinha, R.K., Burnier, L., Bouwens, E.A., and Griffin, J.H. (2012). Biased agonism of protease-activated receptor 1 by activated protein C caused by noncanonical cleavage at Arg46. Blood *120*: 5237–5246.

Mundell, S.J., and Mumford, A. (2018). TBXA2R gene variants associated with bleeding. Platelets *29*: 739–742.

Murakami, T., Horigome, H., Tanaka, K., Nakata, Y., Ohkawara, K., Katayama, Y., et al. (2007). Impact of weight reduction on production of platelet-derived microparticles and fibrinolytic parameters in obesity. Thromb. Res. *119*: 45–53.

Nagata, S. (2018). Apoptosis and Clearance of Apoptotic Cells. Annu. Rev. Immunol. *36*: 489–517.

Neijssen, J., Herberts, C., Drijfhout, J.W., Reits, E., Janssen, L., and Neefjes, J. (2005). Cross-presentation by intercellular peptide transfer through gap junctions. Nature *434*: 83–88.

Nielsen, M.H., Beck-Nielsen, H., Andersen, M.N., and Handberg, A. (2014). A flow cytometric method for characterization of circulating cell-derived microparticles in plasma. J. Extracell. Vesicles *3*:.

Nieswandt, B., Brakebusch, C., Bergmeier, W., Schulte, V., Bouvard, D., Mokhtari-Nejad, R., et al. (2001). Glycoprotein VI but not alpha2beta1 integrin is essential for platelet interaction with collagen. EMBO J. *20*: 2120–2130.

Nishi, C., Toda, S., Segawa, K., and Nagata, S. (2014). Tim4- and MerTK-mediated engulfment of apoptotic cells by mouse resident peritoneal macrophages. Mol. Cell. Biol. *34*: 1512–1520.

Ohtani, Y., Irie, T., Uekama, K., Fukunaga, K., and Pitha, J. (1989). Differential effects of alpha-, beta- and gamma-cyclodextrins on human erythrocytes. Eur. J. Biochem. *186*: 17–22.

Owens, A.P., and Mackman, N. (2011). Microparticles in Hemostasis and Thrombosis. Circ. Res. *108*: 1284–1297.

Packham, M.A., Rand, M.L., Perry, D.W., Ruben, D.H., and Kinlough-Rathbone, R.L. (1996). Probenecid inhibits platelet responses to aggregating agents in vitro and has a synergistic inhibitory effect with penicillin G. Thromb. Haemost. *76*: 239–244.

Pani, B., and Singh, B.B. (2009). Lipid rafts/caveolae as microdomains of calcium signaling. Cell Calcium *45*: 625–633.

Paoluzzi, L., Gonen, M., Gardner, J.R., Mastrella, J., Yang, D., Holmlund, J., et al. (2008). Targeting Bcl-2 family members with the BH3 mimetic AT-101 markedly enhances the therapeutic effects of chemotherapeutic agents in in vitro and in vivo models of B-cell lymphoma. Blood *111*: 5350–5358.

Paredes, R.M., Etzler, J.C., Watts, L.T., and Lechleiter, J.D. (2008). Chemical Calcium Indicators. Methods San Diego Calif *46*: 143–151.

Park, C.-M., Oie, T., Petros, A.M., Zhang, H., Nimmer, P.M., Henry, R.F., et al. (2006). Design, synthesis, and computational studies of inhibitors of Bcl-XL. J. Am. Chem. Soc. *128*: 16206–16212.

Parton, R.G., Hanzal-Bayer, M., and Hancock, J.F. (2006). Biogenesis of caveolae: a structural model for caveolin-induced domain formation. J. Cell Sci. *119*: 787–796.

Paul, B.Z.S., Kim, S., Dangelmaier, C., Nagaswami, C., Jin, J., Hartwig, J.H., et al. (2003). Dynamic regulation of microtubule coils in ADP-induced platelet shape change by p160ROCK (Rho-kinase). Platelets *14*: 159–169.

Paulus, J.M. (1975). Platelet size in man. Blood *46*: 321–336.

Pelegrin, P., and Surprenant, A. (2006). Pannexin-1 mediates large pore formation and interleukin-1β release by the ATP-gated P2X7 receptor. EMBO J. *25*: 5071–5082.

Petrich, B.G. (2009). Talin-dependent integrin signalling in vivo. Thromb. Haemost. *101*: 1020–1024.

Pike, L.J. (2006). Rafts defined: a report on the Keystone Symposium on Lipid Rafts and Cell Function. J. Lipid Res. *47*: 1597–1598.

Pisitkun, T., Shen, R.-F., and Knepper, M.A. (2004). Identification and proteomic profiling of exosomes in human urine. Proc. Natl. Acad. Sci. U. S. A. *101*: 13368–13373.

Podoplelova, N.A., Sveshnikova, A.N., Kotova, Y.N., Eckly, A., Receveur, N., Nechipurenko, D.Y., et al. (2016). Coagulation factors bound to procoagulant platelets concentrate in cap structures to promote clotting. Blood *128*: 1745–1755.

Pol, E. van der, Böing, A.N., Gool, E.L., and Nieuwland, R. (2016). Recent developments in the nomenclature, presence, isolation, detection and clinical impact of extracellular vesicles. J. Thromb. Haemost. JTH *14*: 48–56.

Pol, E. van der, Gemert, M.J.C. van, Sturk, A., Nieuwland, R., and Leeuwen, T.G. van (2012). Single vs. swarm detection of microparticles and exosomes by flow cytometry. J. Thromb. Haemost. JTH *10*: 919–930.

Pol, E. van der, and Harrison, P. (2017). From platelet dust to gold dust: physiological importance and detection of platelet microvesicles. Platelets *28*: 211–213.

Poon, I.K.H., Lucas, C.D., Rossi, A.G., and Ravichandran, K.S. (2014). Apoptotic cell clearance: basic biology and therapeutic potential. Nat. Rev. Immunol. *14*: 166–180.

Praefcke, G.J.K., and McMahon, H.T. (2004). The dynamin superfamily: universal membrane tubulation and fission molecules? Nat. Rev. Mol. Cell Biol. *5*: 133–147.

Preston, R.A., Jy, W., Jimenez, J.J., Mauro, L.M., Horstman, L.L., Valle, M., et al. (2003). Effects of severe hypertension on endothelial and platelet microparticles. Hypertens. Dallas Tex 1979 *41*: 211–217.

Prudent, M., Crettaz, D., Delobel, J., Seghatchian, J., Tissot, J.-D., and Lion, N. (2015). Differences between calcium-stimulated and storage-induced erythrocyte-derived microvesicles. Transfus. Apher. Sci. Off. J. World Apher. Assoc. Off. J. Eur. Soc. Haemapheresis *53*: 153–158.

Putney, J.W. (2010). Pharmacology of store-operated calcium channels. Mol. Interv. *10*: 209–218.

Putney, J.W., Steinckwich-Besançon, N., Numaga-Tomita, T., Davis, F.M., Desai, P.N., D'Agostin, D.M., et al. (2017). The functions of store-operated calcium channels. Biochim. Biophys. Acta Mol. Cell Res. *1864*: 900–906.

Qin, C., Nagao, T., Grosheva, I., Maxfield, F.R., and Pierini, L.M. (2006). Elevated plasma membrane cholesterol content alters macrophage signaling and function. Arterioscler. Thromb. Vasc. Biol. *26*: 372–378.

Quach, M.E., Chen, W., and Li, R. (2018). Mechanisms of platelet clearance and translation to improve platelet storage. Blood *131*: 1512–1521.

Quinter, P.G., Dangelmaier, C.A., Quinton, T.M., Kunapuli, S.P., and Daniel, J.L. (2007). Glycoprotein VI agonists have distinct dependences on the lipid raft environment. J. Thromb. Haemost. JTH *5*: 362–368.

Quinton, T.M., Kim, S., Jin, J., and Kunapuli, S.P. (2005). Lipid rafts are required in Galpha(i) signaling downstream of the P2Y12 receptor during ADP-mediated platelet activation. J. Thromb. Haemost. JTH *3*: 1036–1041.

Raghupathy, R., Anilkumar, A.A., Polley, A., Singh, P.P., Yadav, M., Johnson, C., et al. (2015). Transbilayer lipid interactions mediate nanoclustering of lipid-anchored proteins. Cell *161*: 581–594.

Rao, A.K. (2013). Inherited platelet function disorders: overview and disorders of granules, secretion, and signal transduction. Hematol. Oncol. Clin. North Am. *27*: 585–611.

Raposo, G., and Stoorvogel, W. (2013). Extracellular vesicles: exosomes, microvesicles, and friends. J. Cell Biol. *200*: 373–383.

Raslan, Z., Magwenzi, S., Aburima, A., Taskén, K., and Naseem, K.M. (2015). Targeting of type I protein kinase A to lipid rafts is required for platelet inhibition by the 3',5'-cyclic adenosine monophosphate-signaling pathway. J. Thromb. Haemost. JTH *13*: 1721–1734.

Ratajczak, J., Wysoczynski, M., Hayek, F., Janowska-Wieczorek, A., and Ratajczak, M.Z. (2006). Membrane-derived microvesicles: important and underappreciated mediators of cell-to-cell communication. Leukemia *20*: 1487–1495.

Rehse, M.A., Corpuz, S., Heimfeld, S., Minie, M., and Yachimiak, D. (1995). Use of fluorescence threshold triggering and high-speed flow cytometry for rare event detection. Cytometry *22*: 317–322.

Robert, S., Poncelet, P., Lacroix, R., Arnaud, L., Giraudo, L., Hauchard, A., et al. (2009). Standardization of platelet-derived microparticle counting using calibrated beads and a Cytomics FC500 routine flow cytometer: a first step towards multicenter studies? J. Thromb. Haemost. JTH *7*: 190–197.

Roberts, A.W., Seymour, J.F., Brown, J.R., Wierda, W.G., Kipps, T.J., Khaw, S.L., et al. (2012). Substantial susceptibility of chronic lymphocytic leukemia to BCL2 inhibition: results of a phase I study of navitoclax in patients with relapsed or refractory disease. J. Clin. Oncol. Off. J. Am. Soc. Clin. Oncol. *30*: 488–496.

Roberts, D.E., McNicol, A., and Bose, R. (2004). Mechanism of collagen activation in human platelets. J. Biol. Chem. *279*: 19421–19430.

Rogers, C., Fernandes-Alnemri, T., Mayes, L., Alnemri, D., Cingolani, G., and Alnemri, E.S. (2017). Cleavage of DFNA5 by caspase-3 during apoptosis mediates progression to secondary necrotic/pyroptotic cell death. Nat. Commun. *8*: 14128.

Rosado, J.A., Brownlow, S.L., and Sage, S.O. (2002). Endogenously expressed Trp1 is involved in store-mediated Ca2+ entry by conformational coupling in human platelets. J. Biol. Chem. *277*: 42157–42163.

Rossum, D.B. van, Patterson, R.L., Ma, H.T., and Gill, D.L. (2000). Ca2+ entry mediated by store depletion, S-nitrosylation, and TRP3 channels. Comparison of coupling and function. J. Biol. Chem. *275*: 28562–28568.

Rothmeier, A.S., Marchese, P., Petrich, B.G., Furlan-Freguia, C., Ginsberg, M.H., Ruggeri, Z.M., et al. (2015). Caspase-1-mediated pathway promotes generation of thromboinflammatory microparticles. J. Clin. Invest. *125*: 1471–1484.

Rozenvayn, N., and Flaumenhaft, R. (2001). Phosphatidylinositol 4,5-bisphosphate mediates Ca2+-induced platelet alpha-granule secretion: evidence for type II phosphatidylinositol 5-phosphate 4-kinase function. J. Biol. Chem. *276*: 22410–22419.

Rukoyatkina, N., Mindukshev, I., Walter, U., and Gambaryan, S. (2013). Dual role of the p38 MAPK/cPLA2 pathway in the regulation of platelet apoptosis induced by ABT-737 and strong platelet agonists. Cell Death Dis. *4*: e931.

Sachet, M., Liang, Y.Y., and Oehler, R. (2017). The immune response to secondary necrotic cells. Apoptosis Int. J. Program. Cell Death *22*: 1189–1204.

Sage, S.O., Jarvis, G.E., Jardín, I., Rosado, J.A., and Harper, A.G.S. (2014). The TRPV1 ion channel is expressed in human but not mouse platelets. Platelets *25*: 390–392.

Sage, S.O., Pugh, N., Mason, M.J., and Harper, A.G.S. (2011). Monitoring the intracellular store Ca2+ concentration in agonist-stimulated, intact human platelets by using Fluo-5N. J. Thromb. Haemost. JTH *9*: 540–551.

Saha, S., Anilkumar, A.A., and Mayor, S. (2016). GPI-anchored protein organization and dynamics at the cell surface. J. Lipid Res. *57*: 159–175.

Saksena, S., Sun, J., Chu, T., and Emr, S.D. (2007). ESCRTing proteins in the endocytic pathway. Trends Biochem. Sci. *32*: 561–573.

Salzer, U., Hinterdorfer, P., Hunger, U., Borken, C., and Prohaska, R. (2002). Ca(++)-dependent vesicle release from erythrocytes involves stomatin-specific lipid rafts, synexin (annexin VII), and sorcin. Blood *99*: 2569–2577.

Salzer, U., Zhu, R., Luten, M., Isobe, H., Pastushenko, V., Perkmann, T., et al. (2008). Vesicles generated during storage of red cells are rich in the lipid raft marker stomatin. Transfusion (Paris) *48*: 451–462.

Sandilos, J.K., Chiu, Y.-H., Chekeni, F.B., Armstrong, A.J., Walk, S.F., Ravichandran, K.S., et al. (2012). Pannexin 1, an ATP Release Channel, Is Activated by Caspase Cleavage of Its Pore-associated C-terminal Autoinhibitory Region♦. J. Biol. Chem. *287*: 11303–11311.

Santos, N.C., Martins-Silva, J., and Saldanha, C. (2005). Gramicidin D and dithiothreitol effects on erythrocyte exovesiculation. Cell Biochem. Biophys. *43*: 419–430.

Sapet, C., Simoncini, S., Loriod, B., Puthier, D., Sampol, J., Nguyen, C., et al. (2006). Thrombin-induced endothelial microparticle generation: identification of a novel pathway involving ROCK-II activation by caspase-2. Blood *108*: 1868–1876.

Sarratt, K.L., Chen, H., Zutter, M.M., Santoro, S.A., Hammer, D.A., and Kahn, M.L. (2005). GPVI and α2β1 play independent critical roles during platelet adhesion and aggregate formation to collagen under flow. Blood *106*: 1268–1277.

Savi, P., Zachayus, J.-L., Delesque-Touchard, N., Labouret, C., Hervé, C., Uzabiaga, M.-F., et al. (2006). The active metabolite of Clopidogrel disrupts P2Y12 receptor oligomers and partitions them out of lipid rafts. Proc. Natl. Acad. Sci. U. S. A. *103*: 11069–11074.

Scavone, M., Femia, E.A., and Cattaneo, M. (2017). P2Y12 receptor gene mutations associated with bleeding. Platelets *28*: 421–423.

Scheffer, L.L., Sreetama, S.C., Sharma, N., Medikayala, S., Brown, K.J., Defour, A., et al. (2014). Mechanism of Ca^{2+}-triggered ESCRT assembly and regulation of cell membrane repair. Nat. Commun. *5*: 5646.

Schindelin, J., Arganda-Carreras, I., Frise, E., Kaynig, V., Longair, M., Pietzsch, T., et al. (2012). Fiji: an open-source platform for biological-image analysis. Nat. Methods *9*: 676–682.

Schindl, R., Bergsmann, J., Frischauf, I., Derler, I., Fahrner, M., Muik, M., et al. (2008). 2-aminoethoxydiphenyl borate alters selectivity of Orai3 channels by increasing their pore size. J. Biol. Chem. *283*: 20261–20267.

Schnitzer, J.E., Oh, P., Pinney, E., and Allard, J. (1994). Filipin-sensitive caveolae-mediated transport in endothelium: reduced transcytosis, scavenger endocytosis, and capillary permeability of select macromolecules. J. Cell Biol. *127*: 1217–1232.

Schoenwaelder, S.M., Jarman, K.E., Gardiner, E.E., Hua, M., Qiao, J., White, M.J., et al. (2011). Bcl-xL-inhibitory BH3 mimetics can induce a transient thrombocytopathy that undermines the hemostatic function of platelets. Blood *118*: 1663–1674.

Schoenwaelder, S.M., Yuan, Y., Josefsson, E.C., White, M.J., Yao, Y., Mason, K.D., et al. (2009). Two distinct pathways regulate platelet phosphatidylserine exposure and procoagulant function. Blood *114*: 663–666.

Segawa, K., Kurata, S., Yanagihashi, Y., Brummelkamp, T.R., Matsuda, F., and Nagata, S. (2014). Caspase-mediated cleavage of phospholipid flippase for apoptotic phosphatidylserine exposure. Science *344*: 1164–1168.

Semeraro, F., Ammollo, C.T., Morrissey, J.H., Dale, G.L., Friese, P., Esmon, N.L., et al. (2011). Extracellular histones promote thrombin generation through platelet-dependent mechanisms: involvement of platelet TLR2 and TLR4. Blood *118*: 1952–1961.

Sezgin, E., Levental, I., Grzybek, M., Schwarzmann, G., Mueller, V., Honigmann, A., et al. (2012). Partitioning, diffusion, and ligand binding of raft lipid analogs in model and cellular plasma membranes. Biochim. Biophys. Acta *1818*: 1777–1784.

Sezgin, E., Levental, I., Mayor, S., and Eggeling, C. (2017). The mystery of membrane organization: composition, regulation and roles of lipid rafts. Nat. Rev. Mol. Cell Biol. *18*: 361–374.

Sezgin, E., and Schwille, P. (2011). Fluorescence Techniques to Study Lipid Dynamics. Cold Spring Harb. Perspect. Biol. *3*:.

Shcherbina, A., and Remold-O'Donnell, E. (1999). Role of caspase in a subset of human platelet activation responses. Blood *93*: 4222–4231.

Shekhonin, B.V., Domogatsky, S.P., Muzykantov, V.R., Idelson, G.L., and Rukosuev, V.S. (1985). Distribution of type I, III, IV and V collagen in normal and atherosclerotic human arterial wall: immunomorphological characteristics. Coll. Relat. Res. *5*: 355–368.

Shiraga, M., Miyata, S., Kato, H., Kashiwagi, H., Honda, S., Kurata, Y., et al. (2005). Impaired platelet function in a patient with P2Y12 deficiency caused by a mutation in the translation initiation codon. J. Thromb. Haemost. JTH *3*: 2315–2323.

Simons, K., and Vaz, W.L.C. (2004). Model systems, lipid rafts, and cell membranes. Annu. Rev. Biophys. Biomol. Struct. *33*: 269–295.

Sinauridze, E.I., Kireev, D.A., Popenko, N.Y., Pichugin, A.V., Panteleev, M.A., Krymskaya, O.V., et al. (2007). Platelet microparticle membranes have 50- to 100-fold higher specific procoagulant activity than activated platelets. Thromb. Haemost. *97*: 425–434.

Singh, A.K., Saotome, K., McGoldrick, L.L., and Sobolevsky, A.I. (2018). Structural bases of TRP channel TRPV6 allosteric modulation by 2-APB. Nat. Commun. *9*:.

Skommer, J., Wlodkowic, D., Mättö, M., Eray, M., and Pelkonen, J. (2006). HA14-1, a small molecule Bcl-2 antagonist, induces apoptosis and modulates action of selected anticancer drugs in follicular lymphoma B cells. Leuk. Res. *30*: 322–331.

Son, S.M., Kang, S., Choi, H., and Mook-Jung, I. (2015). Statins induce insulin-degrading enzyme secretion from astrocytes via an autophagy-based unconventional secretory pathway. Mol. Neurodegener. *10*: 56.

Sosinsky, G.E., Boassa, D., Dermietzel, R., Duffy, H.S., Laird, D.W., MacVicar, B., et al. (2011). Pannexin channels are not gap junction hemichannels. Channels Austin Tex *5*: 193–197.

Soslau, G., Mason, C., Lynch, S., Benjamin, J., Ashak, D., Prakash, J.M., et al. (2014). Intracellular matrix metalloproteinase-2 (MMP-2) regulates human platelet activation via hydrolysis of talin. Thromb. Haemost. *111*: 140–153.

Souers, A.J., Leverson, J.D., Boghaert, E.R., Ackler, S.L., Catron, N.D., Chen, J., et al. (2013). ABT-199, a potent and selective BCL-2 inhibitor, achieves antitumor activity while sparing platelets. Nat. Med. *19*: 202–208.

Splettstoesser, F., Florea, A.-M., and Büsselberg, D. (2007). IP3 receptor antagonist, 2-APB, attenuates cisplatin induced Ca2+-influx in HeLa-S3 cells and prevents activation of calpain and induction of apoptosis. Br. J. Pharmacol. *151*: 1176–1186.

Sprague, D.L., Elzey, B.D., Crist, S.A., Waldschmidt, T.J., Jensen, R.J., and Ratliff, T.L. (2008). Platelet-mediated modulation of adaptive immunity: unique delivery of CD154 signal by platelet-derived membrane vesicles. Blood *111*: 5028–5036.

Stachowiak, J.C., Schmid, E.M., Ryan, C.J., Ann, H.S., Sasaki, D.Y., Sherman, M.B., et al. (2012). Membrane bending by protein-protein crowding. Nat. Cell Biol. *14*: 944–949.

Stefanini, L., Paul, D.S., Robledo, R.F., Chan, E.R., Getz, T.M., Campbell, R.A., et al. (2015). RASA3 is a critical inhibitor of RAP1-dependent platelet activation. J. Clin. Invest. *125*: 1419–1432.

Storey, R.F. (2001). The P2Y12 receptor as a therapeutic target in cardiovascular disease. Platelets *12*: 197–209.

Suzuki, J., Imanishi, E., and Nagata, S. (2016). Xkr8 phospholipid scrambling complex in apoptotic phosphatidylserine exposure. Proc. Natl. Acad. Sci. U. S. A. *113*: 9509–9514.

Suzuki, J., Umeda, M., Sims, P.J., and Nagata, S. (2010). Calcium-dependent phospholipid scrambling by TMEM16F. Nature *468*: 834–838.

Swieringa, F., Spronk, H.M.H., Heemskerk, J.W.M., and Meijden, P.E.J. van der (2018). Integrating platelet and coagulation activation in fibrin clot formation. Res. Pract. Thromb. Haemost. *2*: 450–460.

Tait, S.W.G., and Green, D.R. (2013). Mitochondrial regulation of cell death. Cold Spring Harb. Perspect. Biol. *5*:.

Takei, K., McPherson, P.S., Schmid, S.L., and De Camilli, P. (1995). Tubular membrane invaginations coated by dynamin rings are induced by GTP-gamma S in nerve terminals. Nature *374*: 186–190.

Tavoosi, N., Davis-Harrison, R.L., Pogorelov, T.V., Ohkubo, Y.Z., Arcario, M.J., Clay, M.C., et al. (2011). Molecular Determinants of Phospholipid Synergy in Blood Clotting. J. Biol. Chem. *286*: 23247–23253.

Taylor, K.A., Wright, J.R., Vial, C., Evans, R.J., and Mahaut-Smith, M.P. (2014). Amplification of human platelet activation by surface pannexin-1 channels. J. Thromb. Haemost. JTH *12*: 987–998.

Teissier, E., and Pécheur, E.-I. (2007). Lipids as modulators of membrane fusion mediated by viral fusion proteins. Eur. Biophys. J. EBJ *36*: 887–899.

Théry, C., Witwer, K.W., Aikawa, E., Alcaraz, M.J., Anderson, J.D., Andriantsitohaina, R., et al. (2018). Minimal information for studies of extracellular vesicles 2018 (MISEV2018): a position statement of the International Society for Extracellular Vesicles and update of the MISEV2014 guidelines. J. Extracell. Vesicles *7*: 1535750.

Thon, J.N., Schubert, P., Duguay, M., Serrano, K., Lin, S., Kast, J., et al. (2008). Comprehensive proteomic analysis of protein changes during platelet storage requires complementary proteomic approaches. Transfusion (Paris) *48*: 425–435.

Tian, C., Du, L., Zhou, Y., and Li, M. (2016). Store-operated CRAC channel inhibitors: opportunities and challenges. Future Med. Chem. *8*: 817–832.

Trebak, M., Bird, G.S.J., McKay, R.R., and Putney, J.W. (2002). Comparison of human TRPC3 channels in receptor-activated and store-operated modes. Differential sensitivity to channel blockers suggests fundamental differences in channel composition. J. Biol. Chem. *277*: 21617–21623.

Tricoci, P., Huang, Z., Held, C., Moliterno, D.J., Armstrong, P.W., Van de Werf, F., et al. (2012). Thrombin-receptor antagonist vorapaxar in acute coronary syndromes. N. Engl. J. Med. *366*: 20–33.

Tse, C., Shoemaker, A.R., Adickes, J., Anderson, M.G., Chen, J., Jin, S., et al. (2008). ABT-263: a potent and orally bioavailable Bcl-2 family inhibitor. Cancer Res. *68*: 3421–3428.

Tsujinaka, T., Kajiwara, Y., Kambayashi, J., Sakon, M., Higuchi, N., Tanaka, T., et al. (1988). Synthesis of a new cell penetrating calpain inhibitor (calpeptin). Biochem. Biophys. Res. Commun. *153*: 1201–1208.

Turturici, G., Tinnirello, R., Sconzo, G., and Geraci, F. (2014). Extracellular membrane vesicles as a mechanism of cell-to-cell communication: advantages and disadvantages. Am. J. Physiol. Cell Physiol. *306*: C621-633.

Urbanelli, L., Magini, A., Buratta, S., Brozzi, A., Sagini, K., Polchi, A., et al. (2013). Signaling Pathways in Exosomes Biogenesis, Secretion and Fate. Genes *4*: 152–170.

Vaiyapuri, S., Flora, G.D., and Gibbins, J.M. (2015). Gap junctions and connexin hemichannels in the regulation of haemostasis and thrombosis. Biochem. Soc. Trans. *43*: 489–494.

Vaiyapuri, S., Jones, C.I., Sasikumar, P., Moraes, L.A., Munger, S.J., Wright, J.R., et al. (2012). Gap junctions and connexin hemichannels underpin hemostasis and thrombosis. Circulation *125*: 2479–2491.

Vaiyapuri, S., Moraes, L.A., Sage, T., Ali, M.S., Lewis, K.R., Mahaut-Smith, M.P., et al. (2013). Connexin40 regulates platelet function. Nat. Commun. *4*: 2564.

Vance, J.E., and Tasseva, G. (2013). Formation and function of phosphatidylserine and phosphatidylethanolamine in mammalian cells. Biochim. Biophys. Acta *1831*: 543–554.

Vanden Abeele, F., Bidaux, G., Gordienko, D., Beck, B., Panchin, Y.V., Baranova, A.V., et al. (2006). Functional implications of calcium permeability of the channel formed by pannexin 1. J. Cell Biol. *174*: 535–546.

Vanden Berghe, T., Linkermann, A., Jouan-Lanhouet, S., Walczak, H., and Vandenabeele, P. (2014). Regulated necrosis: the expanding network of non-apoptotic cell death pathways. Nat. Rev. Mol. Cell Biol. *15*: 135–147.

Varga-Szabo, D., Authi, K.S., Braun, A., Bender, M., Ambily, A., Hassock, S.R., et al. (2008). Store-operated Ca(2+) entry in platelets occurs independently of transient receptor potential (TRP) C1. Pflugers Arch. *457*: 377–387.

Vasina, E.M., Cauwenberghs, S., Feijge, M. a. H., Heemskerk, J.W.M., Weber, C., and Koenen, R.R. (2011). Microparticles from apoptotic platelets promote resident macrophage differentiation. Cell Death Dis. *2*: e211.

Verderio, C., Gabrielli, M., and Giussani, P. (2018). Role of sphingolipids in the biogenesis and biological activity of extracellular vesicles. J. Lipid Res. *59*: 1325–1340.

Vermes, I., Haanen, C., Steffens-Nakken, H., and Reutelingsperger, C. (1995). A novel assay for apoptosis. Flow cytometric detection of phosphatidylserine expression on early apoptotic cells using fluorescein labelled Annexin V. J. Immunol. Methods *184*: 39–51.

Versteeg, H.H., Heemskerk, J.W.M., Levi, M., and Reitsma, P.H. (2013). New fundamentals in hemostasis. Physiol. Rev. *93*: 327–358.

Vietri, M., Schink, K.O., Campsteijn, C., Wegner, C.S., Schultz, S.W., Christ, L., et al. (2015). Spastin and ESCRT-III coordinate mitotic spindle disassembly and nuclear envelope sealing. Nature *522*: 231–235.

Vlassov, A.V., Magdaleno, S., Setterquist, R., and Conrad, R. (2012). Exosomes: current knowledge of their composition, biological functions, and diagnostic and therapeutic potentials. Biochim. Biophys. Acta *1820*: 940–948.

Voets, T., Prenen, J., Fleig, A., Vennekens, R., Watanabe, H., Hoenderop, J.G., et al. (2001). CaT1 and the calcium release-activated calcium channel manifest distinct pore properties. J. Biol. Chem. *276*: 47767–47770.

Vogel, S., Bodenstein, R., Chen, Q., Feil, S., Feil, R., Rheinlaender, J., et al. (2015). Platelet-derived HMGB1 is a critical mediator of thrombosis. J. Clin. Invest. *125*: 4638–4654.

Vogler, M., Hamali, H.A., Sun, X.-M., Bampton, E.T.W., Dinsdale, D., Snowden, R.T., et al. (2011). BCL2/BCL-X(L) inhibition induces apoptosis, disrupts cellular calcium homeostasis, and prevents platelet activation. Blood *117*: 7145–7154.

Wallentin, L., Becker, R.C., Budaj, A., Cannon, C.P., Emanuelsson, H., Held, C., et al. (2009). Ticagrelor versus clopidogrel in patients with acute coronary syndromes. N. Engl. J. Med. *361*: 1045–1057.

Wang, Y., Fang, C., Gao, H., Bilodeau, M.L., Zhang, Z., Croce, K., et al. (2014). Platelet-derived S100 family member myeloid-related protein-14 regulates thrombosis. J. Clin. Invest. *124*: 2160–2171.

Wang, Z.-T., Wang, Z., and Hu, Y.-W. (2016). Possible roles of platelet-derived microparticles in atherosclerosis. Atherosclerosis *248*: 10–16.

Warner, T.D., Nylander, S., and Whatling, C. (2011). Anti-platelet therapy: cyclo-oxygenase inhibition and the use of aspirin with particular regard to dual anti-platelet therapy. Br. J. Clin. Pharmacol. *72*: 619–633.

Watts, S.W., Morrison, S.F., Davis, R.P., and Barman, S.M. (2012). Serotonin and Blood Pressure Regulation. Pharmacol. Rev. *64*: 359–388.

Webster, B.M., Colombi, P., Jäger, J., and Lusk, C.P. (2014). Surveillance of nuclear pore complex assembly by ESCRT-III/Vps4. Cell *159*: 388–401.

Wei, J., Stebbins, J.L., Kitada, S., Dash, R., Placzek, W., Rega, M.F., et al. (2010). BI-97C1, an optically pure Apogossypol derivative as pan-active inhibitor of antiapoptotic B-cell lymphoma/leukemia-2 (Bcl-2) family proteins. J. Med. Chem. *53*: 4166–4176.

Wei, M., Zhou, Y., Sun, A., Ma, G., He, L., Zhou, L., et al. (2016). Molecular mechanisms underlying inhibition of STIM1-Orai1-mediated Ca2+ entry induced by 2-aminoethoxydiphenyl borate. Pflugers Arch. *468*: 2061–2074.

Weyd, H., Abeler-Dörner, L., Linke, B., Mahr, A., Jahndel, V., Pfrang, S., et al. (2013). Annexin A1 on the surface of early apoptotic cells suppresses CD8+ T cell immunity. PloS One *8*: e62449.

Whiteheart, S.W. (2011). Platelet granules: surprise packages. Blood *118*: 1190–1191.

Willebrords, J., Maes, M., Crespo Yanguas, S., and Vinken, M. (2017). Inhibitors of connexin and pannexin channels as potential therapeutics. Pharmacol. Ther. *180*: 144–160.

Wilson, W.H., O'Connor, O.A., Czuczman, M.S., LaCasce, A.S., Gerecitano, J.F., Leonard, J.P., et al. (2010). Navitoclax, a targeted high-affinity inhibitor of BCL-2, in lymphoid malignancies: a phase 1 dose-escalation study of safety, pharmacokinetics, pharmacodynamics, and antitumour activity. Lancet Oncol. *11*: 1149–1159.

Wiviott, S.D., Braunwald, E., McCabe, C.H., Montalescot, G., Ruzyllo, W., Gottlieb, S., et al. (2007). Prasugrel versus Clopidogrel in Patients with Acute Coronary Syndromes. N. Engl. J. Med. *357*: 2001–2015.

Wolf, P. (1967). The nature and significance of platelet products in human plasma. Br. J. Haematol. *13*: 269–288.

Wolfs, J.L., Wielders, S.J., Comfurius, P., Lindhout, T., Giddings, J.C., Zwaal, R.F., et al. (2006). Reversible inhibition of the platelet procoagulant response through manipulation of the Gardos channel. Blood *108*: 2223–2228.

Wong, P.C., Seiffert, D., Bird, J.E., Watson, C.A., Bostwick, J.S., Giancarli, M., et al. (2017). Blockade of protease-activated receptor-4 (PAR4) provides robust antithrombotic activity with low bleeding. Sci. Transl. Med. *9*:.

Xu, P., Baldridge, R.D., Chi, R.J., Burd, C.G., and Graham, T.R. (2013). Phosphatidylserine flipping enhances membrane curvature and negative charge required for vesicular transport. J. Cell Biol. *202*: 875–886.

Xu, S.-Z., Zeng, F., Boulay, G., Grimm, C., Harteneck, C., and Beech, D.J. (2005). Block of TRPC5 channels by 2-aminoethoxydiphenyl borate: a differential, extracellular and voltage-dependent effect. Br. J. Pharmacol. *145*: 405–414.

Xu, X., Ali, S., Li, Y., Yu, H., Zhang, M., Lu, J., et al. (2016). 2-Aminoethoxydiphenyl Borate Potentiates CRAC Current by Directly Dilating the Pore of Open Orai1. Sci. Rep. *6*: 29304.

Yang, H., Kim, A., David, T., Palmer, D., Jin, T., Tien, J., et al. (2012). TMEM16F forms a Ca2+-activated cation channel required for lipid scrambling in platelets during blood coagulation. Cell *151*: 111–122.

Yano, Y., Shiba, E., Kambayashi, J., Sakon, M., Kawasaki, T., Fujitani, K., et al. (1993). The effects of calpeptin (a calpain specific inhibitor) on agonist induced microparticle formation from the platelet plasma membrane. Thromb. Res. *71*: 385–396.

Ye, Z.-C., Oberheim, N., Kettenmann, H., and Ransom, B.R. (2009). Pharmacological 'cross-inhibition' of connexin hemichannels and swelling activated anion channels. Glia *57*: 258–269.

Yousuf, O., and Bhatt, D.L. (2011). The evolution of antiplatelet therapy in cardiovascular disease. Nat. Rev. Cardiol. *8*: 547–559.

Yu, J., Fischman, D.A., and Steck, T.L. (1973). Selective solubilization of proteins and phospholipids from red blood cell membranes by nonionic detergents. J. Supramol. Struct. *1*: 233–248.

Yuan, A., Farber, E.L., Rapoport, A.L., Tejada, D., Deniskin, R., Akhmedov, N.B., et al. (2009). Transfer of microRNAs by embryonic stem cell microvesicles. PloS One *4*: e4722.

Yuan, S., Chan, H.C.S., Vogel, H., Filipek, S., Stevens, R.C., and Palczewski, K. (2016). The Molecular Mechanism of P2Y1 Receptor Activation. Angew. Chem. Int. Ed Engl. *55*: 10331–10335.

Yun, S.-H., Sim, E.-H., Goh, R.-Y., Park, J.-I., and Han, J.-Y. (2016). Platelet Activation: The Mechanisms and Potential Biomarkers. BioMed Res. Int. *2016*:.

Zerp, S.F., Stoter, R., Kuipers, G., Yang, D., Lippman, M.E., Blitterswijk, W.J. van, et al. (2009). AT-101, a small molecule inhibitor of anti-apoptotic Bcl-2 family members, activates the SAPK/JNK pathway and enhances radiation-induced apoptosis. Radiat. Oncol. Lond. Engl. *4*: 47.

Zhang, J., Sun, X., Zheng, S., Liu, X., Jin, J., Ren, Y., et al. (2014). Myelin basic protein induces neuron-specific toxicity by directly damaging the neuronal plasma membrane. PloS One *9*: e108646.

Zhang, S., Ye, J., Zhang, Y., Xu, X., Liu, J., Zhang, S.H., et al. (2013). P2Y12 protects platelets from apoptosis via PI3k-dependent Bak/Bax inactivation. J. Thromb. Haemost. JTH *11*: 149–160.

Zhang, Y., Chen, X., Gueydan, C., and Han, J. (2018). Plasma membrane changes during programmed cell deaths. Cell Res. *28*: 9–21.

Zhao, L., Liu, J., He, C., Yan, R., Zhou, K., Cui, Q., et al. (2017). Protein kinase A determines platelet life span and survival by regulating apoptosis. J. Clin. Invest. *127*: 4338–4351.

Zhao, Y., Ishigami, M., Nagao, K., Hanada, K., Kono, N., Arai, H., et al. (2015). ABCB4 exports phosphatidylcholine in a sphingomyelin-dependent manner. J. Lipid Res. *56*: 644–652.

Zhou, B., Wang, Y., Zhang, C., Yang, G., Zhang, F., Yu, B., et al. (2018). Ribemansides A and B, TRPC6 Inhibitors from Ribes manshuricum That Suppress TGF-β1-Induced Fibrogenesis in HK-2 Cells. J. Nat. Prod. *81*: 913–917.

Zhou, B.-D., Guo, G., Zheng, L.-M., Zu, L.-Y., and Gao, W. (2015). Microparticles as Novel Biomarkers and Therapeutic Targets in Coronary Heart Disease. Chin. Med. J. (Engl.) *128*: 267–272.

Zhou, H., Iwasaki, H., Nakamura, T., Nakamura, K., Maruyama, T., Hamano, S., et al. (2007). 2-Aminoethyl diphenylborinate analogues: selective inhibition for store-operated Ca2+ entry. Biochem. Biophys. Res. Commun. *352*: 277–282.

Zidovetzki, R., and Levitan, I. (2007). Use of cyclodextrins to manipulate plasma membrane cholesterol content: evidence, misconceptions and control strategies. Biochim. Biophys. Acta *1768*: 1311–1324.

Żmigrodzka, M., Guzera, M., Miśkiewicz, A., Jagielski, D., and Winnicka, A. (2016). The biology of extracellular vesicles with focus on platelet microparticles and their role in cancer development and progression. Tumour Biol. J. Int. Soc. Oncodevelopmental Biol. Med. *37*: 14391–14401.

Zong, W.-X., and Thompson, C.B. (2006). Necrotic death as a cell fate. Genes Dev. *20*: 1–15.

Zwaal, R.F.A., Comfurius, P., and Bevers, E.M. (2004). Scott syndrome, a bleeding disorder caused by defective scrambling of membrane phospholipids. Biochim. Biophys. Acta *1636*: 119–128.

Zwaal, R.F.A., Comfurius, P., and Bevers, E.M. (2005). Surface exposure of phosphatidylserine in pathological cells. Cell. Mol. Life Sci. CMLS *62*: 971–988.